Translational control of Human Epidermal Growth Factor Receptors, *HER2* and *HER4* in response to cellular stresses in breast cancer cells

Arnelle Edwards, BSc.

Thesis submitted to the University of Nottingham
for degree of Doctor of Philosophy

April 2023

Declaration

I declare that the work presented in this thesis is my own work and was conducted in the Gene Regulation & RNA Biology laboratory, School of Pharmacy, University of Nottingham.

Abstract

The human epidermal growth factors (EGFR and HER2-4) are tyrosine kinase cell surface receptors that play key roles in cell signalling, growth, and differentiation. However, HER2 and HER4 are commonly overexpressed in breast cancer contributing to breast cancer aggressiveness.

Translational mechanisms such as internal ribosome entry sites (IRESs) and upstream opening reading frames (uORFs) can mediate translation of specific mRNA under cell stress conditions when global translation is inhibited. Cancer cells can be exposed to many cell stress conditions such as hypoxia and nutrient starvation, and such translational control mechanisms can contribute to overexpression of mRNAs. *EGFR* mRNA contains an IRES in the 5' untranslated region (5' UTR) that maintains expression of a firefly luciferase reporter in response to stress conditions such as hypoxia. However, it is not known if the 5' UTRs of the other *HER* family members (*HER* 2-4) contain an IRES. Additionally, *HER2* mRNA contains a repressive uORF in the 5' UTR and a translational derepression element (TDE) in the 3' UTR. However, it has not been investigated whether *HER2* 5' UTR can mediate an increase in translation in response to glutamine or glucose starvation as seen for *ATF4* and *GCN4* mRNA.

To screen for IRES activity in *HER2* or *HER4* 5' UTRs, bicistronic luciferase constructs were created that contained the 5' UTR of *HER2* or *HER4* between two luciferase reporters. In contrast to *EGFR* 5' UTR, there was no evidence of IRES activity in the 5' UTRs of *HER2* and *HER4* in response to endoplasmic reticulum stress, oxidative stress, low serum conditions, a hypoxia mimic,

genotoxic stress, confluence stress, glutamine starvation and glucose starvation in MCF-7 breast cancer cells.

Additionally, monocistronic constructs were created that contained the 5' UTRs of *HER2* or *HER4* upstream to a single firefly luciferase reporter. In monocistronic constructs, *HER2* and *HER4* 5' UTRs did not increase translation in response to glutamine or glucose starvation in MCF-7 cells. Finally, in contrast to a previous publication, the TDE in *HER2* 3' UTR did not derepress translation under non-stressed conditions or additionally in response to glutamine or glucose starvation.

The work in this thesis investigated the translational control of important oncogenes in stress conditions that are biologically relevant to cancer. Despite not identifying any translational control mechanisms in *HER2* or *HER4* 5' UTRs, the work in this thesis provides a promising approach for characterising the translational control of other important oncogenes that could provide potential therapeutic targets for cancer therapy in the future.

Acknowledgments

Firstly, I would like to thank my supervisors, Keith Spriggs, Cornelia De Moor and Catherine Jopling for sharing their knowledge on the research area that has helped me throughout my time in the lab and writing my thesis.

I would like to thank all members of the Gene Regulation & RNA biology group, past or present who have helped me during my time in the lab and for being a very supportive lab community. I would like to give a special mention to AJ (Abdulmohsin J Alamoudi) for welcoming me into the lab, training me on my core lab experiments and for all his support and kindness. Thank you to Declan Grewcock and Maksim Ivanov for being helpful and kind in the lab.

I would like to thank the DTP team for all the support and encouragement during my PhD and the BBSRC for funding my PhD project.

I am very grateful to my parents, siblings, and friends for all their support and encouragement that has helped me throughout my PhD.

Table of Contents

Abstract ..... **i**
Acknowledgments ..... **iii**
Table of Contents ..... **iv**
List of Figures ..... **viii**
List of Tables ..... **xii**
List of Abbreviations ..... **xiii**
Chapter 1 - Introduction **1**
1. Summary **2**
1.1. Overview of mRNA co-transcriptional processes **2**
1.2. Cap-dependent Translation **3**
1.2.1. Translation Initiation **3**
1.2.2. Translation Elongation **7**
1.2.3. Translation Termination **8**
1.3. Translational Control of Global Protein Synthesis **9**
1.3.1. Regulation of Translation Initiation Factors **10**
1.3.1.1. eIF2α Phosphorylation **10**
1.3.1.2. Regulation of eIF4E **11**
1.3.2. Regulation of Translation Elongation and Termination Factors **12**
1.4. Translational Control: mRNA-specific mechanisms **13**
1.4.1. Internal Ribosome Entry Site-Mediated Translation **14**
1.4.1.1. Viral IRESs **15**
1.4.1.2. Classification of Viral IRESs **15**
1.4.1.3. Cellular IRESs **17**
1.4.1.4. IRES Trans-acting Factors (ITAFs) **19**
1.4.2. Upstream Open Reading Frames **20**
1.4.3. RNA Binding Proteins **25**
1.4.4. Iron Response Elements **25**
1.4.5. MicroRNAs **26**
1.5. Breast Cancer **27**
1.5.1. Molecular Subtypes **28**
1.5.2. Examples of stress-induced translational control in cancer **29**
1.6. Human Epidermal Growth Factor Receptors **31**

1.6.1. Structure.....31
1.6.2. Isoforms.....32
1.6.3. Mechanism of Action.....40
1.6.4. Main Signalling Pathways.....41
1.6.4.1. Mitogen-Activated Protein Kinase Pathway.....41
1.6.4.2. Phosphoinositide 3-Kinase Pathway.....41
1.6.5. Role in Breast Cancer.....42
1.6.6. Translational Regulation.....44
1.6.6.1. *EGFR* 5' UTR IRES.....44
1.6.6.2. *HER2* coding region IRES.....44
1.6.6.3. *HER2* uORF.....45
1.7. Breast Cancer Therapeutics.....46
1.7.1. Overview of current therapeutics.....46
1.7.2. HER2-positive Breast Cancers Therapies.....47
1.7.3. Emerging Therapeutics.....49
1.8. Aims and Objectives.....52
Chapter 2 - Materials and Methods.....53
2.1. Cell Culture.....54
2.1.1. Solutions and Reagents.....54
2.1.2. Cell lines and Maintenance.....54
2.1.3. Transient Transfection.....55
2.1.4. Cell Stress Treatments.....55
2.1.5. Dual-Luciferase Assay.....56
2.1.6. MTT Assay.....57
2.2. Molecular Biology Techniques.....58
2.2.1. Reagent and Solutions.....58
2.2.2. Overview of luciferase constructs used in this thesis.....58
2.2.3. Bicistronic reporters.....60
2.2.4. Polymerase Chain Reaction.....62
2.2.5. Creating 5' UTRs from synthetic oligonucleotides.....62
2.2.6. *HER2* 3' UTR g-block cloning.....66
2.2.7. Primer Sequences.....68
2.2.8. Agarose Gel Electrophoresis.....70
2.2.9. Purification of DNA from Agarose Gel.....70
2.2.10. Restriction Digest.....70

2.2.11. Ligation....73
2.2.12. Polymerase Chain Reaction Colony Screening....73
2.2.13. Protein Extraction....74
2.2.14. Bradford Protein Assay....74
2.2.15. Sodium Dodecyl Sulfate–Polyacrylamide (SDS-PAGE)....74
2.2.16. Western Blotting....76
2.2.16.1. Antibodies....76
2.2.17. RNA Extraction....77
2.2.18. Reverse Transcriptase reaction....77
2.2.19. Quantitative Polymerase Chain Reaction....78
2.3. Bacterial Techniques....80
2.3.1. Reagents and Solutions....80
2.3.2. Preparing competent *E.coli* cells....80
2.3.3. Transformation....81
2.3.4. Purification of Plasmid DNA from a Miniprep/Maxiprep Kit..81
2.4. Statistical Analysis....82
Chapter 3 - *HER2* and *HER4* 5' UTRs did not mediate IRES-dependent translation in response to cell stress....83
3.1. Introduction....84
3.2. Generating *HER2* and *HER4* 5' UTR bicistronic luciferase constructs....85
3.3. *HER2* and *HER4* 5' UTRs are unable to induce firefly luciferase expression under non-stressed conditions....91
3.4. The effect of endoplasmic reticulum stress on the translational control by *HER2* and *HER4* 5' UTRs....93
3.5. The effect of oxidative stress on the translational control by *HER2* and *HER4* 5' UTRs....99
3.6. The effect of hypoxic stress on the translational control by *HER2* and *HER4* 5' UTRs....103
3.7. The effect of low serum conditions on the translational control by *HER2* and *HER4* 5' UTRs....109
3.8. The effect of genotoxic stress on the translational control by *HER2* and *HER4* 5' UTRs....113
3.9. The effect of high cell densities on translational control by *HER2* and *HER4* 5' UTRs....118
3.10. Discussion....121

Chapter 4 - *HER2* and *HER4* 5' UTRs mediated inefficient translation in contrast to *EGFR* 5' UTR in response to glutamine starvation 128

4.1. Introduction 129

4.2. No evidence of IRES activity in *HER2* and *HER4* 5' UTRs in response to glutamine starvation 132

4.3. Investigating the effect of glutamine starvation on the endogenous HER2 protein and *HER2*/*HER4* mRNA expression levels 142

4.4. Creating 5' UTR monocistronic luciferase constructs 146

4.5. *HER2* 5' UTR and *HER4* 5' UTR are unable to increase translation in a monocistronic context in response to glutamine starvation 152

4.6. *HER2* 3' UTR is unable to derepress translation in destabilised firefly luciferase constructs under non-starvation or glutamine starvation 157

4.7. Discussion 167

Chapter 5 - Glucose starvation had no effect on translation mediated by *HER2* or *HER4* 5' UTRs in luciferase reporters 175

5.1. Introduction 176

5.2. *HER2* and *HER4* 5' UTRs do not promote cap-independent translation in response to glucose starvation 178

5.3. Investigating the endogenous HER2 protein and *HER2*/*HER4* mRNA levels in response to glucose starvation 185

5.4. *HER2* and *HER4* 5' UTRs are unable to increase translation in a monocistronic context in response to glucose starvation 189

5.5 Discussion 196

Chapter 6 - Discussion 203

6.1. Summary 204

6.2. Investigating potential IRESs in *HER2* and *HER4* 5' UTRs under various cell stress conditions 204

6.3. Measuring translation in monocistronic firefly luciferase constructs in response to glutamine or glucose starvation 212

6.4. Conclusion 221

References 222

Appendices 273

List of Figures

Figure 1.1. Cap-dependent Translation Initiation 5

Figure 1.2. IRES-mediated Translation 14

Figure 1.3. Translational Control via uORFs 23

Figure 1.4. Multiple Human *HER2/ERBB2* isoforms 34

Figure 1.5. HER2 isoforms produced by alternative splicing, alternative initiation of translation or proteolytic cleavage 35

Figure 1.6. Human *HER4/ERBB4* JM-a isoforms 39

Figure 2.1. The multiple cloning site sequence in the pRF bicistronic plasmid 60

Figure 2.2. Transcription of the pRF plasmid produces a bicistronic mRNA 61

Figure 2.3. *HER2* 5' UTR synthesis from three oligonucleotides 64

Figure 2.4. *HER2* 3' UTR sequence cloned into destabilised p15-*HER2* 5' UTR plasmid 67

Figure 2.5. Schematic showing the location of the qPCR primer on the exons 79

Figure 3.1. Bicistronic luciferase construct-pRF vector map 86

Figure 3.2. Schematic of bicistronic constructs used in this project 87

Figure 3.3. *HER2* and *HER4* 5' UTRs are unable to mediate cap-independent translation in contrast to *EGFR* IRES under non-stressed conditions 92

Figure 3.4. The *Renilla* luciferase expression in response to thapsigargin 95

Figure 3.5. Thapsigargin had no effect on translation mediated by *HER2* and *HER4* 5' UTRs but *EGFR* IRES activity was decreased 96

Figure 3.6. The effect of thapsigargin on the cell viability of MCF-7 cells 98

Figure 3.7. 250 µM of hydrogen peroxide treatment reduced the *Renilla* luciferase expression 101

Figure 3.8. No evidence for IRES activity in *HER2* and *HER4* 5' UTRs in response to 250 µM of hydrogen peroxide treatment 101

Figure 3.9. The effect of 250µM of hydrogen peroxide on the viability of MCF-7 cells 102
Figure 3.10. The *Renilla* luciferase expression in response to $CoCl_2$ treatment 106
Figure 3.11. The hypoxia mimic, $CoCl_2$ was unable to induce firefly expression of the bicistronic constructs 107
Figure 3.12. $CoCl_2$ treatment had no effect on the cell viability of MCF-7 cells 108
Figure 3.13. Overall, low serum conditions were unable to efficiently reduce cap-dependent translation 111
Figure 3.14. No evidence for IRES activity in *HER2* and *HER4* 5' UTRs in response to low serum conditions 112
Figure 3.15. Low **s**erum conditions had no effect on the cell viability of MCF-7 cells 112
Figure 3.16. The *Renilla* luciferase expression in response to UV-B radiation 115
Figure 3.17. The effect of UV radiation on the F/R expression mediated by *EGFR*, *HER2* and *HER4* 5' UTRs 116
Figure 3.18. UV-B radiation decreased the cell viability of MCF-7 cells 117
Figure 3.19. Increasing the seeding cell density increased the *Renilla* luciferase expression 120
Figure 3.20. Increasing the seeding cell density had no effect on the F/R expression mediated from *EGFR*, *HER2* and *HER4* 5' UTRs 120
Figure 4.1. Overall, short-term glutamine starvation had no effect on the *Renilla* expression 134
Figure 4.2. No evidence of IRES activity in *HER2* and *HER4* 5' UTRs in response to short-term glutamine starvation 135
Figure 4.3. The effect of 24 hours of glutamine starvation on the *Renilla* expression 137
Figure 4.4. No evidence of IRES activity in *HER2* and *HER4* 5' UTRs in contrast to *EGFR* IRES in response to 24 hours of glutamine starvation 137

Figure 4.5. Short-term glutamine starvation had no effect on the cell viability of MCF-7 cells 139
Figure 4.6. The effect of long term glutamine starvation on the cell viability of MCF-7 cells 139
Figure 4.7. Increase in phosphorylated eIF2α protein levels in response to 48 hours of non-starvation and glutamine starvation 141
Figure 4.8. Increase in HER2 protein levels in response to 48 hours of glutamine starvation 143
Figure 4.9. The effect of glutamine starvation on *HER2* and *HER4* mRNA levels 145
Figure 4.10. Monocistronic firefly construct-p15 vector map 147
Figure 4.11. Schematic of monocistronic constructs used in this project 148
Figure 4.12. The monocistronic *Renilla* expression co-transfected with each construct in response to glutamine starvation 155
Figure 4.13. *HER4* 5' UTR mediated a decrease in translation in response to 48 hours of glutamine starvation whilst *EGFR* 5' UTR increased translation in a monocistronic context 156
Figure 4.14. Schematic of destabilised monocistronic luciferase constructs used in this project 158
Figure 4.15. Schematic of destabilised p15-*HER2* 5' + 3' UTRs construct used in this project 161
Figure 4.16. Overall, glutamine starvation reduced the monocistronic *Renilla* expression when co-transfected with destabilised monocistronic constructs 163
Figure 4.17. *HER2* 3' UTR was unable to increase translation under non-starvation or glutamine starvation conditions 166
Figure 5.1. 30 minutes and 4 hours of glucose starvation decreased the cell viability of MCF-7 cells 178
Figure 5.2. The expression of phospho-eIF2α in response to glucose starvation 180
Figure 5.3. Overall, the *Renilla* expression was not reduced in response to glucose starvation 183

Figure 5.4. No evidence of IRES activity in *HER2* or *HER4* 5' UTRs in response to glucose starvation in contrast to *EGFR* 5' UTR 184

Figure 5.5. HER2 protein expression in response to non-starvation and glucose starvation 186

Figure 5.6. The effect of glucose starvation on the mRNA levels of *HER2* and *HER4* 188

Figure 5.7. The *Renilla* expression co-transfected with each construct was not affected by glucose starvation in a monocistronic context 191

Figure 5.8. *HER2* and *HER4* 5' UTRs mediated inefficient translation in response to glucose starvation 192

Figure 5.9. *HER2* 3' UTR was unable to derepress translation in non-starvation or glucose starvation conditions 195

List of Tables

Table. 2.1. Chemical Stress Inducers 56
Table 2.2. Constructs made for this project 59
Table 2.3. Oligonucleotides for synthesis of *HER2* 5' UTR 64
Table 2.4. Oligonucleotides for synthesis of *HER4* 5' UTR 66
Table 2.5. PCR primers 68
Table 2.6. qPCR primers 69
Table 2.7. Restriction enzymes and the conditions used in the study 72
Table 2.8. SDS-PAGE 5% Stacking gel components 75
Table 2.9. SDS-PAGE 10% Resolving gel components 75
Table 2.10. cDNA Synthesis Reaction settings 78

List of Abbreviations

4E-BP	eIF4E-Binding Protein
4ICD	HER4 Soluble Intracellular Domain
ABCE1	ATP Binding Cassette Subfamily E Member 1
AGO2	Argonaute2
AHA	Azidohomoalanine
AMPK	AMP-Activated Protein Kinase
APAF1	Apoptotic Peptidase Activating Factor 1
APS	Ammonium Persulfate
A-site	Aminoacyl site
ATF4	Activating Transmembrane Factor 4
ATP	Adenosine Triphosphate
BiP	Immunoglobulin Binding Protein
BIRC2	Baculoviral IAP Repeat Containing 2
BLAST	Basic Local Alignment Search Tool
bp	Base pair
BSA	Bovine Serum Albumin
CDKN1B	Cyclin Dependent Kinase Inhibitor 1B
cDNA	Complementary DNA
$CoCl_2$	Cobalt (II) Chloride Hexahydrate
CrPV	Cricket Paralysis Virus
CTFs	Carboxyl-terminal fragments
DMSO	Dimethyl Sulfoxide
DNA	Deoxyribonucleic Acid
dsRNA	Double-Stranded RNA
E.coli	Escherichia coli
EDTA	Ethylenediaminetetraacetic Acid
eEF2K	eEF2 Kinase
EGF	Epidermal Growth Factor
EGFR	Epidermal Growth Factor Receptor
eIFs	Eukaryotic Initiation Factors
EMCV	Encephalomyocarditis

ER	Endoplasmic Reticulum
ERK	Extracellular Signal Regulated Kinase
E-site	Exit site
ESR	Oestrogen Receptor
ETBs	Engineered toxin bodies
EV71	Enterovirus 71
FBS	Foetal Bovine Serum
FGF	Fibroblast Growth Factors
FMDV	Foot and Mouth Disease Virus
GAPDH	Glyceraldehyde 3-phosphate Dehydrogenase
GCN2/4	General Control Nonderepressible 2/4
GDP	Guanosine Diphosphate
GSPT1	G1 To S Phase Transition 1
GTP	Guanosine-5'-Triphosphate
HER	Human Epidermal Growth Factor Receptor
HIF-1/2α	Hypoxia-Inducible Factor 1/2-Alpha
HRI	Heme-Regulated Inhibitor
HRV	Human Rhinovirus
IGF-IR	Insulin-Like Growth Factor 1 Receptor
IREs	Iron Response Elements
IRES	Internal Ribosome Entry Site
ITAFs	IRES Trans-Acting Factors
KH	K-Homology Domain
LB	Luria-Bertani
NFE2	Nuclear Factor Erythroid 2
nt	Nucleotide
MAPK	Mitogen-Activated Protein Kinase
m^7G	7-Methylguanosine
miRNAs	MicroRNAs
MKNK	MAPK Interacting Serine/Threonine Kinase
M-MLV	Moloney Murine Leukemia Virus
mRNA	Messenger RNA
mTOR	Mammalian Target of Rapamycin

MTT	3-(4,5-Dimethylthiazol-2-yl)-2,5-Diphenyltetrazolium bromide
ODD	Oxygen-dependent degradation
ORF	Open Reading Frame
PABP	Poly(A)-Binding Protein
PBS	Phosphate Buffered Saline
PCR	Polymerase Chain Reaction
qPCR	Quantitative Polymerase Chain Reaction
PEI	Polyethylenimine
PERK	PKR-like ER kinase
PI3K	Phosphoinositide 3-kinase
PKR	Protein Kinase R
P-site	Peptidyl site
PR	Progesterone Receptors
PTB	Polypyrimidine Tract-Binding Protein
PV	Poliovirus
RBDs	RNA Binding Domains
RBPs	RNA Binding Proteins
RISC	RNA-Induced Silencing Complex
RNA	Ribonucleic Acid
RNAase	Ribonuclease
ROS	Reactive Oxygen Species
RRM	RNA Recognition Motif
RT	Reverse Transcription
SDF-1	Stromal Cell-Derived Factor 1
SDS	Sodium Dodecyl Sulfate
SECIS	Selenocysteine Insertion Sequence
SHMT1	Serine Hydroxymethyltransferase1
SREBP-1	Sterol Regulatory Element Binding Protein 1
STAT5	Signal Transducer and Activator of Transcription 5
TACE	Tumour Necrosis Factor-α Converting Enzyme
TβR-I	Type I TGF-β Receptor
TCA	Tricarboxylic Acid Cycle
TCP80	Translational Control 80

TDE	Translational Derepression Element
TDG	Thymine DNA Glycosylase
TEAD	Transcriptional Enhanced Associate Domains
TEMED	Tetramethylethylenediamine
TG	Thapsigargin
TMEV	Theiler's Murine Encephalomyelitis Virus
TNBC	Triple-Negative Breast Cancer
TP53	Tumour Protein 53
tRNA	Transfer Ribonucleic Acid
tRNAi ^{Met}	Initiator Methionyl tRNA
uORFs	Upstream Open Reading Frames
UPR	Unfolded Protein Response
UTR	Untranslated Region
UV	Ultraviolet
VEGF	Vascular Endothelial Growth Factor
VHL	von Hippel-Lindau
XIAP	X-linked Inhibitor of Apoptosis Protein
YAP	Yes-Associated Protein

Chapter 1 - Introduction

1. Summary

The control of gene expression during translation is important for regulating the levels of protein synthesised from messenger RNA (mRNA) within a cell. Proteins are required for many crucial cellular processes such as cell growth, differentiation, homeostasis and responding to environmental stress. Translational regulation allows such processes to be tightly controlled (Krichevsky *et al.,* 1999; Picard *et al.,* 2013). Translational control is important to cancer cells as it allows cells to respond and adapt to stress conditions such as hypoxia and oxidative stress. This is achieved by the downregulation of global protein synthesis to reduce the energy burden on cells and the upregulation of specific mRNAs that can support cancer progression (Lang *et al.*, 2002; Van Den Beucken *et al.*, 2011; Xiao *et al.*, 2022).

1.1. Overview of mRNA co-transcriptional processes

In eukaryotes, the mRNA transcript is initially transcribed from DNA into a pre-mRNA transcript by RNA polymerase II during transcription in the nucleus (Fishburn *et al.,* 2015). Co-transcriptionally, the pre-mRNA undergoes processing to produce a mature mRNA transcript. This involves the addition of the 7-methylguanosine (m^7G) cap at the 5' untranslated region (UTR), splicing out of introns, cleavage at the 3' UTR (except histone mRNAs) and the addition of the poly(A)tail at the 3' UTR (Ahuja *et al.*, 2001; Moteki and Price, 2002; Brugiolo *et al.*, 2013). The m^7G cap is a binding site for eukaryotic initiation factors during translation initiation (Marcotrigiano and Gingras, 1997). The addition of the poly(A)tail at the 3' UTR protects the mRNA from exonuclease degradation and increases mRNA stability (Ford *et al.*, 1997). Alternative splicing events can occur and can involve certain exons being excluded or

certain introns being unspliced. This produces alternative isoforms of a single mRNA which can encode proteins with different functions (Grau-Bové *et al.*, 2018).

1.2. Cap-dependent Translation

The mature mRNA transcript is exported out of the nucleus and into the cytoplasm where translation takes place (Ashkenazy-Titelman *et al.*, 2022). Translation is an important process as proteins produced from mRNA transcripts are essential for various cellular processes such as growth, metabolism, homeostasis, and structure. Many vital cellular molecules are proteins including enzymes, receptors, and transporters (Liebermeister *et al.*, 2014).

There are three main stages of translation: initiation, elongation, and termination. Initiation involves the joining of the 40S and 60S ribosomal subunits onto the mRNA initiation codon with the aid of eukaryotic initiation factors (Lee *et al.*, 2002; Fringer *et al.*, 2007). Elongation involves the delivery of amino acids by tRNA to the ribosome. The amino acids are linked together producing a growing polypeptide chain (Flis *et al.*, 2018). Termination involves the release of the newly formed polypeptide from tRNA and the dissociation of the ribosomal subunits from the mRNA transcript (Trobro and Åqvist, 2007; Barthelme *et al.*, 2011).

1.2.1. Translation Initiation

Cap-dependent translation is the most common mode of translation initiation and involves the binding of eukaryotic initiation factors known as the eIF4F complex (eIF4E, eIF4G, eIF4A) to 5’ end of mRNA (Preiss and Hentze, 2003). eIF4G is a scaffold protein that has two isoforms, eIF4GI and eIF4GII where the

latter isoform is less abundant (Imataka *et al.*, 1998; Coldwell and Morley, 2006). eIF4G can bind eIF4E at the eIF4G amino-terminal domain, eIF4A at the middle and carboxyl domains and PABP at the N-terminus (Imataka *et al.*, 1997 and 1998). eIF4E is known as the cap-binding protein and binds to the m^7G cap at the 5' end of mRNA (Marcotrigiano and Gingras, 1997). The RNA helicase eIF4A has three isoforms, eIF4A1, eIF4A2 and eIF4A3. eIF4A1 and eIF4A2 have roles in translation initiation but eIF4A1 is the more dominant isoform whereas eIF4A3 has a role in RNA processing (Galicia-Vázquez *et al.*, 2015; Mazloomian *et al.*, 2019). In translation initiation eIF4A removes secondary structures on the mRNA transcript (Rozen *et al.*, 1990). PABP interacts with the poly(A)tail at the 3' end of mRNA which causes circularisation of the mRNA transcript (Kahvejian *et al.*, 2005; Gu *et al.*, 2022).

Initiation factors, eIF1, eIF1A and eIF3 bind to the 40S ribosomal subunit. eIF2B converts GDP to GTP allowing GTP to bind to eIF2 (Adomavicius *et al.*, 2019). eIF2-GTP moves $tRNAi^{Met}$ to the peptidyl site (P-site) of the 40S ribosomal subunit to form the 43S preinitiation complex which also binds eIF5B (Passmore *et al.*, 2007; Sokabe and Fraser, 2014). The 43S preinitiation complex then binds to the m^7G cap at the 5' end of mRNA which then scans the mRNA until the AUG codon is recognised (Lind and Åqvist, 2016). The anticodon on $tRNAi^{Met}$ base pairs with the AUG initiation codon which triggers the hydrolysis of GTP and the release of the initiation factors bound to the 40S ribosomal subunit. eIF5B is required for the hydrolysis of GTP which then leads to the 60S subunit being recruited to the 40S subunit to form the 80S ribosome (Figure 1.1) (Lee *et al.*, 2002; Fringer *et al.*, 2007).

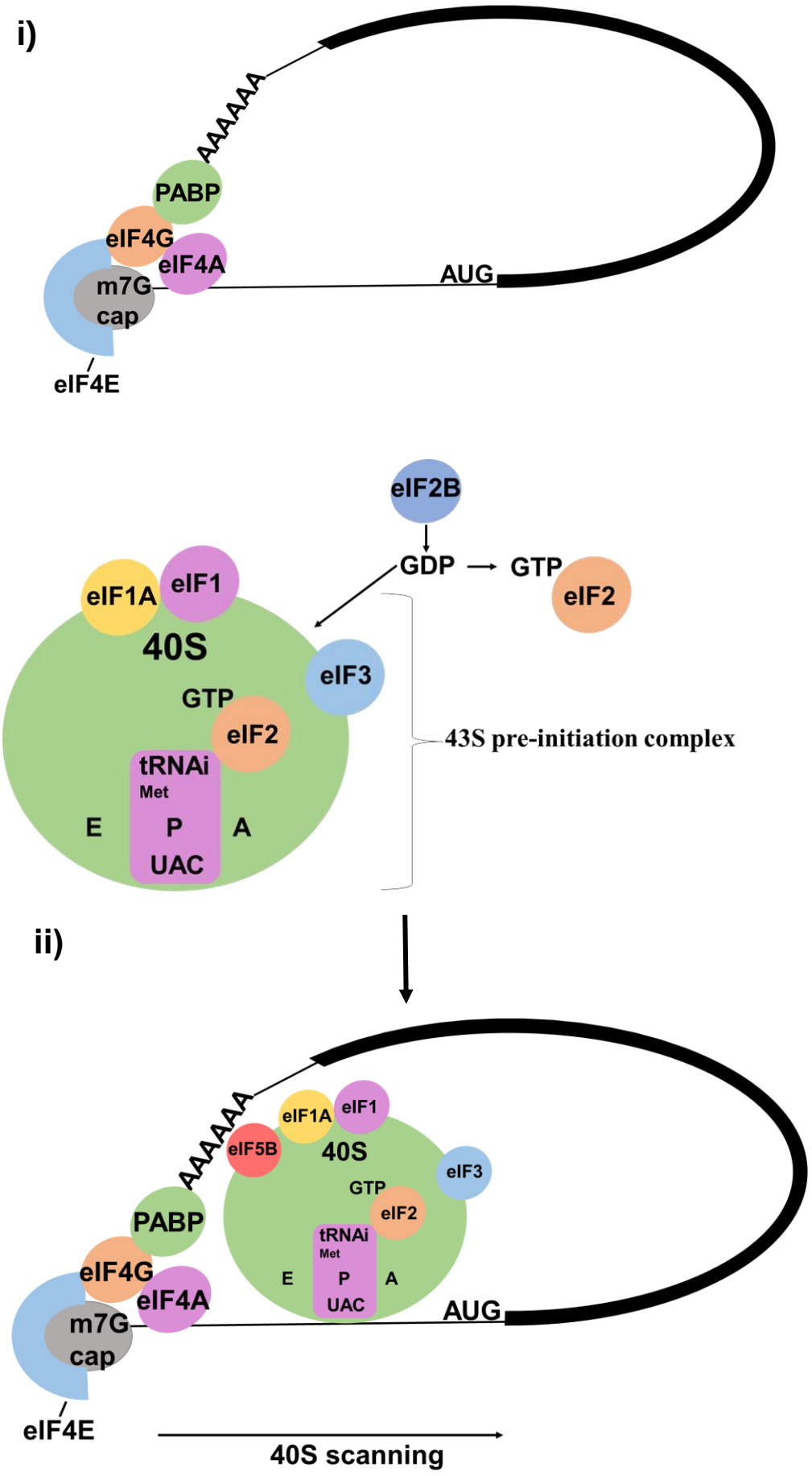
i)
AAAAAA
PABP
eIF4G
eIF4A
m7G
cap
eIF4E
AUG
eIF2B
GDP
GTP
eIF2
eIF1A
eIF1
40S
eIF3
GTP
eIF2
tRNAi
Met
E
P
A
UAC
43S pre-initiation complex
ii)
AAAAAA
eIF1A
eIF1
eIF5B
40S
eIF3
GTP
eIF2
PABP
tRNAi
Met
eIF4G
eIF4A
E
P
A
UAC
m7G
cap
AUG
eIF4E
40S scanning

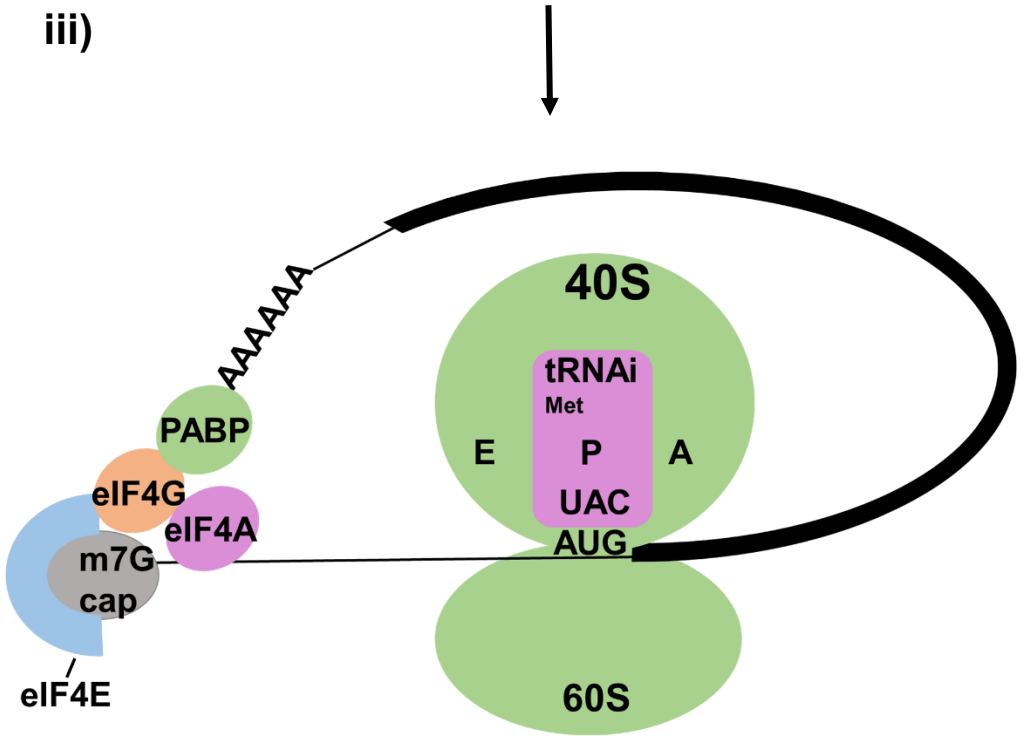

Figure 1.1. Cap-dependent Translation Initiation. i) The binding of the eIF4F complex at the m^7G cap, mRNA circularisation by PABP and formation of the 43S preinitiation complex. ii) Recruitment of $tRNAi^{Met}$ to the P-site of the 40S ribosomal subunit by eIF2-GTP and 40S ribosomal scanning on mRNA. iii) AUG recognition, base-pairing of AUG with the tRNA anti-codon and release of initiation factors from the 40S ribosomal subunit (Image created by the author of this thesis).

1.2.2. Translation Elongation

Eukaryotic translation elongation factors eEF1A and eEF2 are GTP binding proteins with important roles in translation elongation. eEF1B is an GTP exchange factor that provides GTP for the elongation process (Gromadski *et al.*, 2007). eEF1A and eEF1B are the two subunits that form the eEF1 complex. eEF1A is further classified into two isoforms which differ in expression levels in cells, eEF1A1 is widely expressed across cells whereas eEF1A2 is expressed mainly in specific cells such as muscle cells (Chambers *et al.*, 1998; Doig *et al.*, 2013).

Translation elongation starts with the elongation factor, eEF1A-GTP binding to an aminoacylated tRNA and recruiting it to the aminoacyl (A-site) of the ribosome. The anticodon on the aminoacylated tRNA base pairs with the codon on the mRNA at the A-site which triggers the release of a phosphate from GTP which releases eEF1A (Andersen *et al.*, 2001; Dever and Green, 2012). The methionine joined to the tRNA in the P-site is transferred to the aminoacylated tRNA at the A-site and a peptide bond is formed between the methionine in the P-site and the amino acid in the A-site. Next, eEF2-GTP stimulates the translocation of the deacylated tRNA from the P-site into the exit site (E-site) whilst the tRNA joined to the amino acids moves to the P-site. This results in the ribosome moving one codon forward which allows a new aminoacylated tRNA to base pair with the mRNA codon in the A-site of the ribosome. The elongation process continues resulting in a growing amino acid chain (Dever *et al.*, 2018; Flis *et al.*, 2018; Djumagulov *et al.*, 2021).

1.2.3. Translation Termination

Translation termination starts when the A-site of the ribosome encounters one of the three stop codons (UAA, UAG or UGA) on mRNA (Inagaki and Doolittle, 2000). Translation termination is carried out by two main eukaryotic termination factors eRF1 and eRF3. eRF1 contains a carboxyl terminal, a middle domain, and an amino-terminal domain. eRF3-GTP binds to the carboxyl terminal domain of eRF1 and then the amino-terminal domain of eRF1 recognises one of the three stop codon (Taylor *et al.*, 2012). Then GTP is hydrolysed which moves the middle domain of eRF1 into the P-site of the ribosome which allows it to be in close proximity to the tRNA attached to the polypeptide chain in the P-site (Salas-Marco and Bedwell, 2004). The middle domain of eRF1 contains a GGQ motif that promotes nucleophilic attack of the ester bond of the tRNA in the P-site leading to the release of the polypeptide chain. This releases eRF3 from the carboxyl domain of eRF1. (Trobro and Åqvist, 2007).

ABCE1 known as the ATP binding cassette protein is in a 'open' conformation and binds to the carboxyl domain of eRF1 at the 40S and 60S ribosomal junction. Upon ATP binding, ABCE1 then enters a 'close' conformation and releases phosphates from two ATP molecules. The energy released from the ATP molecules causes the dissociation of the 40S and 60S ribosomal subunits and release of eRF1 and ABCE1 (Barthelme *et al.*, 2011; Preis *et al.*, 2014). eIF1 and eIF1A remove tRNA from the P-site of the 40S ribosomal subunit whilst eIF3 releases mRNA from the 40S ribosomal subunit (Pisarev *et al.*, 2007; Pisarev *et al.*, 2010). Alternatively, eIF2D can trigger the release of tRNA in the P-site and the mRNA from the 40S ribosomal subunit. The splitting of the ribosomal subunits by ABCE1 allows them to be recycled for a new round of

translation (Young *et al.*, 2018). Some 40S ribosomal subunits may not be fully recycled and instead remain associated with mRNA. These remaining 40S ribosomal subunits are able to reinitiate translation once a new eIF2-GTP-tRNAi ^{Met} binds to the 40S ribosomal subunit (Bohlen *et al.*, 2019).

Termination efficacy can be reduced by mechanisms such as stop codon readthrough. This involves translating ribosomes not recognising the stop codon and instead continuing translation which can result in the production of extended protein isoforms. The nucleotide sequence surrounding the stop codon and in particularly the nucleotide immediately after the stop codon (the 4th base) can influence the termination efficiency (Mccaughan *et al.*, 1995). Termination signals with a purine as the 4th base have a stronger termination efficiency and are more frequently occur as a termination signal than pyrimidines bases which are more likely to result in stop codon readthrough (Mccaughan *et al.*, 1995).

Additionally, the amino acid selenocysteine is encoded by the stop codon UGA. mRNAs containing a selenocysteine insertion sequence (SECIS) will encode for selenocysteine when the UGA is encountered whereas most mRNAs without the SECIS recognise the UGA as a stop codon and terminate translation (Korotkov *et al.*, 2002).

1.3. Translational Control of Global Protein Synthesis

Translation is an energy demanding process that is tightly regulated. The downregulation of global protein synthesis in response to environmental stress stimuli reduces the energy demand of the cell and helps the cell recover from the stress stimuli. Most translational control of global protein synthesis occurs at the initiation phase by the phosphorylation of eukaryotic initiation factors.

However, some control of general translation rates can occur during translation elongation and termination (Buttgereit and Brand, 1995; Segev and Gerst, 2018).

1.3.1. Regulation of Translation Initiation Factors

1.3.1.1. eIF2α Phosphorylation

The phosphorylation of eIF2α is a key regulator of translation initiation. eIF2α is phosphorylated at serine 51 in response to cellular stress. This reduces the formation of the ternary complex and thus prevents the formation and recruitment of the 43S preinitiation complex to the mRNA 5' UTR (Zhou *et al.*, 2008). There are four main kinases, protein kinase R (PKR), PKR-like ER kinase (PERK), general control nonderepressible 2 (GCN2) and heme-regulated inhibitor (HRI) that are activated by known stress signals. The activation of these kinases leads to eIF2α phosphorylation and inhibition of global translation which is important so that cells can conserve energy for essential survival pathways (Taniuchi *et al.*, 2016).

GCN2 is activated in response UV radiation, oxidative stress, viral infection and accumulation of uncharged tRNA in response to amino acid starvation (Dong *et al.*, 2000; Zhang *et al.*, 2002; Won *et al.*, 2012; Anda *et al.*, 2017). PERK is mainly activated in response to endoplasmic reticulum (ER) stress (Harding *et al.*, 2000a). HRI is activated in response to heme deprivation, osmotic stress and heat shock (Fagard and London, 1981; Lu *et al.*, 2001). PKR is mainly activated in response to double-stranded RNA (dsRNA) mainly in response to viral infections (Elde *et al.*, 2009).

When the α subunit of eIF2 is phosphorylated, eIF2α-(P)-GDP binds to the eIF2B guanine exchange factor. This inhibits the activity of eIF2B which

reduces the concentration of eIF2-GTP needed to form the ternary complex resulting in a reduction in general protein synthesis rates (Bogorad *et al.*, 2017).

1.3.1.2. Regulation of eIF4E

Serine/threonine kinases, Erk 1/2 and MAPK14 activate MKNK1a and MKNK2a in response to stress and mitogenic stimuli (Lee *et al.*, 1994; Graves *et al.*, 1996). MKNK1a and MKNK2a interact with eIF4G which then allows MKNK1a and MKNK2a to phosphorylate eIF4E at serine 209 (Pyronnet *et al.*, 1999; Ueda *et al.*, 2004; Shveygert *et al.*, 2010). The phosphorylation of eIF4E decreases it binding to the m^7G cap, but this is thought to take place after the formation of the eIF4F. Thus phosphorylation of eIF4E allows the release of the components of the eIF4F complex allowing these factors to be available to carry out translation initiation (Scheper *et al.*, 2002). eIF4E phosphorylation can increase cancer cell progression by enhancing the translation of cancer associated genes such as *MYC*, the apoptosis inhibitor *BIRC2* and vascular endothelial growth factor C (*VEGFC*) (Furic *et al.*, 2010; Ruan *et al.*, 2020). Additionally, eIF4E phosphorylation can increase cancer cell survival in response to various stress conditions such as oxidative stress, glutamine starvation and glucose starvation (Martínez *et al.*, 2015).

The mammalian target of rapamycin (mTOR) activity is regulated by growth factor and nutrient availability and is important for regulating translation which can affect cell proliferation (Sancak *et al.*, 2008; Hsu *et al.*, 2011). The activity of the translation inhibitor 4E-BP is regulated by mTOR. 4E-BP can bind to eIF4E blocking the recruitment of eIF4G to eIF4E (Pause *et al.*, 1994; Poulin *et al.*, 1998). Under non-stressed conditions, 4E-BP is phosphorylated by the mTOR which reduces the binding of 4E-BP to eIF4E which allows translation

initiation (Gingras *et al.*, 1999). Under stress conditions such as viral infections, 4E-BP phosphorylation is reduced which increases the binding of 4E-BP to eIF4E therefore decreasing cap-dependent translation (Haghighat *et al.*, 1995; Patel *et al.*, 2002; Salaün *et al.*, 2003; Mazor *et al.*, 2018).

1.3.2. Regulation of Translation Elongation and Termination Factors

Translation elongation can be controlled by the phosphorylation of elongation factors which can increase or reduce overall translation rates. Type I TGF-β receptor (TβR-I) can phosphorylate eEF1A at serine 3000 which prevents the binding of eEF1A to the aminoacylated tRNA. This prevents translation elongation and cell proliferation (Lin *et al.*, 2010). Alternatively, the phosphorylation of eEF1 by multipotential S6 kinase splits eEF1 into its respective subunits (eEF1A and eEF1B) which are then able to carry out their roles in translation elongation (Chang and Traugh, 1998).

eEF2 can be phosphorylated at threonine 56 by eEF2 kinase (eEF2K) which inhibits eEF2 translocase activity (Ovchinnikov *et al.*, 1990). Additionally, phosphorylation of eEF2 by cyclin A-cyclin-dependent kinase 2 at serine 595 enhances eEF2K activity (Hizli *et al.*, 2013). eEF2K can be regulated by nutrient, growth factor and mitogenic status and is activated in response to stress stimuli or starvation conditions by AMP-activated protein kinase (AMPK) (Redpath *et al.*, 1996; Leprivier *et al.*, 2013; Sanchez *et al.*, 2019).

The expression levels of the termination release factor eRF1 has been shown to be controlled by an autoregulatory feedback loop in yeast and plants. The mechanism involves stop codon readthrough which is regulated by near cognate or suppressor tRNAs. For instance, high expression of eRF1 reduces stop codon

readthrough of eRF1 mRNA and triggers non-sense mediated decay that results in a lower expression of eRF1. In response to low levels of eRF1 stop codon readthrough can occur. This prevents non-sense mediated decay which allows translation of eRF1 mRNA (Stansfield *et al.*, 1996; Betney *et al.*, 2012; Nyikó *et al.*, 2017).

1.4. Translational Control: mRNA-specific mechanisms

The regulation of specific mRNAs is important for various biological processes such as early embryotic development, cell differentiation that allows cells to be specialised for a particular function and for local translation in neurons that is important for synaptic function (Seli, 2009; Donlin-Asp *et al.*, 2021; Martin *et al.*, 2022). In addition to regulating global translation rates, cell stress can upregulate the translation of specific mRNAs that are needed for cells to rapidly respond and survive in response to stress stimuli (Xiao *et al.*, 2022).

The mature mRNA contains a coding sequence flanked by a 5' and 3' UTR containing the respective m^7G cap and poly(A)tail. The translation of specific mRNAs can be regulated by motifs or proteins in the 5' or 3' UTRs such as internal ribosome entry sites (IRESs), RNA-binding proteins (RBPs) and upstream open reading frames (uORFs) (Huez *et al.*, 1998; Cava *et al.*, 2022; Nelde *et al.*, 2022). These motifs can affect translation and mRNA stability and are often found in genes involved in diseases such as cancer (Guan *et al.*, 2014).

The average length of a 5' UTR is 100-200 nts and it is thought that longer 5' UTRs have reduced translation efficiency (Chappell *et al.*, 2006; Paek *et al.*, 2015; Karollus *et al.*, 2021). The 3' UTR length can vary from hundreds to thousands of nts with an average length of ~1000 nts (Hendrickson *et al.*, 2009;

Kotagama *et al.*, 2015). In addition, different isoforms of a gene produced by alternative splicing or alternative polyadenylation can produce mRNA with different 5' UTR or 3' UTR lengths. Alternative isoforms can be regulated differently which can have an effect on translation and mRNA stability which can impact the function of a protein (Wang *et al.*, 2008; Resch *et al.*, 2009; Zheng *et al.*, 2018).

1.4.1. Internal Ribosome Entry Site-Mediated Translation

IRESs are cis-acting RNA elements present in the 5' UTR of certain viral or cellular mRNA transcripts. IRESs internally recruit the 40S ribosomal subunit onto the mRNA transcript which can bypass the m^7G cap structure under stress conditions when global translation rates are reduced (Figure 1.2). IRESs are diverse in structure, sequence, and requirements for eukaryotic initiation factors and IRES trans-acting factors (ITAFs) (Chamond *et al.*, 2014). IRESs were first discovered in viral mRNA and are important for some viruses as they allow the translation of viral proteins in the host cell when global translation is inhibited (Jang *et al.*, 1988; Pelletier and Sonenberg, 1988). Later, IRESs were discovered in some cellular mRNAs and are essential for the synthesis of proteins required for the cell to respond to stress stimuli (Macejak and Sarnow, 1991).

Figure 1.2. IRES-mediated Translation. Direct recruitment of the 40S ribosomal subunit bypassing the m^7G cap structure of capped mRNAs under cell stress conditions with the aid of ITAFs (Image created by the author of this thesis).

1.4.1.1. Viral IRESs

IRESs were first discovered in the mRNAs of poliovirus (PV) and encephalomyocarditis (EMCV) which belong to the *picornavirus* family. Picornaviruses do not contain the m^7G cap structure but polioviruses do contain a VPg peptide bound to the 5' UTR of their mRNA (Jang *et al.,* 1988; Pelletier and Sonenberg, 1988). However, some viruses use the host cell capping machinery to cap their 5' UTRs such as *retroviridae* viruses (Wilusz, 2013).

Viruses also require the host cells translational machinery to produce viral proteins. Viruses often cleave eukaryotic initiation factors in the host cells such as components of the eIF4F complex, eIF4G and eIF4A. Therefore, leading to inhibition of protein synthesis in the host cell (Gingras *et al.*, 1996; Belsham *et al.,* 2000; Glaser and Skern, 2000; Zaborowska *et al.*, 2012). IRESs elements naturally allow translation of uncapped viral mRNAs but can also allow the translation of capped viral mRNAs during conditions when global protein synthesis of the host cell is inhibited such as during viral infections (Herbreteau *et al.*, 2005; Chamond *et al.*, 2014).

1.4.1.2. Classification of Viral IRESs

The majority of viral IRESs are categorised into four main classes based on differences in structure, recruitment of the 40S ribosomal subunit and requirements for eukaryotic initiation factors. Class I IRESs are mainly found in *picornavirus* such as PV, human rhinovirus (HRV) and enterovirus 71 (EV71) and have five major domains (II-VI) (Sweeney *et al.,* 2014). Class II IRESs are also found in *picornavirus* such as EMCV, foot-and-mouth disease virus (FMDV) and Theiler's murine encephalomyelitis virus (TMEV) (Yu *et al.,* 2011). Class II IRESs have five major domains designated H-L. Class I and II

IRESs contain a Yn-Xm-AUG motif, which consists of a pyrimidine-rich tract that is 8-10 nts (Yn) separated by a intergenic region of 18-20 nts (Xm) (De Breyne *et al.*, 2009; Yu *et al.*, 2011).

Class I and II IRESs require most eukaryotic initiation factors except for the cap-binding protein eIF4E. eIF4G binds to domain V for class I IRESs and between domains J-K for class II IRESs and stimulates eIF4A activity which restructures the IRES (De Breyne *et al.*, 2009; Yu *et al.*, 2011; Sweeney *et al.*, 2014). For class I IRESs the binding of eIF3 to eIF4G enhances IRES activity. The 40S ribosome is recruited upstream of the initiation codon and is required to scan downstream of the mRNA until the initiation codon is reached (De Breyne *et al.*, 2009; Sweeney *et al.*, 2014; Asnani *et al.*, 2016). Whereas for class II IRESs the 40S ribosome is directly recruited to the initiation codon (Yu *et al.*, 2011).

Class III IRESs include members of the *flaviviridae*, hepatitis C and swine fever virus but also some members of the *picornavirus* including porcine enterovirus 8 and porcine teschovirus type 1 (Chard *et al.*, 2006; Friis *et al.*, 2012). This class of IRESs require a smaller number of eukaryotic initiation factors, eIF2, eIF3 and eIF5 and contains three main domains (II, III and IV). Domain III contains stem-loop structures and a pseudoknot that binds eIF3 (Woo *et al.*, 2012). Additionally, domain III contains a triple C motif that complementary base pairs with the 18S ribosomal RNA on the 40S ribosomal subunit. Domain II then facilities direct recruitment of the 40S ribosome to the AUG codon which is situated in domain IV (Malygin *et al.*, 2013).

Class IV IRESs are members of the *dicistroviridae* family such as cricket paralysis virus (CrPV). This class of IRESs do not require eukaryotic initiation

factors to start translation but the IRES is contained within an intergenic region which directly recruits the 40S ribosomal subunit (Fernández *et al.*, 2014; Murray *et al.*, 2016). For example, the CrPV IRES is highly structured and contain three pseudoknots (I, II and III) as well as stem-loop structures. CrPV IRES undergoes translocation by eEF2 which situates pseudoknot I into the P-site of the 40S ribosomal subunit instead of tRNAi ^{Met}. Translation then takes place from the mRNA codon situated in the A-site of the 40S ribosomal subunit (Fernández *et al.*, 2014).

1.4.1.3. Cellular IRESs

After the discovery of viral IRESs, an IRES was then discovered in the cellular mRNA of the immunoglobulin heavy-chain binding protein (*BiP*) (Macejak and Sarnow, 1991). IRESs have been found in other cellular mRNAs that are needed for cell survival and cell growth and many of which are involved in cancer progression. IRESs have been found in the mRNA 5' UTR of stress response genes *(TP53* and *BiP*) (Macejak and Sarnow, 1991; Khan *et al.*, 2015), growth factors (*VEGF* and fibroblast growth factors (*FGF*)) (Miller *et al.*, 1998; Allera-Moreau *et al.*, 2007), growth factor receptors (insulin-like growth factor 1 receptor (*IGF-IR*), insulin receptor (*IR*) and epidermal growth factor receptor (*EGFR*)) (Giraud *et al.*, 2001; Spriggs *et al.*, 2009; Webb *et al.*, 2015) and genes involved in cell division (*MYC*) (Cécile Nanbru *et al.*, 1997).

IRESs are active in response to specific stress signals, for example, *VEGF* IRES is active in response to hypoxia and glutamine starvation (Abcouwer *et al.*, 2002; Bornes *et al.*, 2007), *TP53* IRES functions in response to glucose starvation and genotoxic stress (Khan *et al.*, 2015; Ji *et al.*, 2017), *FGF* IRES is active in response to oxidative stress, hypoxia and ER stress (Conte *et al.*, 2008; Argüelles

et al., 2014; Philippe *et al.*, 2016) and *MYC* IRES is active in response to hypoxia, genotoxic stress and ER stress (Subkhankulova *et al.*, 2001; Shi *et al.*, 2016).

The RNA structure and sequence of cellular IRES lacks conservation therefore the presence of cellular IRESs cannot be accurately predicted based on structure or sequence (Xia and Holcik, 2009). For example, *FGF-1* IRESs have distinct structure and sequences from the *FGF-2* IRES. *FGF-1* contains a PTB and Unr binding motif but *FGF-2* lacks these motifs but does contain a hnRNP A1 motif (Bonnal *et al.*, 2003; Conte *et al.*, 2009).

The structure of the well-established *MYC* IRES contains two highly structured domains. Domains one and two both contains internal loop structures but domain one also contains two pseudoknots. Ribosomes bind to a region downstream of the pseudoknots in domain one and scan along the mRNA until the initiation codon is reached (Cécile Nanbru *et al.*, 1997; Le Quesne *et al.*, 2001).

Bicistronic reporter constructs have been used to establish the presence of IRESs where translation of the downstream reporter gene can only take place if the inserted 5' UTR within the intercistronic region contains an IRES (Van Eden *et al.*, 2004).There have been doubts over the existence of cellular IRESs due to the possibility of expression of the downstream cistron occurring via alternative splicing or a cryptic promoter which would also produce a monocistronic mRNA (Kozak, 2001, 2005). After discovering a putative IRES based on the expression of the downstream cistron, the use of a promoterless vector is an important control which would rule out the possibility of a cryptic promoter. There should

be no expression from a promoterless vector if an actual IRES is present (Oltean and Banerjee, 2005; Shi *et al.*, 2005). RNA analysis using RT-qPCR can be conducted to rule out alternative splicing to demonstrate that an IRES is present in the bicistronic transcript (Van Eden *et al.*, 2004; Kang *et al.*, 2013). The inclusion of the controls mentioned has provided strong evidence for the presence of IRESs in cellular mRNAs such as *TP53*, *JUN*, *IR*, *FGF-2* and *MYC* (Nanbru *et al.*, 1997; Stoneley *et al.*, 1998; Créancier *et al.*, 2001; Ray *et al.*, 2006; Yang *et al.*, 2006; Audigier *et al.*, 2008; Spriggs *et al.*, 2009; Blau *et al.*, 2012).

1.4.1.4. IRES Trans-acting Factors (ITAFs)

ITAFs are RNA-proteins that can enhance IRES activity or in some cases inhibit IRES activity. Many ITAFs have additional functions in gene expression such as HuR and PSF, which are involved in mRNA stability and pre-mRNA splicing respectively. The function of an ITAF depends on the specific mRNA as well as the cell stress stimuli (Wang *et al.*, 2000; Peng *et al.*, 2006; Lin *et al.*, 2015; Dave *et al.*, 2017).

ITAFs can alter the IRES structure to facilitate or inhibit recruitment and binding of the 40S ribosomal subunit as well as stabilising the preinitiation complex (Shi *et al.*, 2016; Strand *et al.*, 2021). For instance, TCP80 and RNA helicase A are ITAFs that unwind the *TP53* IRES which increases *TP53* translation in response to genotoxic stress (Halaby *et al.*, 2015). Whereas, nucleolin can strengthen the secondary structures of the *TP53* IRES preventing translation of *TP53* mRNA (Takagi *et al.*, 2005). Additionally, the nuclear protein, BANP is an ITAF that binds to *TP53* and enhances its expression in response to glucose starvation (Khan *et al.*, 2015).

Eukaryotic initiation and elongation factors are important ITAFs for class I, II and III viral IRESs (Section 1.4.1.2.) as well as for some cellular IRESs. For example, IRESs of the *MYC* family *(MYCL, MYCN* and *MYC*) differ in their requirement for eukaryotic initiation factors however, they all commonly bind eIF4G and eIF3 (Spriggs *et al.*, 2009).

1.4.2. Upstream Open Reading Frames

Upstream open reading frames (uORFs) are short open reading frames present in the 5' UTR of some mRNAs that contain a stop and start codon upstream to the main ORF on mRNA. uORFs usually repress translation of the downstream coding region thus negatively regulate translation (Vattem and Wek, 2004; Sundaram and Grant, 2014). uORFs commonly modulate translation of genes involved in the cellular response to stress (Vattem and Wek, 2004; Gameiro and Struhl, 2018; McGillivray *et al.*, 2018; Moro *et al.*, 2021). Ribosome stalling can occur at some uORFs which blocks scanning ribosomes from reaching the downstream initiation codons and causes scanning ribosomes to dissociate (Gaba *et al.*, 2001; Bottorff *et al.*, 2022). The length of the uORF can influence ribosome reinitiation after translation of the uORF as longer uORFs have reduced reinitiation efficacy than shorter uORFs (Berkhout *et al.*, 2011).

Additionally, uORFs have been found within some cellular IRESs such as *VEGFA* and cationic amino acid transporter (*SLC7A1*) mRNA. *VEGFA* has two IRESs and a uORF located within the first IRES that negatively regulates translation of the *VEGFA-121* isoform (Bastide *et al.*, 2008; Arcondéguy *et al.*, 2013). Alternatively, *SLC7A1* contains an uORF located within its IRES that modulates the structure of the 5' UTR to enable IRES-mediated translation (Fernandez *et al.*, 2001, 2005; Yaman *et al.*, 2003).

A classic example of uORF mediated regulation is the translation of *GCN4* that encodes a transcription factor in the yeast species, *Saccharomyces cerevisiae* in response to amino acid starvation. There are four uORFs in *GCN4* 5' UTR. In non-stressed conditions ribosomes translate the first uORF on *GCN4* mRNA and then ribosomes reinitiate translation at the second to fourth uORFs on *GCN4* mRNA which inhibits translation at the downstream *GCN4* coding region. In particularly, the 10 nts downstream of the stop codon on *GCN4* uORF4 are important for the inhibitory effects on translation (Miller and Hinnebusch, 1989). In nutrient stress conditions such as glucose or glutamine starvation, there is a general decrease in global translation which results in the phosphorylation of eIF2α (Yang *et al.*, 2000; Mcfarland *et al.*, 2020). This decreases the availability of the ternary complex which results in ribosomes taking longer to acquire and bind to the ternary complex therefore are likely to scan pass the second-fourth uORFs on *GCN4* mRNA. This leads to ribosomes to reinitiate at the *GCN4* coding region leading to an increase in *GCN4* translation (Figure 1.3) (Sundaram and Grant, 2014; Anda *et al.*, 2017).

The regulation of human *ATF4* mRNA by uORFs is a well-known example of uORF regulation in mammalian cells in response to nutrient starvation. *ATF4* mRNA contains two uORFs which regulate the translation of the gene. The first uORF encodes a three amino acid polypeptide whereas the second uORF encodes a 59 amino acid polypeptide that overlap the first 83 nucleotides of the *ATF4* coding sequence. Reinitiation occurs at the second uORF of *ATF4* after translation of the first uORF under normal conditions. Similar to *GCN4, ATF4* translation is regulated by its uORFs in response to glucose or glutamine starvation (Siu *et al.*, 2002; Chen *et al.*, 2014; Han *et al.*, 2021b; Chen *et al.*,

2022). In glucose or glutamine starvation conditions, the reduction in the ternary complex results in ribosomes bypassing the second uORF and translating the *ATF4* coding region which increases translation of *ATF4* mRNA (Figure 1.3) (Vattem and Wek, 2004; Martín-Pérez *et al.*, 2014; Sundaram and Grant, 2014).

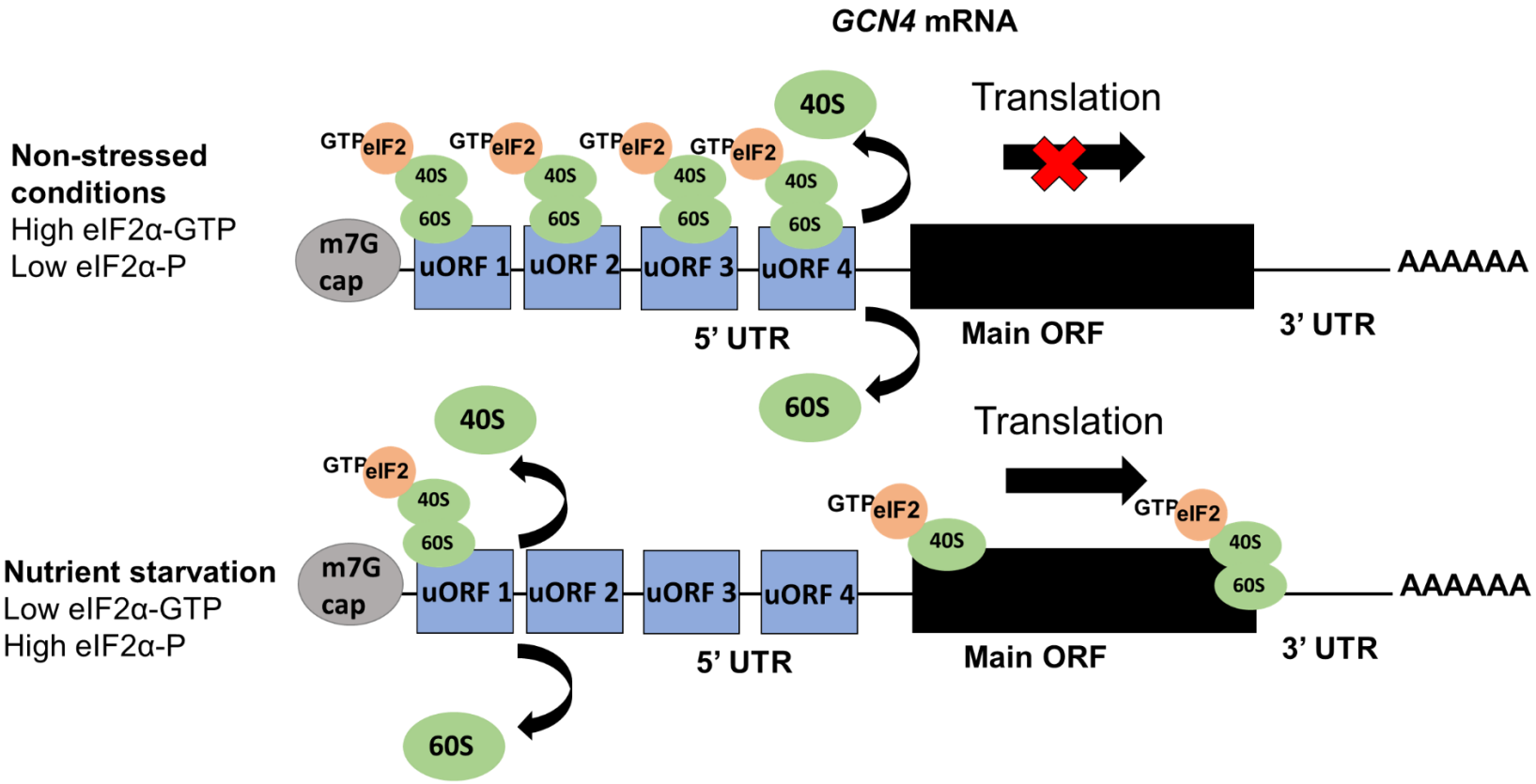
GCN4 mRNA
Non-stressed conditions
High eIF2α-GTP
Low eIF2α-P
Translation
40S
GTP eIF2
40S
60S
m7G cap
uORF 1
uORF 2
uORF 3
uORF 4
5' UTR
Main ORF
3' UTR
AAAAAA
60S
Nutrient starvation
Low eIF2α-GTP
High eIF2α-P

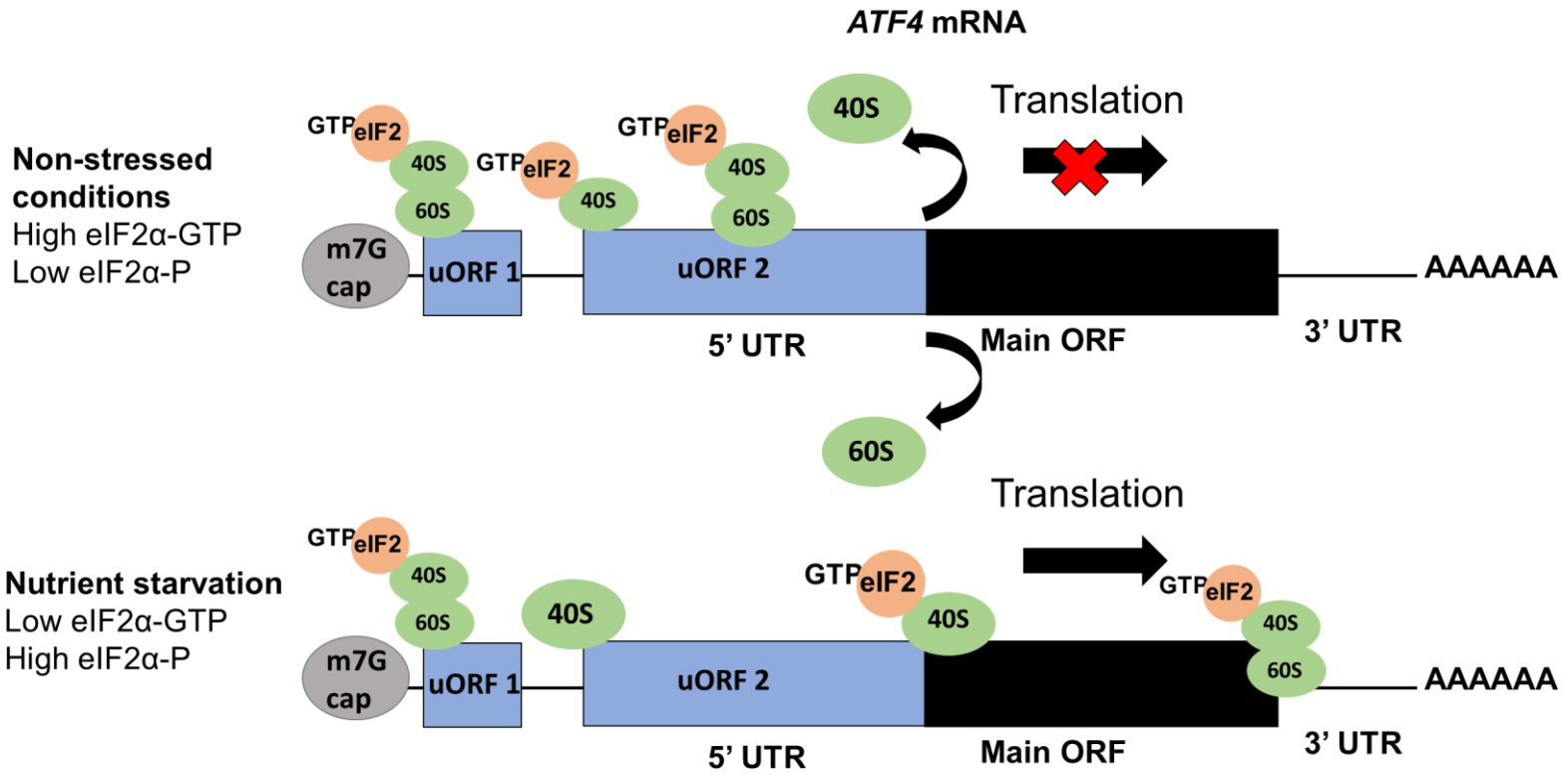

Figure 1.3. Translational control via uORFs. Translation of the main open reading frame (ORF) of *GCN4* and *ATF4* in response to nutrient starvation. Translation of *GCN4* and *ATF4* is repressed under non-stressed conditions when eIF2α-GTP is high and eIF2α phosphorylation is low (eIF2α-P). Under nutrient deprivation when eIF2α-GTP is low and eIF2α-P is high, the translation of *GCN4* and *ATF4* is increased (Image created by the author of this thesis).

1.4.3. RNA Binding Proteins

RBPs have various roles in gene expression including regulating translation and RNA stability. RBPs contain RNA binding domains (RBDs) which enables RBPs to recognise RNA sequences in the 5' or 3' UTR and sometime in the coding region of mRNAs. RNA recognition motif (RRM) is one of the most common RBD that contains approximately 90 amino acids (Nowacka *et al.*, 2019; Liu *et al.*, 2021a). Examples of other RBDs include, K-homology domain (KH) (Grishin, 2001), zinc finger domain (Krishna *et al.*, 2003), DEAD-helicase domain and the double-stranded RNA binding motif (Vukovic *et al.*, 2014; Talwar *et al.*, 2017).

RBPs that interact with IRESs in the 5' UTR of mRNA are called ITAFs. Some can increase or decrease translation depending on the specific mRNA and the cellular conditions. For example, the polypyrimidine tract-binding protein (PTB) contains four RRM domains and can remodel the RNA structure and can increase translation of mRNAs such as *TP53* and APAF1 or decrease translation of certain mRNA such as *BiP* (HSPA5) (Kim *et al.*, 2000; Mitchell *et al.*, 2003; Grover *et al.*, 2008).

1.4.4. Iron Response Elements

Iron-response elements (IREs) are ~30 bp RNA structures present in the 5' UTR or 3' UTR of mRNAs involved in iron metabolism for example IREs are found in the 5' UTR of ferritin and the 3' UTR of transferrin. IREs have a conserved stem-loop structure and are recognised by iron regulatory proteins (IRP), IRP1 and IRP2. The iron status of the cell is important for determining the translation of mRNAs containing a IRE in the 5' UTR (Philpott *et al.*, 1994; Addess *et al.*, 1997).

For example, in low iron conditions, IRP can bind to the IRE located in the 5' UTR of ferritin mRNA. This blocks the binding of the 43 preinitiation complex onto mRNA thereby reducing translation of ferritin which increases iron uptake in cells (Gray and Hentze, 1994). When iron levels are plentiful, iron binds to IREs which induces a conformational change in the mRNA which enhances the binding of eIF4F to the IRE leading to an increase in the translation of ferritin to store excess iron (Ma *et al.*, 2012; Garza *et al.*, 2020).

1.4.5. MicroRNAs

MicroRNAs (miRNAs) are small non-coding RNAs that most commonly interact with the 3' UTR of a gene to inhibit translation and reduce mRNA stability by inducing mRNA degradation (Iliopoulos *et al.*, 2009). Although some miRNAs can interact with the mRNA 5' UTR or coding regions (Kloosterman *et al.*, 2004; Ørom *et al.*, 2008).

The mature miRNAs are produced from primary miRNAs in the nucleus (Lee *et al.*, 2004). A common pathway for the biogenesis of miRNAs involves the recognition of primary miRNAs by a protein called DGCR8. The ribonuclease III enzyme, Drosha can then associate with DGCR8 and cleaves the primary miRNA at the RNA hairpin site producing a 2 nt 3' overhang on the primary miRNA (Han *et al.*, 2004; Zeng *et al.*, 2005). The precursor miRNA is then transported to the cytoplasm by exportin 5 where the miRNA is recognised by Dicer which cleaves the stem-loop of the miRNA into a shorter miRNA. Argonaute2 (AGO2) interacts with Dicer and unwinds the miRNA and one strand is released. The remaining guide strand of the miRNA and AGO2 form part of the RNA-induced silencing complex (RISC). The miRNA guides the

RISC to the target mRNA by partial complementary base-pairing (Yi *et al.*, 2003; Han *et al.*, 2004; Okamura *et al.*, 2004).

GW182 is a scaffold protein that is recruited to RISC and recruits other proteins such as PAN2-PAN3, CCR4-NOT and PABP (Braun *et al.*, 2011; Huntzinger *et al.*, 2013). In the context of translation, CNOT1 a component of CCR4-NOT can interact with eIF4A2 (Wilczynska *et al.*, 2019). eIF4A2 can bind to the 5' UTR of target mRNAs and induce inhibition of translation initiation. Additionally, a reduction in global translation can be carried out in a miRNA-mediated manner. For instance, CNOT1 can also bind to DDX6 which can associate with the 4E-transporter. The 4E-transporter can bind to eIF4E preventing the interaction of eIF4E and eIF4G that is required for translation initiation (Kamenska *et al.*, 2016).

1.5. Breast Cancer

Breast cancer is one of the most prevalent cancers and one of the world's leading causes of death in women (Wild *et al.*, 2020). Breast cancer arises from uncontrolled cell division of the epithelial cells in the breast tissue that form a malignant lump with the potential to metastasise to other areas of the body (Elenbaas *et al.*, 2001).

The hormone oestrogen can bind to oestrogen receptors (ESR1 and ESR2) in breast cells which dimerise and bind to oestrogen responsive elements in the DNA of oestrogen response genes. This can activate transcription factors and mediate cell growth signalling (Powell and Xu, 2008; Sanchez *et al.*, 2010). Oestrogen can activate cell growth signalling via the mitogen-activated protein kinase pathway (MAPK) and in addition this pathway can increase oestrogen

signalling. Dysregulation of oestrogen signalling, and increased oestrogen levels can contribute to breast cancer (Atanaskova *et al.*, 2002).

Women have a higher risk of developing breast cancer due to females having higher oestrogen levels than males (Al-Ajmi *et al.*, 2018). There are several risk factors for developing breast cancer including obesity due to adipose tissue releasing high amounts of oestrogen, high alcohol consumption as alcohol can increase oestrogen metabolism and germline mutations in the tumour suppressor genes, *BRCA -1* and *-2* (Savolainen-Peltonen *et al.*, 2014; Jung *et al.*, 2016; Wang *et al.*, 2018b; Laforest *et al.*, 2020). In addition, to obesity and high alcohol consumption, other environmental causes such as exposure to toxic chemicals, pollutants and ionising radiation can increase the risk of breast cancer (Wolff and Weston, 1997). Additionally, the risk of breast cancer can increase with age due to an increased potential to accumulate somatic mutations over time, however breast cancer is still detected in many women below the age of 40 for example due to germline mutations (Brinton *et al.*, 2008; Milholland *et al.*, 2015).

1.5.1. Molecular Subtypes

Breast cancer can be categorised into four main molecular subtypes, luminal A, luminal B, HER2-positive and triple-negative breast cancer (TNBC) (TNBC is also referred to as basal-like). Luminal A is the most common breast cancer subtype and is positive for ESRs and progesterone receptors (PR) and has low or negative expression of the growth factor receptor, HER2 (Poudel *et al.*, 2019). However, high oestrogen signalling can increase HER2 expression in MCF-7 breast cancer cells that is classified as luminal A (Lattrich *et al.*, 2008). Luminal B is also positive for ESRs, PRs and contains elevated HER2 levels. The luminal

B breast cancer cells have higher proliferation rates than luminal A breast cancer cells (Ahn *et al.*, 2015; Jääskeläinen *et al.*, 2020). TNBCs are negative for ESRs, PRs and HER2 (Perou, 2011). A high proportion of TNBCs are mutant for *TP53* caused by missense mutations. Additionally, TNBCs frequently contain high expression of receptor tyrosine kinases, EGFR, HER3 and KIT (Keam *et al.*, 2011; Darb-Esfahani *et al.*, 2016; Ogden *et al.*, 2020). TNBCs are very aggressive and have poor prognosis as they cannot be treated by hormone or HER2-targeted therapies (Perou, 2011). HER2-positive breast cancer accounts for 15-20% of breast cancer cases and is an aggressive form of breast cancer with a poor prognosis. HER2-positive breast cancers contain high levels of the HER2 protein and MYC (Guarneri *et al.*, 2010). MYC and other oncogenes are also commonly detected in the other breast cancer subtypes (Singhi *et al.*, 2012). In addition, the angiogenesis mediator, VEGF is highly expressed in luminal B, TNBCs and HER2-positive breast cancers (Liu *et al.*, 2011).

1.5.2. Examples of stress-induced translational control in cancer

Cancer cells are exposed to various stress conditions such as hypoxia, oxidative stress, nutrient starvation, and ER stress. As mentioned previously (Section 1.3.1.1.), eIF2α is phosphorylated in response to cell stress conditions causing a reduction in global translation (Taniuchi *et al.*, 2016). However, the translation of mRNAs containing IRESs or uORFs can trigger stress response pathways to allow cancer cells to adapt and survive in response to stress therefore such translational control mechanisms can support breast cancer cell progression (Braunstein *et al.*, 2007; Sundaram and Grant, 2014). However, depending on the severity of the stress and if the stress response is ineffective then apoptosis can be triggered (Cano-González *et al.*, 2018).

For example, ER stress is caused by the accumulation of misfolded and unfolded proteins which can be triggered by various stress conditions such as hypoxia, oxidative stress, glucose starvation and glutamine starvation. ER stress activates the unfolded response pathway (UPR) and PERK is one of the main proteins of the UPR. PERK phosphorylation of eIF2α causes a decrease in global protein synthesis which helps reduce the ER workload and the further accumulation of unfolded proteins (Shi *et al.*, 2016; Han and Wan, 2018). Additionally, PERK activates ATF4 whose translation is mediated by uORFs in the *ATF4* 5' UTR (Section 1.4.2.**)**. ATF4 coordinates the cells response to stress by upregulating genes involved in amino acid uptake and metabolism (Harding *et al.*, 2003; Torrence *et al.*, 2021). ATF4 can increase cell proliferation and migration in some HER2-positive breast cancers (Zeng *et al.*, 2019). However, ATF4 has also been shown to induce pro-apoptosis proteins TRAIL-R2 and capase-8 in some HER2-positive breast cancers (Martín-Pérez *et al.*, 2014).

HIF-1α 5' UTR contains an IRES that can allow it to be translated in hypoxic conditions when global translation is downregulated. HIF-1α dimerises with HIF-1β in the nucleus to form HIF-1. HIF-1 then binds to hypoxia responsive elements (HREs) and induces the transcription of hypoxia responsive genes (Ebert and Bunn, 1998). HIF-1 can upregulate many genes that promote cancer cell growth and progression. For example, HIF-1 can bind to the promoter of *VEGF* (Yoshiji *et al.*, 1997; Konecny *et al.*, 2004; Hu *et al.*, 2016a). Furthermore, *VEGF* 5' UTR contains two IRESs that also stimulate translation of *VEGF* mRNA during hypoxic conditions. VEGF helps provide cancer cells with new blood vessels to help supply nutrients and oxygen to cancer cells to aid their growth and survival (Liu *et al.*, 2011).

1.6. Human Epidermal Growth Factor Receptors

The human epidermal growth factor receptors (HERs), HER2 (EGFR2/ERBB2) and HER4 (EGR4/ERBB4) are tyrosine kinases cell surface receptors. They are members of the epidermal growth factor family which also includes EGFR (HER1/ERBB1) and HER3 (EGFR3/ERBB3). The HERs are responsible for healthy cell signalling, growth, and differentiation. They transduce extracellular signals to promote cell proliferation and survival via two main downstream signalling pathways which are the MAPK and the phosphoinositide 3-kinase (PI3K) pathways. Dysregulation of the HER receptors are commonly seen in many cancers including breast cancer (Zhou and Hung, 2003; Wolf-Yadlin *et al.*, 2006).

1.6.1. Structure

HERs contain an extracellular region, a transmembrane domain that spans the plasma membrane, an intracellular domain containing a juxtamembrane, tyrosine kinase domain and a carboxy-terminal region (Martin-Fernandez *et al.*, 2019). The extracellular domain contains four subdomains (I-IV). Domains I and III of the extracellular regions are ligand binding domains and domains II and IV are cysteine rich regions (Ogiso *et al.*, 2002). The juxtamembrane region contains receptor trafficking signals and a calmodulin binding site (Martín-Nieto and Villalobo, 1998; Choowongkomon *et al.*, 2005). The tyrosine kinase domain contains a N-terminal and C-terminal region that contain ATP binding sites (Lee *et al.*, 2006; Galdadas *et al.*, 2021). The C-terminal tail contains tyrosine kinase residues that are phosphorylated upon receptor activation (Kovacs *et al.*, 2015).

1.6.2. Isoforms

There are multiple mRNA transcript variants of *HER2* (*ERBB2*), Figure 1.4 shows the schematics of multiple human *HER2* transcripts that includes the 5' UTR, exon regions and 3' UTR. A number of HER2 isoforms have been described in the literature and are produced by alternative splicing, alternative initiation of translation or proteolytic cleavage. These include delta-16-HER2, HER2-p100, herstatin, HER2-pI9, HER2-pI12 and HER2 carboxyl-terminal fragments (CTFs) also referred to as p95-HER2 (Figure 1.5) (Pedersen *et al.*, 2009; Yang *et al.*, 2022) . Delta-16-HER2 is produced from the deletion of exon 16 in the extracellular domain. This results in unpaired cysteine residues that lead to increased strength of HER2 dimers (Volpi *et al.*, 2019). p100-HER2 results from inclusion of intron 15 that contains a premature termination codon resulting in a HER2 protein with only an extracellular domain. p100-HER2 interferes with dimer formation and is associated with inhibition of cancer cell growth (Aigner *et al.*, 2001). Herstatin is produced from the inclusion of intron 8 that contains a premature termination codon which generates a HER2 extracellular domain and a novel C-terminal region. Herstatin can bind to the extracellular domain of the full length HER2 via its C-terminal region and is associated with inhibition of cancer growth (Silipo *et al.*, 2017). HER2-pI9 contains partial inclusion of intron 9 and HER2-I12 retains the full intron 12. HER2-pI9 has low phosphorylation activity whilst HER2-I12 can activate downstream signalling (Hart *et al.*, 2021). HER2 CTFs are produced by alternative initiation of translation at methionine 611 or 687. (Yuan *et al.*, 2003; Anido *et al.*, 2006; Pedersen *et al.*, 2009). In addition, HER2 CTFs can be produced by proteolytic cleavage of the full length HER2 by alpha-secretase

producing CTFs that contain a transmembrane domain and nuclear localisation signal. Proteolytic cleavage of the full length HER2 by gamma-secretase can generate HER2 CTFs lacking the transmembrane domain but retaining the nuclear localisation signal (Godfrey *et al.*, 2022). HER2 CTFs that retain the transmembrane domain are active and can dimerise and induce downstream signalling (Parra-Palau *et al.*, 2010). They are also detected in 30 % of HER2-positive breast cancer cases (Sáez *et al.*, 2006).

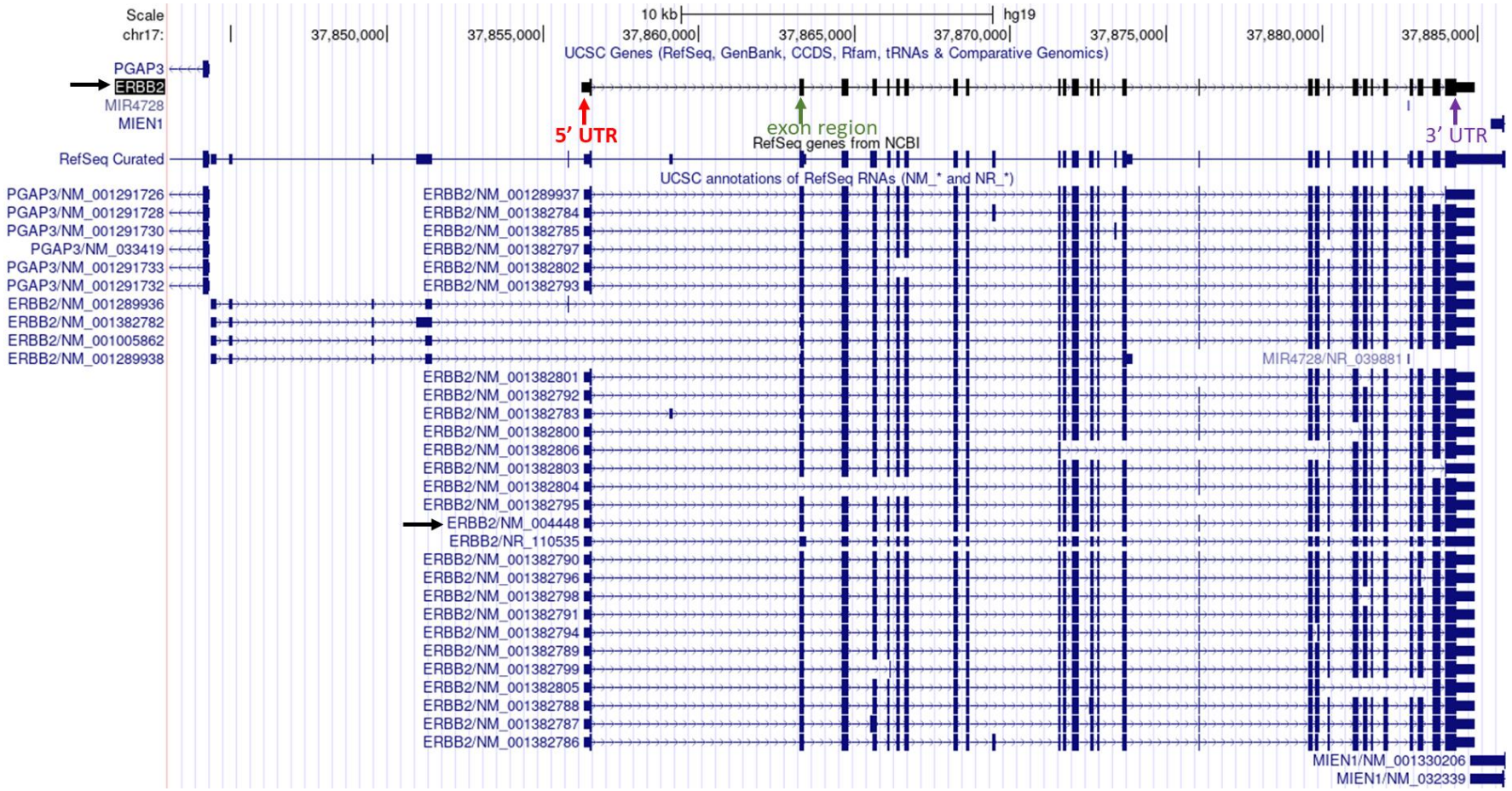

Figure 1.4. Multiple Human *HER2/ERBB2* isoforms. Schematics of 31 human *HER2/ERBB2* isoforms showing the 5' UTR, exons and 3' UTR on chromosome 17 from the UCSC genome browser. Black arrows: transcript variant 1 mRNA (*HER2/ERBB2* isoform used in this project). Red arrows: 5' UTR, green arrows: an exon region and purple arrow: 3' UTR. (Nassar *et al.*, 2023).

A) WT HER2

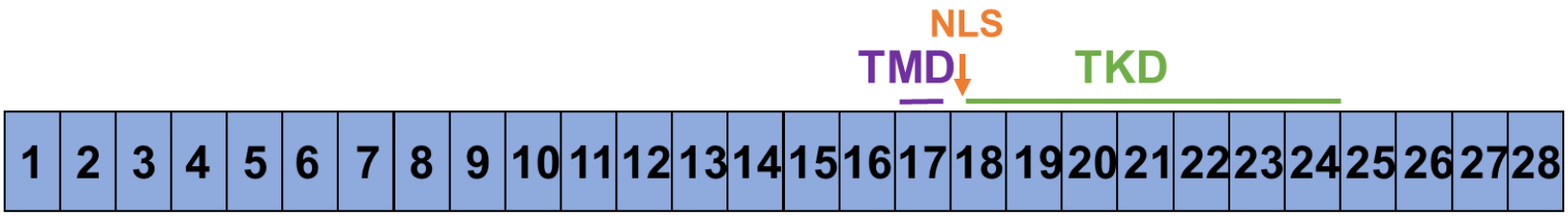

B) delta-16-HER2

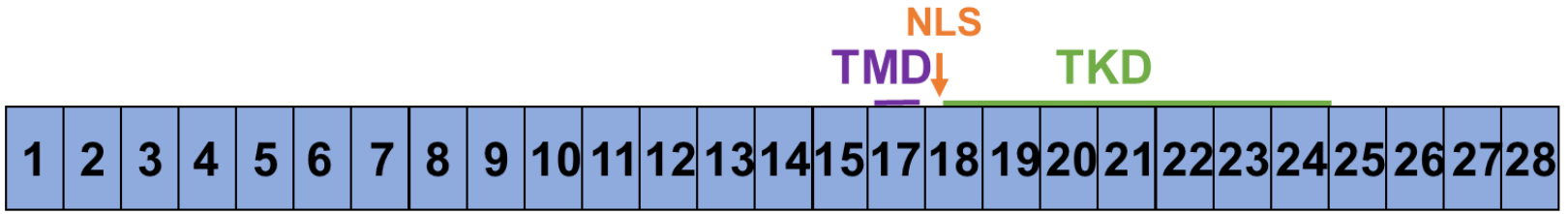

C) HER2-p100

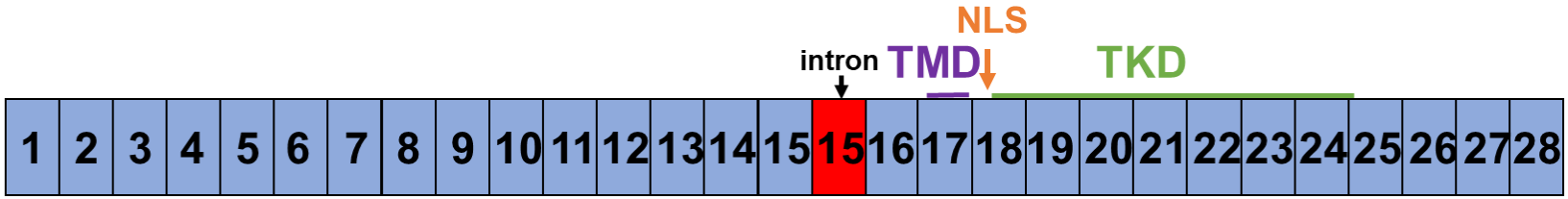

D) **Herstatin**

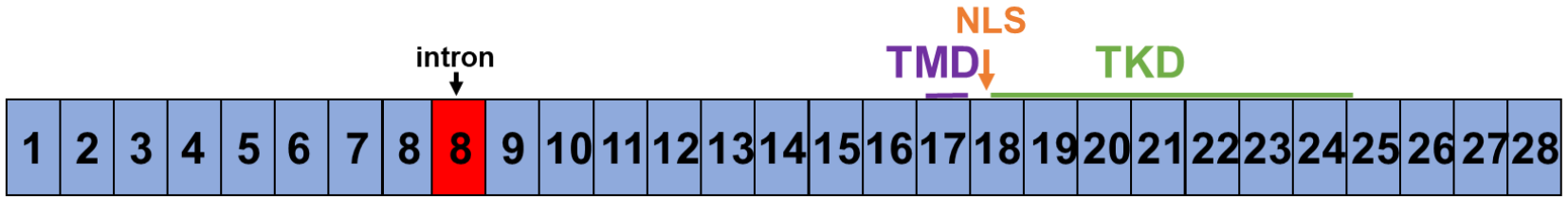

E) **HER2-pI9**

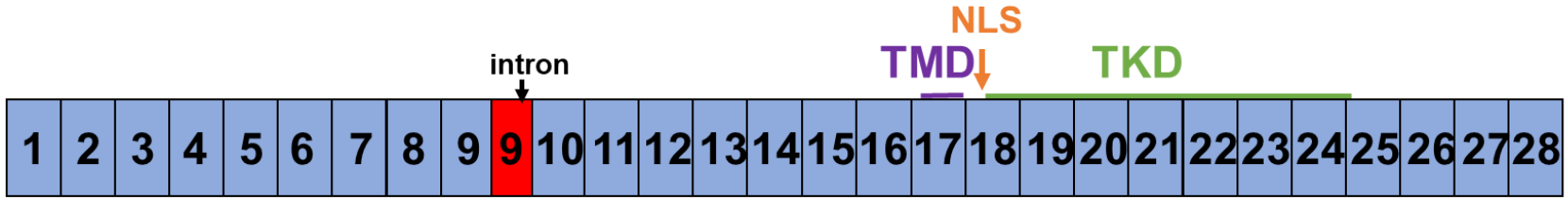

F) **HER2-I12**

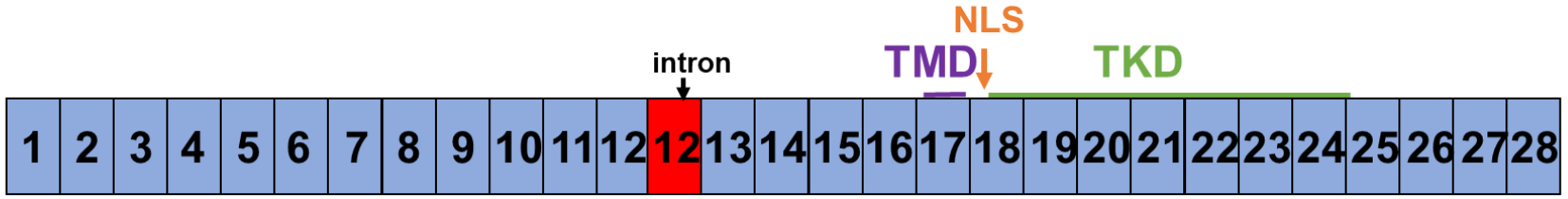

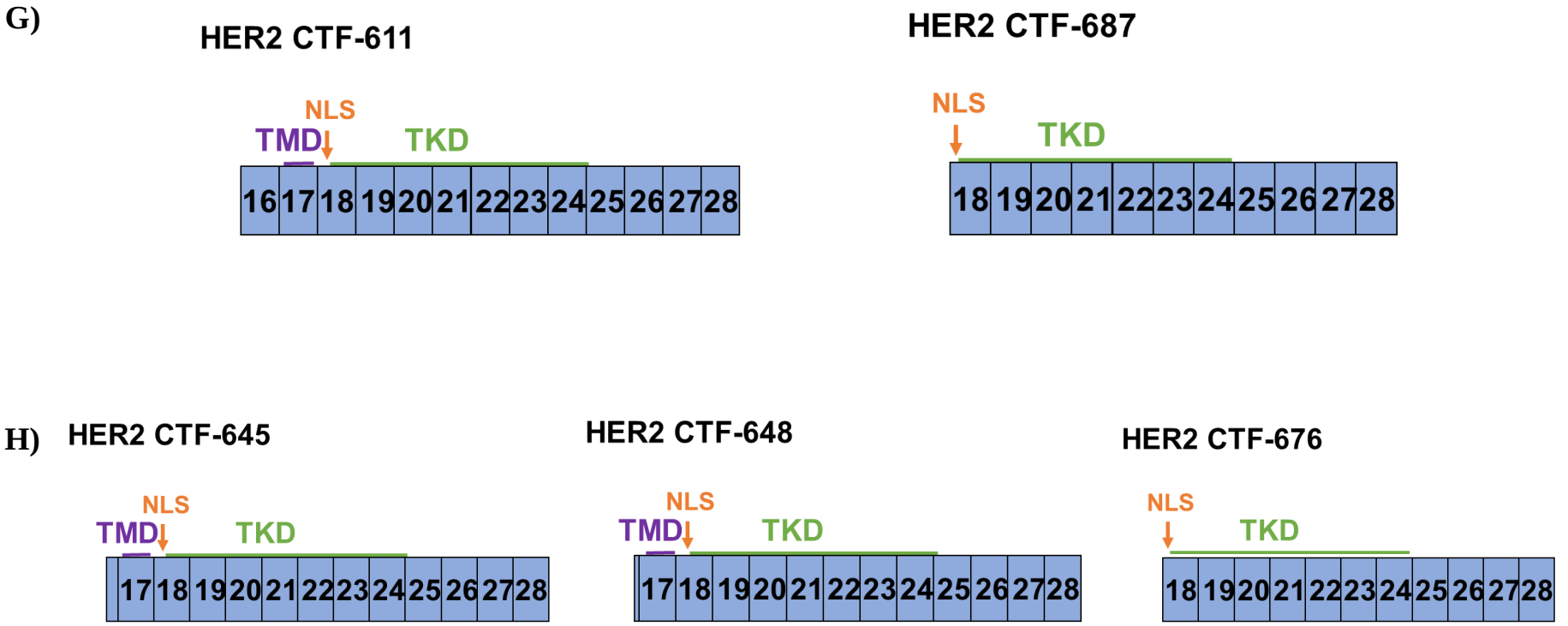

Figure 1.5. HER2 isoforms produced by alternative splicing, alternative initiation of translation or proteolytic cleavage. A) Wildtype HER2 (WT). B) Delta-16-*HER2* produced by the deletion of exon 16. C) p100-*HER2* and D) Herstatin, are generated by the retention of intron 15 and 8 respectively that contains a pre-mature stop codon. E) *HER2*-pI9 contains partial retention of intron 9. F) *HER2*-I12 produced by the full retention of intron 12. G) HER2 CTFs 611 and 687 produced by alternative translation at exons 15 and 17 respectively. H) HER2 CTFs generated by the proteolytic cleavage by alpha (α) starting at 645 or 648 which contain a TMD and NLS. HER2 CTFs cleaved by gamma (γ) secretase, producing CTFs starting at 676 lacking the TMD. TMD= transmembrane domain. TKD= tyrosine kinase domain. NLS= nuclear localisation signal. Exons are indicated as a blue box. Introns are indicated as a red box. (Image created by the author of this thesis).

HER4 has four main isoforms produced from alternative splicing of the juxtamembrane domain (JM) and cytoplasmic domain (CYT); JM-a/CYT1, JM-a/CYT2, JM-b/CYT1 and JM-b/CYT2. JM-a is encoded by exon 16 whilst JM-b is encoded from exon 15b. Figure 1.6. shows the mRNA 5' UTR, exons and 3' UTR of the JM-a/CYT1 and JM-a/CYT2 isoforms from the UCSC genome browser. The difference between the JM isoforms is that JM-a can be cleaved by tumour necrosis factor-α converting enzyme (TACE) and γ-secretase (Rio *et al.*, 2000; Strunk *et al.*, 2007). CYT1 is produced from inclusion of exon 26 that contains 16 amino acids that include a binding site for the p85 subunit of PI3K, and for proteins containing WW domains that can bind to proline-rich sequences. CYT1 can therefore trigger the PI3K/AKT pathway and is associated with increased cancer progression whilst CYT2 is produced from the exclusion of exon 26 and lacks the 16 amino acid residue (Elenius *et al.*, 1999; Tan *et al.*, 2010).

However, there has been conflicting reports that have shown CYT2 to increase the growth of mammary epithelial cells whilst CYT1 is associated with decreased growth of some mammary epithelial cells. CYT1 has a lower stability than CYT2 and can interact with the WW domain of E3 ubiquitin ligase leading to degradation of CYT1 (Muraoka-Cook *et al.*, 2009). However, both CYT1 and CYT2 have been identified in breast cancer cells (Junttila *et al.*, 2005).

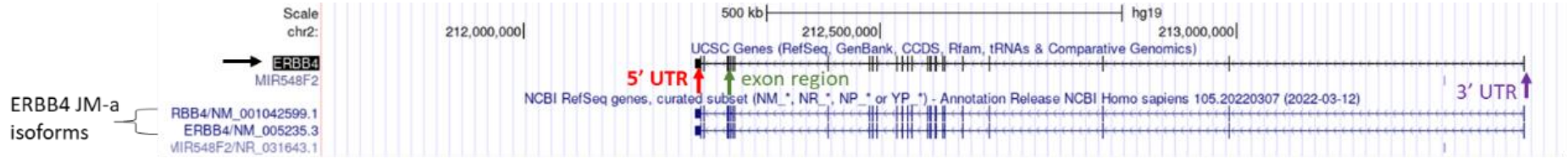

Figure 1.6. Human *HER4/ERBB4* JM-a isoforms. Schematics of the human *HER4/ERBB4* JM-a isoforms (CYT1/CTY2). Human *HER4/ERBB4* JM-a isoforms showing the 5' UTR, exons and 3' UTR on chromosome 2. The JM-a isoforms are the two *HER4/ERBB4* isoforms available from the UCSC genome browser. Black arrow: transcript variant JM-a/CVT-1 mRNA (*HER4/ERBB4* isoform used in this project). Red arrow: 5' UTR, green arrow: an exon region and purple arrow: 3' UTR (Nassar *et al.*, 2023).

1.6.3. Mechanism of Action

HER family members transduce extracellular signalling to trigger intracellular cell proliferation pathways. Apart from HER2, ligand binds to the extracellular domain of the receptors (Arkhipov *et al.*, 2013). EGFR binds EGF, betacellulin, epiregulin, heparin-binding EGF-like growth factor, TGF-alpha and amphiregulin. HER3 and HER4 bind neuregulin (NRG). HER4 also binds betacellulin, epiregulin and heparin-binding EGF-like growth factor (Komurasaki *et al.*, 1997; Sanders *et al.*, 2013; South *et al.*, 2013; Huang *et al.*, 2021).

A ligand binds between extracellular domains I and III, this brings these domains into closer contact. Then a conformational change takes place where the dimerisation arm of domain II is uncoupled from domain IV. This exposes domain II and allows it to be accessible to form a dimer with another receptor of the same type (homodimer) or a heterodimer with another HER (Liu *et al.*, 2012). HER2 extracellular domains exist in an open conformation making it a preferred dimerisation partner for other HERs (Alvarado et al., 2009). The conformational change that takes place upon ligand binding, allows ATP to bind to the intracellular cytoplasmic tyrosine kinase domains (Honegger *et al.*, 1987). Dimerisation allows two receptors to be in close proximity thereby allowing each receptor to phosphorylate and activate the cytoplasmic domain of its dimerisation partner through an autophosphorylation process. Alternatively, receptor kinase activity can be activated by transphosphorylation from other kinases such as SRC (Yarden and Schlessinger, 1987; El-Hashim *et al.*, 2017). HER3 has weak kinase activity due to differences in the amino acid residues of the HER3 cytoplasmic domain (Sierke *et al.*, et al., 1997; Shi *et al.*, 2010).

1.6.4. Main Signalling Pathways

1.6.4.1. Mitogen-Activated Protein Kinase Pathway

The MAPK pathway is activated by the phosphorylation of the tyrosine kinase domains of the HERs which creates binding sites for adaptor proteins such as GRB and SRC to bind to via their sequence homology 2 (SH2) domains. These adaptor proteins also contain SH3 domains that can bind to other proteins. For example, the SH3 domain of GRB can then bind to the SH3 domain of sons of sevenless (SOS) which converts GDP to GTP (Lemmon *et al.,* 1994; Jadwin *et al.,* 2018). SOS activates RAS-GTP which then activates the serine/threonine kinase RAF. RAF phosphorylates MEK which triggers a series of phosphorylation reactions of MAPKs leading to the activation of ERK (Kamioka et al., 2010). ERK can move to the nucleus and activate transcription factors such as AP-1 (JUN and FOS) (Hu *et al.*, 1997; Monje *et al.*, 2005).

AP-1 can then bind to 12-O-tetradecanoylphorbol-13-acetate (TPA) response elements or cAMP response elements (CRE) on target genes such as cyclin genes involved in the cell cycle (Lee *et al.*, 1987; Ghee *et al.*, 1998).

1.6.4.2. Phosphoinositide 3-Kinase Pathway

Class I PI3K contains a p85 regulatory subunit and a p110 catalytic subunit. The SH2 domain within the p85 subunit of PI3K binds to the phosphorylated tyrosine kinase residues of the HERs this results in activation of the p110 catalytic domain (Geltz and Augustine, 1998; Jiménez *et al.*, 2002).

PI3K then phosphorylates phosphatidylinositol 4,5-bisphosphate (PIP2) to phosphatidylinositol-3,4,5-triphosphate (PIP3) (Zhang *et al.*, 2019b).

Phosphatase and tensin homolog (*PTEN*) can dephosphorylate PIP3 to PIP2 thereby regulating the PI3K pathway (Chen *et al.*, 2016).

PIP3 can bind to proteins containing pleckstrin homology (PH) domains such as PDK1 (Ziemba *et al.*, 2013). AKT is then phosphorylated by PDK1 and mTORC-RICTOR at threonine 308 and serine 473 respectively (Hresko and Mueckler, 2005; Dangelmaier *et al.*, 2014). AKT can then phosphorylate and inhibit target proteins such as the tumour suppressor TSC2 an inhibitor of mTOR therefore increasing mTOR activity (Inoki *et al.*, 2002). Additionally, AKT can promote cell survival by phosphorylating and inhibiting many proteins involved in apoptosis such as forkhead box O (FOXO) transcription factors, glycogen synthase kinase 3 (GSK3) and Bad (Datta *et al.*, 1997; Bloedjes *et al.*, 2020).

1.6.5. Role in Breast Cancer

HER2 and HER4 are commonly overexpressed in breast cancers. HER2 is overexpressed in 30% of breast cancers and high HER2 expression is indicative of HER2-positive breast cancers (Carlsson *et al.*, 2004). HER4 is expressed in ESR1-positive and HER2-positive breast cancers (Czopek *et al.*, 2013; Morrison *et al.*, 2013; Nafi *et al.*, 2014; Wege *et al.*, 2018).

Although, HER4 can increase breast cancer survival it can also induce apoptosis in cancer cells and decrease cancer cell survival. The conflicting effects of HER4 activity depends on the release and localisation of the HER4 soluble intracellular domain (4ICD) produced from the proteolytic cleavage of the JM-a domain by TACE (Junttila *et al.*, 2005; Naresh *et al.*, 2006; Lanotte *et al.*, 2020). In the nucleus 4ICD can act as a transcriptional activator by interacting with various proteins such as ESR1, yes-associated protein (YAP) and STAT5A (Komuro *et*

al., 2003; Zhu *et al.*, 2006; Han *et al.*, 2016). For example, 4ICD interacts with ESR1 at oestrogen response elements on the promoters of oestrogen response genes including PR and stromal cell-derived factor 1 (SDF-1) contributing to breast cancer cell growth (Zhu *et al.*, 2006). However, the localisation of the 4ICD to the cytoplasm is associated with decreased cancer cell survival. This is due to the 4ICD accumulating in the mitochondria and activating BAK via the 4ICD BH3 domain. This leads to the efflux of cytochrome c from the mitochondria and apoptosis. However, the activity of BCL2 can inhibit the interaction of the 4ICD BH3 domain and BAK which can prevent apoptosis in some breast cancers containing the cytoplasmic 4ICD (Naresh *et al.*, 2006).

Overexpression of HER2 and HER4 results in constitutive activation of the receptors and an increase in downstream growth factor signalling contributing to cancer progression. HER2 activation of MAPK and PI3K downstream signalling pathways can stimulate MYC phosphorylation at serine 62 leading to increase in MYC stability which enhances cell growth of breast cancer cells (Risom *et al.*, 2020).

A small portion of the overexpression of the HERs is due to gene amplification. *HER2* gene amplification accounts for 15-20% of HER2 overexpression (Yamashita *et al.*, 2020). However, translational upregulation is thought to account for a proportion of HERs overexpression as observed for EGFR. For instance, *EGFR* gene amplification accounts for only ~6% of EGFR overexpression (Bhargava *et al.*, 2005). Additionally, EGFR proteins levels have shown to increase under hypoxia with no change in *EGFR* mRNA levels in cancer cell lines (Franovic *et al.*, 2007).

Mutations in the HER2 and HER4 proteins can also contribute to cancer progression. The L755S mutation is the most prevalent HER2 mutation that occurs in the tyrosine kinase domain. The L755S mutation stabilises the tyrosine kinase residues into an active state resulting in an increase in phosphorylation of the tyrosine kinase residues (Xu *et al.*, 2017; Li *et al.*, 2019; Gaibar *et al.*, 2020). HER4 E563K and E872K mutations in the tyrosine kinase domain increase phosphorylation of the tyrosine kinase residues (Canfield *et al.*, 2015; Kawahara and Simizu, 2022).

1.6.6. Translational Regulation

1.6.6.1. *EGFR* 5' UTR IRES

EGFR which is a closely related family member of HER2 and HER4, contains an IRES in the *EGFR* 5' UTR that directly recruits the 40S ribosome between 23 and 56 nts upstream to the initiation codon (Webb *et al.*, 2015). *EGFR* IRES has a requirement for the RNA helicase eIF4A which is needed to unwind secondary structures. *EGFR* IRES activity has been observed in SH-SY5Y, MCF-7, HeLa and Huh7 cells (Webb *et al.*, 2015; Smalley, 2016). Additionally, luciferase reporters have been used to show that *EGFR* IRES can maintain expression in response to stress conditions such as hypoxia (Webb *et al.*, 2015; Smalley, 2016; Alamoudi, 2020).

1.6.6.2. *HER2* coding region IRES

Recently, it has been shown that HER2 CTFs are produced by IRES-mediated translation from the *HER2* coding region (Godfrey *et al.*, 2022). This study found that although *HER2* CTFs are more efficiently translated in a cap-dependent manner, HER2 CTFs can also be produced by cap-independent translation. Insertion of a hairpin that is proposed to inhibit cap-dependent

translation reduced the expression of the full length HER2 but the expression of HER2 CTFs maintained at least half its expression. This study also ruled out the possibility of HER2 CTFs produced by alternative splicing or a cryptic promoter activity (Godfrey *et al.*, 2022).

1.6.6.3. *HER2* uORF

HER2 5' UTR contains a 21 nucleotide uORF that causes translational repression of the *HER2* coding region (Child *et al,* 1999a, 1999b). The translational repression by the uORF is due to ribosomes being unable to reinitiate translation after translating the uORF. The repression of translation is independent of the peptide sequence of the uORF despite the sequence being conserved amongst mammalian species. The translation inhibition is due to the short length of the five nucleotide intercistronic region between the *HER2* uORF and the *HER2* main ORF. Increasing the intercistronic regions alleviates the uORF inhibitory effects as it allows ribosomes more time to reinitiate translation downstream from the uORF. Translation of the *HER2* gene can take place via leaky scanning or some ribosomes reinitiating despite the intercistronic gap (Child *et al,* 1999b). Additionally, *HER2* mRNA is translated more efficiently in transformed cells (MCF-7, BT474 and COS-7 cells) this is due to the over expression of the cap-binding protein, eIF4E enhancing ribosomal scanning (Child 1999b, 1999a; Spevak *et al.*, 2006).

It has been shown that the *HER2* 3' UTR can derepress translation of the *HER2* uORF. *HER2* 3' UTR derepression activity has shown to be higher in breast cancer cell lines that have a higher expression of the HER2 protein such as SKBR-3 and BT474 cells and has moderate activity in MCF-7 cells (Mehta *et al.,* 2006). Additionally, *HER2* 3' UTR has shown to derepress translation of

other mRNAs such as SHIP-2 uORF however derepression activity was greater for *HER2* uORF. The region on *HER2* 3' UTR responsible for the derepression activity in the Mehta 2006 study, is a 73 nt translational derepression element (TDE). HuR, hnRNP A1, hnRNP C1/C2 and PABP were detected in SKBR-3 cells and have found to be TDE RBPs that may be important for derepression activity (Mehta *et al.,* 2006). The TDE PBPs complex has also been detected in other breast cancer cells such as AU565, BT474 and MCF-7 cells (Mehta *et al.,* 2006).

1.7. Breast Cancer Therapeutics

1.7.1. Overview of current therapeutics

Most breast cancer patients undergo a lumpectomy or mastectomy to remove the cancer in the breast. Surgery is often combined with radiation therapy which uses X-rays or radioactive particles to damage the DNA of cancer cells. This can kill remaining cancers cells as well as preventing cancer reoccurrence (Admoun and Mayrovitz, 2021).

Anti-cancer medicines are given as an adjunctive therapy with the aim to further treat the cancer cells, prevent metastasis or cancer reoccurrence. The type of anti-cancer medicine used generally depends on the molecular subtype of the breast cancer. Endocrine therapy (e.g. tamoxifen) are generally used to treat hormone receptor positive breast cancers (Furr *et al.,* 1984; Liu *et al.,* 2014). Chemotherapy and biological therapy are usually given to breast cancer with low or negative ESR expression and HER2-positive breast cancers (Ferraro *et al.,* 2013; Modi *et al.,* 2020; Weisman *et al.,* 2022).

Breast cancer cells can develop intrinsic resistance to anti-cancer drugs prior to treatment or cancer cells can acquire resistance during treatment reducing efficacy of treatment and often leading to reoccurrence and metastasis (Wander *et al.*, 2020). Multi-drug resistance is a key driver of cancer cell resistance and can result in the resistance of cancer cells to anti-cancer drugs via several mechanisms such as increased drug efflux, decrease in drug uptake, changes in expression levels or activity of the target protein, induction of DNA repair mechanisms, changes in the tumour microenvironment, activation of enzymes targeting drugs and genetic heterogeneity (Shen *et al.*, 2000; Fedier *et al.*, 2001; Huang *et al.*, 2003; Reim *et al.*, 2009; Martinez-Outschoorn *et al.*, 2011; Nanayakkara *et al.*, 2018; Baslan *et al.*, 2020; Wiegmans *et al.*, 2021).

1.7.2. HER2-positive Breast Cancers Therapies

There are different therapies that are used to treat HER2-positive breast cancers such as antibodies, small molecule tyrosine kinase inhibitors and antibody drug conjugates. Trastuzumab is a monoclonal antibody that is used to treat breast cancers overexpressing HER2 and it targets the HER2 protein present at the plasma membrane. Trastuzumab binds to the extracellular domain IV of HER2 preventing ligand independent homodimerisation and thus blocking intracellular MAPK and PI3K signalling pathways (Ghosh *et al.*, 2011). Additionally, upon binding to HER2 extracellular domain, trastuzumab can trigger an immune response resulting in cancer cell apoptosis (Arnould *et al.*, 2006). The monoclonal antibody pertuzumab binds to the extracellular II domain of HER2 and prevents HER2 heterodimers and thus downstream signalling (Franklin *et al.*, 2004).

Tyrosine kinase inhibitors target members of the HER family and are used for the treatment of HER2-positive breast cancer. Pyrotinib and neratinib target EGFR, HER2 and HER4 whilst lapatinib targets EGFR and HER2 (Rabindran *et al.*, 2004; Wood *et al.*, 2004; Dai *et al.*, 2020; Chilà *et al.*, 2021; Wang *et al.*, 2021). Additionally, tucatinib is a specific inhibitor of HER2 (Debusk *et al.*, 2021). Tyrosine kinase inhibitors bind to the ATP binding site at cysteine residues of the intracellular tyrosine kinase domain. This prevents ATP binding to the receptors which blocks autophosphorylation of the tyrosine kinase residues therefore preventing downstream signalling (Fang *et al.*, 2020).

Antibody drug conjugates involve the binding of a cytotoxic drug to an antibody that is delivered to the cancer cells upon antibody-receptor binding. Trastuzumab emtansine contains trastuzumab covalently bound by a thioether linker to the cytotoxic compound, emtansine (Park *et al.*, 2021). In addition to inhibiting HER2 dimerisation, trastuzumab delivers emtansine specifically to HER2-positive breast cancer cells. The binding of trastuzumab to HER2 extracellular domain IV results in endocytosis of trastuzumab emtansine into endosomes which is subsequently delivered to lysosomes. Trastuzumab is degraded in the lysosomes whilst emtansine is released. Emtansine then binds to microtubules preventing their polymerisation leading to inhibition of mitosis which triggers apoptosis (Lewis Phillips *et al.*, 2008; Erickson *et al.*, 2012; Baselga *et al.*, 2016).

Trastuzumab deruxtecan is also used for the treatment of HER2-positive breast cancer. Trastuzumab delivers deruxtecan in a similar mechanism to trastuzumab emtansine. However, when deruxtecan is release from lysosomes it enters the nucleus where it inhibits the activity of topoisomerase I which leads to DNA

damage and interferes with breast cancer DNA replication leading to apoptosis (Modi *et al.*, 2020b; Yin *et al.*, 2021).

Somatic mutations in various domains of HER2 can lead to drug resistance of HER-targeted therapies, for example, mutations in exons 19, 20 or 21 of HER2 tyrosine kinase domain blocks the binding of several tyrosine kinase inhibitors which allows phosphorylation of the tyrosine kinase domain that triggers downstream signalling (Wen *et al.*, 2015; Robichaux *et al.*, 2018). The L755S HER2 mutation causes resistance to trastuzumab and lapatinib (Li *et al.*, 2019). A common S310F mutations in the extracellular domain II of HER2 prevents pertuzumab from binding to the HER2 extracellular domain (Zhang *et al.*, 2019c). The truncated HER2 CTF (p95-HER2) isoform lacks an extracellular domain and has shown to be resistant to trastuzumab but lapatinib is still effective in targeting HER2 CTFs (Scaltriti *et al.*, 2007, 2010).

1.7.3. Emerging Therapeutics

Cancer vaccines are active immunotherapies that are being tested for the treatment of HER2-positive breast cancers. Nelipepimut-S is a cancer vaccine that is in phase III clinical trial which targets breast cancer cells expressing HER2 protein (Mittendorf *et al.*, 2019). Nelipepimut-S is a peptide derived from the extracellular domain of HER2 which is used in conjunction with granulocyte macrophage-colony stimulatory factor (GM-CSF) which stimulates T lymphocytes (Groenewegen and De Gast, 1999). Nelipepimut-S is recognised by helper CD4+ and memory CD8+ T-lymphocytes. Cytotoxic CD8+ T-lymphocytes then trigger apoptosis of cancer cells (Bailur *et al.*, 2015).

Protein degraders conjugated to HER2 targeting antibodies have been developed to specifically target HER2-positive cells. For example, ORM-509 has recently been developed and contains a protein degrader called SMol006 conjugated to pertuzumab that bind to HER2-positive cells. SMol006 targets the G1 to S phase transition protein 1 (GSPT1) in the cytosol of cells. Upon release into cells, pertuzumab is degraded by lysosomes whilst SMol006 targets and degrades GSPT1 causing cell death of HER2-positive cells. ORM-509 has shown strong efficacy in HER2 expressing cells and in vivo xenograft models (Palacino *et al.*, 2022; Swain *et al.*, 2023).

Engineered toxin bodies (ETBs) combined with HER2 targeting antibodies can be used to target HER2-positive breast cancers. MT-S111 is an ETB currently in phase 1 clinical trial for the treatment of HER2-positive tumours including breast cancer. The ETB contains a deimmunised Shiga-like Toxin A subunit fused to a HER2 targeting antibody. MT-S111 induces cell toxicity by permanently inactivating ribosomes. In addition, MT-S111 targets a different epitope of HER2 than other HER2 targeting antibodies such as trastuzumab. Therefore, MT-S111 could be used in conjunction with current HER2-positive breast cancer therapeutics. The mechanism of action of MT-S111 is distinct from conventional HER2-positive breast cancer therapies, so may be used to target breast cancer cells resistant to current therapeutics (Van Tine *et al.*, 2022; Swain *et al.*, 2023).

Antisense oligonucleotides have been used to treat some rare disease; but none have currently been approved for cancer treatment. However, antisense oligonucleotides have shown promising results as a future therapy for cancer (Chi *et al.*, 2000). Antisense oligonucleotides are usually single-stranded short

nucleotide sequences that have a complementary nucleotide sequence to the target mRNA. Antisense oligonucleotides can bind to mRNA and act as a steric block of the translation machinery and the 40S ribosomal subunit or induce mRNA degradation by endonuclease, RNAase H which recognises DNA-RNA duplexes (Liang *et al.*, 2017; Holgersen *et al.*, 2021).

Antisense oligonucleotides with a 2′-*O*-methyl modification have shown to reduce IRES mediated translation of hepatitis C virus. The 2′-*O*-methyl antisense oligonucleotides can bind to the IIId domain of the IRES which blocks 40S ribosomal binding (Tallet-Lopez *et al.*, 2003). Antisense oligonucleotides with a phosphorothionate and 2′-*O*-methyl modifications have been designed against *EGFR* 5’ UTR. They have shown to reduce *EGFR* IRES activity in luciferase assays as well as reducing EGFR protein levels via a RNAase H dependent mechanism in MCF-7 and MDA-MB-231 breast cancer cells (Alamoudi, 2020).

1.8. Aims and Objectives

HER2 and HER4 are overexpressed in breast cancer due to gene amplification and somatic mutations within the HER proteins (Canfield *et al.*, 2015; Gaibar *et al.*, 2020; Yamashita *et al.*, 2020; Kawahara and Simizu, 2022). However, translational regulation has been thought to play a role in their overexpression in breast cancer cells that are exposed to various cell stress conditions (Yang *et al.*, 2000). An IRES in *EGFR* 5' UTR has previously been identified and shown to maintain expression in response to stress conditions such as hypoxia in various cell lines such as MCF-7 breast cancer cells (Webb *et al.*, 2015). However, an IRES has not currently been identified in the 5' UTRs of the other HER family members which may contribute to their overexpression in breast cancer cells. Additionally, *HER2* 5' UTR may mediate an increase in translation under glutamine or glucose starvation as previously seen for other mRNAs containing uORF such as *ATF4* and *GCN4* (Gameiro and Struhl, 2018; Zhang *et al.*, 2018; Chen *et al.*, 2022).

The first aim of this thesis was to investigate whether *HER2* or *HER4* contain an IRES in their 5' UTR. To test this, bicistronic luciferase constructs were used to screen for IRES activity under various cancer-associated cell stress conditions in MCF-7 breast cancer cells (Chapter 3). The second aim was to test if *HER2* and *HER4* 5' UTRs could mediate an increase in translation in response to glutamine starvation (Chapter 4) or glucose starvation (Chapter 5) using monocistronic luciferase constructs. Finally, the effect of *HER2* 3' UTR on derepressing the translational inhibition caused by the *HER2* 5' UTR was tested in response to glutamine starvation (Chapter 4) and glucose starvation (Chapter 5).

Chapter 2 - Materials and Methods

2.1. Cell Culture

2.1.1. Solutions and Reagents

Phosphate buffered saline (PBS): 4.3mM disodium hydrogen phosphate, 1.5mM potassium dihydrogen phosphate, 137mM sodium chloride, 2.7mM potassium chloride, pH 7.4.

High Glucose Dulbecco's Modified Eagle Medium (DMEM) (Sigma Aldrich)

Gibco Opti-MEM reduced serum media (Thermofisher Scientific)

Foetal bovine serum (Thermofisher Scientific)

L-Glutamine (Sigma-Aldrich)

Trypsin-EDTA (FisherScientific)

2 mg/ml 3-(4,5-dimethylthiazol-2-yl)-2,5-diphenyltetrazolium bromide (MTT) solution (Sigma-Aldrich)

2.1.2. Cell lines and Maintenance

MCF-7 human breast adenocarcinoma cells were provided by the Spriggs lab and grown in cell culture grade T75 flasks in DMEM supplemented with 10% Gibco foetal bovine serum (FBS) and 2 mM L-Glutamine. The cells were maintained at 37°C under a humidified atmosphere containing 5% CO_2. Cells were grown to 70-80 % confluence then were subcultured by removing exhausted media, washing with 5 ml of PBS, and detaching the cells from the flask with 1ml of 1x trypsin. Cells were diluted in fresh media and seeded 1:5 (cells: media) in a T75 flask.

2.1.3. Transient Transfection

MCF-7 cells were seeded at a density of $1x10^4$ cells per well in a 24-well plate unless stated otherwise. 3 µg of polyethylenimine (PEI) (provided by Abdulmohsin Alamoudi, University of Nottingham) was added to 1 µg of plasmid DNA at a 1: 3 ratio of DNA to PEI in 50 µl per well of Gibco Opti-MEM reduced serum media. The PEI/DNA solution was left to incubate for 20 minutes whilst the exhausted cell media was removed from the cells and replaced with 1 ml of fresh DMEM. After the 20 minutes incubation, the PEI/DNA solution was added to cells. MCF-7 cells were left to incubate at 37˚C, 5% CO_2 for 24 hours before being treated or assayed for luciferase activity.

2.1.4. Cell Stress Treatments

24 hours after transfection, MCF-7 cells were exposed to the cell stress treatments described in this section. MCF-7 cells were treated with the following chemical reagents (Table 2.1); different concentrations of cobalt (II) chloride hexahydrate ($CoCl_2$) made up in fresh media or an untreated DMEM control, different concentrations of thapsigargin in DMSO or untreated controls containing the equivalent DMSO percentage to treated cells, and hydrogen peroxide (H_2O_2) made up in DMEM or an untreated DMEM control. The concentrations of $CoCl_2$, thapsigargin and H_2O_2 applied to cells are specified in Chapter 3. To induce genotoxic stress MCF-7 cells were exposed to a UV-B light 280-315 nm (UVM-57 lamp, UVP Inc) for 10 seconds or 20 seconds. To expose MCF-7 cells to low serum conditions cells were incubated with DMEM containing 0.5% FBS (Thermo Fisher Scientific) or control media containing 10% FBS for 24 hours. To induce glutamine or glucose starvation, MCF-7 were incubated with DMEM glutamine-free/sodium pyruvate-free media or glucose-

free/sodium pyruvate-free media respectively (Thermo Fisher Scientific), supplemented with 10% dialysed FBS (Merck Life Science Ltd) at various timepoints (specified in Chapters 4 and 5).

Table 2.1. Chemical stress inducers

Reagent	**Solute**	**Stock Concentration**	**Supplier**	**Duration of treatment**	**Stressor**
Cobalt (II) chloride hexahydrate ($CoCl_2$)	DMEM	5mM	Sigma	24 hours	Hypoxic mimic
Thapsigargin	DMSO	1 µM	Sigma	24 hours	Endoplasmic reticulum stress (ER)
Hydrogen peroxide (H_2O_2)	DMEM	30% w/v	VWR Chemicals BDH	24 hours	Oxidative stress

2.1.5. Dual-Luciferase Assay

After transfection with luciferase plasmids and exposure to cell stressors for the specified duration of time (described in Section 2.1.4 and Chapters 3-5), the media was removed from MCF-7 cells then cells were washed once with PBS. PBS was removed completely before cells were lysed with 50 µl of 1x passive lysis buffer (Promega) which was added to each well of a 24 well plate. Cells were dissociated from the wells by scraping and 5 µl of cell lysate was added to a black rounded 96 well plate. Luciferase activity was measured using a dual-luciferase assay kit (Promega). 25 µl of each luciferase reagent, LarII (firefly luciferase) followed by Stop&Glo (*Renilla* luciferase) was added to each well

and the luminescence was measured using a Glomax luminometer (Promega) over a 10 second integration time after the addition of each reagent.

2.1.6. MTT Assay

MCF-7 cells were seeded into a 96 well plate at a density of $1x10^3$ cells per well. Plates were incubated at 37˚C, 5% CO_2 for 24 hours before being treated. Cells were treated with cell stress inducers (Section 2.1.4.). After treatment, 2 mg/ml 3-(4,5-dimethylthiazol-2-yl)-2,5-diphenyltetrazolium bromide (MTT) (Sigma-Aldrich) dissolved in PBS solution was added to each well. Plates were then shaken for five minutes at 150 RPM using a gyratory rocker then incubated at 37 ˚C, 5% CO_2 for 2.5 hours. Media was aspirated, then 150 µl of DMSO was added to each well to resuspend the formazan product. The plate was then shaken for five minutes at 150 RPM using a gyratory rocker to allow the formazan product to mix into the solvent. Then the optical density was read at 560 nm using a Microplate Plate Reader (BioTek).

2.2. Molecular Biology Techniques

2.2.1. Reagent and Solutions

1X TAE: 40 mM Tris base, 40 mM acetic acid, 1 mM EDTA pH 8.0

RIPA buffer: 140Mm sodium chloride, 25mM Tris (pH 7.4), 1mM EGTA, 1mM EDTA, 1% Triton X-100, 10% glycerol, 0.1% sodium dodecyl-sulfate (SDS), 0.5 % sodium deoxycholate

1X Tris-Glycine Buffer: 55 mM Tris Base, 1.92 M Glycine, 5% methanol

10X SDS-PAGE Buffer: 250 mM Tris base, 1.93 M glycine and 1% SDS

10X TBS: Tris base 0.2 M, 1.5M sodium chloride, pH adjusted to 7.4 with hydrogen chloride

TBST: 1X TBS supplemented with 0.1% Tween 20 detergent (Sigma)

1X CutSmart Buffer: 50 mM potassium acetate,20 mM Tris-acetate,10 mM magnesium acetate ,100 µg ml BSA, pH 7.9 at 25°C (NEB)

1X NEBuffer 2.1: 50 mM sodium chloride, 10 mM Tris-hydrochloric acid, 10 mM magnesium chloride, 100 µg ml BSA, pH 7.9 at 25°C (NEB)

2.2.2. Overview of luciferase constructs used in this thesis

The luciferase plasmids pRF (*Renilla*/firefly luciferase) (Stoneley et al., 2000), p15 (firefly luciferase) and p80 (*Renilla* luciferase) (Webb, 2012) were provided by the Spriggs lab and used as controls in the luciferase experiments. The CMV-LUC2CP/ARE plasmid was provided by the De Moor lab (Younis *et al.*, 2010). In addition, pRF-*β-tubulin*-5’ UTR, pRF-*EGFR* 5’ UTR (Smalley, 2016) and

p15-*EGFR* 5' UTR (Webb, 2012) were provided by the Spriggs lab. Constructs made for this thesis are in Table 2.2 and were stored at -20°C.

Table 2.2. Constructs made for this project. Constructs made during this thesis, the template DNA source and the template DNA concentration used for cloning. All plasmids were stored at -20°C.

Construct	**Luciferase**	**Cloning modification**	**Template DNA source and concentration used in PCR reactions**
pRF-*HER2* 5' UTR	*Renilla*/Firefly	Addition of *HER2* 5' UTR into pRF	200 ng of *HER2* 5' UTR oligonucleotide DNA
pRF-*HER4* 5' UTR	*Renilla*/Firefly	Addition of *HER4* 5' UTR into pRF	200 ng of *HER4* 5' UTR oligonucleotide DNA
p15-*HER2* 5' UTR	Firefly	Addition of *HER2* 5' UTR into p15	1 ng of pRF-*HER2* 5' UTR
p15-*HER4* 5' UTR	Firefly	Addition of *HER4* 5' UTR into p15	1 ng of pRF-*HER4* 5' UTR
Destabilised p15	Firefly	Addition of hCl-hPEST into p15	1 ng of CMV-LUC2CP/ARE
Destabilised p15-*HER2* 5' UTR	Firefly	Addition of hCl-hPEST into p15-*HER2* 5' UTR	1 ng of CMV-LUC2CP/ARE
Destabilised p15-*HER2* 5' UTR + 3' UTR	Firefly	Addition of *HER2* 3' UTR into destabilised p15-*HER2* 5'UTR	50 ng of *HER2* 3' UTR g-block (Figure 2.4)

2.2.3. Bicistronic reporters

The pRF plasmid is the bicistronic reporter used in this thesis (Section 2.2.2). pRF contains a SV40 promoter and two luciferase reporter genes, *Renilla* and firefly luciferase (vector map-Figure 3.1). The intercistronic region between the luciferase ORFs contains restriction sites for cloning of a 5' UTR sequence (Figure 2.1) (schematics showing the specific 5' UTR sequences used in this project are shown in Figure 3.2). The SV40 promoter allows transcription of pRF which produces a bicistronic mRNA containing both *Renilla* and firefly luciferase (Figure 2.2). Translation of *Renilla* luciferase occurs in a cap-dependent manner. However, firefly luciferase can only be translated if the 5' UTR cloned into the intercistronic region contains an IRES that would allow translation of firefly luciferase in a cap-independent manner. The F/R ratio is the raw firefly luminescence signal divided by the *Renilla* luminescence signal. The F/R ratio normalises the firefly luminescence signal to account for variations in transfection efficiency among replicates.

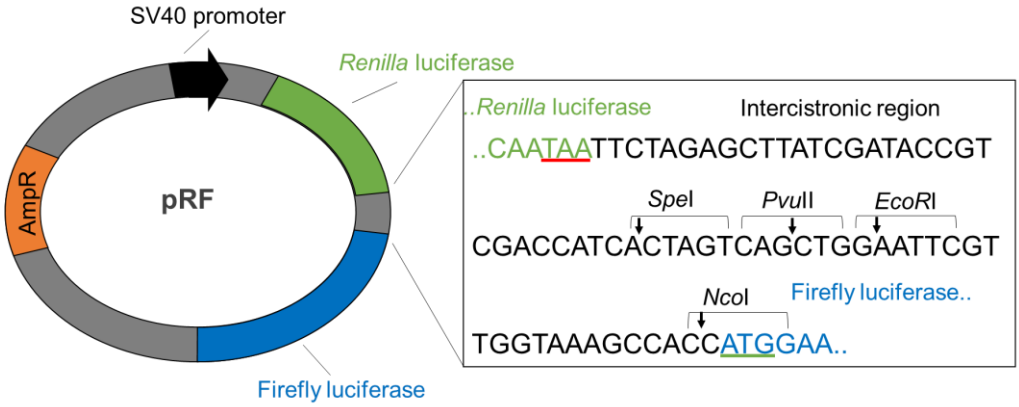

Figure 2.1. The multiple cloning site sequence in the pRF bicistronic plasmid. The sequence showing the end of *Renilla* luciferase, the intercistronic region containing *Spe*I, *Pvu*II, *Eco*RI and *Nco*I restriction sites, and the start of firefly luciferase. Start codons are underlined green and stop codons are underlined red. The black arrow indicates the restriction enzyme cutting location. AmpR= ampicillin resistance gene (Image created by the author of this thesis).

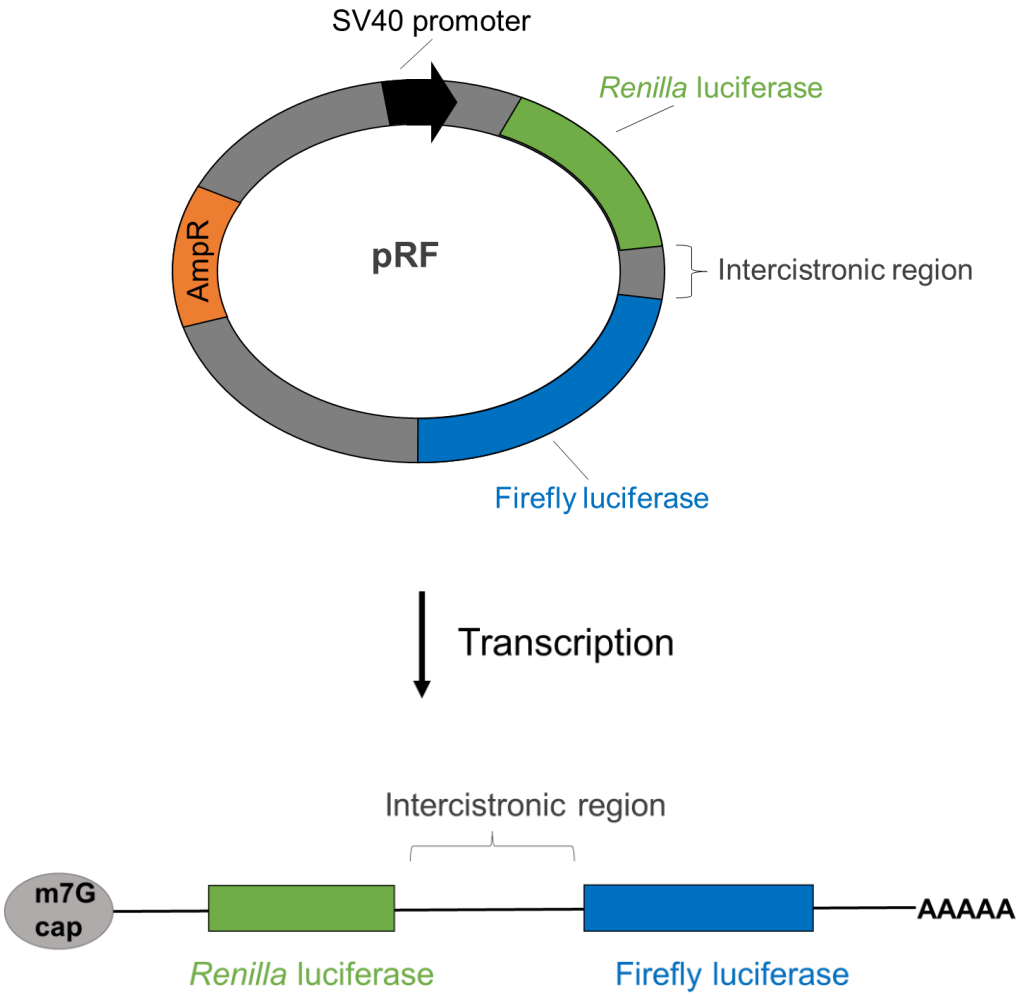

Figure 2.2. Transcription of the pRF plasmid produces a bicistronic mRNA. (Image created by the author of this thesis).

2.2.4. Polymerase Chain Reaction

DNA templates were added to the following PCR for amplification according to the manufacturer's instructions (NEB) (see Table 2.2. for specific concentrations of each DNA template used) to produce the following PCR reaction; 1x Phusion GC Buffer, 10 mM dNTPs, 3% DMSO, 0.5 µM of each forward and reverse primer (primers: Table 2.5) and 1 unit of Phusion high-fidelity DNA polymerase which was made up to a final volume of 50 µl. A touch-down PCR method was used to increase the specificity of the PCR reaction and to avoid amplifying non-specific sequences. DNA was initially denatured at 98-°C for 30 seconds. Then the DNA entered a cycle of denaturation at 98-°C for 10 seconds, annealing that lasted for 20 seconds per cycle and started at 72-°C for the first cycle only then the annealing temperature was decreased by 0.5-°C every cycle until 66 -°C was reached and an extension at 72-°C for 40 seconds. 35 cycles were completed before the final extension at 72-°C for 20 seconds. For amplification of hCL1-hPEST (obtained from the CMV-LUC2CP/ARE plasmid) the same PCR setting were used as described above except an annealing temperature of 55°C for 20 seconds was used for all 35 cycles. The PCR products were stored at -20°C until required.

2.2.5. Creating 5' UTRs from synthetic oligonucleotides

HER2/ERBB2 5' UTR (accession number; NM_004448.3) (indicated in Figure 1.4) and *HER4/ERBB4* 5' UTR (accession number; NM_005235.2) (indicated in Figure 1.6) (referred to as *HER2* and *HER4* in this thesis) were amplified from synthetic oligonucleotides (Tables- 2.3 and 2.4).

The oligonucleotides were first resuspended in distilled water to 100 mM. *HER2* 5' UTR was synthesised from 3 oligonucleotides (Table 2.3 and Figure 2.3a). There was 22 bp of complementarity between oligonucleotides 1 and 2, and 20 bp of complementarity between oligonucleotides 2 and 3. First, 0.3 µl of oligonucleotides 1 and 2 were annealed together with 1x Phusion GC Buffer, 3% DMSO and distilled water in a PCR machine at 60 °C overnight. The annealed oligonucleotides were extended from the oligonucleotide sequences without primers using 10 mM dNTPs and 1 unit of Phusion high-fidelity DNA polymerase to a total volume of 25 µl using the PCR settings described in Section 2.2.4. Then 0.6 µl of oligonucleotide 3 was added to the same reaction mixture and annealed to the product of oligonucleotides 1 and 2 at 60 °C overnight. The sequences were subsequently extended again without primers as described above. Then the product of the 3 oligonucleotides was amplified with forward and reverse primers (Table 2.5) using the PCR settings described in section 2.2.4 (Figure 2.3b). The PCR product was then visualised by agarose gel and purified (described in sections 2.2.8-2.2.9).

For *HER4* 5' UTR only one synthetic oligonucleotide was used as a template due to the short 5' UTR sequence of *HER4* 5' UTR. *HER4* 5' UTR oligonucleotide was then amplified with forward and reverse primers (Table 2.5) using the PCR settings described in section 2.2.4. The PCR products of both *HER2* and *HER4* 5' UTRs were then re-amplified to obtain more template DNA with the PCR settings described in section 2.2.4 but with a 100 µl reaction volume (DNA concentrations: Table 2.2). The PCR products were then visualised on an agarose gel, purified, digested, and ligated into the pRF plasmid (described in sections 2.2.8-2.2.11.) and screened via colony PCR (section

2.2.12.). Then successfully sequencing was confirmed by Sanger sequencing (Appendix Figures 37-38).

Table 2.3. Oligonucleotides for synthesis of *HER2* 5' UTR. Three oligonucleotides annealed together to produce *HER2* 5' UTR template DNA for cloning into pRF. Region showing complementarity to the forward primer and reverse primer (primers: Table 2.5).

	***HER2* 5' UTR DNA oligonucleotide sequences (5'-3')**
1	GCTTGCTCCCAATCACAGGAGAAGGAGGAGGTGGAGGAGGAG GGCTGCTTGAGGAAGTATAAGAATGAAGTTGTGAAGCTGAGAT TCCCCTCCATTGGGACC
2	GCGCAGTAAAGGGCCCCGTGGGAAGGGGCGCGCGGCTGCCCG GGGGGCTCCCCTGGTTTCTCCGGTCCCAATGGAGGGGAATCTC
3	CATGGTGCTCACTGCGGCTCCGGCCCCATGGCTCCGGCTGGAC CCGGCTGGGAGGGCGCGGGGCGCGGGGTGCTGCGAGGGGTGG GGGCCGGGCGCGCGGCGCAGTAAAGGGCCCCGTG

A

HER2 5' UTR oligo 1

5'-
GCTTGCTCCCAATCACAGGAGAAGGAGGAGGTGGAGGAGG
AGGGCTGCTTGAGGAAGTATAAGAATGAAGTTGTGAAGCT
GAGATTCCCCTCCATTGGGACC-3'

HER2 5' UTR oligo 2

5'-
GCGCAGTAAAGGGCCCCGTGGGAAGGGGCGCGCGGCTGCC
CGGGGGGCTCCCCTGGTTTCTCCGGTCCCAATGGAGGGGAA
TCTC-3'

HER2 5' UTR oligo 3

5'-
CATGGTGCTCACTGCGGCTCCGGCCCCATGGCTCCGGCTGG
ACCCGGCTGGGAGGGCGCGGGGCGCGGGGTGCTGCGAGGG
GTGGGGGCCGGGCGCGCGGCGCAGTAAAGGGCCCCGTG-3'

B

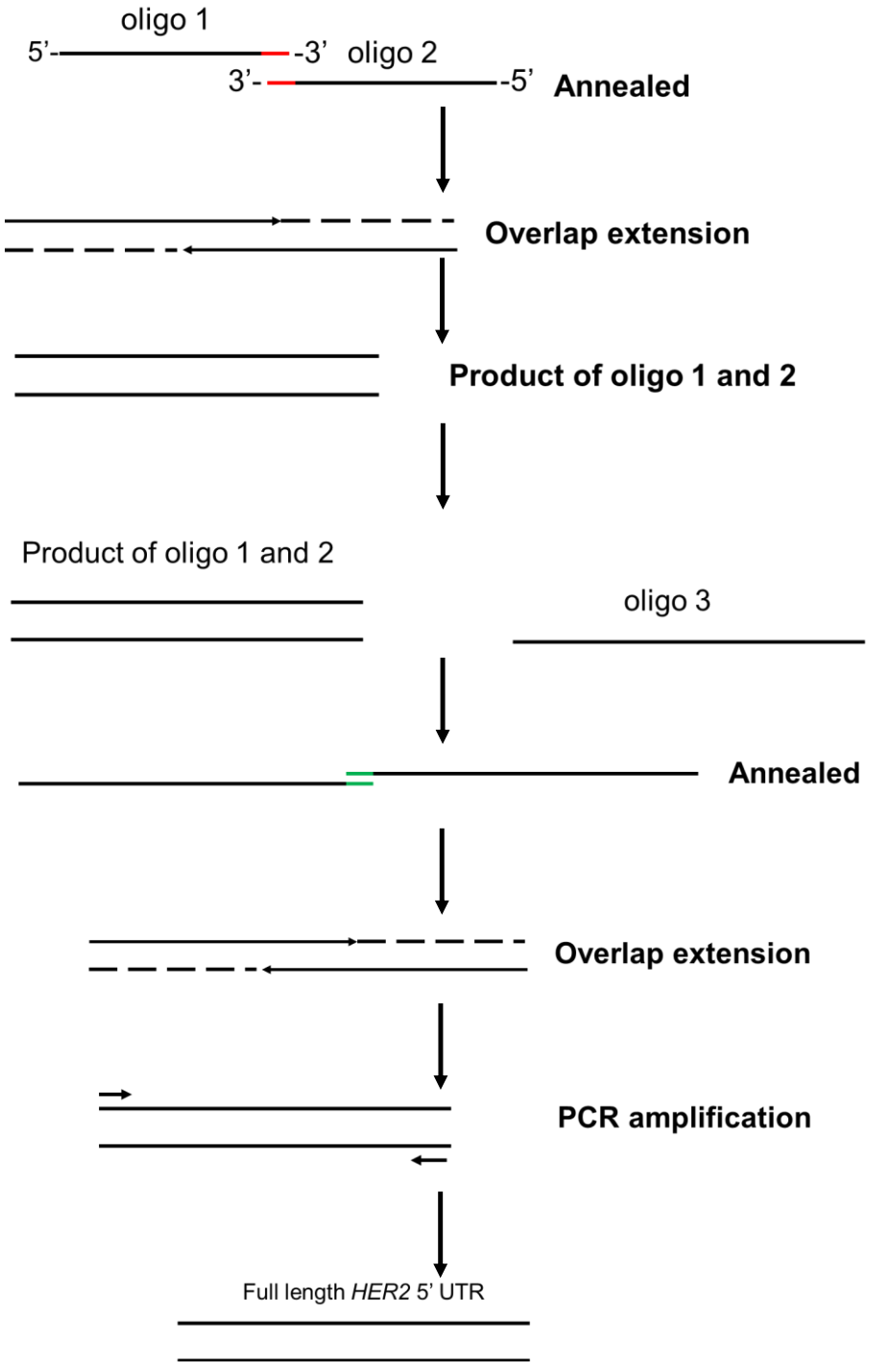

Figure 2.3. *HER2* 5' UTR synthesis from three oligonucleotides. A) DNA sequence of 3 oligonucleotides. Blue = sequence of complementarity to primers, red= sequence of complementarity between oligonucleotides 1 and 2, and green= sequence of complementarity between oligonucleotides 2 and 3. B) Schematic showing the synthesis of *HER2* 5' UTR from three oligonucleotides. Black small arrows= forward and reverse primers. Oligo= oligonucleotide.

Table 2.4. Oligonucleotides for synthesis of *HER4* 5' UTR. A single oligonucleotide used as a template for cloning into pRF. Region showing complementarity to the forward primer and reverse primer (primers: Table 2.5).

***HER4* 5' UTR oligonucleotide sequence (5'-3')**
CACGCGCGCCCGGCTGGGGGATCTCCTCCGCGTGCCCGAAAGGG GGATATGCCATTTGGACATGTAATTGTCAGCACGGGATCTGAGAC TTCCAAAAAATG

2.2.6. *HER2* 3' UTR g-block cloning

500 ng of g-block containing the sequence of *HER2* 3' UTR (Integrated DNA Technologies) (Figure 2.4) was resuspended and diluted with nuclease-free water to a final concentration of 50 ng/µl. *HER2* 3' UTR sequence was amplified from the 50 ng of the g-block using a forward primer containing a *Pml*I restriction site and a reverse primer containing a *Fse*I restriction sites. The PCR was performed using the settings described in Section 2.2.4. The *HER2* 3' UTR sequence was then digested using *Pml*I and *Fse*I before being cloned into destabilised p15-*HER2* 5'UTR using these restriction sites. Successful cloning was confirmed by Sanger sequencing (Appendix-Figure 43).

Figure 2.4. *HER2* 3' UTR sequence cloned into destabilised p15-*HER2* 5' UTR plasmid . Sequence shows the last 20 nt of firefly luciferase ORF, vector sequences between ORFs, hCL1 and hPEST sequence, *Pml*I restriction site, *HER2* 3' UTR sequence and *Fse*I restriction site.

2.2.7. Primer Sequences

Table 2.5. PCR primers

Primers for cloning into pRF	
Primer Name	**Sequences (5'-3')**
HER2 5' UTR *Eco*RI forward	ATGCTGAATTCGCTTGCTCCCAATCACAG
HER2 5' UTR *Bsp*HI reverse	ATGCATCATGATGCTCACTGCGGCTCCGG
HER4 5' UTR *Eco*RI forward	ATGCTGAATTCCACGCGCGCCCGGCTGG
HER4 5'UTR *Nco*I reverse	ATGCACCATGGTTTGGAAGTCTCAGATCC
Primers for subcloning into p15	
HER2 5' UTR *Hind*III forward	TCACTAGTCAGCTGAAGCTTGCTTGCTCCC
HER2 5' UTR *Hind*III reverse	GTTTTTGGCGTCTTAAGCTTGGTGCTCACT
HER4 5' UTR *Hind*III forward	TCACTAGTCAGCTGAAGCTTCACGCGCGCC
HER4 5' UTR *Hind*III reverse	GTTTTTGGCGTCTTAAGCTTTTTTTGGAAG
Primers for subcloning into p15 and p15-*HER2* 5' UTR	
hCL1-hPEST *Eco*RI forward	GCCGTGAATTCTGCTTGCAAGAACTGGTTCAG
hCL1-hPEST *Fse*I reverse	GTACAGGCCGGCCATCTAGACTGCACGTGGACG TTGATCCTGGCGCTGGTAA
Primers for cloning into destabilised p15-*HER2* 5' UTR	
HER2 3' UTR *Pml*I forward	GTGTGACACGTGACCAGAAGGCCAAGTC

HER2 3’ UTR *Fse*I reverse	GTAATGGCCGGCCAGCTGTTTTCCAAAATATATTTGCAAATGG

Table 2.6. qPCR primers

Primer Name	**Sequences (5’-3’)**
GAPDH forward	TCGGAGTCAACGGATTTGGT
GAPDH reverse	TTCCCGTTCTCAGCCTTGAC
β-actin forward	AGCACAGAGCCTCGCCTTT
β-actin reverse	TCATCATCCATGGTGAGCTG
HER2 forward	GACTCTGGAAGAGATCACAGGTTA
HER2 reverse	CTTGCAGGGTCAGCGAGT
HER4 forward	TGCAGACACCATTCATTGGC
HER4 reverse	TATGGCAACGTCCACATCCT

2.2.8. Agarose Gel Electrophoresis

DNA was separated according to its molecular weight by electrophoresis from an agarose gel. A 1% w/v agarose gel was melted in 1X TAE buffer in a volume of 50 ml and cast in a plastic tray after the addition of 2 µl of 10mg/ml ethidium bromide solution (Sigma-Aldrich) or 1X SYBR safe DNA gel stain (Thermo Fisher Scientific). DNA was mixed with 6X loading dye (NEB) and loaded onto wells alongside a 1 kb or 1kb plus DNA ladder (NEB). The gel was submerged in 1X TAE buffer and a voltage of 100 V was applied to the DNA for 1 hour. Then the DNA was visualised using a UV transilluminator.

2.2.9. Purification of DNA from Agarose Gel

DNA was excised from gels using a scalpel and purified using the Monarch Gel Extraction kit (NEB) following manufacture's protocol. Adaptations to the manufacture's protocol included eluting the DNA with 12 µl of DNA Elution Buffer (NEB). The DNA concentration was determined using a Nanodrop 1000 spectrophotometer (Thermo Scientific) by measuring optical absorbance at 260 nm. The 280/260 and 260/230 ratios were used to check the DNA purity.

2.2.10. Restriction Digest

1 µg of DNA was digested with restriction enzymes in the appropriate restriction digestion buffer according to the manufacturer's instructions (NEB). 50 µl reactions were performed at 37°C for 1 hour. Calf Intestinal Alkaline Phosphatase (NEB) was added 30 minutes into the reaction containing the plasmid DNA, to dephosphorylate the plasmid DNA and prevent re-ligation. After the restriction digestion, enzymes were heat inactivated. Table 2.7

provides details of the enzymes and buffers and conditions used for the restriction digestion reactions.

Table 2.7. Restriction enzymes and the conditions used in the study. The restriction enzyme, the reaction buffer, reaction temperature and the deactivation temperature and duration used in this project. According to manufacturer's instructions, NEB.

Enzyme Name	**Buffer**	**Reaction Temperature**	**Deactivation Temperature and Time**	**Plasmid/Insert the enzyme digested**	**Plasmid the insert (s) were cloned into**
*Bsp*HI	1X CutSmart Buffer	37°C	80°C for 20 minutes	Insert: *HER2* 5' UTR	pRF
EcoRI	1X NEBuffer 2.1	37°C	65°C for 20 minutes	Plasmids: pRF, p15, p15-*HER2* 5' UTR	N/A
				Inserts: *HER2* 5' UTR, *HER4* 5' UTR	pRF
				Insert: hCL1-hPEST	p15, p15-*HER2* 5' UTR
*Nco*I	1X NEBuffer 2.1	37°C	80°C for 20 minutes	Plasmid: pRF	N/A
				Insert: *HER4* 5' UTR	pRF
*Hind*III	1X NEBuffer 2.1	37°C	80°C for 20 minutes	Plasmid: p15	N/A
				Inserts: *HER2* 5' UTR, *HER4* 5' UTR	p15
*Fse*I	1X CutSmart Buffer	37°C	65°C for 20 minutes	Plasmids: p15, p15-*HER2* 5' UTR and destabilised p15-*HER2* 5' UTR	N/A
				Insert: hCL1-hPEST	p15, p15-*HER2* 5' UTR
				Insert: *HER2* 3'UTR	destabilised p15-*HER2* 5' UTR
*Pml*I	1X CutSmart Buffer	37°C	65°C for 20 minutes	Plasmid: destabilised p15-*HER2* 5' UTR	N/A
				Insert: *HER2* 3' UTR	destabilised p15-*HER2* 5' UTR

2.2.11. Ligation

DNA fragments were ligated into DNA plasmids using T4 DNA ligase (NEB). Reactions consisted of 2 µl of 10X DNA ligase buffer (NEB), 1 µl T4 DNA ligase and a ratio of 7:1 insert to vector at a total volume of 20 µl. The reactions were incubated at 16°C overnight in a PCR machine. The reactions were transferred to ice and 5 µl of ligation reaction was transformed into typically 50 µl of competent DH5α *E.coli* cells (Section 2.3.3.).

2.2.12. Polymerase Chain Reaction Colony Screening

A single colony of DH5α *E.coli* (originally supplied from Invitrogen) was picked from the agar plates using a pipette tip (Section 2.3.3.) and used as a template for the PCR reaction. The single colony was mixed into the following reaction mixture according to the manufacturer's instructions (NEB); 1x Phusion GC Buffer, 10 mM dNTPs, 3% DMSO, 0.5 µM of each forward and reverse primer and 0.4 units of Phusion high-fidelity DNA polymerase to a final volume of 20 µl.

The reactions were performed in a PCR machine and the initial denaturation temperature was 98 °C for 5 minutes to burst open and release the DNA from the bacterial cells. Then the DNA entered a cycle of denaturation at 98 °C for 10 seconds, annealing at 66.5°C 20 seconds and an extension at 72 °C for 40 seconds. 35 cycles were completed before the final extension at 72 °C for 20 seconds. The DNA produced from the PCR was then visualised by gel electrophoresis.

2.2.13. Protein Extraction

MCF-7 cells were seeded at a density of 0.3 x10^6 in a 6-well plate for protein extractions. Following glutamine or glucose starvation (Section 2.1.4.) cells were scraped in PBS. Then cells were centrifuged at 4000 RPM for 30 minutes and the supernatant was discarded. The cell pellet was lysed in RIPA buffer (RIPA buffer recipe-2.2.1) supplemented with cOmplete Mini Protease Inhibitor Cocktail (Roche) diluted to 1X, and phosphatase inhibitors; 20 mM sodium fluoride and 5 mM sodium orthovanadate. Lysed cells were incubated on ice for 10 minutes before being centrifuged at 13,000 RPM for 10 minutes and the supernatant was collected. Protein lysates were stored at -80°C until required.

2.2.14. Bradford Protein Assay

A Bradford assay was performed to measure the protein concentration of each sample. This was carried out by mixing 2µl of protein sample, 798 µl of dH_20 and 200 µl of Bradford Reagent (BioRad). The samples were left to incubate for 10 minutes then the optical density of each sample was measured at 595 nm. The protein concentration of each sample was calculated from a standard curve that was made from a blank (no BSA) and a series of BSA standards (Thermo Scientific) with concentrations of 2 µg/ml, 4 µg/ml, 6 µg/ml,8 µg/ml and 10 µg/ml. All protein samples and BSA standards were carried out in triplicate.

2.2.15. Sodium Dodecyl Sulfate–Polyacrylamide (SDS-PAGE)

Sodium dodecyl sulfate–polyacrylamide gel was made from a 10% resolving gel and a 5% stacking gel according to the components in Tables- 2.8 and 2.9. ~15 ml of resolving gel was poured between two 1.5 mm glass plates (~7.5 ml per gel) immediately after the addition of TEMED. Isopropanol was layered

over the top and the gel was left to set for 20 minutes. Isopropanol was poured off each plate and then ~2.4 ml of stacking gel was poured to each 1.5 mm glass plate immediately after the addition of TEMED. The gel lane comb was placed on top of the 1.5 mm glass plates and the stacking gel was left to set for 20 minutes.

10-30µg of protein was denatured in 1X SDS loading dye (200 mM Tris-Cl (pH 6.8), 400 mM DTT, 8% SDS, 0.4% bromophenol blue and 40% glycerol) at 100 ºC for 5 minutes. Protein samples were separated onto a 10% SDS-PAGE gel in 1X SDS running buffer at 150 V until the dye front reached the bottom of the gel.

Table 2.8. SDS-PAGE 5% Stacking gel components

Reagents	**Reagent volume**
H_2O	3.4 ml
30% w/v Acrylamide	0.83 ml
1.0 M Tris pH 6.8	0.63 ml
10% w/v SDS	0.05 ml
10% w/v APS	0.05 ml
TEMED	0.005 ml

Table 2.9. SDS-PAGE 10% Resolving gel components

Reagent	**Reagent volume**
H_2O	5.9 ml
30% w/v Acrylamide	5 ml
1.5 M Tris pH 8.8	3.8 ml
10% w/v SDS	0.15 ml
10% w/v APS	0.15 ml
TEMED	0.006 ml

2.2.16. Western Blotting

Proteins were transferred onto a nitrocellulose membrane soaked in 1X Tris-Glycine Buffer (recipe 2.2.1) at either 60 V for 2 hours or 30 V overnight using a wet-transfer machine (Bio-Rad). Membranes were stained with Ponceau S staining solution (0.1% w/v Ponceau S in 5% acetic acid) to confirm successful transfer of proteins. Then Ponceau S staining solution was removed from the membranes using TBS. Membranes were blocked in TBST (TBS supplemented with 0.1% Tween, Sigma) containing 5% BSA powder (Fisher Scientific). 10 mM sodium fluoride and 1 mM sodium orthovanadate were supplemented to the blocking and primary antibody solutions. Primary antibodies were incubated overnight in TBST at 4 °C. Membranes were washed 3x for 5 minutes in TBST then incubated in appropriate secondary antibody for 1 hour at room temperature. Membranes were washed 3x for 5 minutes then were incubated in developing solution (Pierce ECL Western Blotting Substrate, Thermo Scientific) for 1 minute. Images were detected via chemiluminescence signals using a Western Blot imager, LAS-4000 Fujifilm.

2.2.16.1. Antibodies

The anti-HER2 rabbit polyclonal antibody (Cell Signalling, Cat# 2242) was used at a 1:1000 dilution, eIF2α rabbit polyclonal antibody (Cell Signalling, Cat# 9722) was used at a 1:1000 dilution, Phospho-eIF2α rabbit polyclonal antibody (Ser51) (Cell Signalling, Cat# 9721) was used at a 1:500 dilution, anti-lamin A/C (4C11) mouse monoclonal antibody (Cell Signalling, Cat# 4777) served as a loading control and was used at a 1:1000 dilution, anti-rabbit IgG HRP-linked secondary antibody (Cell Signalling, Cat# 7074) was used at a 1:3000 dilution

and anti-mouse IgG HRP-linked secondary antibody (Cell Signalling, Cat# 7076) was used at a 1:3000 dilution.

2.2.17. RNA Extraction

Total RNA was isolated from confluent MCF-7 cells plated on a 6-well plate by first detaching cells from the wells using 1x trypsin. Then cells were pelleted at 2,000 RPM for 5 minutes. RNA was extracted using RNeasy Plus Mini Kit (Qiagen) following the manufacturer's protocol. RNA was eluted with 50 µl of RNase free water for 1 minute at 10,000 rpm. RNA concentration was measured using Nanodrop 1000 spectrophotometer (Thermo Scientific) by measuring optical absorbance at 260 nm. RNA samples were stored at -80˚C until required.

2.2.18. Reverse Transcriptase reaction

RNA was diluted to 100 ng/ µl with ddH20 and was reverse transcribed into cDNA using GoScript Reverse Transcriptase Kit (Promega). According to the manufacture's protocol, 1 µl of 100 ng/µl RNA and 0.5 µl of 0.5 ng/µl Random Primers were made up to 5 µl with ddH20. Then the reaction mix was then heated at 70 °C for 5 minutes. The RNA/Random Primer Mix were chilled on ice for 5 minutes, then centrifuged and chilled on ice for a further 10 minutes. Then the reverse transcriptase mix was made with the following reagents: 4 µl of 5X Go Script Reaction Buffer, 4 µl of 3.2 mM $MgCl_2$, 1µl of 0.5 mM of PCR Nucleotide Mix and 1µl of GoScript Reverse Transcriptase (RT enzyme; M-MLV) which was made up to 15 µl with nuclease-free water. Then the 15 µl reverse transcriptase mix was added to the 5 µl RNA/Random Primer Mix producing a final volume of 20 µl and the sample was reversed transcribed using the thermocycler setting in Table 2.10.

Table 2.10. cDNA synthesis reaction settings. The reaction temperature and duration for each segment used for cDNA synthesis

Segment	**Temperature (°C)**	**Time (mins)**
Anneal	25	05:00
Extend	42	59:00:00
Inactivation of reverse transcriptase	75	15:00
Hold	4	N/A

2.2.19. Quantitative Polymerase Chain Reaction

qPCRs reactions were carried out using GoTaq qPCR Master Mix (Promega) using the Rotorgene machine (Qiagen). Primers were designed using NCBI Primer3 and BLAST (Figure 2.5). A master mix was made using 0.2 µl of each forward and reverse primer (100mM) (Table 2.6), 20 µl of GoTaq Master Mix and 17.4 µl of nuclease-free water to a total volume of 38 µl per reaction. 9.5 µl of mastermix was added per tube then 0.5 µl of cDNA was added to each tube. The reaction was carried out using the following settings: initial denaturation for 10 minutes at 95˚C; 40 cycles at 95 ˚C for 10 seconds, 58 ˚C for 15 seconds and 72 ˚C for 20 seconds. The fold change of each sample was calculated using the -ΔΔCt method relative to GAPDH house-keeping gene. No reverse transcriptase (-RT) and non-template controls were conducted to check for genomic DNA and reagent contamination respectively (Appendix-Figures 14-19, 28 and 30).

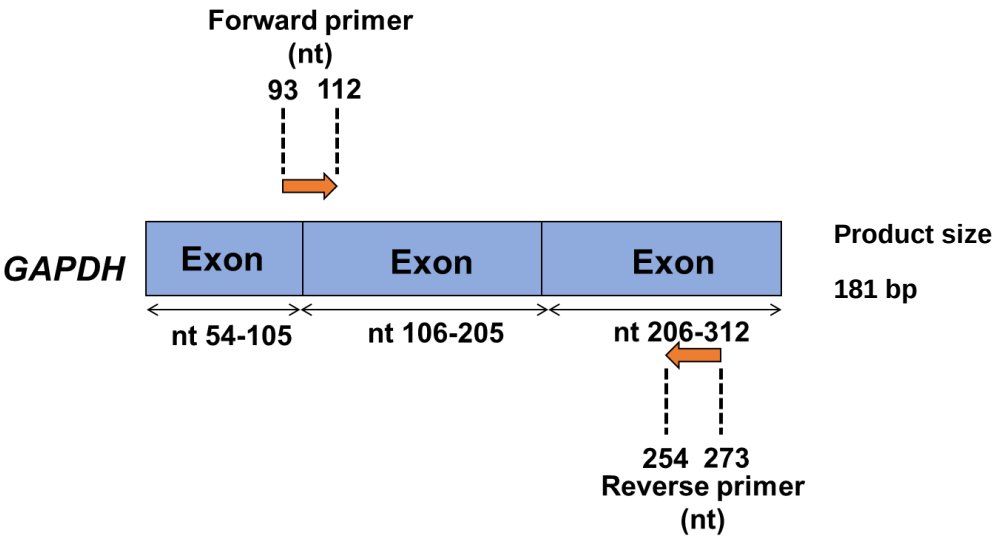
Forward primer
(nt)
93 112
GAPDH
Exon
Exon
Exon
Product size
181 bp
nt 54-105
nt 106-205
nt 206-312
254 273
Reverse primer
(nt)

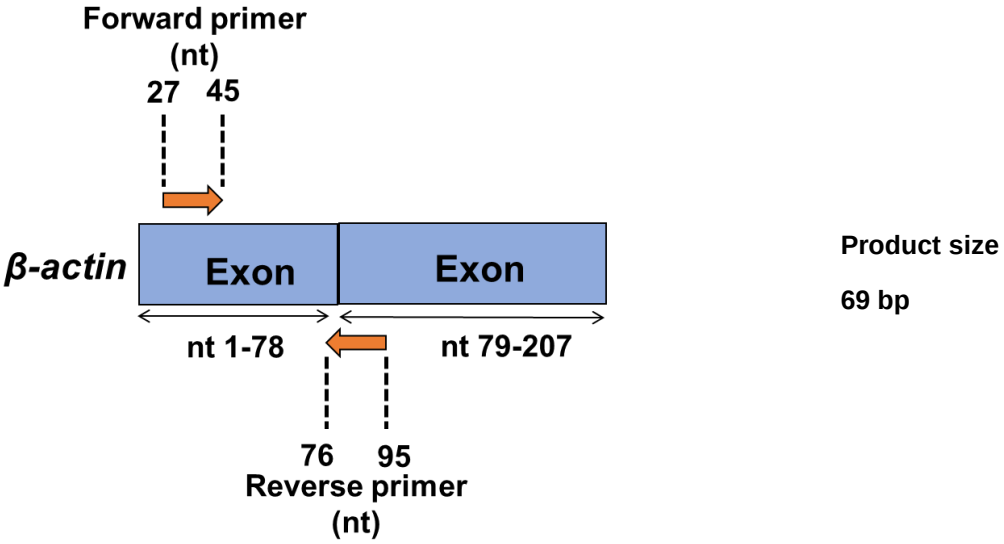
Forward primer
(nt)
27 45
β-actin
Exon
Exon
Product size
69 bp
nt 1-78
nt 79-207
76 95
Reverse primer
(nt)

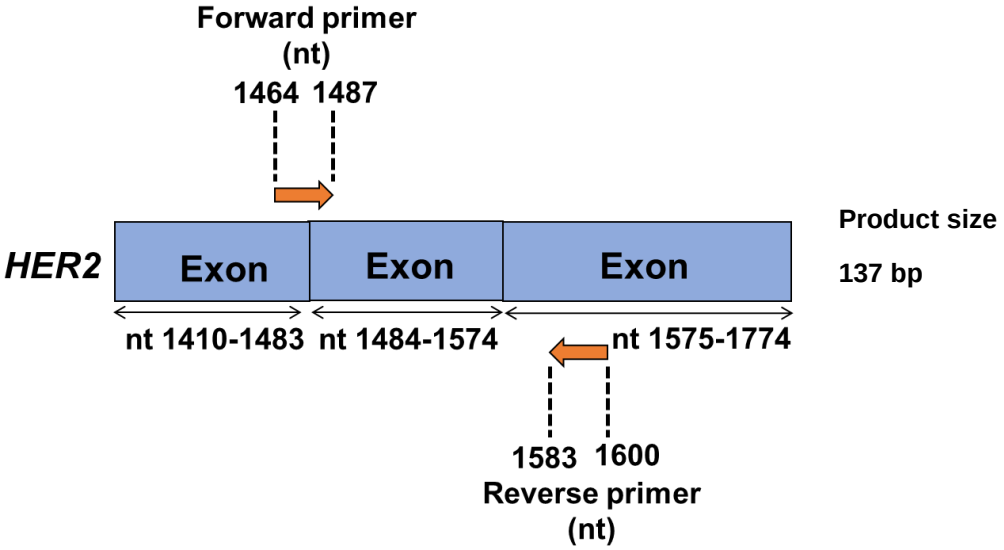
Forward primer
(nt)
1464 1487
HER2
Exon
Exon
Exon
Product size
137 bp
nt 1410-1483
nt 1484-1574
nt 1575-1774
1583 1600
Reverse primer
(nt)

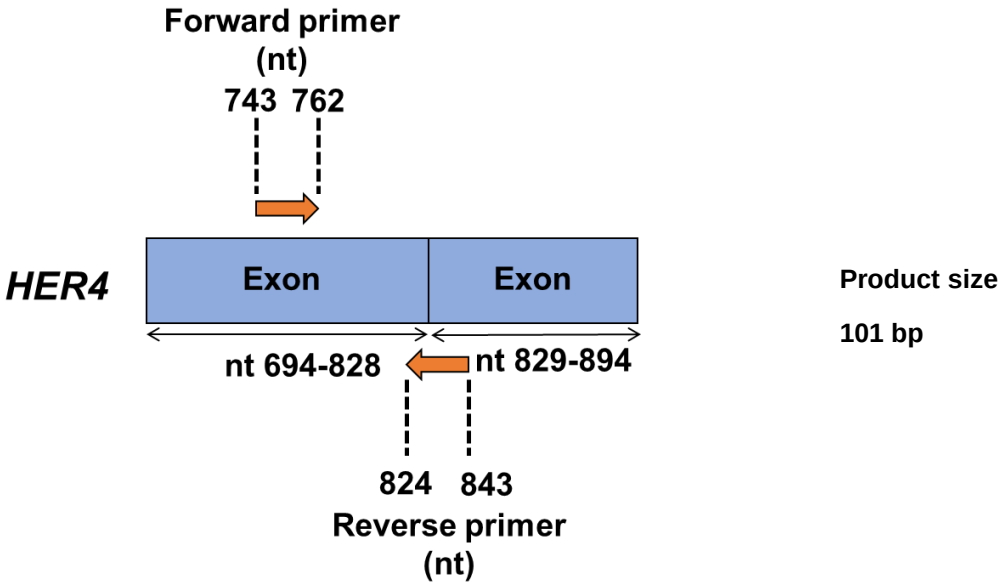

Figure 2.5. Schematic showing the location of the qPCR primer on the exons. The location of the qPCR primers in Table 2.5, on exons of *GAPDH* (accession number: NM_002046.7), *β-actin* (accession number: NM_001101.5) *HER2* (accession number: NM_004448.3) and *HER4* (accession number: NM_005235.2).

2.3. Bacterial Techniques

2.3.1. Reagents and Solutions

TFB1:30mM KOAc, 10mM CaCl2, 50mM MnCl2, 100mM RbCl, 15% glycerol

TFB2:10mM MOPS pH 6.5, 75mM CaCl2, 10mM RbCl, 15% glycerol

2.3.2. Preparing competent *E.coli* cells

A single colony was used to grow a 5 ml culture of DH5α *E.coli* cells overnight. The 5 ml culture was used to inoculate 250 ml culture of LB supplemented with 20 mM of $MgSO_4$. This was grown in a shaker incubator at 37°C until the optical density measured at A600 was between 0.4 and 0.6. The remaining steps were all performed at 4°C. Cells were pelleted by centrifuging at 4000 RPM for 10 minutes and resuspended in 100 ml of ice cold TBF1 and incubated on ice for 5

minutes. Cells were pelleted again at 4000 RPM for 10 minutes and resuspended in 6 ml of ice-cold TBF2 and incubated on ice for 60 minutes. The cells were aliquoted (200µl) then snapped frozen in liquid nitrogen and stored at -80 until required.

2.3.3. Transformation

5 µl of ligation mixture was added to 50 µl of competent DH5α *E.coli* cells and the mixtures were incubated on ice for 30 minutes. Then the mixture was heat-shocked at 42°C for 45 seconds, then was recovered on ice for 5 minutes. The mixture was then added to 750 µl of LB and incubated in a shaking incubator (215 RPM) at 37°C for 1 hour. Cells were then pelleted by centrifuging at 7,000 RPM for 2 minutes. The supernatant was removed, and cells were resuspended in 50-100 µl of LB and spread evenly onto agar plates containing ampicillin (100 µg/ml). Plates were incubated upside down at 37°C overnight.

2.3.4. Purification of Plasmid DNA from a Miniprep/Maxiprep Kit

A single colony of DH5α *E.coli* cells were used to start a culture in 10 ml of LB containing 10 µl of 100 µg/-ml ampicillin. Plasmid DNA was isolated and miniprepped using the NucleoSpin Plasmid Quick Purekit (Macherey-Nagel) following the manufacturer's instructions. DNA was eluted in 50 µl of nuclease-free water. Large-scale isolation of plasmid DNA was carried out using Plasmid Maxiprep Kit (Qiagen) following the manufacturer's instructions and DNA was eluted in 200 µl of nuclease-free water.

2.4. Statistical Analysis

Luciferase and MTT data was conducted using a t-test with Bonferroni-Dunn's correction. The *Renilla* luciferase and F/R p-values are stated in the Results chapters. qPCR analysis was conducted using a Mann-Whitney t-test with Bonferroni-Dunn's correction to compare two groups. All error bars represent the standard deviation. $p<0.05$ was determined statistically significant. All statistical analysis was conducted using GraphPad Prism (version 9.4.1, GraphPad Software, Inc).

Densitometric analysis was conducted for the western blots. The intensity of a given band was measured as the total volume under the peak in Image J v1.53e. Background values were obtained by measuring the total volume under the peak of an area where no protein was loaded. Then the background intensity was subtracted from each protein intensity. The values for the protein of interest was divided by lamin a/c loading control or total eIF2α levels.

Chapter 3 - *HER2* and *HER4* 5' UTRs did not mediate IRES-dependent translation in response to cell stress

3.1. Introduction

As mentioned in Chapter 1, Section 1.3.1.1, translation is regulated in response to cellular stress due to the phosphorylation of eIF2α. The phosphorylation of eIF2α leads to a reduction in cap-dependent translation but translation of specific mRNAs can take place via IRES-mediated translation (Zhou *et al.*, 2008). This is important for cancer cells as many cellular mRNAs containing IRESs often encode for growth factors, growth factor receptors and transcription factors that are commonly overexpressed in many cancers and aid cancer cell survival (Stein *et al.*, 1998; Webb *et al.*, 2015; Li *et al.*, 2016). IRESs are active in response to specific cellular stress conditions (Smalley, 2016). IRES activation can be cell-type specific and can be dependent on the presence of certain ITAFs (Créancier *et al.*, 2001; Cobbold *et al.*, 2008).

Many cellular stress conditions such as hypoxia and oxidative stress are commonly observed in cancers and can aid cancer cell progression (Mahalingaiah and Singh, 2014; Hoffmann *et al.*, 2018; Zenin *et al.*, 2022). *HER2* and *HER4* have been upregulated in response to some cellular stress conditions (discussed in this chapter) and have increased the expression of some genes involved in cell stress pathways such as *HIFα*, leading to an increase in cancer cell growth and survival (Paatero *et al.*, 2014; Jarman *et al.*, 2019).

The aim of this chapter was to determine whether *HER2* and *HER4* 5' UTRs contain an IRES present in non-stressed conditions or in response to ER stress, oxidative stress, hypoxia, low serum conditions, genotoxic stress and confluence stress. These stress conditions are observed in many cancers and some of these stress conditions have shown to affect the translation of other cellular IRESs (Lewis *et al.*, 2008; Riley *et al.*, 2010; Argüelles *et al.*, 2014; Halaby *et al.*, 2015;

Webb *et al.*, 2015; Yan *et al.*, 2020). Each stress condition was tested on MCF-7 breast cancer cells using bicistronic luciferase reporters containing *HER2* or *HER4* 5' UTRs inserted into the intercistronic region. The identification of an IRES in the 5' UTR of *HER2* and *HER4* could be an important therapeutic target for cancer therapy.

3.2. Generating *HER2* and *HER4* 5' UTR bicistronic luciferase constructs

To assess whether *HER2* and *HER4* 5' UTRs contain an IRES, each 5' UTR was cloned into a bicistronic luciferase plasmid, pRF (Figure 3.1). Bicistronic reporter systems containing firefly (*Photinus pyralis*) -luciferase downstream of a *Renilla reniformis* luciferase open reading frame are widely used for assessing IRES activity (Stoneley *et al.*, 2000; Allera-Moreau *et al.*, 2007). *Renilla* luciferase is translated in a cap-dependent manner whereas firefly luciferase is only produced if an IRES is present in the intercistronic region (Nanbru *et al.*, 1997; Stoneley *et al.*, 2000). The *Renilla* luciferase activity is used to normalise the firefly luciferase expression and acts as an internal control to account for differences in transfection efficiency. The firefly luciferase expression is divided by the *Renilla* luciferase expression and referred to as the F/R ratio. Successful cloning of *HER2* and *HER4* 5' UTRs was confirmed by Sanger sequencing described in Chapter 2 (plasmids-Table 2.2 and primers-Table 2.5). *EGFR* 5' UTR was previously shown to contain an IRES and was used as positive control (Smalley, 2016). *β-tubulin* 5' UTR is known to not contain IRES activity and was used as a negative control (Smalley, 2016). A pRF vector containing no 5' UTR inserted into the intercistronic region was also used as a negative control

(Stoneley et al., 2000). All the constructs used in this chapter are shown in Figure 3.2.

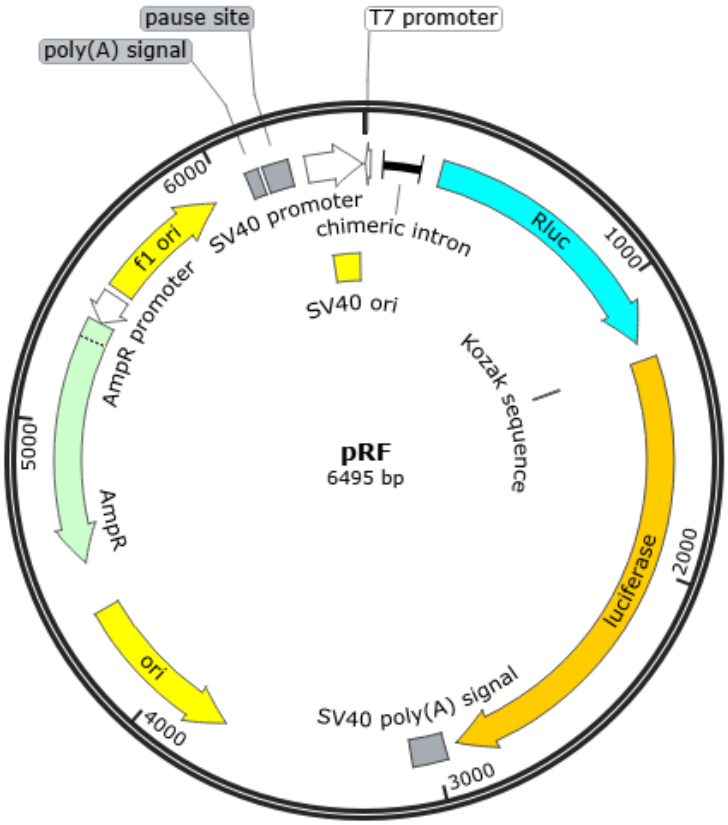

Figure 3.1. Bicistronic luciferase construct-pRF vector map. pRF plasmid contains a SV40 promoter upstream to luciferase open reading frames. The 5' UTRs were cloned in the intercistronic region in pRF between the *Renilla* luciferase and firefly luciferase open reading frames.

i)

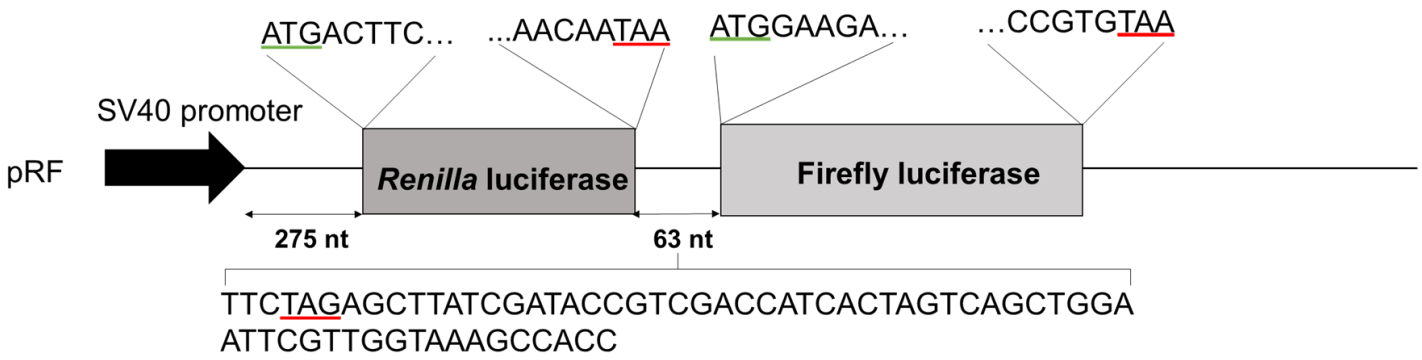
ATGACTTC…
...AACAATAA
ATGGAAGA…
…CCGTGTAA
SV40 promoter
pRF
Renilla luciferase
Firefly luciferase
275 nt
63 nt
TTCTAGAGCTTATCGATACCGTCGACCATCACTAGTCAGCTGGA
ATTCGTTGGTAAAGCCACC

ii)

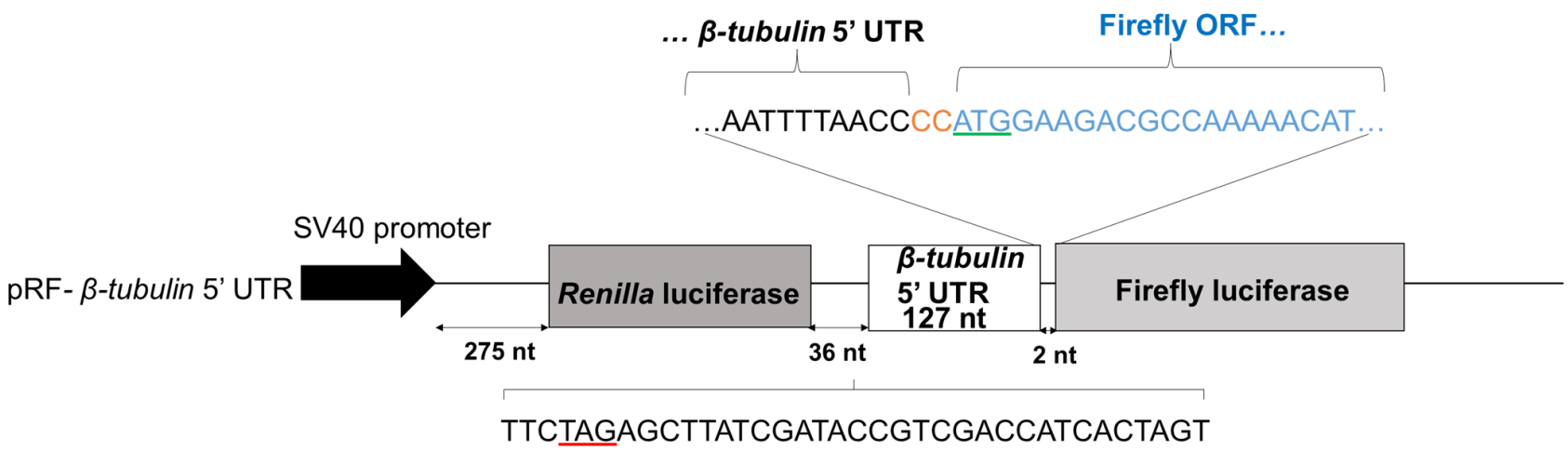
… β-tubulin 5' UTR
Firefly ORF…
…AATTTTAACCCCATGGAAGACGCCAAAAACAT…
SV40 promoter
pRF- β-tubulin 5' UTR
Renilla luciferase
β-tubulin
5' UTR
127 nt
Firefly luciferase
275 nt
36 nt
2 nt
TTCTAGAGCTTATCGATACCGTCGACCATCACTAGT

iii)

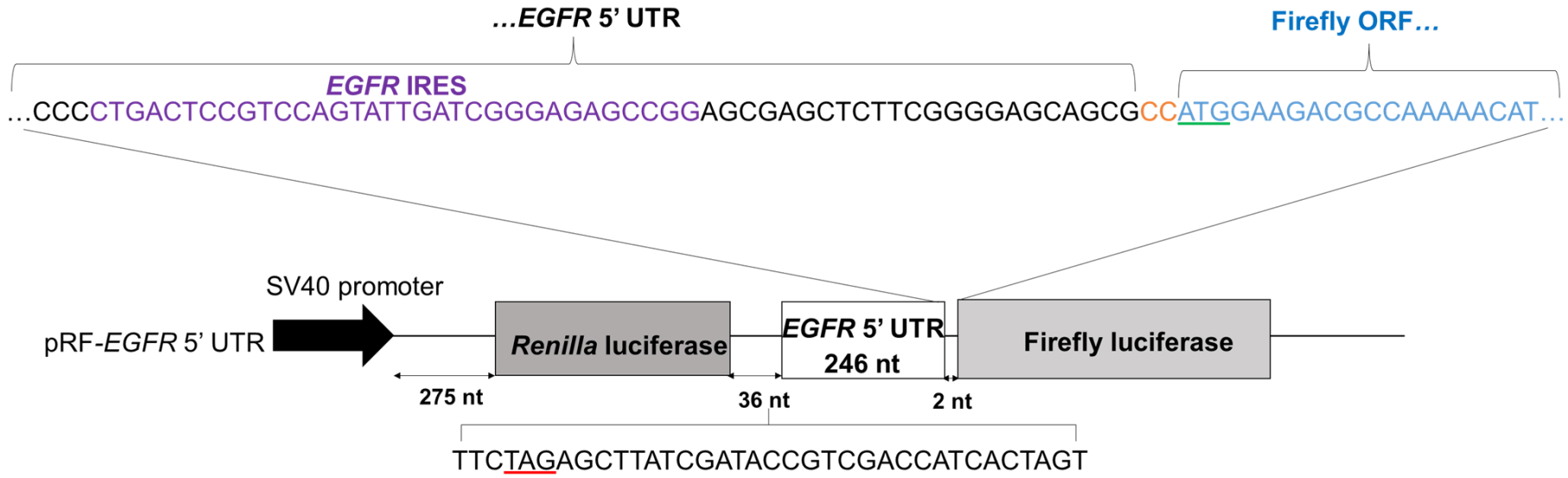
…EGFR 5' UTR
Firefly ORF…
EGFR IRES
…CCCCTGACTCCGTCCAGTATTGATCGGGAGAGCCGGAGCGAGCTCTTCGGGGAGCAGCGCCATGGAAGACGCCAAAAACAT…
SV40 promoter
pRF-EGFR 5' UTR
Renilla luciferase
EGFR 5' UTR
246 nt
Firefly luciferase
275 nt
36 nt
2 nt
TTCTAGAGCTTATCGATACCGTCGACCATCACTAGT

iv)

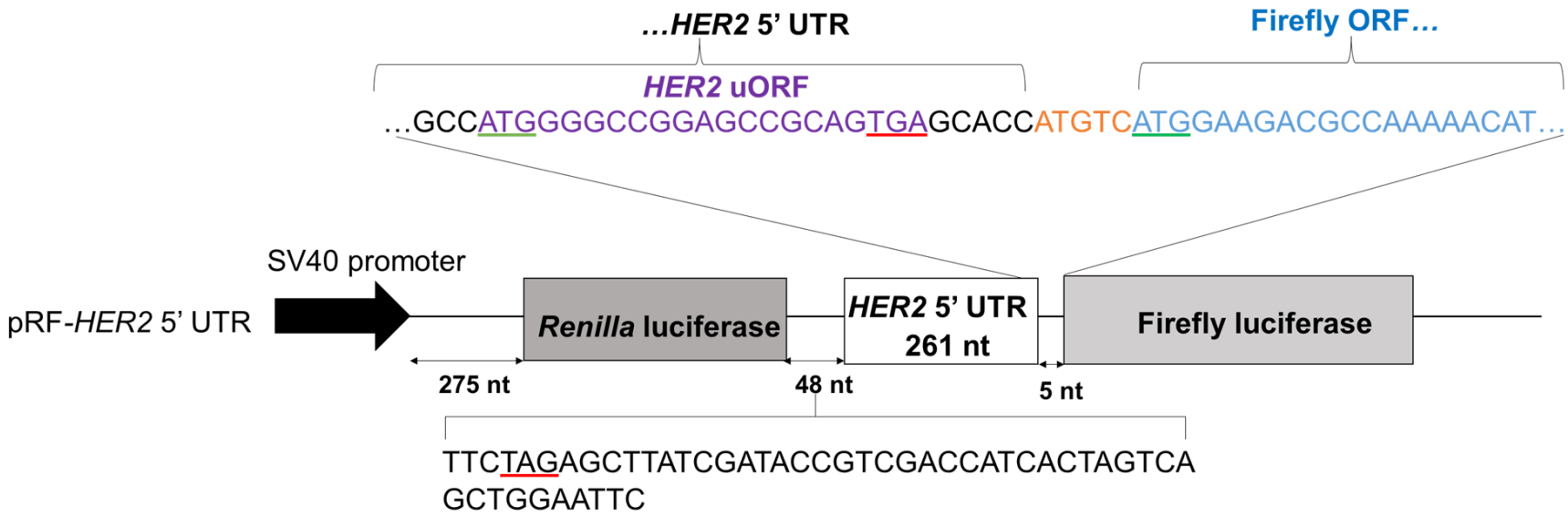
…HER2 5' UTR
Firefly ORF…
HER2 uORF
…GCCATGGGGCCGGAGCCGCAGTGAGCACCATGTCATGGAAGACGCCAAAAACAT…
SV40 promoter
pRF-HER2 5' UTR
Renilla luciferase
HER2 5' UTR
261 nt
Firefly luciferase
275 nt
48 nt
5 nt
TTCTAGAGCTTATCGATACCGTCGACCATCACTAGTCA
GCTGGAATTC

v)

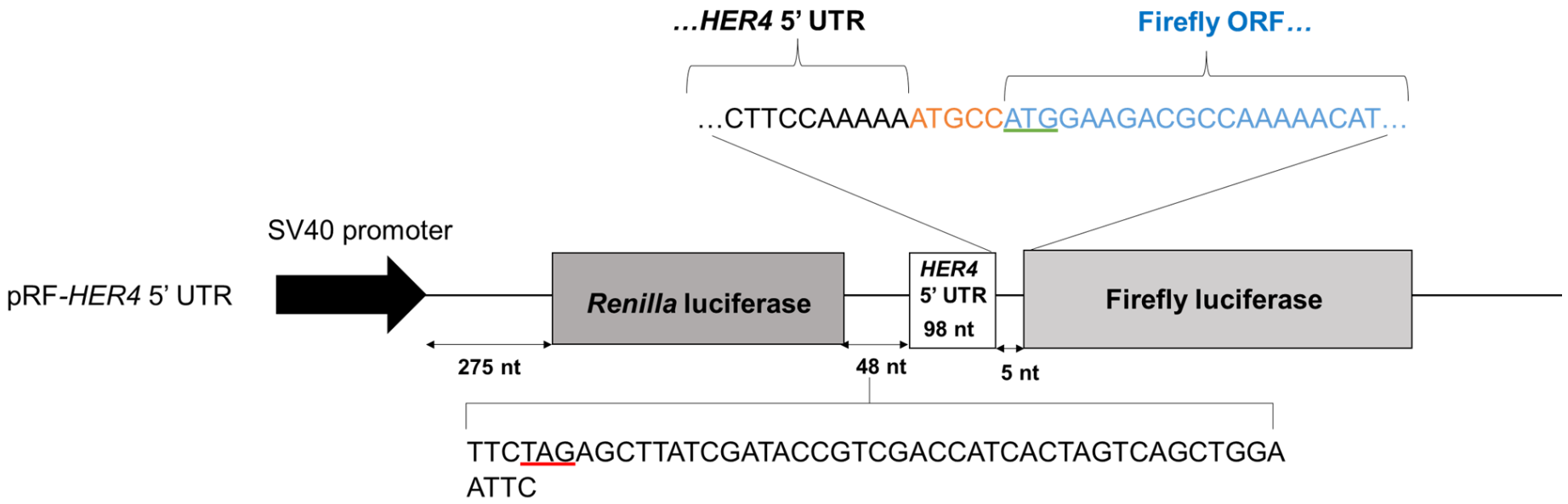

Figure 3.2. Schematics of the bicistronic constructs used in this project. i) pRF plasmid containing no 5' UTR inserted into the intercistronic region was used as a negative control. *Renilla* and firefly luciferase start and stop codons are underlined green or red respectively. The *Renilla* and firefly luciferase ORF sequences are the same for all the bicistronic constructs. ii) pRF-*β-tubulin* 5' UTR was used as a negative control. iii) *EGFR* 5' UTR IRES (*EGFR* IRES highlighted purple, source: Webb, 2012) was used as positive control and referred to as pRF-*EGFR*-5' UTR. The 5' UTRs of *HER2* and *HER4* were cloned in the intercistronic region in pRF between the *Renilla* luciferase and firefly luciferase open reading frames and referred to as iv) pRF-*HER2* 5' UTR (*HER2* uORF is highlighted purple) and v) pRF-*HER4* 5'UTR respectively. Start codons are underlined green and stop codons are underlined red.

3.3. *HER2* and *HER4* 5' UTRs are unable to induce firefly luciferase expression under non-stressed conditions

Initially, the bicistronic constructs were transfected into unstressed MCF-7 cells to determine if there was evidence of IRES activity mediated by *HER2* and *HER4* 5' UTRs under non-stressed conditions. It was found that there was some background firefly luciferase and F/R expression from pRF (Appendix Figure 1 and Figure 3.3). The *Renilla* luciferase expression of the bicistronic constructs were at similar levels except for bicistronic constructs containing *β-tubulin* 5' UTR which had a slightly higher expression. This could be due to variation in cell numbers (Appendix Figure 1). However, the firefly luciferase and the F/R expression mediated from *β-tubulin* 5' UTR was still at background levels (Appendix Figure 1 and Figure 3.3). *EGFR* 5' UTR showed a 5.5-fold increase in the F/R expression compared to pRF (Figure 3.3). This was due to *EGFR* IRES increasing the translation of firefly luciferase (Appendix Figure 1). However, the firefly luciferase and the F/R expression mediated from *HER2* 5' UTR was 4.7- folds lower than pRF indicating that *HER2* 5' UTR blocked readthrough signals. *HER4* 5' UTR mediated background firefly luciferase and F/R levels similar to the negative controls (Appendix Figure 1 and Figure 3.3).

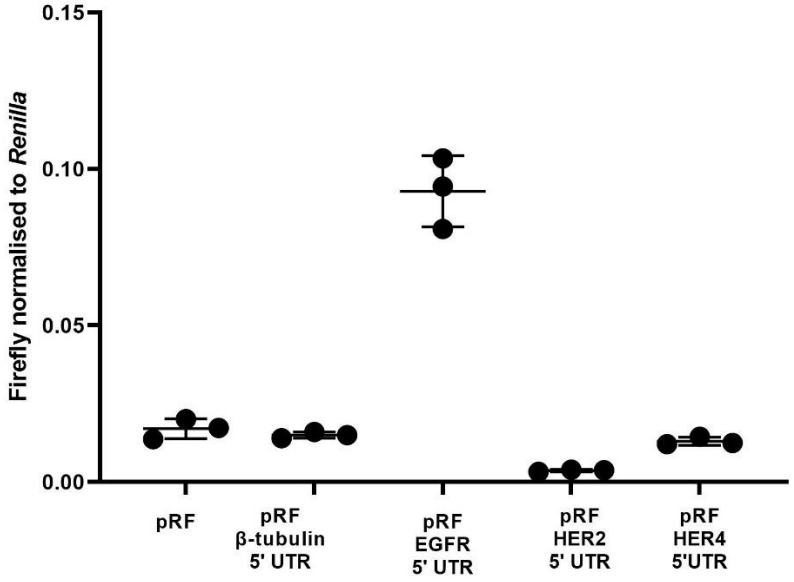

Figure 3.3. *HER2* and *HER4* 5' UTRs are unable to mediate cap-independent translation in contrast to *EGFR* IRES under non-stressed conditions. MCF-7 cells were transfected with bicistronic constructs containing both *Renilla* and firefly luciferase open reading frames. 24 hours post-transfection cells were lysed and the F/R activity was measured. Data represents one independent experiment taken in triplicate. All error bars represent the standard deviation.

3.4. The effect of endoplasmic reticulum stress on the translational control by *HER2* and *HER4* 5' UTRs

After establishing in contrast to *EGFR*, that *HER2* and *HER4* 5' UTRs do not show IRES activity under unstressed conditions, next it was investigated whether they might contain IRESs that only become active in response to cellular stress. The first cellular stress tested was ER stress which has shown to maintain the translation of other cellular IRESs such as *MYC* in response to ER stress. Furthermore, MYC expression can be regulated by HER2 (Park *et al.*, 2005; Nair *et al.*, 2013; Shi *et al.*, 2016). In addition, Nuclear Factor Erythroid 2 (NFE2) is activated by PERK and can aid the survival of HER2-positive breast cancer cells in response to ER stress by degrading misfolded proteins (Cullinan *et al.*, 2003; Singh *et al.*, 2015; Chen *et al.*, 2017). NFE2 can also increase the expression of HER2 and HER4 (Khalil *et al.*, 2016; Kankia *et al.*, 2021).

To determine if *HER2* or *HER4* 5' UTRs contain an IRES that is active under ER stress, MCF-7 cells were transfected with bicistronic luciferase reporters and were exposed to different concentrations of ER stress inducer thapsigargin (0.5 µM, 1 µM and 2 µM) or the equivalent percentage of DMSO as a control. First, the *Renilla* luciferase expression was assessed to determine if thapsigargin could reduce cap-dependent translation and induce cell stress. Overall, it was found that the *Renilla* luciferase expression was not reduced in response to thapsigargin indicating that cells were not sufficiently stressed. The exception to this was a reduction in the *Renilla* luciferase expression in response to 1 µM of thapsigargin from pRF ($p<0.001$) and bicistronic constructs containing *EGFR* 5' UTR ($p=0.051$) demonstrating it reduced cap-dependent translation in this condition for these two constructs at 1 µM of thapsigargin treatment (Figure

3.4). There was an unexpected increase in the *Renilla* expression from pRF in response to 2 µM of thapsigargin (p=0.006) (Figure 3.4). However, more replicates are needed as variations could be due to other factors such as differences in cell numbers.

The firefly luciferase and the F/R expression from pRF was overall not affected by thapsigargin treatment at concentrations of 0.5 µM (p= 0.605) and 2 µM (p=0.142) except for an unexpected increase in the F/R expression in response to 1 µM of thapsigargin (p<0.001) (Figure 3.5). However, there was a decrease in the firefly luciferase expression from pRF in response to 1 µM of thapsigargin treatment (Appendix 2). This is unlikely to be biologically relevant given that the firefly luciferase and the F/R expression was at background levels (Appendix Figure 2 and Figure 3.5). The *EGFR* IRES had no effect on the firefly luciferase and the F/R expression in response to 0.5 µM (p=0.137) of thapsigargin (Appendix Figure 2 and Figure 3.5). However, *EGFR* IRES induced a statistically significant decrease on the firefly luciferase and the F/R expression in response to 1 µM (p=0.012) and 2 µM (p= 0.047) of thapsigargin (Appendix Figure 2 and Figure 3.5). This is consistent with previous reports that found that *EGFR* IRES reduced firefly luciferase activity in response to 1 µM of thapsigargin (Smalley, 2016). There was no change in the firefly luciferase and the F/R expression mediated from bicistronic constructs containing *HER2* or *HER4* 5' UTRs in response to 0.5 µM (p=0.920 and p=0.309), 1 µM (p=0.443 and p=0.923) and 2 µM (p=0.870 and p=0.611) of thapsigargin respectively (Appendix Figure 2 and Figure 3.5). This suggests that there was no evidence of IRES activity in *HER2* or *HER4* 5' UTRs in response to thapsigargin.

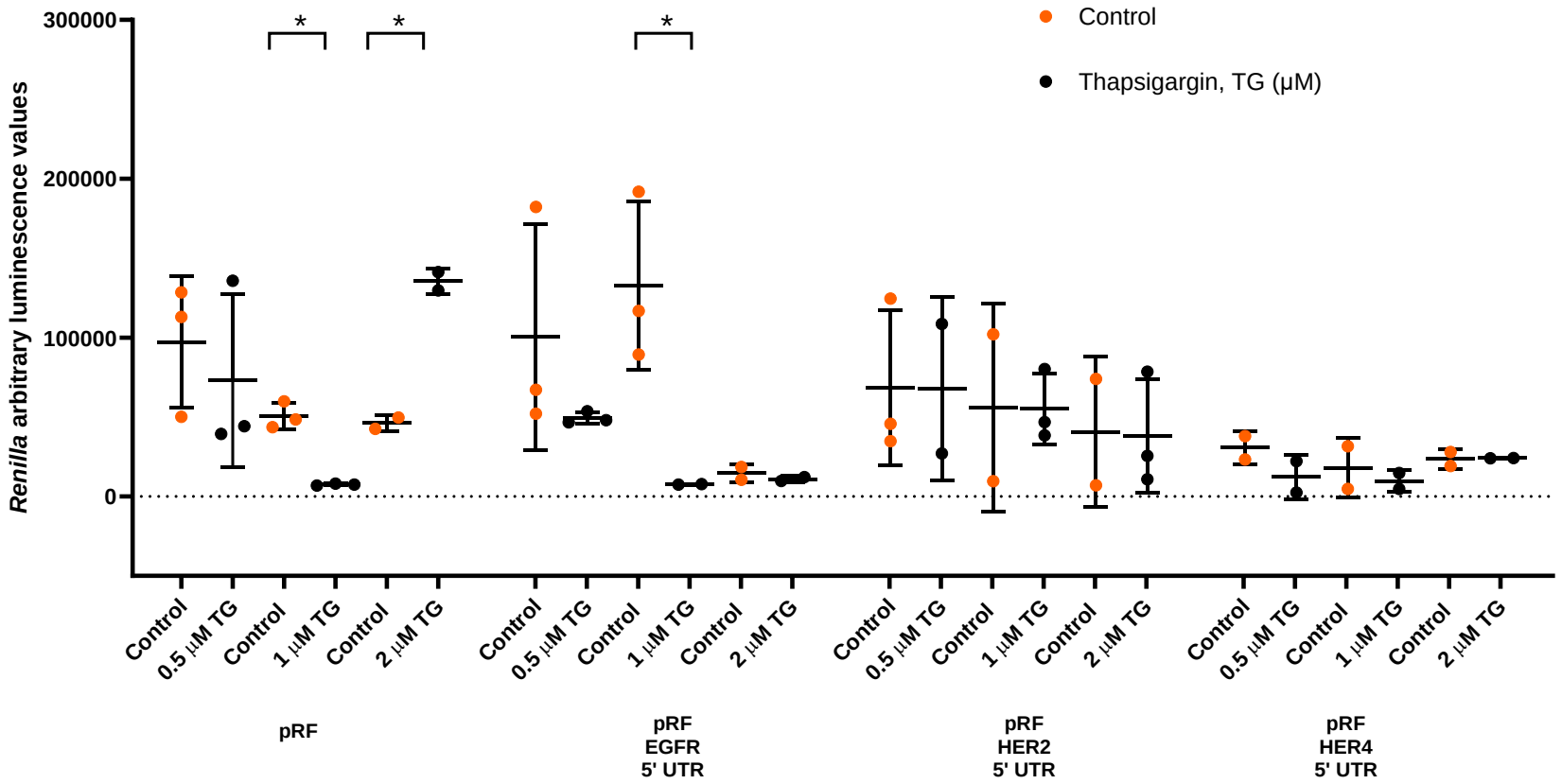

Figure 3.4. The *Renilla* luciferase expression in response to thapsigargin. MCF-7 cells were transfected with bicistronic constructs. 24 hours post-transfection MCF-7 cells were exposed to either 0.5 μM, 1 μM or 2 μM of thapsigargin (black) or respective DMSO controls (orange). 24 hours later cells were lysed and the *Renilla* luciferase expression was measured. Data represents the average of two-three independent experiments each carried out in triplicate. All error bars represent the standard deviation. $p<0.05$ was determined statistically significant using a t-test with Bonferroni-Dunn's correction.

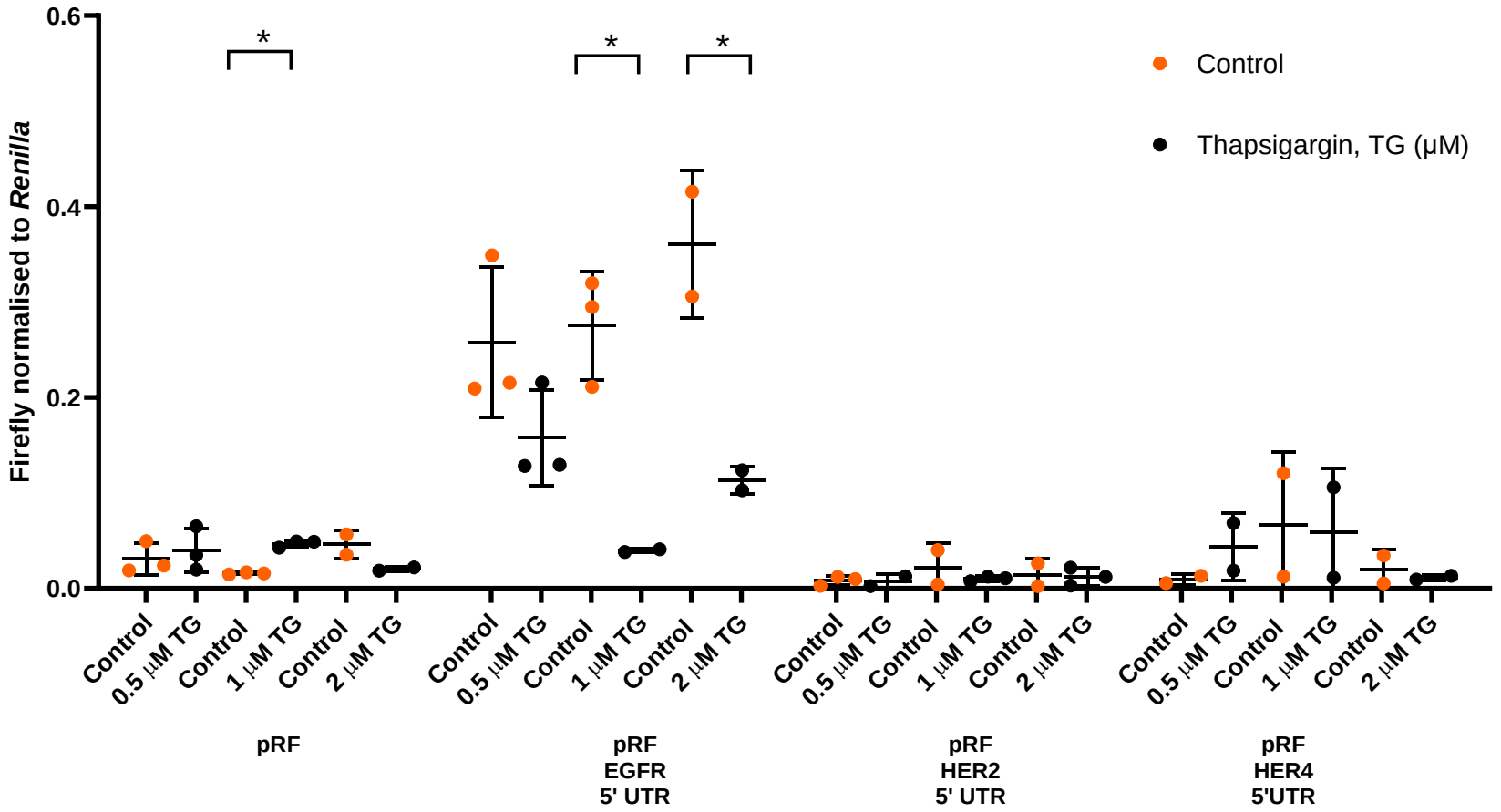

Figure 3.5. Thapsigargin had no effect on translation mediated by *HER2* and *HER4* 5' UTRs but *EGFR* IRES activity was decreased. MCF-7 cells were transfected with bicistronic constructs containing both *Renilla* luciferase and firefly luciferase open reading frames. 24 hours post-transfection MCF-7 cells were exposed to either 0.5 μM, 1 μM or 2 μM of thapsigargin (black) or respective DMSO controls (orange). 24 hours later cells were lysed and the F/R activity was measured. Data represents the average of two-three independent experiments each carried out in triplicate. All error bars represent the standard deviation. $p<0.05$ was determined statistically significant using a t-test with Bonferroni-Dunn's correction.

As the *Renilla* luciferase expression was not efficiently reduced in response to thapsigargin (Figure 3.4), next it was investigated whether thapsigargin treatment could reduce the cell viability of MCF-7 which would give an indication to whether thapsigargin induced ER stress.

The results from the MTT data found that there was a 50.2%, 18.6% and 55.3% decrease in the cell viability of MCF-7 cells in response to 0.5 µM, 1 µM and 2 µM of thapsigargin respectively, from the average of two independent experiments (Figure 3.6). This indicates that thapsigargin treatments did reduce the cell viability of MCF-7 cells. However, one experimental repeat showed a low cell viability at the 0.1% DMSO control which was compared with the 1 µM of thapsigargin condition. This may be due to low cell numbers at this replicate. Additional repeats should be conducted to see if there is a similar percentage decrease at 1 µM of thapsigargin like the other concentrations of thapsigargin. Previous experiments shown that 1 µM of thapsigargin caused a 39% reduction in the cell viability of MCF-7 cells (Smalley, 2016).

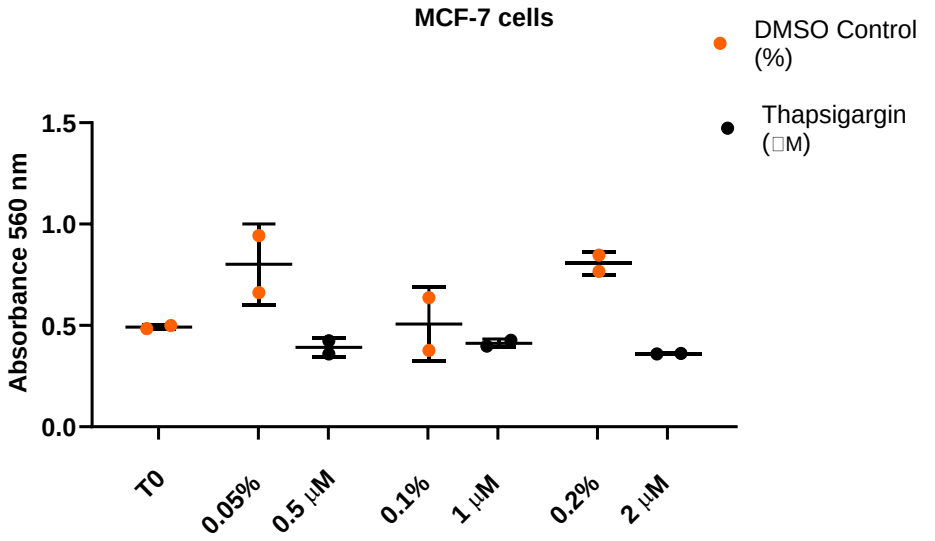

Figure 3.6. The effect of thapsigargin on the cell viability of MCF-7 cells. MCF-7 cells were exposed to either 0.5 µM, 1 µM or 2 µM of thapsigargin (black) or respective controls containing the equivalent percentage of DMSO (%) (orange). After 24 hours the cell viability was measured by MTT assay. T0= time-zero readings taken at the start of treatment. Data represents the average of two independent experiments from at least four technical replicates. Percentage decrease was calculated from the average of two independent experiments and was compared to the respective % DMSO control. Error bars represent the standard deviation.

3.5. The effect of oxidative stress on the translational control by *HER2* and *HER4* 5' UTRs

NFE2 a regulator of HER2 and HER4 can also protect cancer cells from oxidative stress by upregulating antioxidant genes (Chen *et al.*, 2017; Zhang *et al.*, 2019a). Breast cancer patients overexpressing *HER2* have shown to have an increase in oxidative stress in comparison to *HER2* negative patients, together this suggests that *HER2* may be translated in response to oxidative stress (Victorino *et al.*, 2014). In addition, oxidative stress has shown to activate the IRESs of some cellular mRNA such as FGF and XIAP (Argüelles *et al.*, 2014). Next, it was investigated if *HER2* and *HER4* 5' UTRs contain an IRES active in response to oxidative stress. To assess this bicistronic luciferase reporters containing the 5' UTRs were tested in response to 250 µM of hydrogen peroxide treatment.

The *Renilla* luciferase expression was assessed to check if hydrogen peroxide decreased cap-dependent translation. The *Renilla* luciferase expression was reduced in response to 250 µM of hydrogen peroxide treatment indicating that cap-dependent translation was reduced. This was except for constructs containing *HER2* 5' UTR which may be due to variability in the cell confluency between replicates (Figure 3.7). To determine the effect of hydrogen peroxide treatment on the translation mediated by the 5' UTRs the F/R was measured. There was a decrease in the background firefly luciferase and the F/R levels from pRF in response to hydrogen peroxide treatment ($p=0.005$) (Appendix Figure 3 and Figure 3.8). There was a decrease in the firefly luciferase expression from *EGFR* IRES in response to 250 µM of hydrogen peroxide (Appendix Figure 3). There was a slight decrease in the F/R expression mediated

by *EGFR* IRES but this was determined to be statistically insignificant (p= 0.063) (Figure 3.8).There was no change in the firefly luciferase or the F/R levels mediated from *HER2* and *HER4* 5' UTRs in response to hydrogen peroxide treatment (p=0.324 and p=0.492 respectively) (Appendix Figure 3 and Figure 3.8). The data showed no evidence for IRES activity in *HER2* and *HER4* 5' UTRs in response to hydrogen peroxide treatment.

Next, an MTT assay was conducted to measure if hydrogen peroxide reduced the cell viability of MCF-7 cells that would indicate that stress was induced. There was an increase in the viability of MCF-7 cells in response to 250 µM of hydrogen peroxide, indicating that cells were able to withstand this treatment and therefore unlikely to have been stressed. However, this was determined to be statistically insignificant (p=0.102) and therefore more replicates would need to be carried out to confirm the effects shown (Figure 3.9).

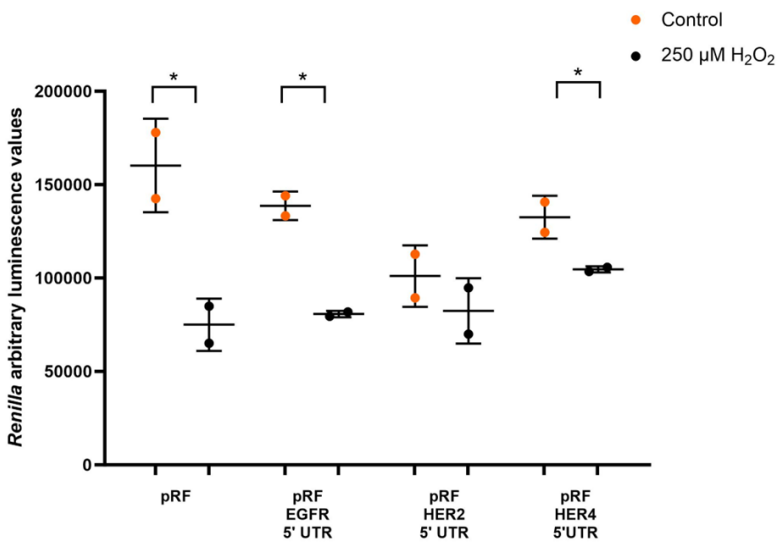

Figure 3.7. 250 μM of hydrogen peroxide treatment reduced the *Renilla* luciferase expression. MCF-7 cells were transfected with bicistronic constructs. 24 hours post-transfection MCF-7 cells were exposed to 250 μM of hydrogen peroxide (H_2O_2) (black) or were untreated (orange) for 24 hours. Then cells were lysed and the *Renilla* luciferase expression was measured. Data represents the average of two independent experiments each carried out in triplicate. All error bars represent the standard deviation. $p<0.05$ was determined statistically significant using a t-test with Bonferroni-Dunn's correction.

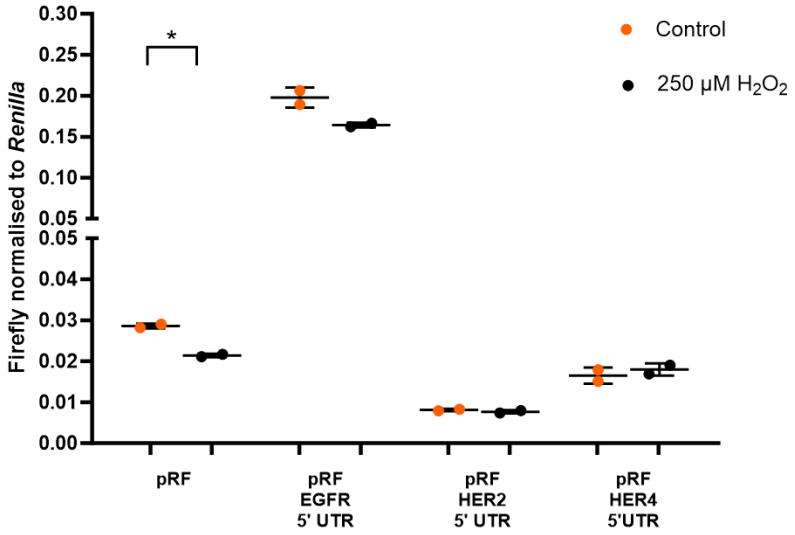

Figure 3.8. No evidence for IRES activity in *HER2* and *HER4* 5' UTRs in response to 250 μM of hydrogen peroxide treatment. MCF-7 cells were transfected with bicistronic constructs. 24 hours post-transfection MCF-7 cells were exposed to 250 μM of hydrogen peroxide (H_2O_2) (black) or were untreated (orange) for 24 hours. 24 hours later cells were lysed and the F/R activity was measured. Data represents the average of two independent experiments each carried out in triplicate. All error bars represent the standard deviation. $p<0.05$ was determined statistically significant using a t-test with Bonferroni-Dunn's correction.

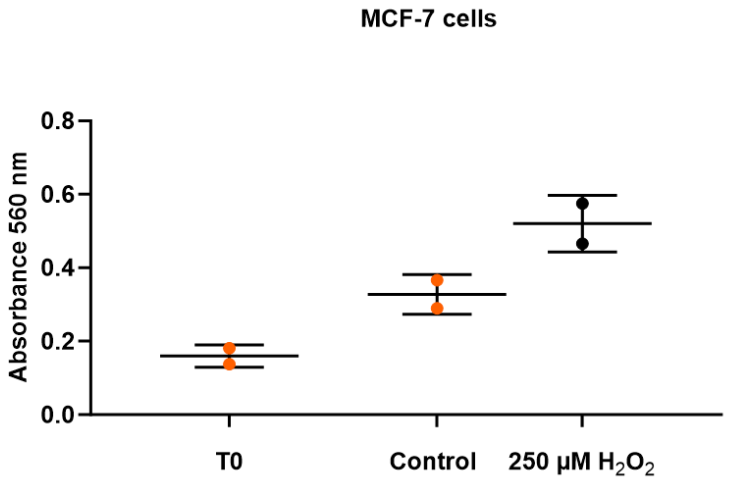

Figure 3.9. The effect of 250µM of hydrogen peroxide on the viability of MCF-7 cells. Cells were exposed to either 250 µM of hydrogen peroxide (H_20_2) (black) or were untreated (orange) for 24 hours before a MTT assay was conducted. T0= time-zero readings taken at the start of treatment. Data represents two independent experiments from at least four technical replicates. Error bars represent the standard deviation. $p<0.05$ was determined statistically significant using a t-test with Bonferroni-Dunn's correction.

3.6. The effect of hypoxic stress on the translational control by *HER2* and *HER4* 5' UTRs

HER2 and *HER4* PI3K signalling have shown to upregulate HIF expression leading to the transcription of genes that promote cancer cell progression such as *VEGF*. This shows that *HER2* and *HER4* have a role in regulating hypoxia. (Jarman *et al.*, 2019; Laughner *et al.*, 2001; Paatero *et al.*, 2012). Additionally, EGFR a closely related family member and dimerisation partner of HER2 and HER4, contains an IRES in the *EGFR* 5' UTR that is active in response to hypoxic stress (Liu *et al.*, 2012; Webb *et al.*, 2015; Jeon *et al.*, 2017).

Therefore, it was tested whether *HER2* and *HER4* 5' UTRs contain an IRES active in response to hypoxia. To assess this MCF-7 cells were transfected with bicistronic luciferase constructs and then were treated with different concentrations (75 µM, 100 µM and 150 µM) of hypoxia mimic $CoCl_2$. $CoCl_2$ mimics hypoxia by binding to the oxygen-dependent degradation (ODD) domain of HIF-1α and HIF-2α. This inhibits the hydroxylation of HIF-α by prolyl hydroxylases and prevents the subsequent degradation by VHL which results in the stabilisation of HIF-1α and HIF-2α (Yuan *et al.*, 2003).

To determine if $CoCl_2$ was able to reduce cap-dependent translation the *Renilla* luciferase expression from each bicistronic construct was measured. Surprisingly, there was an increase in the *Renilla* luciferase expression from pRF in response to $CoCl_2$ indicating that $CoCl_2$ increased cap-dependent translation in MCF-7 cells transfected with pRF. However, the increase from pRF may be due to low transfection at the control condition, as the *Renilla* expression at the $CoCl_2$ conditions was at similar levels to the other bicistronic reporters. There

was also a statistically significant increase in the *Renilla* expression from bicistronic constructs containing *HER2* 5' UTR in response to 75 µM and 100 µM of $CoCl_2$. In addition, there was a decrease in the *Renilla* expression from bicistronic constructs containing *HER4* 5' UTR in response to 75 µM and 150 µM of $CoCl_2$ and no change at 100 µM. There was a slight decrease in the *Renilla* luciferase expression from bicistronic constructs containing *EGFR* 5' UTR at all three concentrations of $CoCl_2$ but this was statistically insignificant (Figure 3.10). As $CoCl_2$ overall did not reduce the *Renilla* luciferase expression of the bicistronic constructs, the results indicate that $CoCl_2$ was unable to decrease cap-dependent translation. Overall, the results suggests that hypoxic stress may have not been efficiently induced.

75 µM of $CoCl_2$ had previously been reported to have no effect on *EGFR* IRES activity in MCF-7 cells (Smalley, 2016). To confirm this effect and determine if higher concentrations of $CoCl_2$ could increase *EGFR* IRES activity and detect IRES activity in the 5' UTRs of *HER2* and *HER4*, the F/R expression was measured from each bicistronic construct. There was found to be an increase in the firefly luciferase expression from pRF in response to $CoCl_2$ (Appendix Figure 4). There was a decrease in the F/R from pRF in response to $CoCl_2$ but this was determined to be statistically insignificant at 75 µM ($p=0.082$), 100 µM ($p=0.062$) and 150 µM ($p=0.051$) of $CoCl_2$ (Figure 3.11). There was a slight decrease in the firefly luciferase expression from *EGFR* IRES in response to 75 µM and 100 µM of $CoCl_2$ but this was statistically insignificant. There was no change in the F/R from *EGFR* IRES in response to 75 µM ($p=0.590$) or higher concentrations of $CoCl_2$ at 100 µM ($p=0.928$) and 150 µM ($p=0.604$) (Appendix Figure 4 and Figure 3.11). There was an increase in the firefly luciferase

expression from constructs containing *HER2* 5' UTR in response to 100 μM of $CoCl_2$. There was also a decrease in the firefly luciferase expression from constructs containing *HER4* 5' UTR in response to 75 μM and 150 μM of $CoCl_2$ (Appendix Figure 4). However, there was found to be no change in the F/R expression from constructs containing *HER2* or *HER4* 5' UTRs in response to 75 μM ($p=0.583$ and $p=0.280$ respectively), 100 μM ($p=0.458$ and $p=0.233$ respectively) and 150 μM ($p=0.835$ and $p=0.062$ respectively) (Figure 3.11). This indicates that there is no IRES activity in *HER2* and *HER4* 5' UTRs in response to $CoCl_2$ treatment.

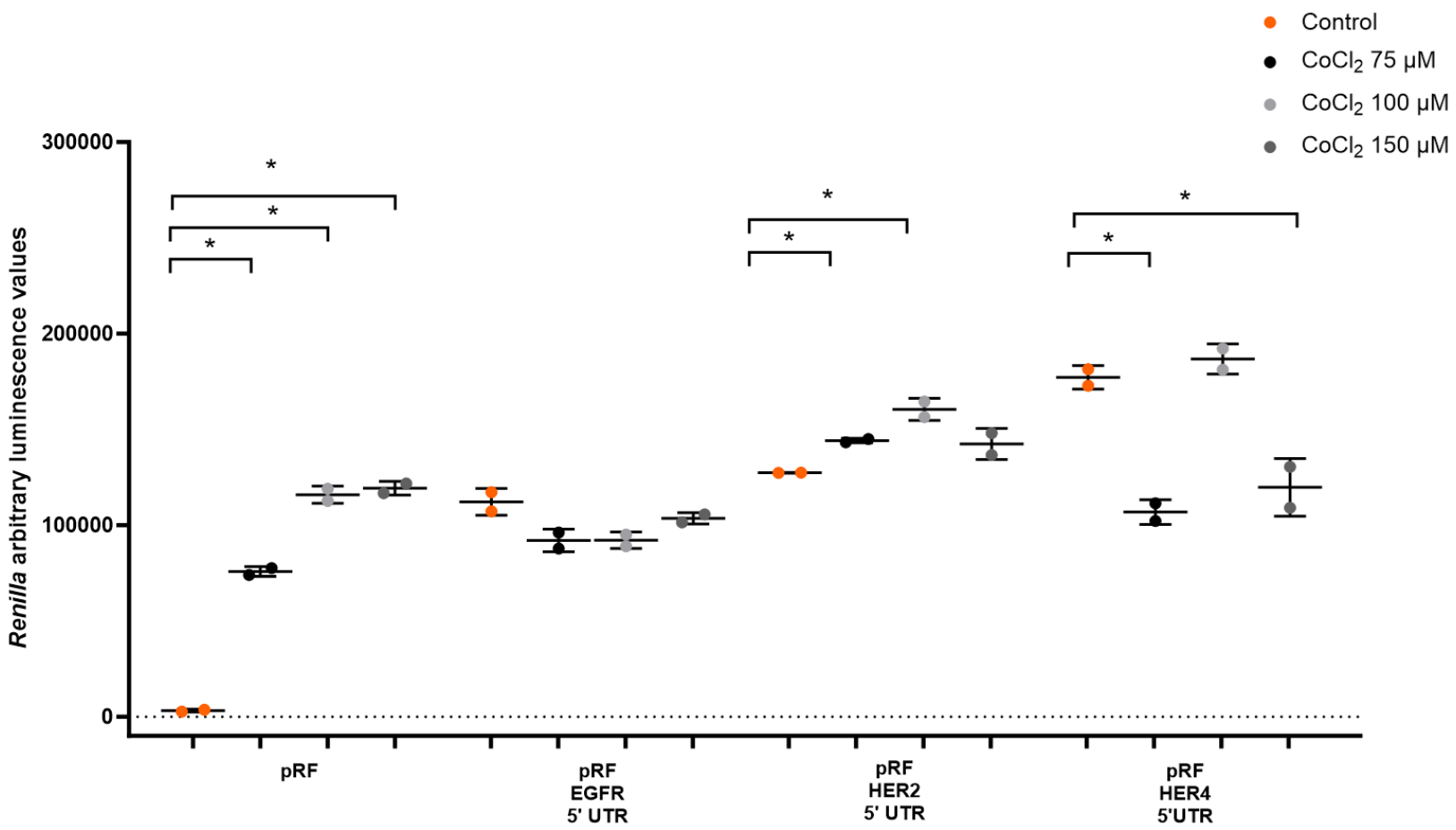

Figure 3.10. The *Renilla* luciferase expression in response to $CoCl_2$ treatment. MCF-7 cells were transfected with bicistronic constructs containing both *Renilla* and firefly luciferase open reading frames. 24 hours post-transfection MCF-7 cells were exposed to 75 µM, 100 µM or 150 µM of $CoCl_2$ (black, light grey or dark grey respectively) or were untreated (orange) for 24 hours. Then cells were lysed and the *Renilla* luciferase expression was measured. Data represents the average of two independent experiments each carried out in triplicate. All error bars represent the standard deviation. $p<0.05$ was determined statistically significant using a t-test with Bonferroni-Dunn's correction.

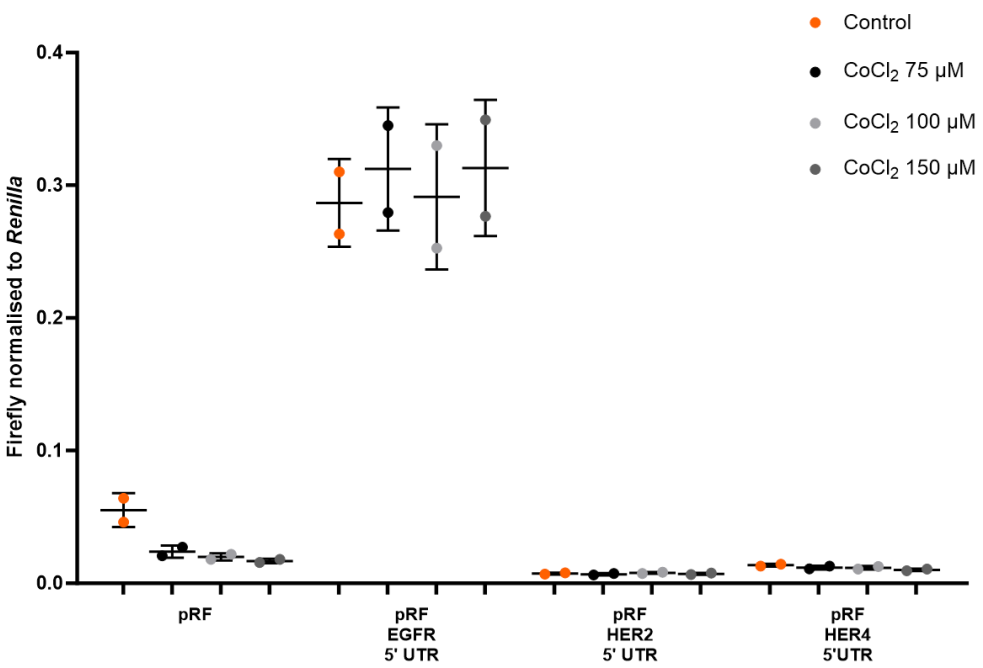

Figure 3.11. The hypoxia mimic, $CoCl_2$ was unable to induce firefly luciferase expression of the bicistronic constructs. MCF-7 cells were transfected with bicistronic constructs containing both *Renilla* and firefly luciferase open reading frames. 24 hours post-transfection MCF-7 cells were exposed to 75 µM, 100 µM or 150 µM of $CoCl_2$ (black, light grey or dark grey respectively) or were untreated control (orange) for 24 hours. Then cells were lysed and the F/R activity was measured. Data represents the average of two independent experiments each carried out in triplicate. All error bars represent the standard deviation. $p<0.05$ was determined statistically significant using a t-test with Bonferroni-Dunn's correction.

An MTT assay was conducted to measure if $CoCl_2$ could reduce the cell viability of MCF-7 cells. It was found that $CoCl_2$ had no effect on the cell viability of MCF-7 cells (Figure 3.12). This indicates that hypoxic stress may have not been induced in response to different concentration of $CoCl_2$ in MCF-7 cells.

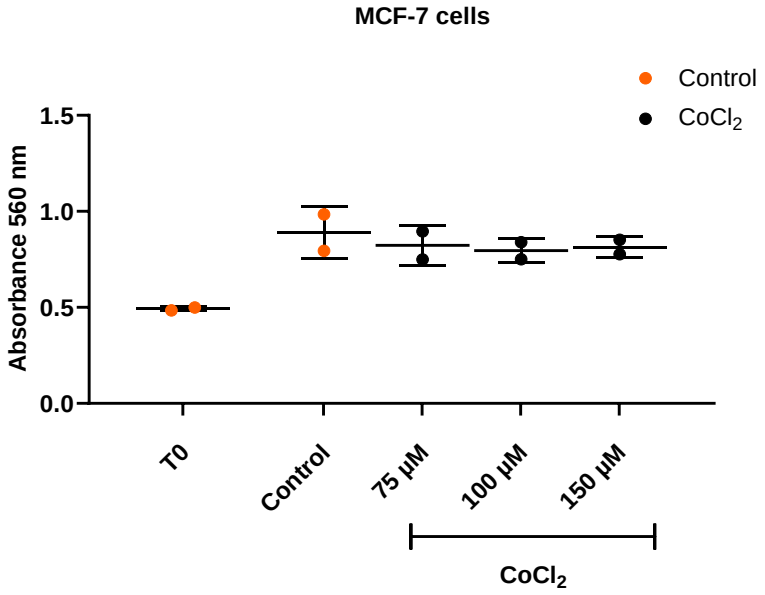

Figure 3.12. $CoCl_2$ treatment had no effect on the cell viability of MCF-7 cells. Cells were exposed to either 75 µM, 100 µM or 150 µM of $CoCl_2$ (black) or were untreated (orange) for 24 hours before an MTT assay was conducted. T0= time-zero readings taken at the start of treatment. Data represents two independent experiments from at least four technical replicates.

3.7. The effect of low serum conditions on the translational control by *HER2* and *HER4* 5' UTRs

Many cancers are dependent on the presence of nutrients such as growth factors and amino acids. Cancer cells are often deprived of such nutrients which is mimicked by serum starvation in tissue culture. In response to growth factor deprivation cap-dependent translation is inhibited. Some IRESs have shown to be active in response to serum starvation such as XIAP, CDKN1B and SREBP-1 (Coleman *et al.*, 2009; Riley *et al.*, 2010; Damiano *et al.*, 2010). This demonstrates that serum starvation can affect translation. *HER4* expression has shown to be increased in response to serum starvation and *HER4* expression can protect cancer cells from serum starvation (Hua *et al.*, 2012; Wang *et al.*, 2018a). Therefore, there is potential that an IRES could mediate an increase in *HER4* expression or closely related family member *HER2* in response to low serum conditions.

To test the effects of low serum conditions on translation, MCF-7 cells were transfected with bicistronic constructs and the serum levels in the media was reduced from 10% FBS to 0.5% FBS. First, the *Renilla* luciferase expression was measured to determine if low serum conditions could reduce cap-dependent translation. There was no change in the *Renilla* luciferase expression in response to 0.5% FBS indicating that cap-dependent translation was not reduced. The exception to this was a reduction in the *Renilla* luciferase expression from constructs containing *β-tubulin* 5' UTR ($p=0.004$) (Figure 3.13). The difference in response of the *Renilla* luciferase expression of the bicistronic construct containing *β-tubulin* 5' UTR and the other bicistronic constructs is unexpected. This is because the *Renilla* expression is controlled by the same SV40 promoter

across the bicistronic constructs so it would be expected that the *Renilla* luciferase expression behaves the same across the bicistronic constructs especially given that they are subjected to the same conditions.

Next, the F/R expression was measured from each bicistronic construct to determine if *HER2* and *HER4* 5' UTRs contain an IRES active in response to low serum conditions. There was no change in the firefly luciferase expression from each bicistronic construct in response to low serum conditions except for constructs containing *β-tubulin* 5' UTR where the firefly luciferase expression was decreased (Appendix Figure 5). However, as the *Renilla* expression also decreased for constructs containing *β-tubulin* 5' UTR this resulted in no change in the F/R expression (p=0.518) (Figure 3.14). In addition, there seemed to be an increase in the firefly expression mediated by *EGFR* IRES in response to serum starvation, however this was not statistically significant (Appendix Figure 5). There was no effect of low serum conditions on pRF (p=0.882). There was no change in the F/R mediated by *EGFR* IRES in response to low serum conditions (p=0.671). *HER2* and *HER4* 5' UTR (p=0.449 and p=0.980 respectively) mediated similar F/R readings to the negative controls which indicates that there is no evidence of IRES activity in *HER2* and *HER4* 5' UTRs in response to low serum conditions (Figure 3.14).

To determine if low serum conditions had an effect on the cell viability of MCF-7 cells, cells were treated with DMEM containing 0.5% FBS and a MTT assay was conducted. It was found that DMEM containing 0.5% FBS had no effect on the cell viability of MCF-7 cells. Therefore, it is unlikely that low serum conditions induced stress in this study (Figure 3.15).

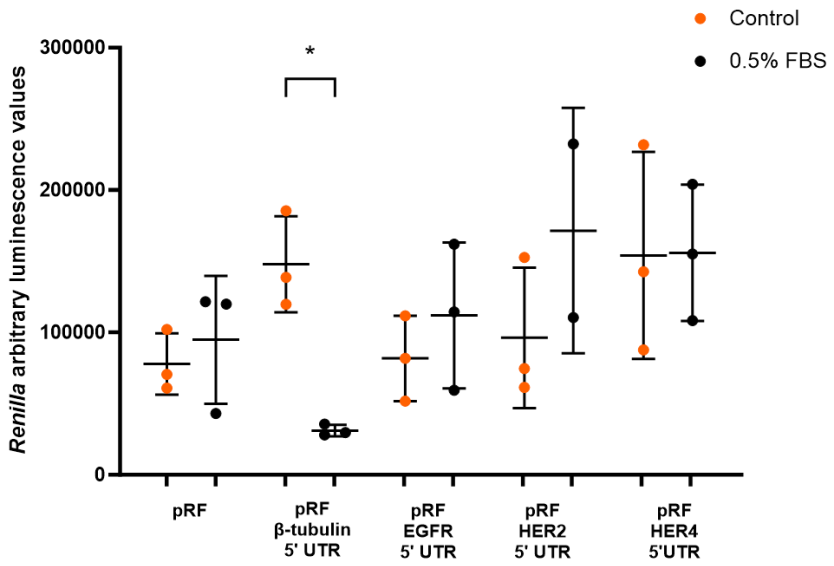

Figure 3.13. Overall, low serum conditions were unable to efficiently reduce cap-dependent translation. MCF-7 cells were transfected with bicistronic constructs. 24 hours post-transfection MCF-7 cells were exposed to media containing 0.5% FBS to provide low serum conditions (black) or media containing 10% FBS as a control (orange) for 24 hours. Then cells were lysed and the *Renilla* luciferase expression was measured. Data represents the average of two-three biological repeat each carried out in triplicate. All error bars represent the standard deviation. $p<0.05$ was determined statistically significant using a t-test with Bonferroni-Dunn's correction.

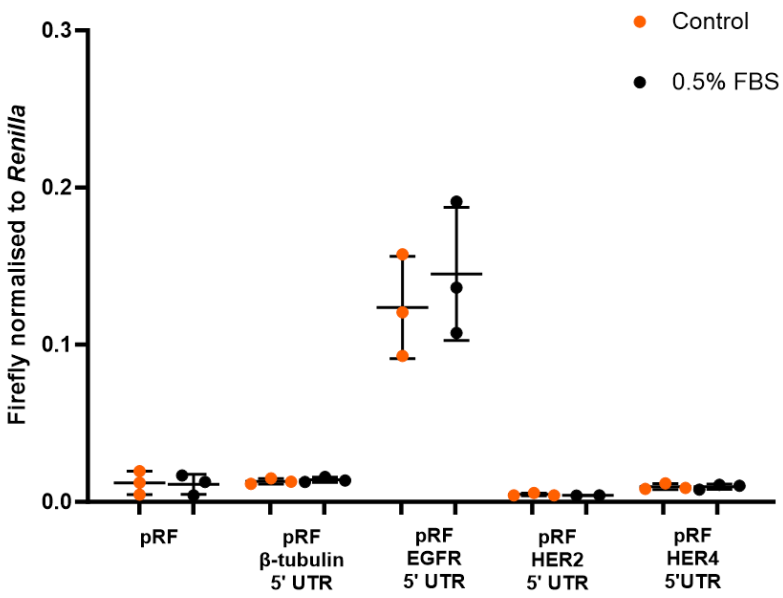

Figure 3.14. No evidence for IRES activity in *HER2* or *HER4* 5' UTRs in response to low serum conditions. MCF-7 cells were transfected with bicistronic constructs. 24 hours later MCF-7 cells were exposed to media containing 0.5% FBS to provide low serum conditions (black) or media containing 10% FBS as a control (orange) for 24 hours. Then cells were lysed and the F/R activity was measured. Data represents the average of two-three biological repeat each carried out in triplicate. All error bars represent the standard deviation. $p<0.05$ was determined statistically significant using a t-test with Bonferroni-Dunn's correction.

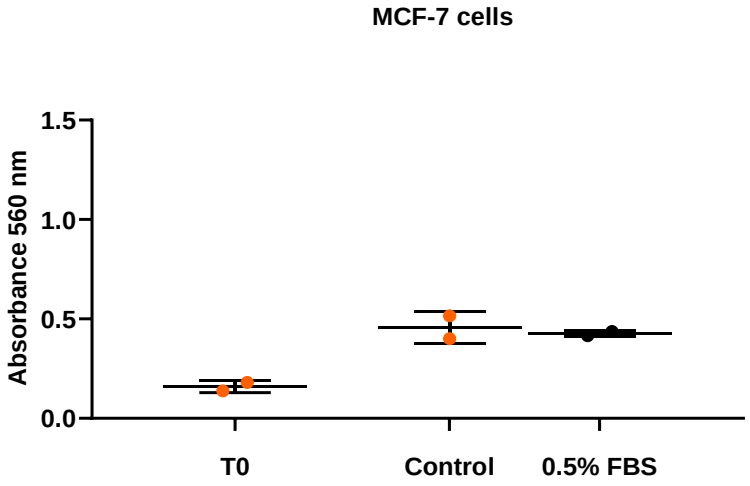

Figure 3.15. Low serum conditions had no effect on the cell viability of MCF-7 cells. Cells were exposed to DMEM media containing either 0.5 % FBS to provide low serum conditions (black) or 10% FBS as a control (orange) before an MTT assay was conducted. T0= time-zero readings taken at the start of treatment. Data represents two biological repeats from at least four technical replicates. Error bars represent the standard deviation.

3.8. The effect of genotoxic stress on the translational control by *HER2* and *HER4* 5' UTRs

Genotoxic stress can be induced by UV-B which can form mutagenic lesions and photoproducts such as cyclobutane pyrimidine dimers and pyrimidine 6-4 pyrimidone photoproducts commonly inducing C to T mutations in DNA (Goto *et al.*, 2015; Horrell *et al.*,2015). However, the repair of these lesions by nucleotide excision repair (NER) has shown to be reduced in some breast cancers (Navaraj *et al.*, 2005; Berndt *et al.*, 2006). The UV resistance associated gene is upregulated in breast cancers and increases the expression of proteins such as cyclins and SRC (Sencan *et al.*, 2021). In addition, HER2 is activated in response to UV and activates the PI3K pathway to prevent inhibition of the S-phase of the cell cycle in keratinocyte carcinoma cells (Madson *et al.*, 2009).

UV radiation has shown to activate other cellular IRES such as SHMT1 and APAF1 IRESs (Ungureanu *et al.*, 2006; Fox *et al.*, 2009). Next, it was investigated whether *HER2* 5' UTR or *HER4* 5' UTRs contain an IRES that could mediate an increase in expression in response to UV radiation in breast cancer cells.

To assess the effect of UV-B radiation on cap-dependent translation, MCF-7 cells were exposed to UV-B radiation for 10 or 20 seconds and the *Renilla* luciferase expression was measured. There seemed to be a slight increase in the *Renilla* expression from the bicistronic reporters in response to 20 seconds of UV-B, however this was insignificant (Figure 3.16). As the *Renilla* expression did not decrease the results suggest that cap-dependent translation was not inhibited (Figure 3.16).

Next, to determine if *HER2* or *HER4* 5' UTRs contain an IRES active in response to UV-B radiation, the F/R expression from each bicistronic construct was measured. At 10 seconds of UV-B exposure there was a slight decrease in the firefly luciferase from pRF however this was determined to be statistically insignificant. There was no change in the firefly luciferase expression of pRF in response to 20 seconds of UV-B and no change in the F/R from pRF in response to 10 or 20 seconds of UV-B radiation (p=0.270 and p=0.679 respectively) (Appendix Figure 6 and Figure 3.17). There was a decrease in the firefly luciferase expression mediated by *EGFR* 5' UTR in response to 10 seconds of UV but this was statistically insignificant. However, there was a statistically significant increase in the firefly luciferase expression mediated from *EGFR* IRES in response to 20 seconds of UV-B (Appendix Figure 6). However, there was no change in the F/R expression in response to 10 or 20 seconds UV-B from *EGFR* IRES (p=0.867 and p=0.461 respectively) (Figure 3.17).

There was no effect of 10 seconds of UV-B on the firefly luciferase and the F/R expression mediated by *HER2* 5' UTR (p=0.206), but there was found to be a statistically significant increase in the firefly luciferase and F/R expression mediated by *HER2* 5' UTR in response to 20 seconds of UV-B compared to the control (p=0.030) (Appendix Figure 6) (Figure 17).There was no change in the firefly luciferase expression but there was a statistically significant decrease in the F/R expression mediated by *HER4* 5' UTR in response to 10 seconds of UV-B radiation (p=0.045) (Appendix Figure 6) (Figure 17). There was a statistically significant increase in the firefly luciferase expression mediated by *HER4* 5' UTR in response to 20 seconds of UV-B (Appendix Figure 6). However, as there was an observed increase in the *Renilla* expression this resulted in no change in

the F/R expression in response to 20 seconds of UV-B (p=0.702) (Figure 3.17). The changes in the F/R mediated by *HER2* and *HER4* 5' UTR are unlikely to be biologically significant given that the F/R expression was at similar or lower levels than the pRF negative control and that the *Renilla* luciferase expression was also not decreased in response to UV-B radiation. This shows that *HER2* and *HER4* 5' UTRs do not contain an IRES active in response to UV-B radiation in MCF-7 cells.

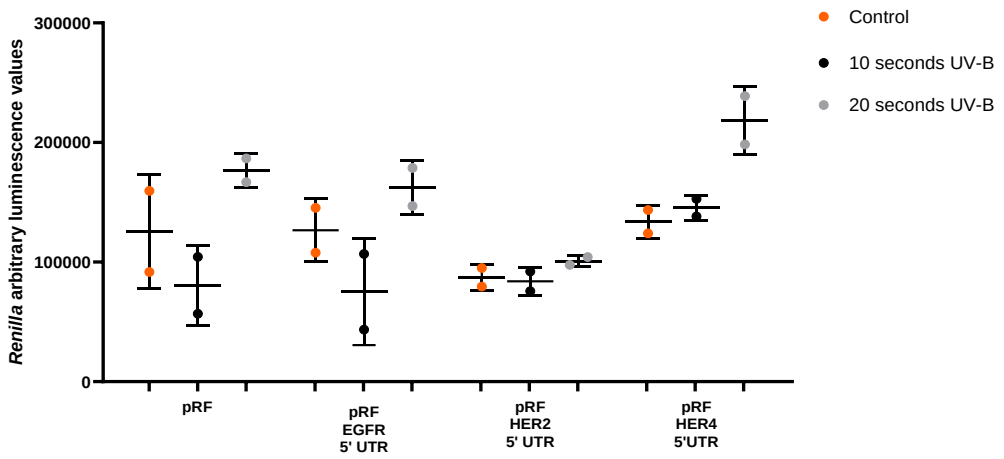

Figure 3.16. The *Renilla* luciferase expression in response to UV-B radiation. MCF-7 cells were transfected with bicistronic constructs. 24 hours post-transfection MCF-7 cells were exposed to UV-B radiation (302 nm) for 10 seconds (black) or 20 seconds (grey) to induce genotoxic stress or were untreated (orange) for 24 hours. After each timepoint cells were lysed, and the *Renilla* luciferase expression was measured. Data represents the average of two independent experiments each carried out in triplicate. All error bars represent the standard deviation. $p<0.05$ was determined as statistically significant using a t-test with Bonferroni-Dunn's correction.

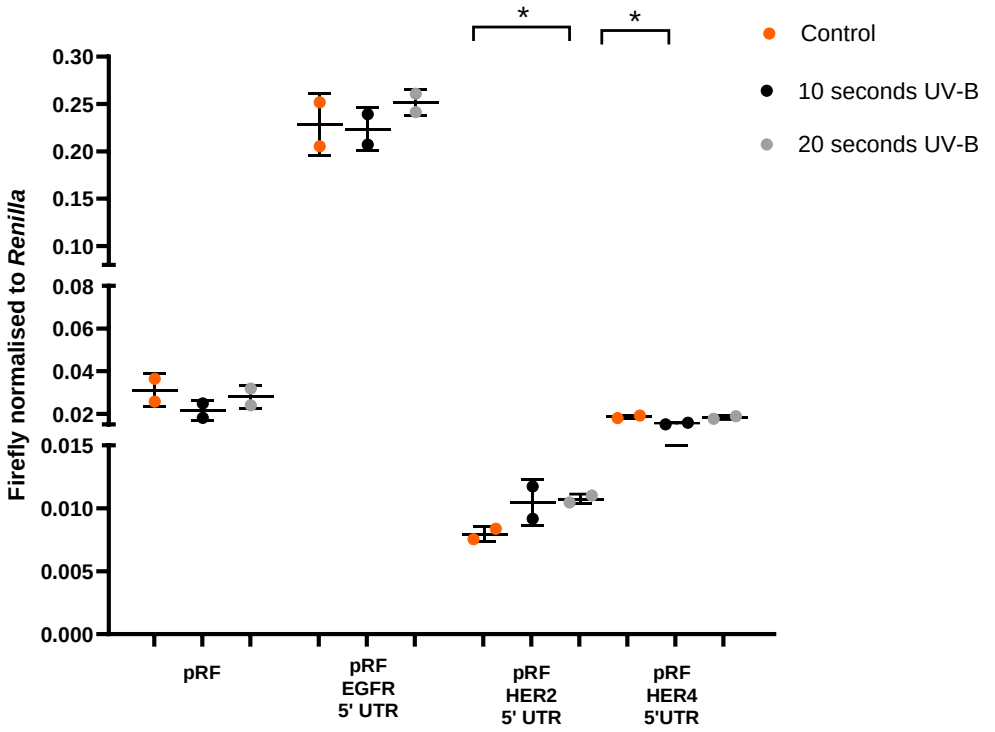

Figure 3.17. The effect of UV radiation on the F/R expression mediated by *EGFR*, *HER2* and *HER4* 5' UTRs. MCF-7 cells were transfected with bicistronic constructs. 24 hours post-transfection MCF-7 cells were exposed to UV-B radiation (302 nm) for 10 seconds (black) or 20 seconds (grey) to induce genotoxic stress or were untreated (orange) for 24 hours. After each timepoint cells were lysed, and the F/R activity was measured. Data represents the average of two independent experiments each carried out in triplicate. All error bars represent the standard deviation. $p<0.05$ was determined as statistically significant using a t-test with Bonferroni-Dunn's correction.

The cell viability was next assessed in response to UV-B radiation to determine if UV-B radiation was able to stress MCF-7 cells. It was found that 20 seconds of UV-B exposure caused a 60.8% reduction in the cell viability of MCF-7 cells (Figure 3.18). This indicates that 20 seconds of UV-B radiation may have induced cell stress by causing DNA damage leading to cell cycle arrest and a reduction in viable cells (Wang *et al.*, 2017a).

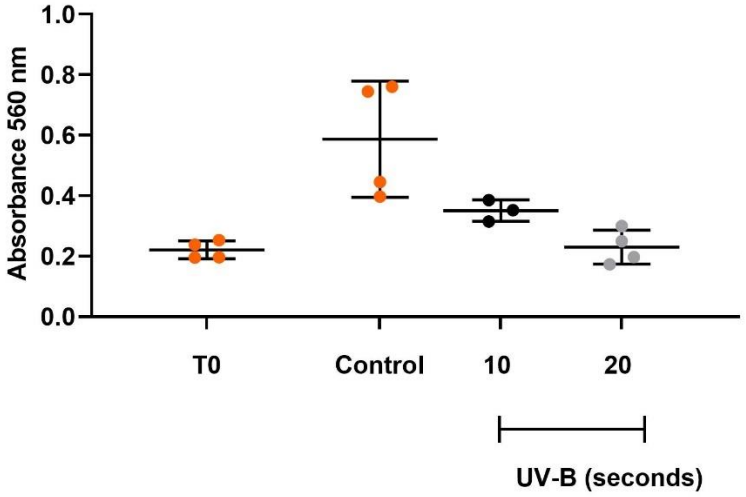

Figure 3.18. UV-B radiation decreased the cell viability of MCF-7 cells. Cells were exposed to UV-B radiation (302 nm) for 10 seconds or 20 seconds (black or grey respectively) or control (orange). After each time-point cell viability was measured by MTT assay. T0= time-zero readings taken at the start of treatment. MCF-7 cells. Data represents a single independent experiment. Percentage decrease was calculated from the average of a single independent experiment from four technical replicates. Error bars represent the standard deviation.

3.9. The effect of high cell densities on translational control by *HER2* and *HER4* 5' UTRs

Cancer cells lose contact inhibition and continue to proliferate even at high cell densities (Eagle and Levine, 1967). The hippo signalling pathway controls cell growth and apoptosis but dysregulation of the pathway can lead to key components such as YAP binding to transcriptional enhanced associate domains (TEAD) and inducing the transcription of genes involved in cell proliferation (Zhao *et al.*, 2008; Tariki *et al.*, 2014). HER4 expression has shown to be increased in response to high cell densities (Hua *et al.*, 2012). In addition, HER2 and HER4 have shown to increase YAP signalling so have a role in regulating cell density which can increase cancer cell progression (Haskins, Nguyen and Stern, 2014; Aharonov *et al.*, 2020). To determine if *HER2* or *HER4* 5' UTRs contain an IRES active in response to high cell densities, MCF-7 cells were seeded at 3X and 6X more than the original cell density of 10,000 cells per well in a 24-well plate before being transfected with each bicistronic construct.

The *Renilla* luciferase expression was assessed to determine the effect of high cell densities on cap-dependent translation. There was an increase in the *Renilla* expression in response to an increase in cell densities (Figure 3.19). This trend was observed across two independent experiments (Figure 3.19 and Appendix Figure 7). However, one independent is shown in Figure 3.19 due to variations when combining independent experiments. The increase in *Renilla* expression may be due to an increase in the number of cells expressing the luciferase constructs.

Next, the F/R expression was measured to determine if high cell densities could induce IRES activity. It was found that increasing the seeding density of cells from 10,000 cells per well to 30,000 or 60,000 cells per well increased the firefly luciferase expression from the bicistronic constructs (Appendix Figure 8). There was no effect on the F/R expression from the bicistronic constructs in response to increasing cell densities (Figure 20).

The results from a second independent experiment also showed an increase in the firefly luciferase expression from the bicistronic constructs in response to an increase in cell density (Appendix Figure 9). However, in the second independent experiment, there was a varied response in the F/R expression. There was an increase in the F/R expression mediated by *EGFR* 5' UTR in response to 60,000 cells per well and *HER4* 5' UTR at 30,000 and 60,000 cells per well. There was a decrease in the F/R expression mediated by *HER2* 5' UTR in response to high cell densities (Appendix Figure 10). The expression from *HER2* and *HER4* 5' UTR are at background levels so unlikely to be biologically relevant. Overall, increasing the cell density seems to increase both the *Renilla* and firefly luciferase expression of the bicistronic constructs. However, due to variations in the F/R expression between the two independent experiments more replicates would need to be conducted to determine the effect of cell density on the reporters.

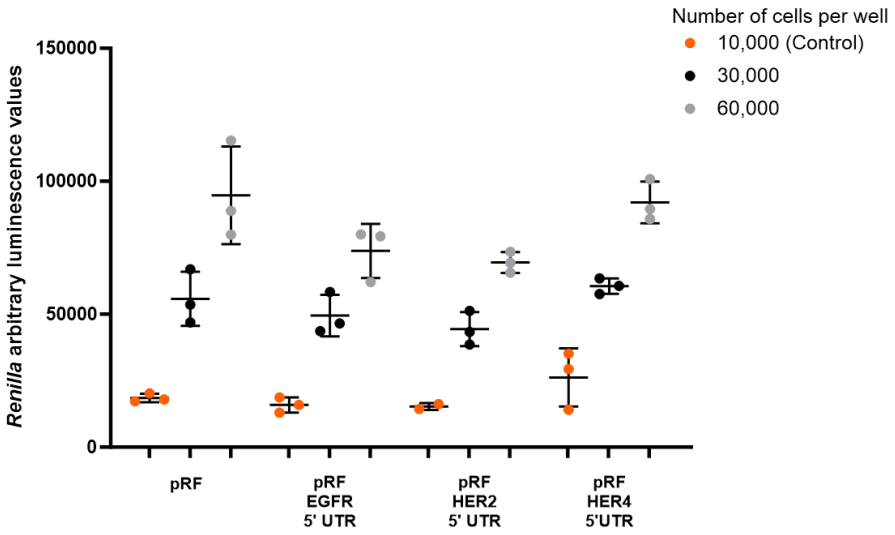

Figure 3.19. Increasing the seeding cell density increased the *Renilla* luciferase expression. MCF-7 cells were seeded at high cell densities; 30,000 (black) and 60,000 (grey) or at the original cell density of 10,000 cells per well (orange). 24 hours later MCF-7 cells were transfected with bicistronic constructs. 24 hours post-transfection cells were lysed, and the *Renilla* luciferase expression was measured. Data of one independent experiment carried out in triplicate but representative of two independent experiments.

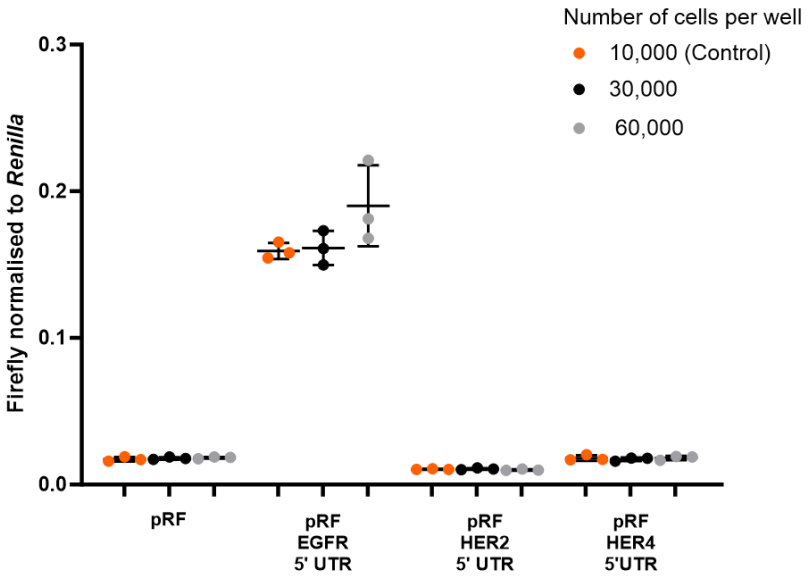

Figure 3.20. Increasing the seeding cell density had no effect on the F/R expression mediated from *EGFR*, *HER2* and *HER4* 5' UTRs. MCF-7 cells were seeded at high cell densities; 30,000 (black) and 60,000 (grey) or at the original cell density of 10,000 cells per well (orange). 24 hours later MCF-7 cells were transfected with bicistronic constructs. 24 hours post-transfection cells were lysed, and the F/R activity was measured. Data represents one independent experiments carried out in triplicate.

3.10. Discussion

The aim of this chapter was to determine whether the 5' UTRs of *HER2* or *HER4* contain an IRES active in breast cancer cells by screening various cell stress conditions in MCF-7 cells using bicistronic luciferase reporters. Cancer cells are exposed to various cell stress conditions such as hypoxia which have been shown to increase the translation of specific mRNA via internal ribosome entry such as *EGFR* (Fukumura *et al.*, 2001; Webb *et al.*, 2015). As HER2 and HER4 are key oncogenes that are responsible for mediating downstream signalling cascades that increase cancer cell growth it would be important to investigate whether these receptors are regulated at the translational level and if translation is mediated by an IRES which could be a potential therapeutic target for cancer (Monsey *et al.*, 2010).

Previously, *EGFR* IRES did not upregulate the F/R expression in response to low serum conditions, $CoCl_2$, UV-B exposure and hydrogen peroxide treatment, however *EGFR* IRES activity was still maintained in these conditions in MCF-7 cells (Alamoudi, 2020; Smalley, 2016). *EGFR*, *HER2* and *HER4* can dimerise and mediate downstream signalling pathways that increase cell proliferation which can cause aberrant signalling in cancer. Therefore, as *EGFR* contains an IRES that mediates expression of the downstream firefly luciferase cistron in response to stress conditions, there is potential for its dimerisation partners *HER2* and *HER4* to also contain an IRES to mediate their expression in cancer cells. Especially, as IRESs are often found in mRNAs of other proto-oncogenes that respond to stress and regulate cell growth such as *MYC*, *TP53*, *VEGF*, *IR* and *IGF-1R* (Miller *et al.*, 1998; Stoneley *et al.*, 2000; Giraud *et al.*, 2001; Ray, Grover and Das, 2006; Spriggs *et al.*, 2009).

The data confirmed the previously observed effects of thapsigargin, $CoCl_2$, low serum conditions and UV-B radiation on *EGFR* IRES activity in MCF-7 cells. Although, *EGFR* IRES did decrease the F/R expression in response to hydrogen peroxide treatment, this was determined as statistically insignificant and therefore more repeats would need to be carried out to confirm the effects shown in response to oxidative stress. Additionally, *EGFR* IRES was found to not be affected by high cell densities except for one independent experiment where there was an increase in response to 60,000 cells per well (Appendix Figure 10). Although, the hypoxia mimic $CoCl_2$ was able to maintain *EGFR* IRES activity, it was unable to statistically significantly reduce the *Renilla* expression. This is in contrast to previous reports that found that *EGFR* IRES maintained the firefly luciferase expression and reduced the *Renilla* expression in response to hypoxia (1% O_2) induced by a hypoxic chamber in MCF-7 cells (Webb *et al.*, 2015). This indicates that the hypoxia mimic $CoCl_2$ may be a poor model to stimulate hypoxia which is also evaluated from previous studies based on 75 µM of $CoCl_2$ (Smalley, 2016). Although in this study higher concentrations of $CoCl_2$ (100µM and 150 µM) were tested which were not included in previous studies. This was to investigate if higher concentrations of $CoCl_2$ could induce IRES activity whilst reducing the *Renilla* expression (Smalley, 2016). Overall, this suggests that a hypoxia chamber is a better way of studying the translational control by a 5' UTR in response to hypoxia as it provides true hypoxic conditions (1% O_2).

The *EGFR* IRES has previously been shown to decrease the F/R expression in response to 1µM of thapsigargin which was consistent with this study but in this study it was also found that 2 µM of thapsigargin decreased *EGFR* IRES activity (Webb *et al.*, 2015; Smalley 2016). However, it is important to mention that the

F/R expression of pRF was increased in response to 1 µM of thapsigargin. Although the F/R expression was at background levels, the firefly expression from pRF should not be affected by thapsigargin treatment. This difference may be due to differences in the transfection efficiency of pRF in the thapsigargin-treated and non-treated cells. *MYC* IRES activity is increased in response to ER stress and hypoxia and can be included as a positive control in such conditions (Webb *et al.*, 2015; Shi *et al.*, 2016; Hantelys *et al.*, 2019). Especially as, *MYC* IRES activity is dependent on MAPK signalling which the HER/EGFR family regulate (Shi *et al.*, 2016). Additionally, MYC and HER2 are commonly co-amplified in breast cancer and they both cooperate to drive cell proliferation in cancer cells (Park *et al.*, 2005; Nair *et al.*, 2013).

However, there was no evidence of IRES activity in the 5' UTRs of *HER2* and *HER4* in non-stressed cells and in response to thapsigargin, $CoCl_2$, low serum conditions and oxidative stress in MCF-7 cells. However, there was an increase in the F/R expression mediated by *HER2* 5' UTR in response to 20 seconds of UV-B exposure and decrease in the F/R mediated by *HER4* 5' UTR at 10 second exposure (Figure 3.17). Additionally, one independent high cell density experiment showed no effect mediated by *HER2* and *HER4* 5' UTRs (Figure 3.20). However, another independent experiment showed an increase in the F/R mediated by *HER4* 5' UTR in response to high cell densities and a decrease in the F/R mediated by *HER2* 5' UTR (Appendix Figure 10). This experiment was conducted by seeding cells at the various cell densities before transfecting cells with each bicistronic which may have affected the transfection efficiency. In addition, other factors such as the quality and topology of the construct could also affect the transfection efficiency. However, these results are unlikely to

biological relevant as the F/R was at background levels. Additionally, more replicates of these experiments are needed to see if the effects shown are consistent.

For the hypoxia mimic experiment, the *Renilla* luciferase expression from pRF was lower in the control condition than in response to $CoCl_2$ which would indicate that the *Renilla* luciferase expression increased in response to $CoCl_2$. However, the *Renilla* luciferase expression of pRF in response to $CoCl_2$ was similar to the *Renilla* luciferase expression from the control and $CoCl_2$ conditions from the other 5' UTR-bicistronic constructs. This indicates that transfection efficiency was reduced in the pRF control condition. There was a varied response in the *Renilla* expression among bicistronic reporters. For example, there was an increase in the *Renilla* expression from bicistronic reporters containing *HER2* 5' UTR in response to 75 μM and 100 μM of $CoCl_2$. In addition, a decrease in the *Renilla* expression was observed from bicistronic reporters containing *HER4* 5' UTR response to 75 μM and 150 μM $CoCl_2$. This not only suggests that $CoCl_2$ is not effective in reducing cap-dependent translation but also that there was issues with the transfection efficiency. Additionally, there was found to be an increase in the *Renilla* from pRF in response to 2μM of thapsigargin. There was also a decrease in the *Renilla* luciferase expression in response to an 1μM of thapsigargin from pRF and constructs containing *EGFR* 5' UTR which indicates that cap-dependent translation was reduced in this condition. There was also a decrease in the *Renilla* luciferase expression from constructs containing *β-tubulin* 5' UTR in response to low serum conditions. The results showed a decrease in the *Renilla* expression in response to hydrogen peroxide for the bicistronic constructs except

constructs mediated by *HER2* 5' UTR. The variation in the *Renilla* luciferase expression across the bicistronic constructs is unexpected as the *Renilla* luciferase expression is driven by the same SV40 promoter in each bicistronic construct, therefore these results are unexplained. However, the variability between constructs could arise from differences in transfection efficiency which could be due to differences in cell numbers, cell lysis, DNA quality, topology of the DNA, cell passage number and cell health (Young *et al.*, 2004). Generation of stable cell lines that have each construct incorporated into the genome of cells may be advantageous when transfecting each construct over many experiments.

Overall, the *Renilla* luciferase expression was not efficiently reduced in response to thapsigargin, $CoCl_2$, low serum conditions and UV-B radiation. 250 µM of hydrogen peroxide did reduce the *Renilla* expression from most bicistronic constructs. The conditions where the *Renilla* expression did not decrease suggests that cap-dependent translation was not inhibited. This indicates that cell stress may not have been induced. As the *Renilla* luciferase expression was unable to decrease cap-dependent translation of most conditions, MTT assays were then conducted to determine if the stress conditions reduced the cell viability of MCF-7 cells. A reduction in the cell viability indicates a reduction of viable of cells which would suggest that cells were being stressed.

There was found to be no effect of $CoCl_2$ and low serum conditions on the cell viability of MCF-7 cells. Thapsigargin and 20 seconds of UV-B radiation did result in a reduction in the cell viability of MCF-7 cells. In addition, hydrogen peroxide increased the cell viability but this was not statistically significant as more replicates are needed. However, an MTT assay does not directly indicate if cell stress occurred as it is possible that cells could have been stressed but the

stress may have not quite affected the cell viability. Therefore, a more sensitive read-out of cell stress would be more appropriate such as measuring eIF2α phosphorylation levels in response to each stress condition which would show that cap-dependent translation was inhibited. In addition, [^{35} S]-methionine incorporation assays could be carried out to measure if each stress could reduce global translation rates (Nagelreiter *et al.*, 2018).

Bicistronic luciferase constructs have been able to detect the existence of many cellular IRESs. They have also been an important model to measure the translational control by a 5' UTR especially as the presence of an IRES is difficult to accurately predict by RNA structure using bioinformatical methods due to cellular IRESs having a low conservation of sequence or structure (Stoneley and Willis, 2004). However, the bicistronic luciferase constructs tested did not measure the translation of the endogenous mRNA which may require other features of the mRNA to influence IRES activity.

In this chapter various stress conditions were used to screen for potential IRES activity in the 5' UTRs of *HER2* and *HER4* mRNA, as IRESs can respond differently to each stress. Although the results from this chapter indicate that it is unlikely that *HER2* and *HER4* contain an IRES, it is still possible for an IRES to exists in the 5' UTRs of these mRNAs active under specific concentrations or exposure time of a stress condition. Therefore, it would have been useful to investigate a smaller number of stresses and optimise each stress condition by using higher concentrations of each chemical used to induce stress or longer time points of each condition. Additionally, the cell stress conditions could be tested in other cell lines that express HER2 and HER4 to determine if the effects are cell-type specific.

Finally, bicistronic luciferase reporters used in this chapter only give an insight into cap-independent translation. As mentioned in the Section 1.6.6.3, *HER2* uORF causes translational repression of the downstream coding region in luciferase reporters (Child, Miller and Geballe, 1999b). *ATF4* uORF has previously been shown to be regulated by glutamine or glucose starvation (Sundaram and Grant, 2014; Gameiro and Struhl, 2018; Zhang *et al.*, 2018; Chen *et al.*, 2022). The use of monocistronic luciferase reporters would allow the effect of *HER2* and *HER4* 5' UTRs on cap-dependent manner to measured which is investigated more in the next chapters.

Chapter 4 - *HER2* and *HER4* 5' UTRs mediated inefficient translation in contrast to *EGFR* 5' UTR in response to glutamine starvation

4.1. Introduction

Cancer cells are highly dependent on glutamine as an energy source to support their rapid cell proliferation (DeBerardinis *et al.*, 2007). Glutamine can enter cells through amino acid transporter, SLC1A5 (Van Geldermalsen *et al.*, 2016; Alfarsi *et al.*, 2021). Glutamine is then converted to glutamate and ammonia in the mitochondria by glutaminase enzymes, this is referred to as glutaminolysis which can activate mTORC1 (Wang *et al.*, 2010; Tsai *et al.*, 2021). Glutamate is then converted to α-ketoglutarate by glutamate dehydrogenase, releasing ammonia and NADPH. α-ketoglutarate enters the tricarboxylic acid cycle (TCA) which produces energy in the form of ATP for cells (Weil-Malherbe and Gordon, 1971; Mailloux *et al.*, 2009). MYC increases cancer cells dependency to glutamine and glutaminolysis by inhibiting the expression of miR-23 which targets glutaminase enzymes (Gao *et al.*, 2009).

In response to glutamine starvation GCN2 phosphorylates eIF2α reducing global protein synthesis (Harding *et al.*, 2000b). However, translation of specific mRNA can take place such as the uORF-mediated translation of *ATF4* in response to glutamine starvation (Section 1.4.2.) (Gameiro and Struhl, 2018; Zhang *et al.*, 2018). ATF4 upregulates the amino acid transporter, SLC7A5 which increases the uptake of branched chain amino acids into cells as an energy source (Chen *et al.*, 2014). SLC7A5 is highly expressed in HER2-positive breast cancers (Törnroos *et al.*, 2022). In addition, VEGF expression is increased in response to glutamine starvation which is suggested to be via IRES-mediated translation. VEGF stimulates angiogenesis in tumours deprived of glutamine (Abcouwer *et al.*, 2002). Additionally, mRNAs involved in glutamine

metabolism such as *MYC* and *TP53* contain IRESs in their 5' UTR (Stoneley *et al.*, 1998; Ray, Grover and Das, 2006).

In response to glutamine starvation, oncogenic MYC can also increase the expression of a glutamine synthetase, glutamate ammonia ligase. This occurs by MYC binding to the promoter of a DNA demethylation enzyme called thymine DNA glycosylase (TDG). This leads to an increase in TDG expression and the activity of glutamine synthetase which increases the uptake of amino acids in breast cancer cells which aids cancer cell survival (Bott *et al.*, 2015).

In addition, in response to glutamine starvation p53 can promote cancer cell survival by upregulating the arginine transporter, SLC7A3. This increases the influx of arginine and activation of mTORC1 which has shown to promote cancer cell growth in mouse embryotic fibroblasts and xenograft tumour models (Lowman *et al.*, 2019).

As mentioned in Section 1.6.6.3, *HER2* 5' UTR contains a 21 nt uORF that causes translational repression of the *HER2* coding region (Child *et al.*, 1999a, 1999b). In addition, *HER2* 3' UTR contains a translation derepression element (TDE) that interacts with the *HER2* uORF and derepresses the translational inhibition mediated by *HER2* uORF (Mehta *et al.*, 2006). This shows that the *HER2* 3' UTR has a vital role in the translational control of *HER2* mRNA.

HER2 has shown to increase the expression of glutaminases via a NF-KB mechanism (Qie *et al.*, 2014). In addition, HER2 signalling via the MAPK pathway can activate ESR which has shown to increase MYC expression and subsequently glutamine metabolism (Chen *et al.*, 2015). This shows that HER2 has a role in glutamine metabolism.

The aim of this chapter was to investigate the translational control by *HER2* 5' UTR and *HER4* 5' UTR in response to glutamine starvation. This was carried out using monocistronic luciferase constructs that allow translation in a cap-dependent or cap-independent manner. It is hypothesised that the translational control by *HER2* 5' UTR will adopt a similar translational control mechanism in response to glutamine starvation conditions similarly to other genes containing uORFs in their 5' UTR such as *ATF4* (Gameiro and Struhl, 2018; Zhang *et al.*, 2018). As mentioned in Chapter 3, *HER2* and *HER4* 5' UTRs are unlikely to contain an IRES. However, IRESs can be active under specific stress conditions. The experiments in this study will also determine if *HER*2 and *HER4* 5' UTRs contain an IRES active in response to glutamine starvation using bicistronic luciferase constructs. Investigating the translational control of these genes in glutamine starvation conditions can reveal vital mechanisms in the 5' UTRs of the genes. This is important as HER2 and HER4 are oncogenes and finding mechanisms responsible for an upregulation of translation in glutamine starvation conditions that cancer cells can adapt and grow in, can reveal key therapeutic targets for cancer.

4.2. No evidence of IRES activity in *HER2* and *HER4* 5' UTRs in response to glutamine starvation

HER2 has shown to increase glutaminolysis via a NF-KB mechanism (Qie *et al.*, 2014). In addition, HER2 can upregulate MYC expression and subsequently glutamine metabolism in breast cancer cells (Chen *et al.*, 2015). Additionally, given that the mRNAs of some oncogenes involved in glutamine metabolism contain IRESs, it was investigated whether *HER2* 5' UTR contains an IRES that may be active in response to glutamine starvation.

To determine if *HER2* 5' UTR or *HER4* 5' UTR contain an IRES active in response to glutamine starvation, bicistronic luciferase constructs were transfected into MCF-7 cells starved of glutamine for 30 minutes or 4 hours. 30 minutes and 4 hours of glutamine starvation has previously been shown to metabolically stress transformed and non-transformed MCF10A, this was indicated by an reduction in global translation (Gameiro and Struhl, 2018). Therefore, these time points were chosen in this study.

First, the *Renilla* expression was measured to determine if glutamine starvation caused a decrease in cap-dependent translation. Overall, there was no change in the *Renilla* expression in response to 30 minutes or 4 hours of glutamine starvation (Figure 4.1). The exception to this was a decreased in the *Renilla* expression from bicistronic constructs containing *EGFR* 5' UTR in response to 30 minutes of glutamine starvation indicating a reduction in cap-dependent translation in cells containing the *EGFR* 5' UTR-bicistronic constructs. Also, an increase in the *Renilla* expression was observed for pRF in response to 4 hours

of glutamine starvation (Figure 4.1). Overall, cap-dependent translation was not efficiently reduced in response to glutamine starvation.

To determine if 30 minutes or 4 hours of glutamine starvation could induce IRES activity the F/R expression of each bicistronic construct was measured. Unexpectedly, there was an increase in the firefly luciferase and the F/R expression from pRF in response to 30 minutes of glutamine starvation, however the expression of pRF was still near background (Appendix Figure 11 and Figure 4.2). There was an increase in the F/R expression mediated by *EGFR* 5' UTR in response to 30 minutes of glutamine starvation (Figure 4.2). There seemed to also be an increase in the firefly luciferase expression, however there was some variability in the replicates (Appendix Figure 11). This indicates that *EGFR* IRES activity was increased in response to 30 minutes of glutamine starvation, whilst the *Renilla* expression decreased for bicistronic constructs containing *EGFR* 5' UTR at this timepoint. However, it was not determined if this was statistically significant as only one independent experiment was conducted. There was no observed effect of 30 minutes of glutamine starvation on the firefly luciferase and the F/R expression mediated by the 5' UTRs of *β-tubulin*, *HER2* and *HER4* (Appendix Figure 11) (Figure 4.2). Additionally, there was no change in the F/R and firefly luciferase expression of any of the bicistronic constructs in response to 4 hours of glutamine starvation (Appendix Figure 11). This shows that there was no evidence of IRES activity in the 5' UTRs of *HER2* and *HER4* in response to short term glutamine starvation.

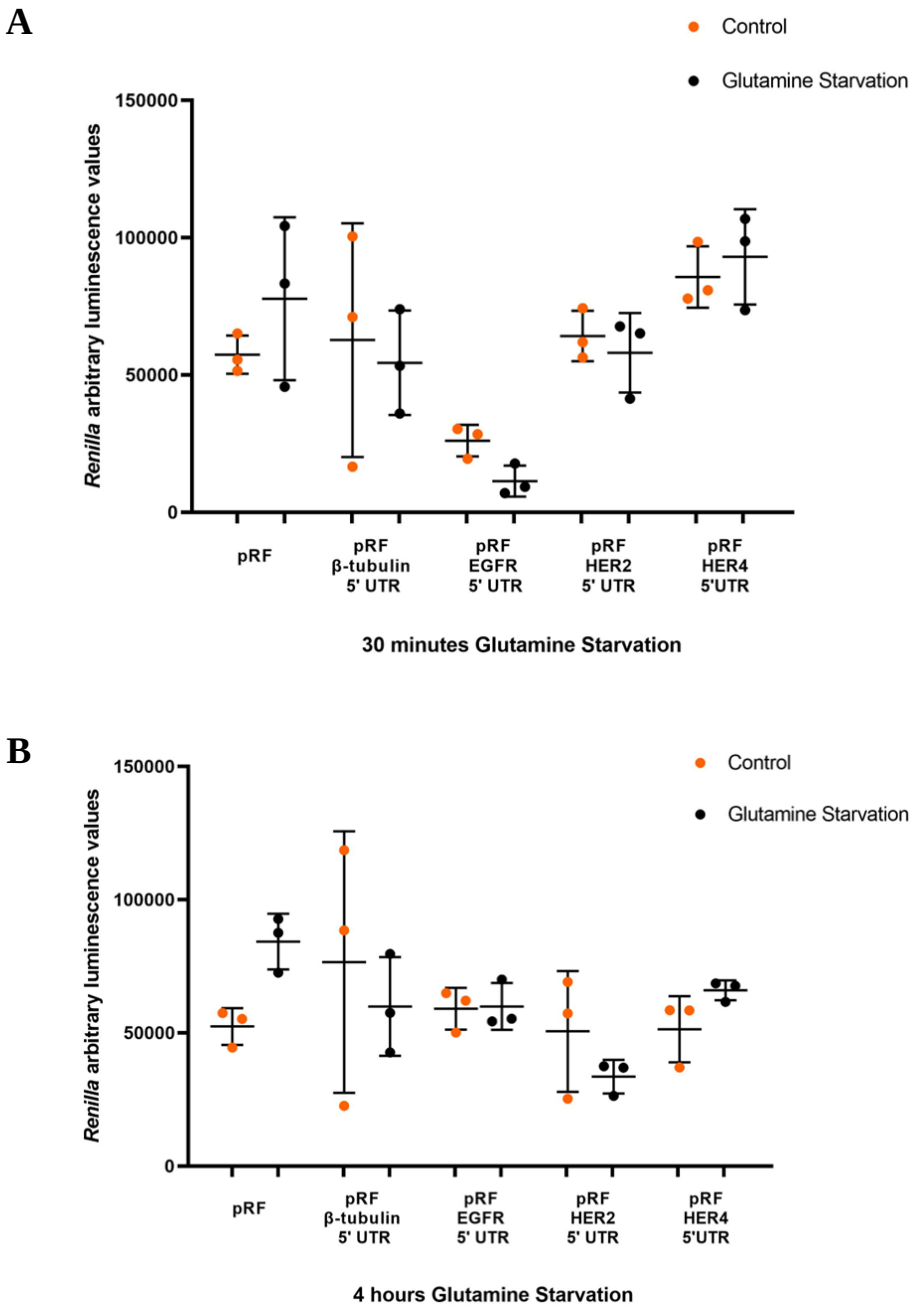

Figure 4.1. Overall, short-term glutamine starvation had no effect on the *Renilla* expression. MCF-7 cells were transfected with each bicistronic construct. 24 hours post-transfection cells were starved of glutamine for 30 minutes or 4 hours (black) or non-starved (orange). After each timepoint cells were then lysed and the *Renilla* expression was measured. A) 30 minutes of glutamine starvation. B) 4 hours of glutamine starvation. Data represents one independent experiment carried out in triplicate. All error bars represent the standard deviation.

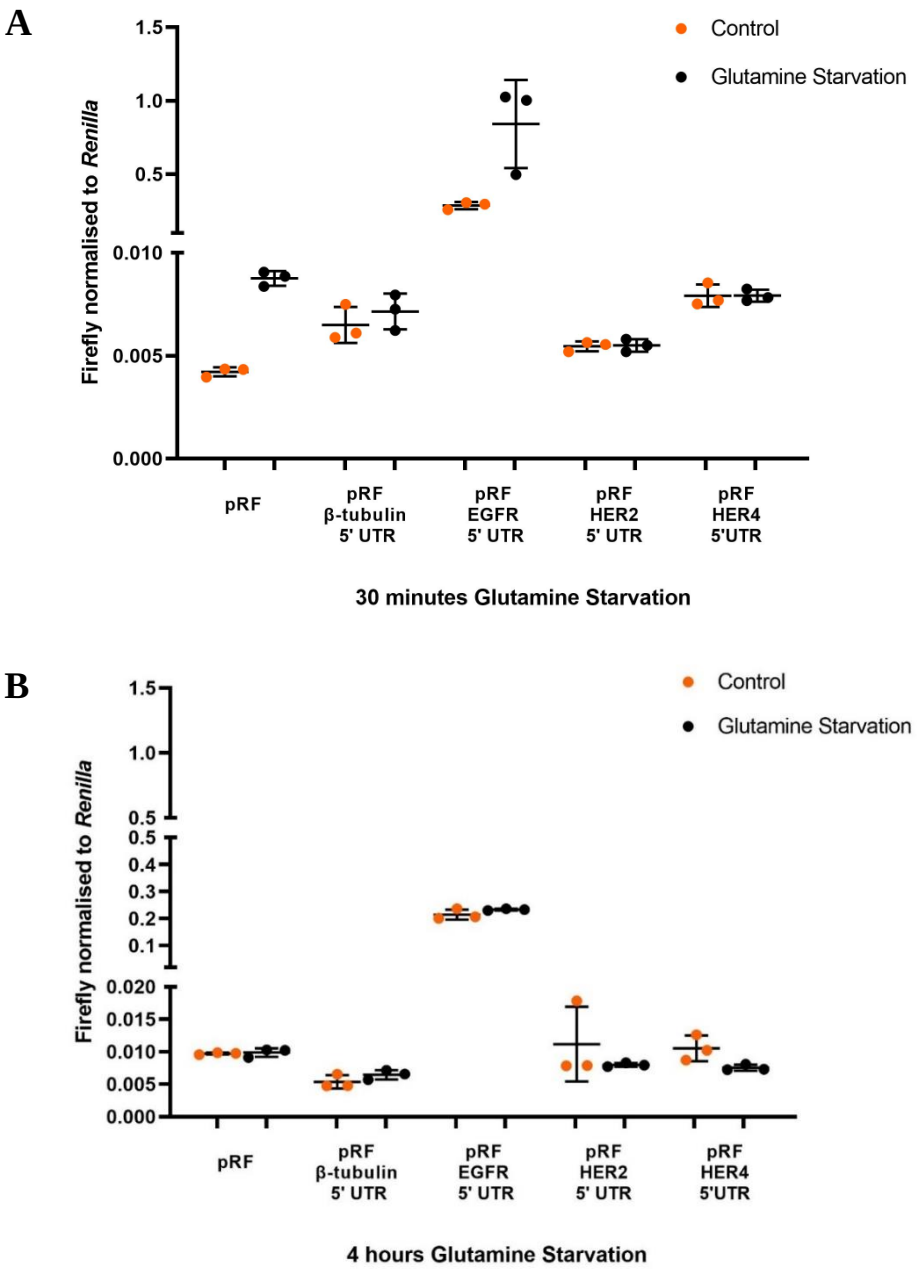

Figure 4.2. No evidence of IRES activity in *HER2* or *HER4* 5' UTRs in response to short-term glutamine starvation. MCF-7 cells were transfected with each bicistronic construct. 24 hours post-transfection cells were starved of glutamine for 30 minutes or 4 hours (black) or non-starved (orange). After each timepoint cells were then lysed, and the F/R expression was measured. A) 30 minutes of glutamine starvation. B) 4 hours of glutamine starvation. Data represents one independent experiment carried out in triplicate. All error bars represent the standard deviation.

As shorter timepoints of glutamine starvation were unable to consistently reduce the *Renilla* expression, next MCF-7 cells were starved of glutamine for 24 hours to determine if cap-dependent translation could be reduced in this condition. It was found that the *Renilla* expression was reduced for pRF and constructs containing *β-tubulin* 5' UTR and *HER2* 5' UTR. The *Renilla* expression from constructs containing *EGFR* 5' UTR and *HER4* 5' UTR seemed to be reduced in response to glutamine starvation. However, as there was variation in the technical replicates the reduction in the *Renilla* expression was not as great as the other reporters and therefore more replicates would need to be carried out (Figure 4.3). This shows that cap-dependent translation may be reduced in response to 24 hours of glutamine starvation but more experiments would need to be conducted to confirm this.

Then the F/R expression was measured to determine if the 5' UTRs contain an IRES active in response to 24 hours of glutamine starvation. It was found that 24 hours of glutamine starvation reduced the firefly luciferase expression as well as the *Renilla* expression resulting in no effect of 24 hours of glutamine starvation on the F/R expression from pRF or constructs containing *β-tubulin* 5' UTR (Appendix Figure 12 and Figure 4.4). There was no change in the firefly luciferase expression from *EGFR* IRES. However, the decrease in the *Renilla* expression resulted in an increase in F/R levels in response to 24 hours of glutamine starvation (Appendix Figure 12 and Figure 4.4). However, constructs containing *HER2* or *HER4* 5' UTR produced firefly luciferase and F/R levels similar to the negative controls (Appendix Figure 12 and Figure 4.4). This shows that in contrast to *EGFR, HER2* and *HER4* 5' UTRs do not mediate IRES activity in response to 24 hours of glutamine starvation.

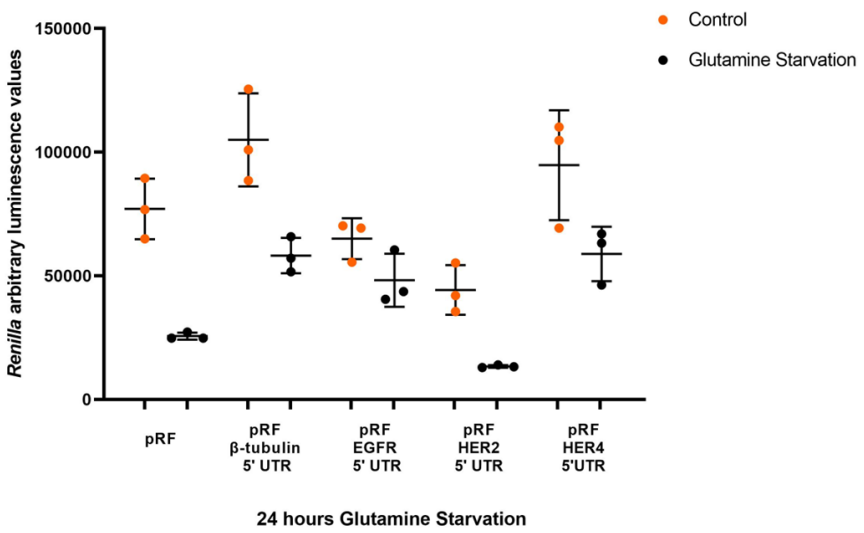

Figure 4.3. The effect of 24 hours of glutamine starvation on the *Renilla* expression. MCF-7 cells were transfected with each bicistronic construct. 24 hours post-transfection cells were starved of glutamine for 24 hours (black) or non-starved (orange). Cells were then lysed and the *Renilla* expression was measured. Data represents one independent experiment carried out in triplicate. All error bars represent the standard deviation.

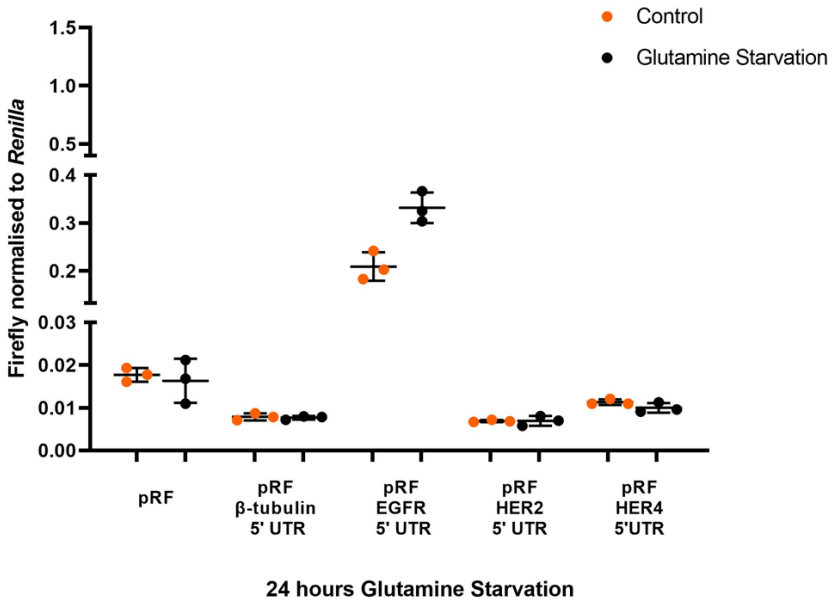

Figure 4.4. No evidence of IRES activity in *HER2* or *HER4* 5' UTRs in contrast to *EGFR* IRES in response to 24 hours of glutamine starvation. MCF-7 cells were transfected with each bicistronic construct. 24 hours post-transfection cells were starved of glutamine for 24 hours (black) or non-starved (orange). Cells were then lysed, and the F/R expression was measured. Data represents one independent experiment carried out in triplicate. All error bars represent the standard deviation.

As Figure 4.1 and Figure 4.3 showed that the *Renilla* expression was not efficiently decreased in response to glutamine starvation, an MTT assay was carried out to determine if short term or long-term glutamine starvation could reduce the cell viability of MCF-7 cells. First, the effect of short-term glutamine starvation was measured and there was found to be no effect of 30 minutes and 4 hours of glutamine starvation on the cell viability of MCF-7 cells (Figure 4.5). This is in contrast to transformed and non-transformed MCF10A cells (Gameiro and Struhl, 2018).

Next, MCF-7 cells were starved of glutamine for 24 hours, 48 hours and 72 hours. Then an MTT assay was conducted to determine if longer time periods could have an effect on the cell viability of MCF-7 cells. There was a 55.1% and 62.1% reduction in the cell viability of MCF-7 cells in response to 48 hours and 72 hours of glutamine starvation, respectively (Figure 4.6). This indicates that long term glutamine starvation may be able to induce cell stress.

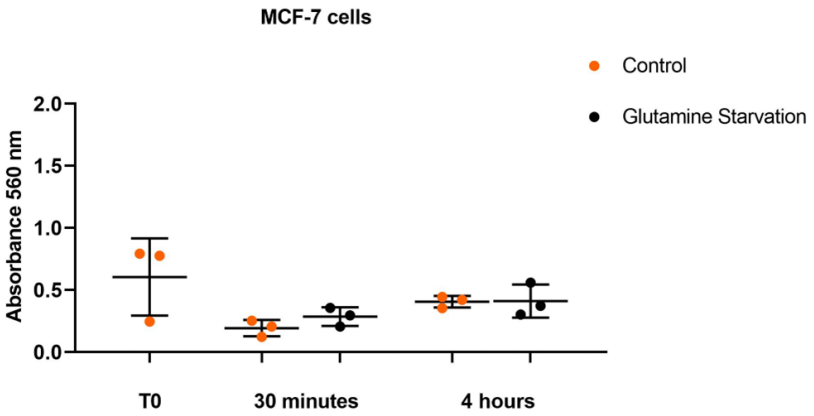

Figure 4.5. Short-term glutamine starvation had no effect on the cell viability of MCF-7 cells. MCF-7 cells were starved of glutamine for 30 minutes or 4 hours (black) or were not starved (orange). After each time-point cell viability was measured by MTT assay. T0= time-zero readings taken at the start of treatment. Data represents three biological repeats (N=6). Error bars represent the standard deviation. $p<0.05$ was determined as statistically significant using a t-test with Bonferroni-Dunn's correction.

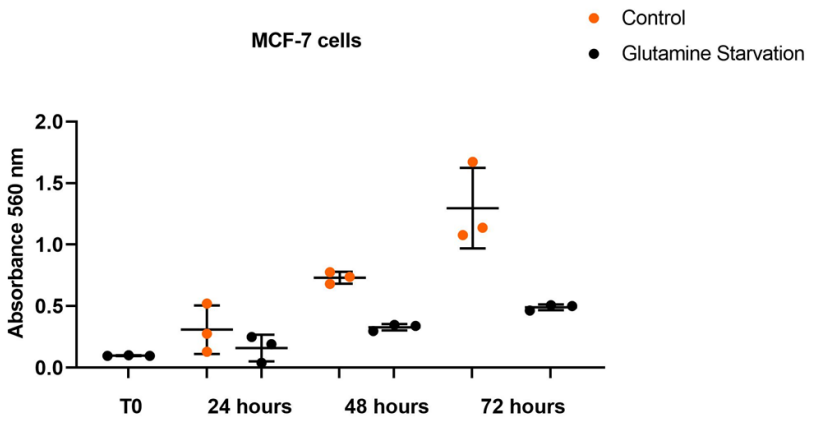

Figure 4.6. The effect of long term glutamine starvation on the cell viability of MCF-7 cells. MCF-7 cells were starved of glutamine for 24, 48 and 72 hours (black) or were not starved (orange). After each time-point cell viability was measured by MTT assay. T0= time-zero readings taken at the start of treatment. Data represents one independent experiment each taken in triplicate. Error bars represent the standard deviation. Percentage decrease was calculated from the average of a single independent experiment.

The MTT assay gave an indirect indication that long-term glutamine starvation was affecting cell viability, so next a western blot was carried to determine if glutamine starvation induced eIF2α phosphorylation which is a more direct way of monitoring cell stress. For the western blots, 24 hours of glutamine starvation was used to determine if a more sensitive read-out could indicate cell stress at this timepoint. 48 hours of glutamine starvation was used as a reduction in the cell viability was observed in this condition from the MTT assay results.

There was no change in the total eIF2α levels in response to glutamine starvation. However, using phospho-specific antibodies there was found to be an increase in the phosphorylated form of eIF2α in response to 48 hours of glutamine starvation in comparison to the 24 hours non-starvation and 24 hours glutamine starvation conditions (Figure 4.7). This indicates that eIF2α phosphorylation increases in a time-dependent manner in response to glutamine starvation. Protein levels of phosphorylated eIF2α also increased at the 48 hour non-starvation timepoint in comparison to the 24 hours non-starvation timepoint (Figure 4.7). This suggests that a substance in the cell media is depleted at 48 hours that is stressing cells and leading to eIF2α phosphorylation in response to 48 hours of non-starvation and glutamine starvation.

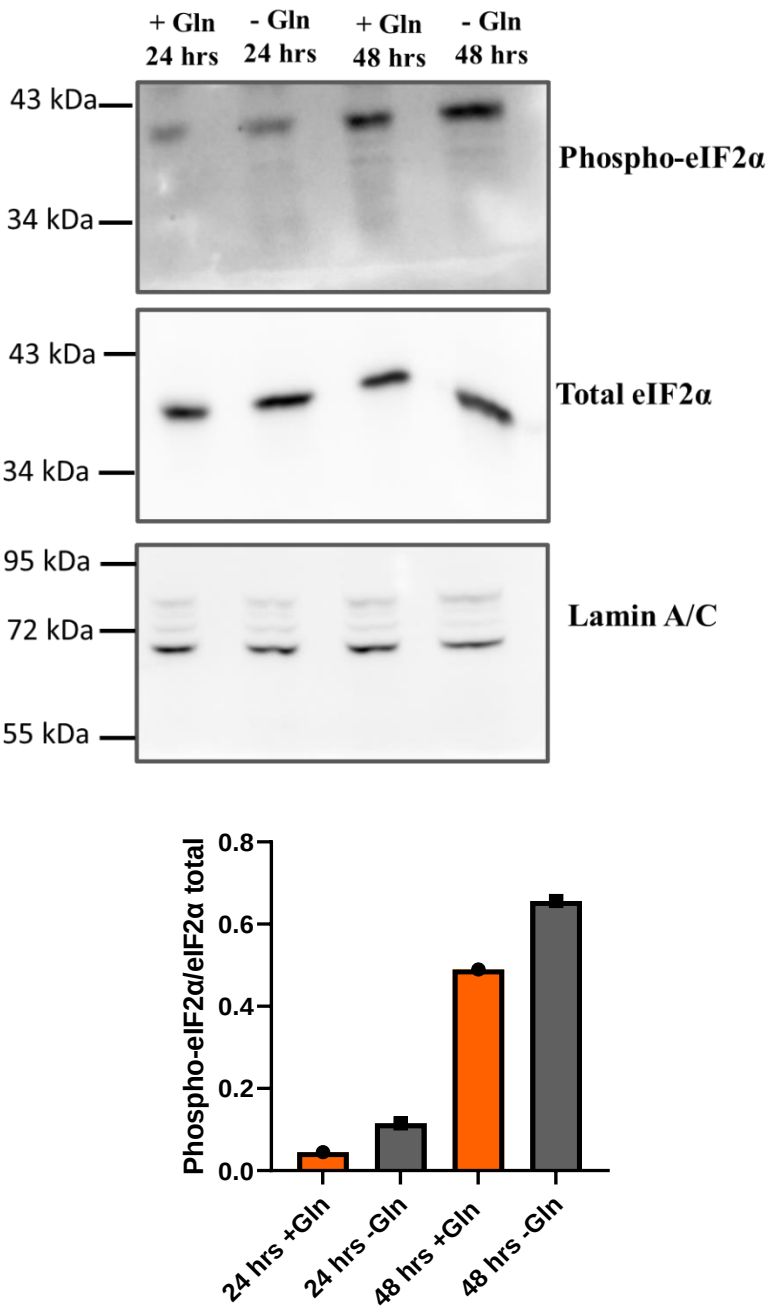

Figure 4.7. Increase in phosphorylated eIF2α protein levels in response to 48 hours of non-starvation and glutamine starvation. Western blots of phosphorylated eIF2α (38 kDa), total eIF2α (38 kDa) and lamin a/c (loading control) (lamin a; 74 kDa, lamin c; 63 kDa; lamin a/c antibody bands usually observed between 60-80 kDa) were carried out on the lysates from MCF-7 cells starved of glutamine for 24 hours and 48 hours (-Gln). The lysates from MCF-7 cells incubated in glutamine containing media for 24 hours and 48 hours were used as a control (+Gln). Densitometric analysis shown of phosphorylated eIF2α relative to total eIF2α. One independent experiment of each blot was carried out.

4.3. Investigating the effect of glutamine starvation on the endogenous HER2 protein and *HER2*/*HER4* mRNA expression levels

As it is hypothesised that the translation of *HER2* may increase in response to glutamine starvation, western blots were carried out to investigate if glutamine starvation could increase endogenous HER2 protein expression. It was found that HER2 protein expression was higher in response to 48 hours of glutamine starvation in comparison to both 24 hours and 48 hours non-starvation controls (Figure 4.8). This shows that HER2 protein levels increased in response to 48 hours of glutamine starvation.

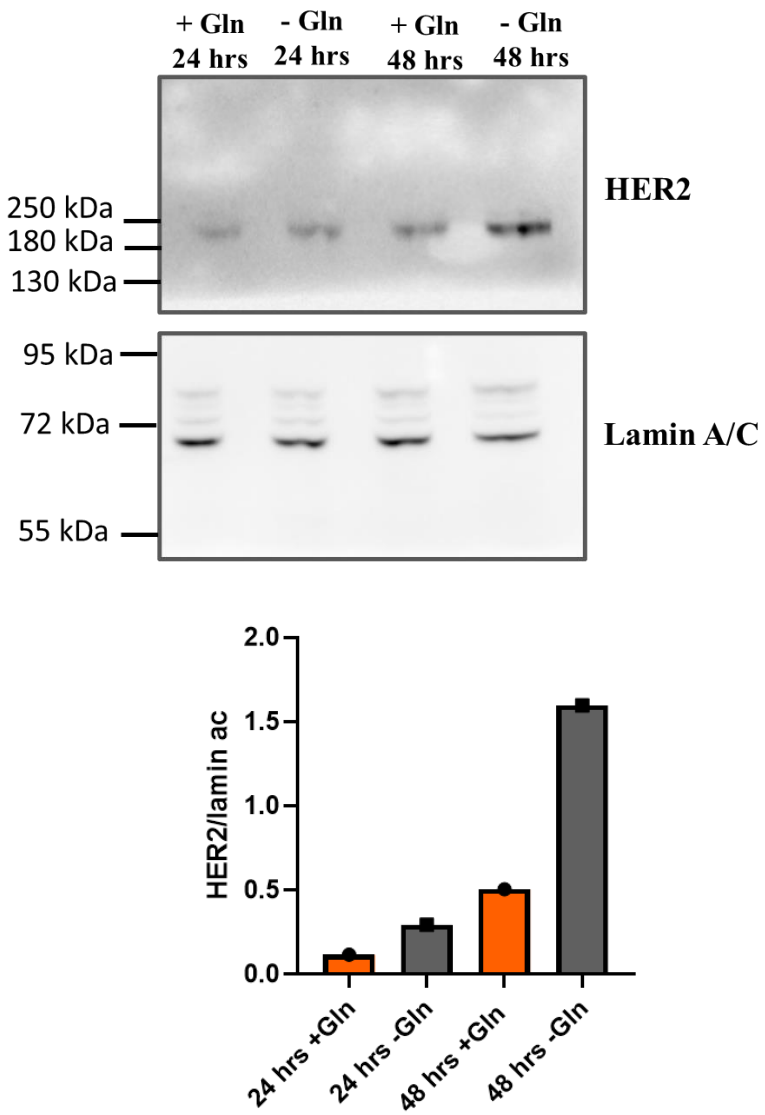

Figure 4.8. Increase in HER2 protein levels in response to 48 hours of glutamine starvation. Western blots of HER2 (185 kDa) and lamin a/c (loading control) (lamin a; 74 kDa, lamin c; 63 kDa; lamin a/c antibody bands usually observed between 60-80 kDa) were carried out on the lysates from MCF-7 cells starved of glutamine for 24 hours and 48 hours (-Gln). The lysates from MCF-7 cells incubated in glutamine containing media for 24 hours and 48 hours were used as a control (+Gln). Densitometric analysis shown of HER2 relative to lamin a/c loading control. One independent experiment of each blot was carried out.

Next, it was investigated at what level HER2 protein was increased following glutamine starvation. qPCR analysis was carried out to determine if there were any changes in the endogenous mRNA levels of *HER2* and *HER4* in response to glutamine starvation. This is important to see if changes in transcription of the genes or mRNA stability have an impact on the efficiency of mRNA translation under glutamine starvation. There was an observed increase in *HER2* mRNA expression in response to 24 hours and 48 hours of glutamine starvation, however this was determined to be statistically insignificant ($p=0.127$ and $p=0.127$). There was found to be a statistically significant increase in the mRNA levels of *HER4* in response to 24 hours and 48 hours of glutamine starvation ($p=0.008$ and $p=0.008$ respectively). As expected, there was no change in the mRNA levels of *β-actin* reference gene in response to 24 hours and 48 hours of glutamine starvation ($p=0.159$ and $p=0.159$ respectively) (Figure 4.9). This indicates that glutamine starvation did increase the transcription of *HER2* and *HER4*, although this was not statistically significant for *HER2*.

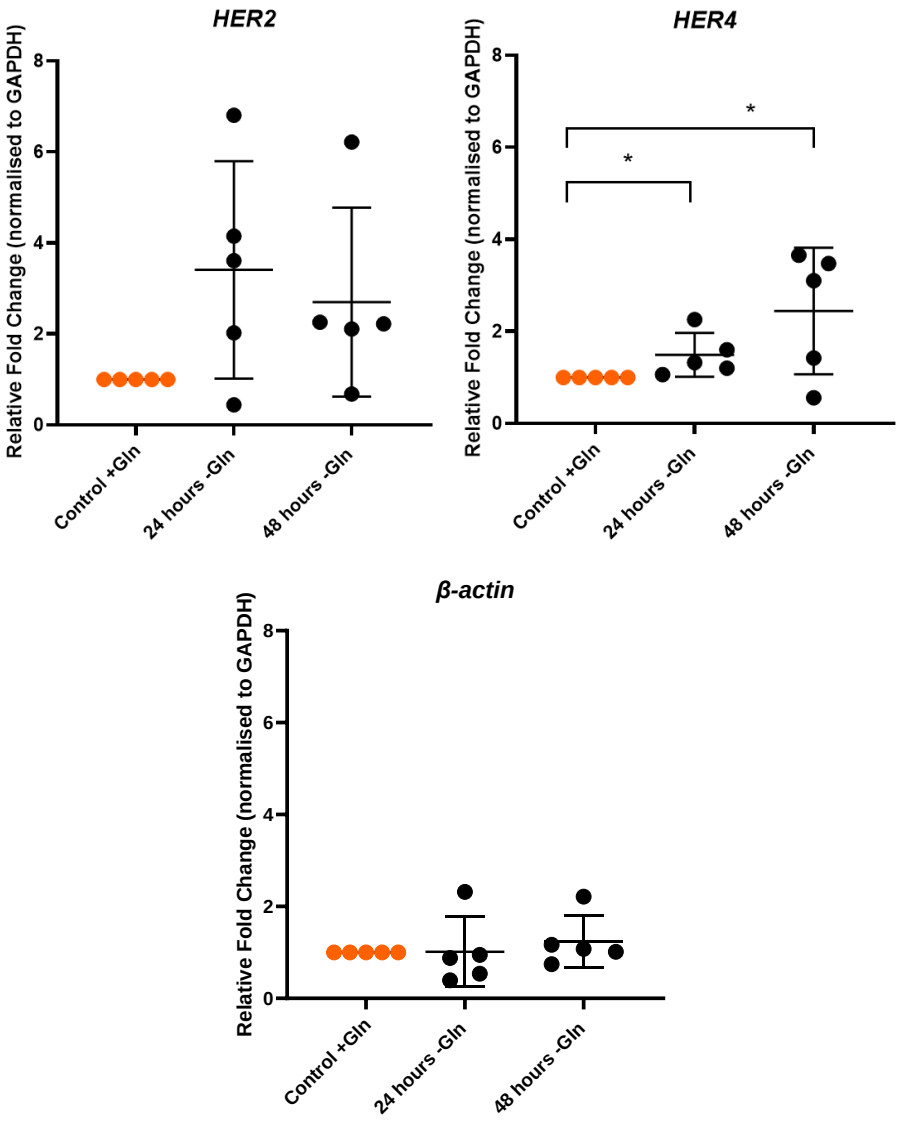

Figure 4.9. The effect of glutamine starvation on *HER2* and *HER4* mRNA levels. MCF-7 cells were incubated in media containing glutamine (+Gln) for 24 hours as a control (orange) or cells were starved of glutamine (-Gln) for 24 hours or 48 hours (black). After each timepoint total RNA was extracted before being reverse transcribed into cDNA which was used as the qPCR template. Data displayed as fold change normalised to GAPDH house-keeping gene using the $2^{-\Delta\Delta CT}$ method. Data represents the average of five independent experiments each carried out in triplicate. All error bars represent the standard deviation. $p<0.05$ was determined as statistically significant (*). A Mann-Whitney t-test with Bonferroni-Dunn's correction was used for comparisons of two groups: 24 hours and 48 hours of glutamine starvation conditions compared separately to the 24 hour non-starvation control.

4.4. Creating 5’ UTR monocistronic luciferase constructs

To determine if the 5’ UTRs of *HER2* and *HER4* could mediate an increase in translation in a cap-dependent manner in response to glutamine starvation the 5’ UTRs were cloned into monocistronic luciferase plasmids. Translation in a monocistronic context can occur in a cap-dependent or cap-independent manner. The firefly luciferase monocistronic vector originally from pGL4.15 (referred to as p15) contains a CMV promoter upstream to the firefly luciferase open reading frame (Figure 4.10). The 5’ UTRs were cloned into p15 upstream of firefly luciferase using *Hind*III restriction sites and successful cloning was confirmed by Sanger sequencing described in Chapter 2 (Table 2.2 and Table 2.5) (Figure 4.11). A p15 vector that contains a single firefly luciferase open reading frame generates efficient translation and was used as a control (Webb, 2012 and Smalley, 2016). Additionally, *EGFR* 5’ UTR had previously been cloned into p15 using *Hind*III restriction sites and was used as a comparison plasmid (Figure 4.11) (Smalley, 2016). pGL4.80 (p80) (Promega) monocistronic *Renilla* plasmid was co-transfected into cells and was used as a transfection control to normalise firefly luciferase expression (Appendix-Figures 33 and 34).

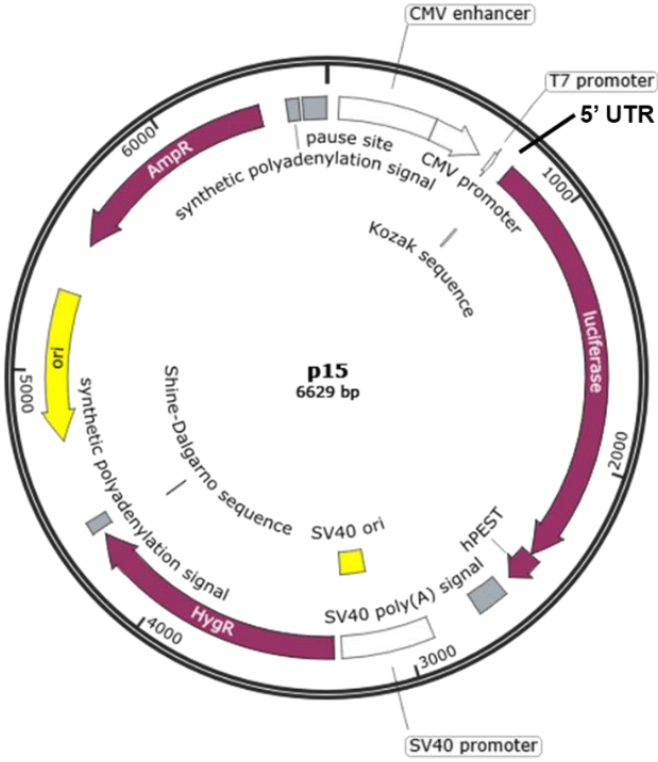

Figure 4.10. Monocistronic firefly luciferase construct-p15 vector map. p15 originally from pGL4.15 with a cytomegalovirus (CMV) promoter upstream to firefly luciferase. The 5' UTRs cloned into p15 upstream to firefly luciferase.

i)

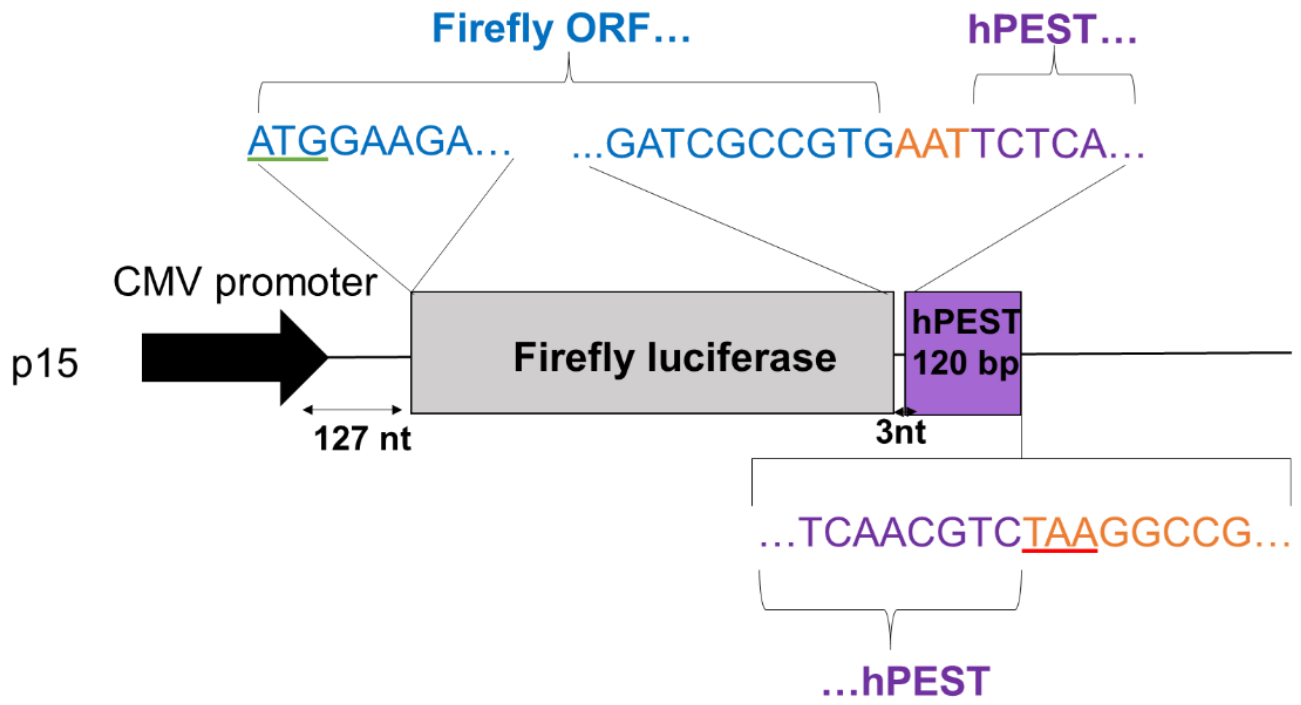
Firefly ORF…
hPEST…
ATGGAAGA…
…GATCGCCGTGAATTCTCA…
CMV promoter
p15
Firefly luciferase
hPEST
120 bp
127 nt
3nt
…TCAACGTCTAAGGCCG…
…hPEST

ii)

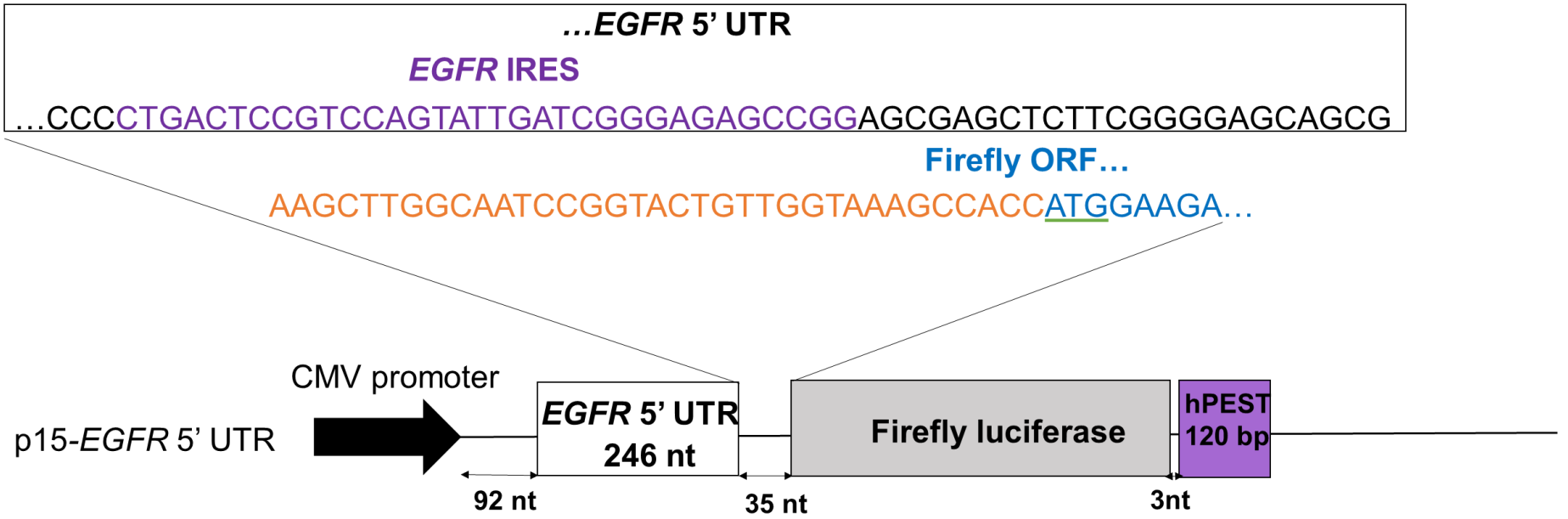
…*EGFR* 5’ UTR
EGFR IRES
…CCCCTGACTCCGTCCAGTATTGATCGGGAGAGCCGGAGCGAGCTCTTCGGGGAGCAGCG
Firefly ORF…
AAGCTTGGCAATCCGGTACTGTTGGTAAAGCCACCATGGAAGA…
CMV promoter
p15-*EGFR* 5’ UTR
EGFR 5’ UTR
246 nt
Firefly luciferase
hPEST
120 bp
92 nt
35 nt
3nt

iii)

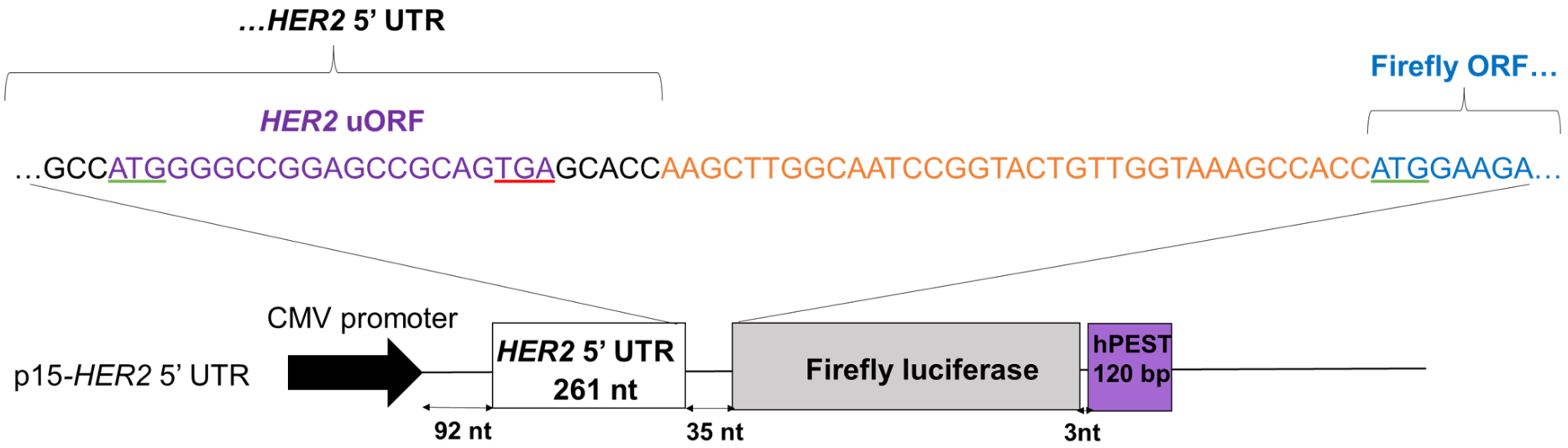
…HER2 5' UTR
HER2 uORF
Firefly ORF…
…GCCATGGGGCCGGAGCCGCAGTGAGCACCAAGCTTGGCAATCCGGTACTGTTGGTAAAGCCACCATGGAAGA…
CMV promoter
p15-HER2 5' UTR
HER2 5' UTR
261 nt
Firefly luciferase
hPEST
120 bp
92 nt
35 nt
3nt

iv)

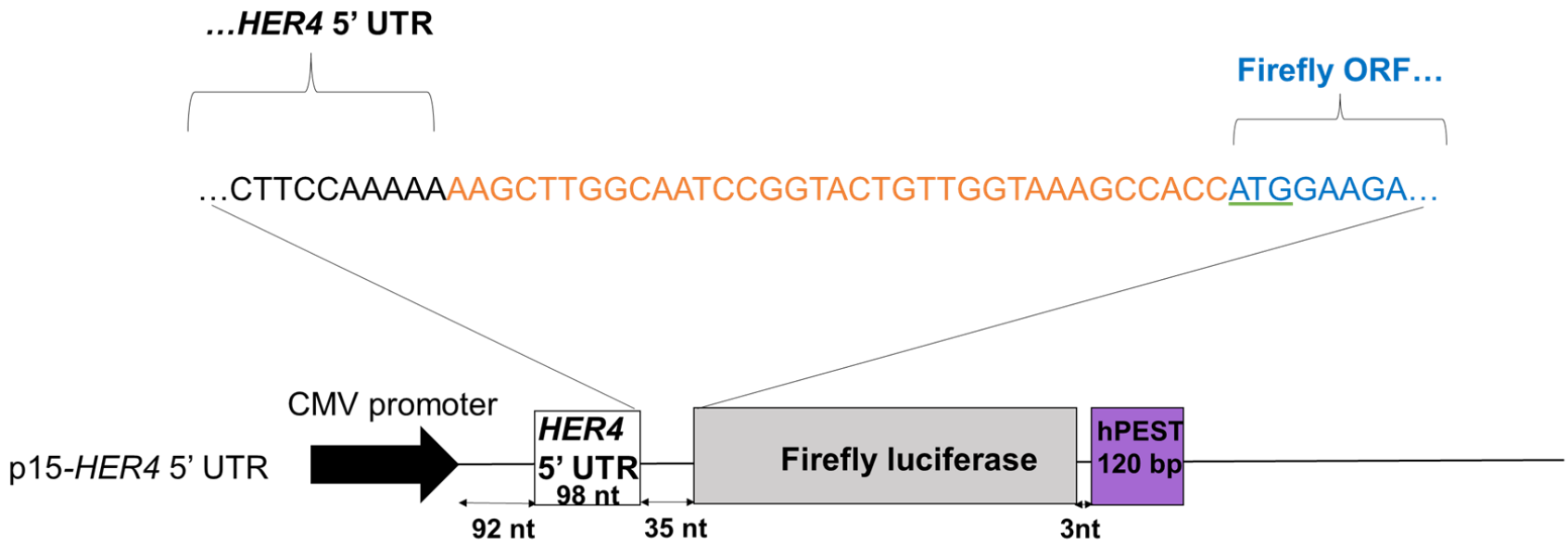

Figure 4.11. Schematic of monocistronic constructs used in this project. i)The p15 plasmid and ii) p15-*EGFR*-5' UTR containing *EGFR* 5' UTR upstream to firefly luciferase were used as controls (*EGFR* IRES highlighted purple, source: Webb, 2012). The 5' UTRs of *HER2* and *HER4* were cloned upstream to firefly luciferase in p15 monocistronic luciferase vector and referred to as iii) p15-*HER2* 5' UTR (*HER2* uORF is highlighted purple) and iv) p15-*HER4* 5' UTR. Firefly luciferase and hPEST sequences are in frame. Start codons are underlined green and stop codons are underlined red.

4.5. *HER2* 5' UTR and *HER4* 5' UTR are unable to increase translation in a monocistronic context in response to glutamine starvation

There was no observation of IRES activity in the 5' UTRs of *HER2* and *HER4* in response to glutamine starvation so next it was investigated whether either *HER2* or *HER4* 5' UTR could allow an increase in translation in response to glutamine starvation in a monocistronic context. Translation in a monocistronic context can take place via cap-dependent or cap-independent translation. The previously identified uORF in *HER2* 5' UTR may allow translation in a cap-dependent manner.

First, it was assessed whether glutamine starvation reduced the *Renilla* expression in a monocistronic context which would indicate a decrease in cap-dependent translation. Figure 4.12 suggests that the *Renilla* expression was reduced in response to 24 hours of glutamine starvation. However, due to variations between biological replicates this was found to be statistically insignificant except for *Renilla* constructs co-transfected with *HER4* 5' UTR. In response to 48 hours of glutamine starvation the *Renilla* expression was reduced for all the monocistronic constructs except constructs containing *EGFR* 5' UTR. Although the *Renilla* expression was not statistically significant when co-transfected with some of the monocistronic firefly constructs, the data suggests that cap-dependent translation was reduced in response to glutamine starvation (Figure 4.12).

Next, the F/R expression was assessed in non-stressed conditions. It was found that *EGFR* 5' UTR was able to produce F/R expression levels similar to p15

(Figure 4.13). This shows that *EGFR* can mediate efficient translation in a monocistronic construct via its IRES. *HER2* and *HER4* 5' UTR produced lower F/R expression levels than p15 and *EGFR* 5' UTR (Figure 4.13). This shows that there was inefficient translation mediated from *HER2* and *HER4* 5' UTRs compared to p15 and *EGFR* 5' UTR in non-stressed conditions.

To determine the effect of glutamine starvation on the translation mediated by each 5' UTR, the F/R expression was measured in MCF-7 cells starved of glutamine. There was a lower firefly luciferase expression from p15 in response to 24 and 48 hours of glutamine starvation, however this was insignificant at the 24 hour timepoint due to variation across independent experiments (Appendix Figure 20). It was found that 24 hours and 48 hours of glutamine starvation had no effect on the F/R expression from p15 ($p=0.548$ and $p=0.270$ respectively) (Figure 13). There was a decrease in the firefly luciferase expression mediated by *EGFR* 5' UTR across some replicates in response to glutamine starvation. However, as there was variation across replicates this was statistically insignificant (Appendix Figure 20).There seemed to be an increase in the F/R expression mediated by *EGFR* 5' UTR in response to 24 hours of glutamine starvation, however this was statistically insignificant ($p=0.087$) (Figure 13). However, the firefly luciferase expression had a similar trend to the *Renilla* expression resulting in a 1.4-fold increase in the F/R expression mediated by *EGFR* 5' UTR in response to 48 hours of glutamine starvation ($p=0.036$) (Appendix Figure 20) (Figure 13). There was found to be a decrease in the firefly luciferase expression from constructs containing *HER2* 5' UTR resulting in no effect of 24 hours or 48 hours of glutamine starvation on the F/R expression from constructs containing *HER2* 5' UTR ($p=0.486$ and $p=0.078$ respectively)

(Appendix Figure 20) (Figure 13). However, there was a 1.5-fold decrease ($p=0.004$ and $p=0.049$ respectively) in the firefly luciferase and the F/R expression mediated from *HER4* 5' UTR in response to 24 hours and 48 hours of glutamine starvation (Appendix Figure 20) (Figure 13). These results show that glutamine starvation is unable to increase translation mediated by *HER2* 5' UTR or *HER4* 5' UTR.

A

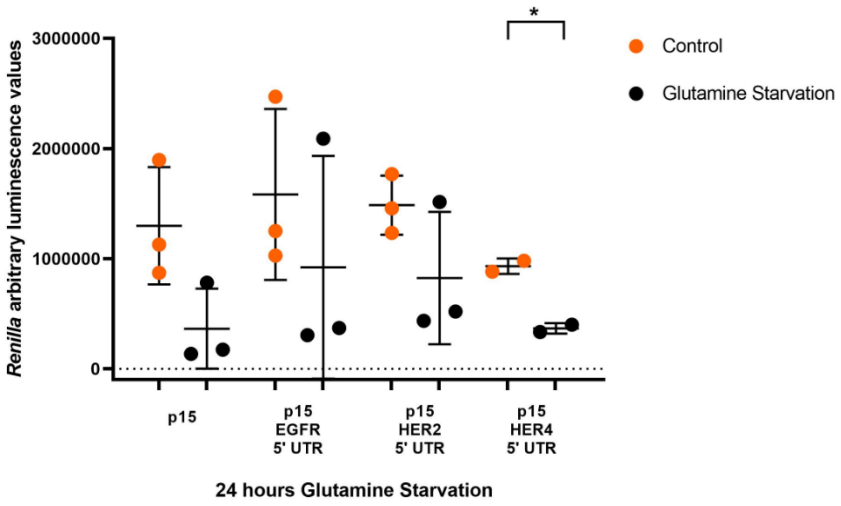

B

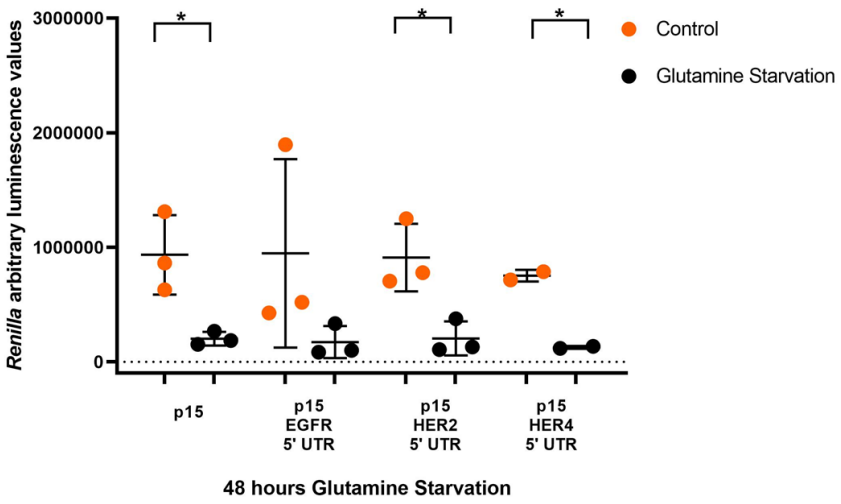

Figure 4.12. The monocistronic *Renilla* expression co-transfected with each construct in response to glutamine starvation. MCF-7 cells were transfected with firefly luciferase monocistronic constructs containing the 5' UTRs and co-transfected with p80 *Renilla* luciferase construct. 24 hours later were exposed to either DMEM containing glutamine control media (orange) or DMEM containing no glutamine media (black). After each timepoint cells were lysed, and the *Renilla* expression was measured. A) 24 hours of glutamine starvation. B) 48 hours of glutamine starvation. Data represents the average of two-three independent experiment carried out in triplicate. All error bars represent the standard deviation. $p<0.05$ was determined as statistically significant (*). A t-test with Bonferroni-Dunn's correction was used for comparisons of each construct in starvation conditions compared to their non-starvation control.

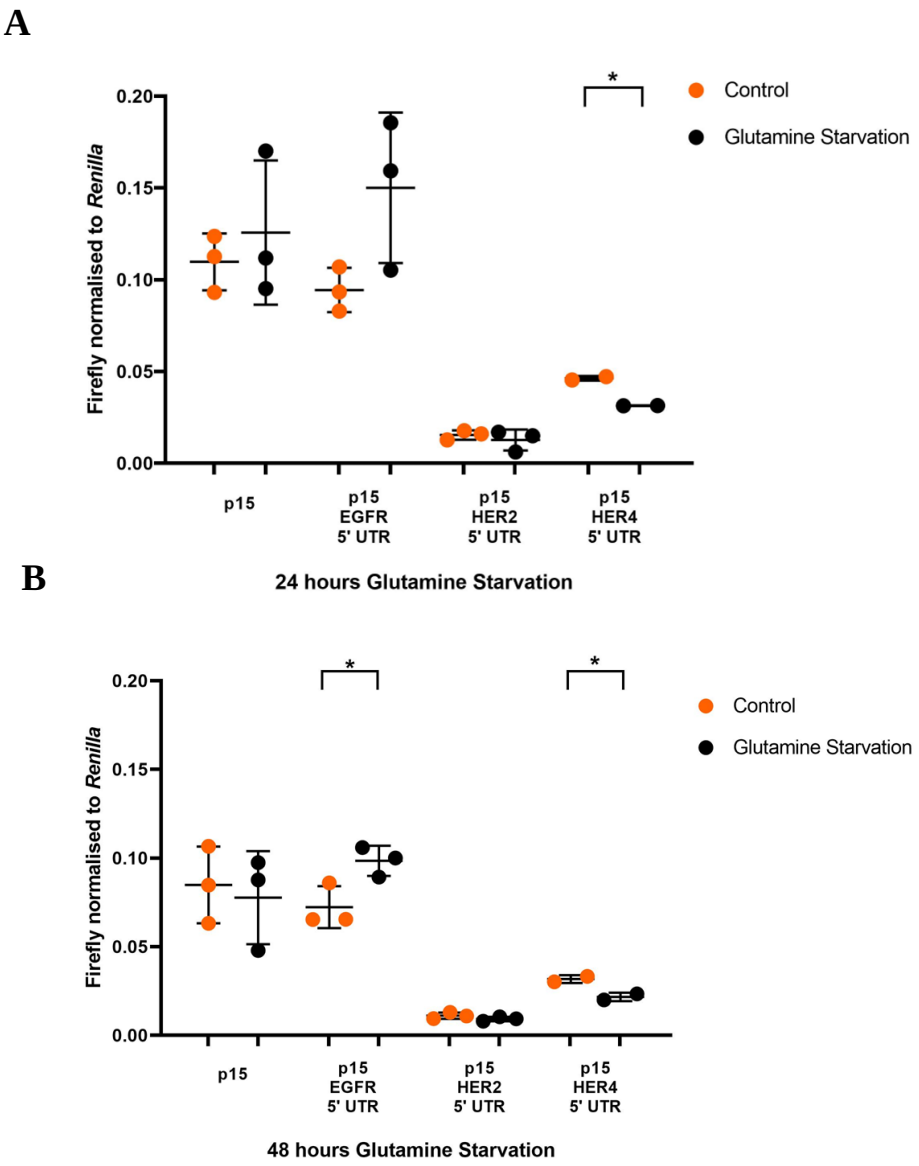

Figure 4.13. *HER4* 5' UTR mediated a decrease in translation in response to 48 hours of glutamine starvation whilst *EGFR* 5' UTR increased translation in a monocistronic context. MCF-7 cells were transfected with firefly luciferase monocistronic constructs containing the 5' UTRs and co-transfected with p80 *Renilla* luciferase construct. 24 hours later were exposed to either DMEM containing glutamine control media (orange) or DMEM containing no glutamine media (black). After each timepoint cells were lysed, and the F/R expression was measured. A) 24 hours of glutamine starvation. B) 48 hours of glutamine starvation. Data represents the average of two-three independent experiments each carried out in triplicate. All error bars represent the standard deviation. $p<0.05$ was determined as statistically significant (*). A t-test with Bonferroni-Dunn's correction was used for comparisons of each construct in starvation conditions compared to their non-starvation control.

4.6. *HER2* 3’ UTR is unable to derepress translation in destabilised firefly luciferase constructs under non-starvation or glutamine starvation

Destabilised firefly luciferase constructs were created to reduce the potential accumulation of luciferase protein in cells and to measure if a change in expression can be detected in response to glutamine starvation. hCL1 degradation sequence was added to monocistronic constructs to reduce the half-life of firefly luciferase. The half-life of luciferase reporters without any degradation sequence is 3 hours. However, the half-life with the addition of hPEST or both hCL1 and hPEST is 1 hour and 0.4 hours respectively (Almond *et al.*, 2004). hCL1 and hPEST protein degradation sequences were subcloned from CMV-LUC2CP/ARE (Promega) into p15 monocistronic plasmids (primers -Table 2.5). The hCL1 and hPEST sequences were cloned into p15 and p15-*HER2* 5’ UTR downstream from the firefly luciferase open reading frame. The constructs are referred to as destabilised p15 and destabilised p15-*HER2* 5’ UTR respectively due to containing two protein degradation sequences (Figure 4.14) (plasmids-Table 2.2). Successful cloning was confirmed by Sanger sequencing. Destabilised p15 and destabilised p15-*HER2* 5’ UTR were co-transfected with p80 *Renilla* luciferase constructs to normalise the firefly luciferase expression.

i)

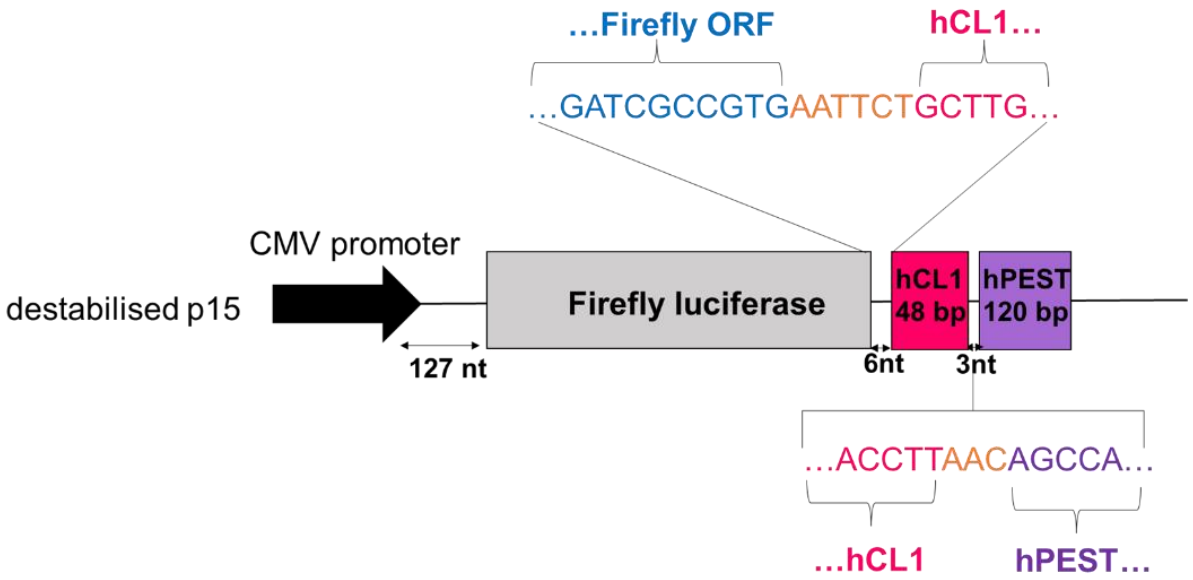
…Firefly ORF
hCL1…
…GATCGCCGTGAATTCTGCTTG…
CMV promoter
destabilised p15
Firefly luciferase
hCL1
48 bp
hPEST
120 bp
127 nt
6nt
3nt
…ACCTTAACAGCCA…
…hCL1
hPEST…

ii)

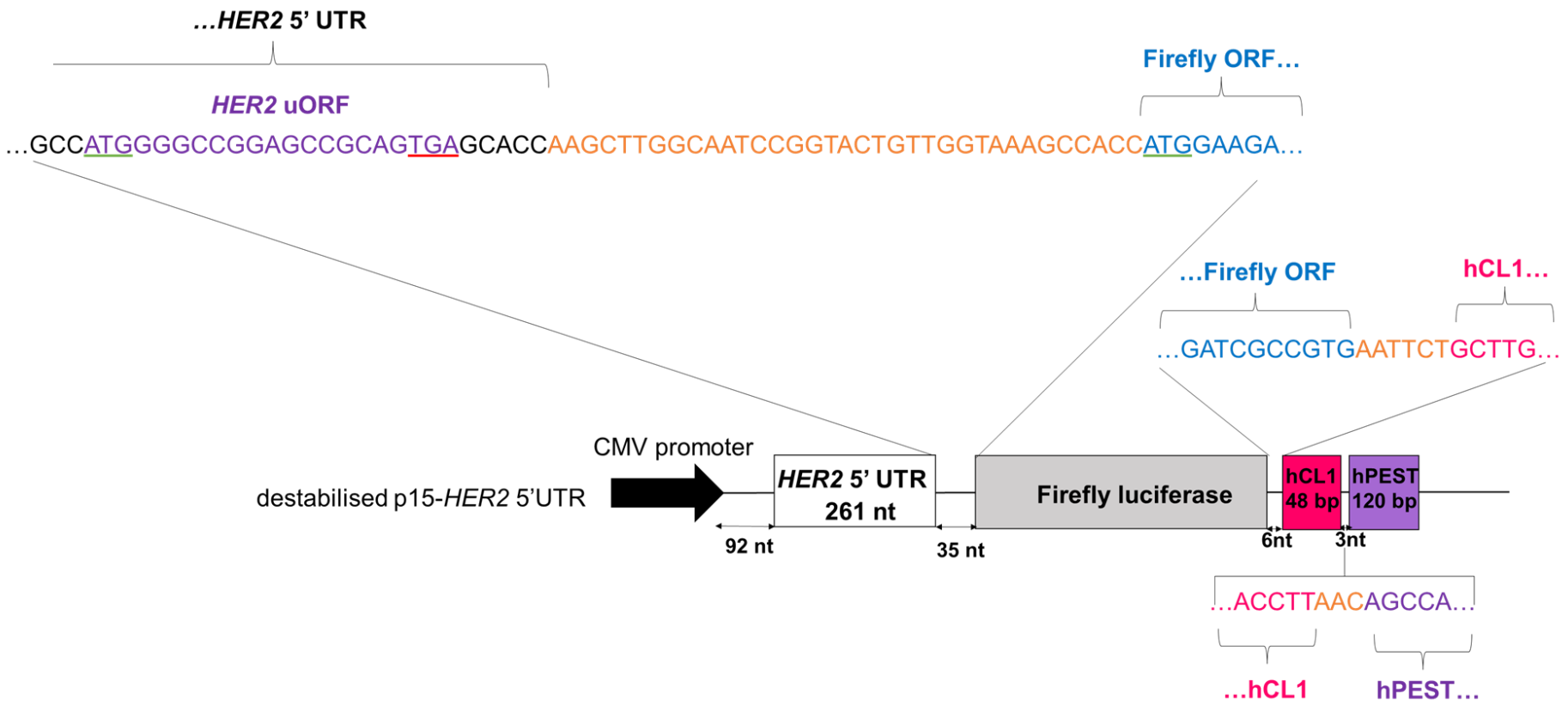

Figure 4.14. Schematic of destabilised monocistronic luciferase constructs used in this project. hCL1 and hPEST protein degradation sequences were subcloned into i) p15 and ii) p15-*HER2* 5' UTR downstream to firefly luciferase open reading frame. Firefly luciferase and hCL1 sequences are in frame. Start codons are underlined green and stop codons are underlined red.

The *HER2* 3’ UTR has previously been shown to derepress the translational inhibition caused by the *HER2* uORF (Mehta et al., 2006). To determine if *HER2* 3’ UTR can derepress translation and mediate translation in response to glutamine starvation, *HER2* 3’ UTR was cloned into destabilised p15-*HER2* 5’ UTR constructs. *HER2* 3’ UTR was produced from a g-block (Integrated DNA Technologies, Inc) described in Section 2.2.6. and was cloned into destabilised p15-*HER2* 5’UTR and referred to as destabilised p15-*HER2* 5’ + 3’ UTRs (Figure 4.15). Successful cloning was confirmed by Sanger sequencing.

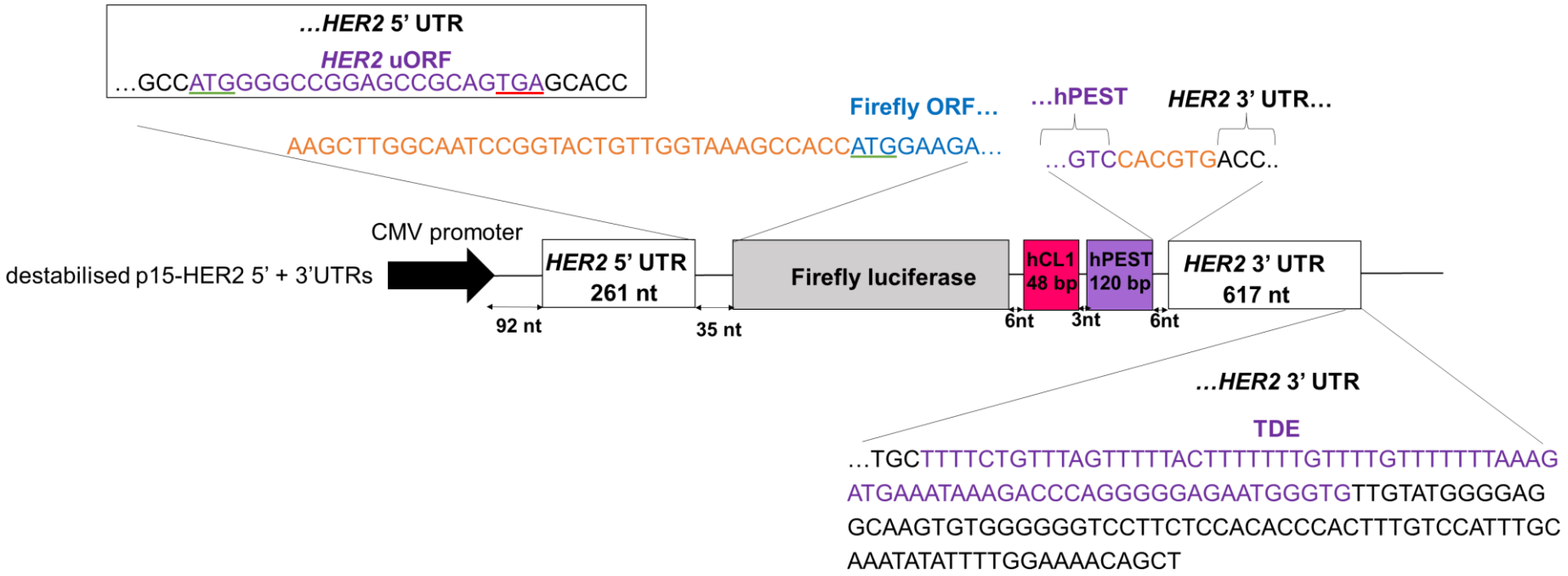

Figure 4.15. Schematic of destabilised p15-*HER2* 5' + 3' UTRs construct used in this project. *HER2* 3' UTR was cloned into destabilised p15-*HER2* 5'UTR downstream to hCL1 and hPEST protein degradation sequences. *HER2* uORF region in the 5' UTR and *HER2* 3' UTR translational derepression element (TDE) are annotated and highlighted purple. hPEST and *HER2* 3' UTR sequences are in frame. Start codons are underlined green and stop codons are underlined red.

Figure 4.13 showed that *HER2* 5' UTR was unable to mediate a change in translation in response to glutamine starvation. To test this further and determine if destabilising the firefly luciferase would allow a change to be detected in response to glutamine starvation mediated by *HER2* 5' UTR, destabilised monocistronic constructs were transfected into MCF-7 cells. As Figure 4.12 showed that the reduction in the *Renilla* expression was not consistently statistically significant, it was first checked whether the monocistronic *Renilla* expression was reduced when transfected with destabilised luciferase constructs. The *Renilla* expression was decreased in response to glutamine starvation when transfected with destabilised monocistronic constructs. The exception to this was destabilised monocistronic constructs containing *HER2* 5' and 3' UTR in response to 24 hours of glutamine starvation (Figure 4.16). Overall, Figure 4.16 indicates that cap-dependent translation was reduced in this experiment.

A

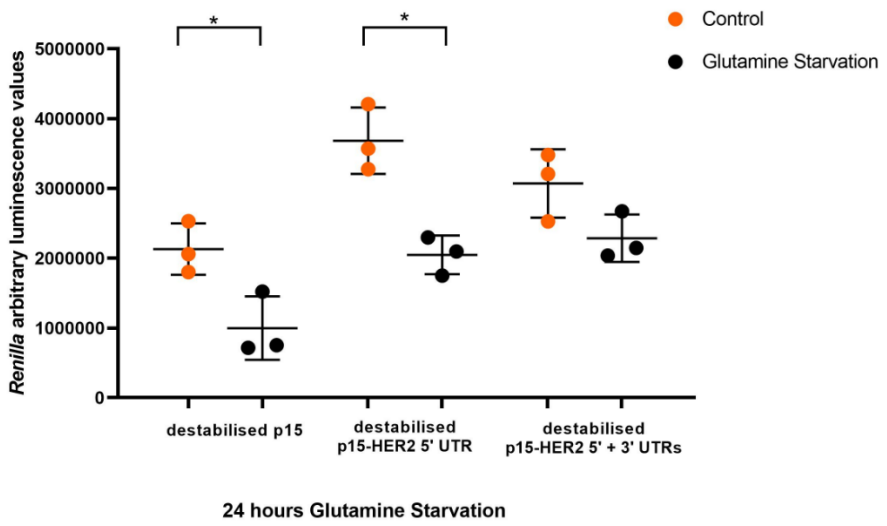

B

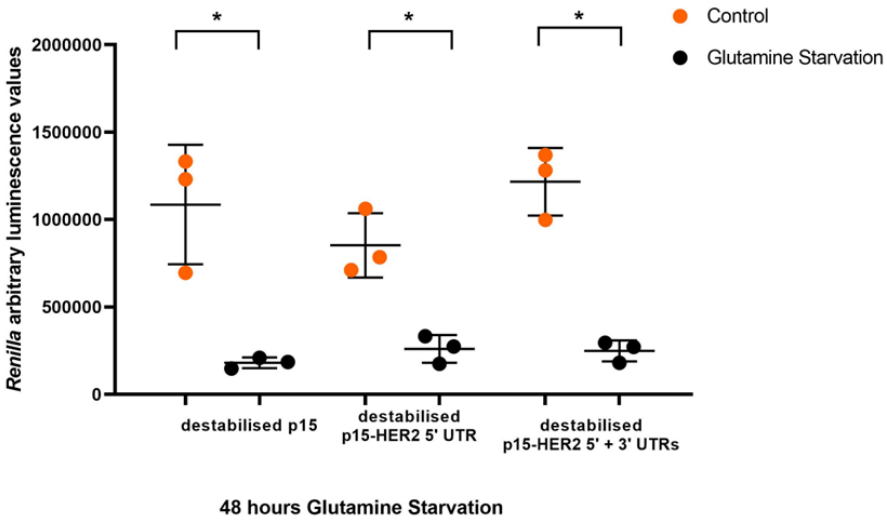

Figure 4.16. Overall, glutamine starvation reduced the monocistronic *Renilla* expression when co-transfected with destabilised monocistronic constructs. MCF-7 cells were transfected with firefly luciferase monocistronic constructs containing the 5' UTRs and co-transfected with p80 *Renilla* luciferase construct and 24 hours later were exposed to either DMEM containing glutamine control media (orange) or DMEM containing no glutamine media (black). After each timepoint cells were lysed, and the *Renilla* expression was measured. A) 24 hours of glutamine starvation. B) 48 hours of glutamine starvation. Data represents the average of three independent experiment carried out in triplicate. All error bars represent the standard deviation. $p<0.05$ was determined as statistically significant (*). A t-test with Bonferroni-Dunn's correction was used for comparisons of each construct in starvation conditions compared to their non-starvation control.

Next, it was checked whether the firefly luciferase expression from destabilised p15 firefly luciferase monocistronics was above background. The raw firefly luciferase expression levels from non-starvation control cells transfected with each destabilised p15 firefly luciferase monocistronic construct was compared to untransfected cells. It was found that destabilised p15 luciferase monocistronics produced over a 1000-fold increase in firefly expression compared to untransfected cells. Destabilised p15-*HER2* 5' UTR monocistronics produced at least over a 100-fold (24 hour control) or over 10-fold (48 hour control) higher firefly expression compared to untransfected cells. Destabilised p15-*HER2* 5' + 3 UTR monocistronics produced at least over a 100-fold higher firefly expression compared to untransfected (Appendix-Table 1). This shows that the luciferase expression from the destabilised constructs was above background levels and not due to background luminescence signals in the detector of the luminometer.

The F/R expression of each destabilised firefly luciferase construct was measured to determine the effects of destabilising firefly luciferase on translation mediated by each construct. In non-stressed conditions, *HER2* 5' UTR produced lower F/R expression levels than p15. This shows that *HER2* 5' UTR mediated less inefficient translation compared to p15 in destabilised constructs. Next, it was investigated whether destabilising firefly luciferase could detect a change in F/R expression in response to glutamine starvation. It was found that there was no change in the firefly luciferase and F/R expression of destabilised p15 in response to 24 hours of glutamine starvation ($p=0.437$) (Appendix Figure 21) (Figure 4.17). There was a decrease in the firefly luciferase expression of p15 in response to 48 hours of glutamine starvation, but

no change in the F/R expression (p=0.993) (Appendix Figure 21) (Figure 4.17). In addition, there was no change in the firefly luciferase and F/R expression from destabilised firefly luciferase constructs containing *HER2* 5' UTR in response to 24 hours or 48 hours of glutamine starvation (p=0.697 and p>0.999 respectively) (Appendix Figure 21) (Figure 4.17). This shows that *HER2* 5' UTR is unable to increase expression in response to glutamine starvation when the expression of firefly luciferase is destabilised.

Next, the destabilised firefly luciferase construct containing both *HER2* 5' UTR and *HER2* 3' UTR was tested to determine if *HER2* 3' UTR would increase the translation of firefly luciferase in response to glutamine starvation. To determine if *HER2* 3' UTR can derepress translation the F/R expression was first assessed in non-stressed conditions. There was no change in the firefly luciferase and F/R expression from destabilised firefly luciferase constructs containing both *HER2* 5' and 3' UTR compared to destabilised firefly luciferase constructs containing only *HER2* 5' UTR in non-starved MCF-7 cells at the 24 hour (p=0.836) and 48-hour timepoints (p=0.189) (Appendix Figure 21) (Figure 4.17). This shows that *HER2* 3' UTR is unable to derepress translation in this study. Then to determine if glutamine starvation could induce *HER2* 3' UTR derepression activity, MCF-7 cells were starved of glutamine. There was no effect of glutamine starvation on the derepression activity of *HER2* 3' UTR in response to 24 hours (p=0.956) or 48 hours (p=0.240) of glutamine starvation (Figure 4.17). This suggests that glutamine starvation has no effect on the translational regulation of *HER2*.

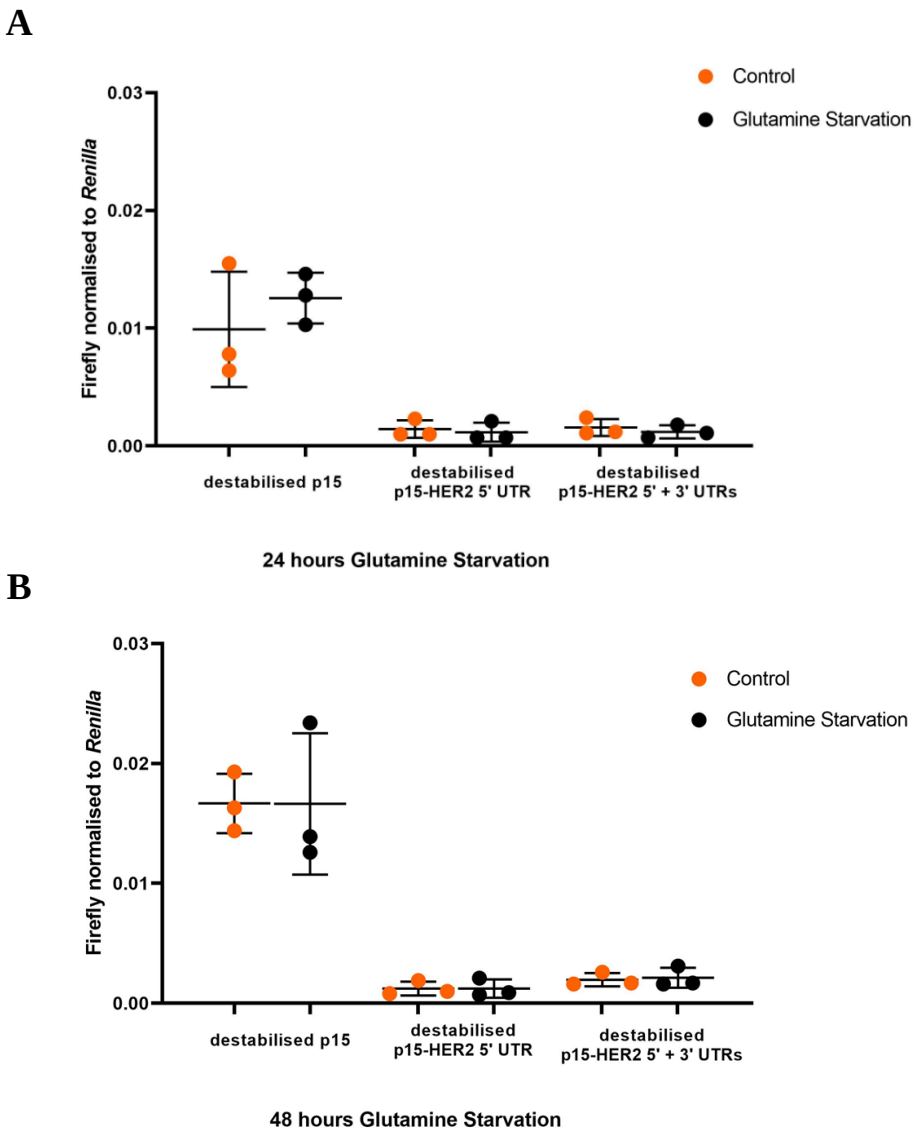

Figure 4.17. *HER2* 3' UTR was unable to increase translation under non-starvation or glutamine starvation conditions. MCF-7 cells transfected for 24 hours with destabilised firefly luciferase monocistronic constructs; destabilised p15, destabilised p15-*HER2* 5' UTR and destabilised *HER2* 5' + 3' UTR and co-transfected with p80 *Renilla* luciferase construct. After each timepoint cells were lysed after being exposed to DMEM containing glutamine (orange) or DMEM containing no glutamine (black). A) 24 hours of glutamine starvation. B) 48 hours of glutamine starvation. Then the F/R activity was measured. Data represents the average of three independent experiments each carried out in triplicate. All error bars represent the standard deviation. $p<0.05$ was determined as statistically significant using a t-test with Bonferroni-Dunn's correction.

4.7. Discussion

The results presented in this chapter demonstrate the translational control by *HER2, HER4* and *EGFR* 5' UTRs under conditions of glutamine starvation. This was important to investigate as cancer cells are dependent on glutamine for survival but are often deprived of glutamine due to their high cell proliferation (DeBerardinis *et al.,* 2007). Additionally, some cancer cells have adapted to glutamine starvation conditions which has been mediated by oncogenic MYC and p53 leading to an increase in glutaminolysis (Gao *et al.*, 2009; Lowman *et al.,* 2019). As HER2 regulates MYC expression and has shown to regulate glutamine metabolism in cancer cells it was therefore important to investigate the translational control of *HER2* in response to glutamine starvation (Qie *et al.*, 2014; Chen *et al.,* 2015). Additionally, as HER4 is a dimersation partner of HER2 that induces intracellular signalling it is also possible that there is translational control of *HER4* in response to glutamine starvation which could reveal potential therapeutic targets for cancer (Monsey *et al.,* 2010).

Despite there being no clear evidence of IRES activity in response to various cell stress conditions tested in Chapter 3, it was first investigated if *HER2* and *HER4* contain an IRES in response to glutamine starvation given the role of HER2 in glutamine metabolism as mentioned above and that an IRES can be active only under specific stress conditions. The results found no evidence for IRES activity in the 5' UTRs of *HER2* and *HER4* in response to the glutamine starvation timepoints tested. However, *EGFR* IRES had increase activity in response to 30 minutes and 24 hours of glutamine starvation. This is an important novel finding as *EGFR* has shown to increase glutamine metabolism in cancer cells therefore, targeting *EGFR* IRES may be a therapeutic target for

cancer cells dependent on glutamine starvation (Yang *et al.*, 2020). In addition, the *Renilla* expression was reduced for constructs containing *EGFR* 5' UTR in response to 30 minutes of glutamine starvation and there seemed to be a reduction at the 24 hour timepoint for some replicates. However, the *Renilla* expression was not reduced in response to 4 hours of glutamine starvation. Overall, indicating that cap-dependent translation was not efficiently reduced in bicistronic luciferase constructs containing *EGFR* 5' UTR in response to glutamine starvation. In addition, the results should be taken with caution as an unexplained increase was observed for pRF in response to 30 minutes of glutamine starvation. Furthermore, only one independent experiment was conducted therefore more repeats would need to be carried out to confirm the effects mediated by *EGFR* 5' UTR and pRF.

As mentioned, the *Renilla* expression was reduced for constructs containing *EGFR* 5' UTR in response to 30 minutes but there was no change in the *Renilla* expression from the other bicistronic constructs at this timepoint. There was also an increase in the *Renilla* expression from pRF in response to 4 hours of glutamine starvation. In addition, in response to 24 hours of glutamine starvation the *Renilla* expression was reduced for pRF and constructs containing *β-tubulin* 5' UTR and *HER2* 5' UTR but a lesser reduction was observed for constructs containing *EGFR* 5' UTR or *HER4* 5'UTR. Overall, this shows that there is variability in the *Renilla* expression across constructs and that cap-dependent translation is not efficiently reduced in these conditions. This may be due to differences in *Renilla* protein stability across constructs or difference in the topology of constructs affecting the transfection efficiency. Alternatively, cells could be co-transfected with beta-galactosidase to normalise the firefly

luciferase expression, however the sources of potential variability such as cell lysis could still arise (Howcroft, *et al.*, 1997).

As the *Renilla* expression was not consistently decreased, the cell viability was checked to give an indication to whether stress was being induced. 48 and 72 hours of glutamine starvation was able to decrease the cell viability of MCF-7 cells. Despite not seeing a reduction in the cell viability in response to 24 hours of glutamine starvation this timepoint was taken further in addition to 48 hours of glutamine starvation, given that there was variability with the *Renilla* expression and that MTT assay is an indirect way to measure cell stress. The 72 hours of glutamine starvation timepoint tested in the MTT assay was not used for detection of eIF2α phosphorylation or in the luciferase assays. This was due to the possibility of cells non-starved at a 72 hour timepoint inducing eIF2α phosphorylation as seen for Figure 4.7 at the 48 hour timepoint, potentially due to the depletion of certain nutrients.

Western blots were included as a more sensitive read out in this chapter to determine if eIF2α is phosphorylated in response to glutamine starvation which would cause a reduction in cap-dependent translation and thus induce stress. 24 hours of glutamine starvation appeared to have little effect on eIF2α phosphorylation. This indicates that cells were not stressed enough at this timepoint which is consistent with the MTT data. Therefore, it is important to consider that no change observed in the luciferase data at this timepoint may be due to cell stress not occurring. eIF2α was found to be phosphorylated in response to 48 hours of glutamine starvation, however as mentioned the phosphorylated form of eIF2α was also detected at the 48 hours non-starvation condition. The detection of eIF2α phosphorylation at the 48 hours non-starvation

timepoint may be a reason for no change detected in response to glutamine starvation in the luciferase assays. However, despite stress being detected at the 48 hours non-starvation condition, 48 hours of glutamine starvation was still investigated further in addition to 24 hours of glutamine starvation. This is because it is possible more western blots repeats will need to be carried out to determine if the effects at the 48-hour timepoint are consistent or are due to other factors such as the condition of the particular passage of MCF-7 cells or environmental factors at the time of the experiment. In the future, measuring the expression of ATF4 in response to glutamine starvation would provide a positive control in the western blot experiment.

It was predicted that *HER2* 5' UTR may increase HER2 expression in response to glutamine starvation in a similar manner to *ATF4* uORF, so HER2 protein levels were measured. There was an increase in HER2 protein levels in response to 48 hours of glutamine starvation which could allow HER2 to mediate oncogenic signalling in response to glutamine starvation, therefore aiding cancer cell growth. To determine at what level HER2 protein was expressed, qPCR analysis was carried out to measure the endogenous *HER2* and *HER4* mRNA levels. There was shown to be an increase in *HER2* mRNA levels in response to glutamine starvation indicating that changes in transcription may be mediating the increase in HER2 protein levels. However, the increase in *HER2* mRNA levels in response to glutamine starvation were determined to be statistically insignificant due to variations across independent experiments. There was an increase in *HER4* mRNA levels in response to glutamine starvation indicating that transcription of *HER4* mRNA is increase in these conditions. However, due

to the variability in the qPCR data it is difficult to make firm conclusions on this data.

Next, to determine if *HER2* 5' UTR mediated an increase in translation in response to glutamine starvation, monocistronic luciferase constructs were tested where translation can occur via cap-dependent or cap-independent translation. Additionally, *HER4* 5' UTR was included to determine if *HER4* 5' UTR could mediate efficient translation in response to glutamine starvation. The p15 construct can mediate efficient translation in a cap-dependent manner. It was found that *EGFR* 5' UTR can efficiently mediate translation in a monocistronic context at similar levels to p15. However, *HER2* and *HER4* 5' UTRs mediated a lower F/R expression than p15 and *EGFR* 5' UTR under non-stressed conditions. This indicates that *HER2* and *HER4* 5' UTRs mediated inefficient translation compared to p15 and *EGFR* 5' UTR. In addition, *HER2* and *HER4* 5' UTRs were unable to increase translation in response to glutamine starvation. Additionally, it was found that *HER4* 5' UTR decreased translation in response to glutamine starvation. In the future, it would be useful to measure the protein expression of HER4 to determine if HER4 protein levels are decreased in response to glutamine starvation which could indicate that translation of *HER4* mRNA is downregulated in these conditions.

The monocistronic *Renilla* expression was overall reduced when co-transfected with p15-destabilised monocistronic constructs (Figure 4.16). The expression of the *Renilla* construct co-transfected with p15 monocistronic constructs seemed to be reduced in response to glutamine starvation (Figure 4.12). However, statistical significance could not be consistently determined due to variations between independent experiments, therefore more repeats would be needed to

confirm that the *Renilla* expression is reduced in these conditions (Figure 4.12). The differences may be due to factors such as cell passage number, cell health and differences in the topology of the p80 plasmids between the experiments. Therefore, it is difficult to determine if cap-dependent translation was efficiently reduced in response to glutamine starvation. In the future it would be useful to measure the effect of glutamine starvation on global protein synthesis at various time points to determine the timepoint when cap-dependent translation is decreased.

Luciferase proteins have a high stability so can accumulate at high levels in cells (Feeney *et al.*, 2016). This can make it difficult to detect a change in response to glutamine starvation. Monocistronic p15 already contains a hPEST degradation sequence but the addition of hCL1 degradation sequence can reduce protein stability by 2-fold (Promega Corporation, revised 2020). Therefore, the firefly luciferase protein was destabilised by the addition of a hCL1 sequence. It was found that destabilised firefly luciferase constructs containing *HER2* 5' UTR had no effect on detecting a change on the F/R expression in response to glutamine starvation.

It has previously been reported that *HER2* 3' UTR can derepress translation of *HER2* 5' UTR in firefly luciferase constructs in a range of breast cancer cells including MCF-7 cells (Mehta *et al.*, 2006). Therefore, *HER2* 3' UTR was cloned downstream of the degradation sequences to investigate if it was able to derepress translation and mediate a change in translation in response to glutamine starvation. It was found that the *HER2* 3' UTR was unable to derepress translation under non-stressed conditions or in response to glutamine starvation. This contrasts with the literature that found that *HER2* 3' UTR can

derepress luciferase translation under non-stressed conditions. The isoform in a previous study used a different *HER2* 3' UTR isoform which may affect the results (Mehta *et al.*, 2006).

The translation of the endogenous *HER2* and *HER4* most likely require factors of the translational machinery and other features of the mRNA for translation which may also vary across different cell lines. Additionally, HER2 and HER4 overexpression contributes to cancer progression therefore it would be useful to test the translational control mediated by each 5' UTR in cell lines that highly express HER2 and HER4. Especially as *HER2* 3' UTR derepression activity is greater in cells that contain a higher expression of HER2 such as SKBR-3 cells compared to MCF-7 cells (Mehta et al., 2006). The translation of firefly luciferase may be different to the endogenous genes. The use of GFP reporters could be used in addition to western blots to test the translation of the endogenous protein tagged to the GFP this way transfection efficiency can also be monitored.

The results did show that HER2 protein was expressed in response to 48 hours of glutamine starvation to investigate the reason for the increase, ribosome profiling data can be assessed. This can measure the association of ribosomes with the endogenous *HER2* mRNA in response to glutamine starvation. This would give an indication to which area of mRNA is being actively translated and would reveal if *HER2* uORF is mediating the increase in HER2 protein levels in response to glutamine starvation.

Overall, this chapter found that *HER2* 5' UTR and *HER4* 5' UTR were unable to mediate an increase in translation in response to glutamine starvation.

However, glucose starvation has also shown to regulate uORFs mediated translation (Lohse *et al.*, 2011; Hu *et al.*, 2016b). This is important as many cancer cells rely on glucose as a main energy source and some cancer cells have reprogrammed their metabolism in response to glucose starvation, so this is investigated in the next chapter.

Chapter 5 - Glucose starvation had no effect on translation mediated by *HER2* or *HER4* 5' UTRs in luciferase reporters

5.1. Introduction

In addition to glutamine, glucose is another important nutrient for many cancer cells. Many cancer cells reprogramme glucose metabolism to increase aerobic glycolysis which is known as the Warburg effect instead of producing energy from oxidative phosphorylation. Despite, glycolysis being a less inefficient way of producing ATP than oxidative phosphorylation, cancer cells increase the rate of glycolysis to meet their ATP demands (Warburg Berlin-Dahlem, 1925; Hanahan and Weinberg, 2011).

The oncogene MYC can increase cancer cells dependency on glucose. For example, MYC can bind to E box regions of glycolytic genes upregulating their expression which leads to an increase in glycolysis (Kim *et al.*, 2004). In addition, whilst wild type p53 has tumour suppressor functions such as decreasing the expression of glucose transporters, mutant p53 can increase glycolysis and is associated with the upregulation of glycolytic enzymes (Schwartzenberg-Bar-Yoseph *et al.*, 2004; Zhang *et al.*, 2013; Harami-Papp *et al.*, 2016).

Similar to the response to glutamine starvation, when cells are starved of glucose GCN2 phosphorylates eIF2α decreasing global translation rates. Translational control of specific mRNAs can occur in response to glucose starvation. *ATF4* and *GCN4* uORFs upregulate translation of their mRNA in response to glucose starvation (Chen *et al.*, 2022). Additionally *TP53* IRES increases the expression of p53 in response to glucose starvation (Khan *et al.*, 2015).

HER2 has a role in glucose metabolism. For example, HER2 signalling via the PI3K pathway can promote the expression of the sodium glucose transporter,

SGLT1 which can increase glucose uptake in HER2-positive breast cancer cells (Wang *et al.*, 2020a). In addition, HER2 has shown to increase the expression of glycolytic enzymes such as lactate dehydrogenase which stimulates lactate production in breast cancer cells (Zhao *et al.*, 2009). Moreover, cancer cells exhibit high concentrations of lactic acid generated from glycolysis. Lactate produced form lactic acid can help some cancer cells survive under glucose starvation by activating the PI3K/AKT/mTOR pathway leading to activation of BCL2 that inhibits apoptosis in glucose starved cancer cells (Huang *et al.*, 2015). Moreover, HER4 can upregulate MYC expression and subsequently increase the expression of MYC target genes such as glycolytic genes (Han *et al.*, 2021a). However, the proliferation of some breast cancer cells has shown to be reduced in response to glucose starvation, but this has shown to not trigger apoptosis in some cancer cells (Khajah *et al.*, 2022).

eIF2α phosphorylation was detected in 48 hours of glutamine starvation conditions and non-starvation conditions in Chapter 4, which may be a reason that *HER2* uORF did not upregulate translation. Therefore, the correlation between eIF2α phosphorylation and *HER2* 5' UTR driven translation was investigated during glucose starvation. This would show if *HER2* 5' UTR is able to upregulate translation as previously seen for *ATF4* and *GCN4*. The translational control by both *HER4* 5' UTR and *HER2* 5' UTR were investigated in response to glucose starvation using monocistronic luciferase reporters. The experiments in this study will also show if *HER2* and *HER4* 5' UTRs contain an IRES active in response to glucose starvation by using bicistronic luciferase reporters.

5.2. *HER2* and *HER4* 5' UTRs do not promote cap-independent translation in response to glucose starvation

First, to establish appropriate conditions that induce glucose starvation conditions, an MTT assay was first carried out to assess the viability of MCF-7 cells. This would give an indirect indication to whether glucose starvation could induce stress in MCF-7 cells. There was found to be a 65.6% (p=0.041) and a 70.1% (p=0.023) decrease in the cell viability of MCF-7 cells in response to 30 minutes and 4 hours of glucose starvation respectively, from the average of three independent experiments (Figure 5.1). This indicates that MCF-7 cells are sensitive to glucose starvation and cell stress may have been induced.

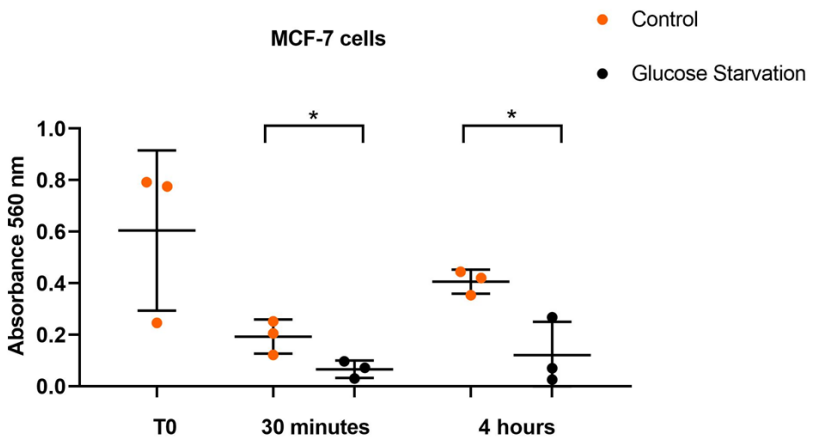

Figure 5.1. 30 minutes and 4 hours of glucose starvation decreased the cell viability of MCF-7 cells. MCF-7 were incubated with media containing glucose (orange) or containing no glucose (black) for 30 minutes or 4 hours. After each time-point cell viability was measured by MTT assay. T0= time-zero readings taken at the start of treatment. Data represents three independent experiments (N=6). Error bars represent the standard deviation. $p<0.05$ was determined as statistically significant (*) using a t-test with Bonferroni-Dunn's correction. Percentage decrease was calculated from the average of three independent experiments.

As the MTT data showed that 30 minutes and 4 hours of glucose starvation decreased the cell viability of MCF-7 cells, which gave an indication that cells were stressed. Next, western blots were carried out to determine if eIF2α was phosphorylated in response to glucose starvation which would provide a more sensitive indication of cell stress occurring. Densitometric analysis confirmed that eIF2α phosphorylation increased in response to 30 minutes of glucose starvation compared to the 30 minute non-starvation control. There was also a slight increase in eIF2α phosphorylation in response to 4 hours of glucose starvation compared to 4 hour non-starvation controls (Figure 5.2). However, eIF2α phosphorylation was greater in response to 30 minutes of glucose starvation compared to 4 hours of glucose starvation (Figure 5.2).

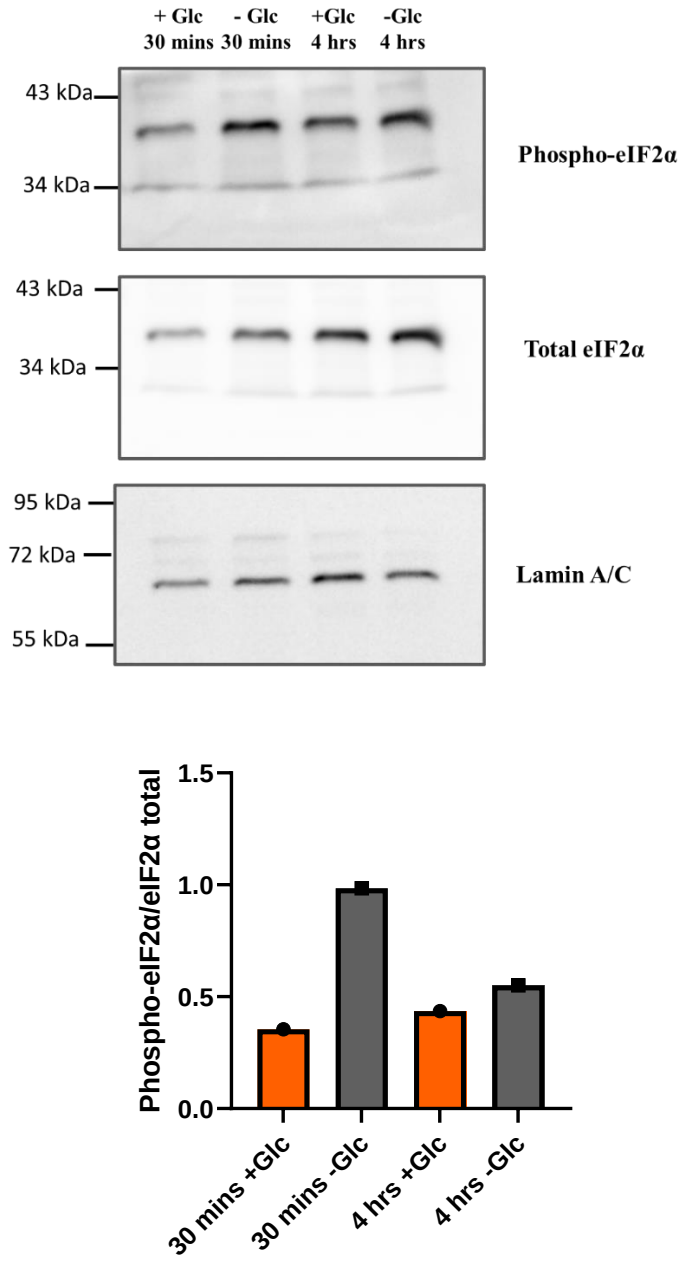

Figure 5.2. The expression of phospho-eIF2α in response to glucose starvation. Western blots of phosphorylated eIF2α (38 kDa), total eIF2α (38 kDa) and lamin a/c (loading control) (lamin a; 74 kDa, lamin c; 63 kDa; lamin a/c antibody bands usually observed between 60-80 kDa) were carried out on the lysates from MCF-7 cells starved of glucose for 30 minutes and 4 hours (-Glc). MCF-7 cells incubated in glucose containing media for 30 minutes and 4 hours were used as a control (+Glc). Densitometric analysis shown of phosphorylated eIF2α relative to total eIF2α. One independent experiment of each blot was carried out.

IRES mediated translation can take place in response to glucose starvation for some mRNAs such as *SLC7A1* and *TP53* (Fernandez *et al.*, 2002; Khan *et al.*, 2015). Next, it was investigated whether *HER2* or *HER4* 5' UTRs contain IRES activity in response to glucose starvation. In addition, *EGFR* 5' UTR was also tested to measure whether glucose starvation had an effect on *EGFR* IRES activity.

To determine if glucose starvation could induce IRES activity in the 5' UTRs, bicistronic luciferase reporters were transfected into MCF-7 cells, then cells were starved of glucose for 30 minutes or 4 hours. First, the *Renilla* expression was assessed to measure if glucose starvation reduced cap-dependent translation. There was no change in the *Renilla* expression in response to glucose starvation. The exception to this was an unexpected increase in the *Renilla* expression in response to 30 minutes of glucose starvation from pRF. In addition, there was a decrease in the *Renilla* expression in response to 4 hours of glucose starvation from constructs containing *EGFR* 5' UTR (Figure 5.3). There also seemed to be a reduction in the *Renilla* expression from constructs containing *HER2* 5' UTR in response to 30 minutes of glucose starvation and overall, a higher *Renilla* expression from constructs containing *HER4* 5' UTR in response to 30 minutes of glucose starvation. However, there was variability so more biological repeats are needed to determine if the variation in the *Renilla* expression across constructs is consistent (Figure 5.3). Overall, the *Renilla* expression was not efficiently reduced in response to glucose starvation indicating that cap-dependent translation was not sufficiently decreased.

Next, the F/R expression was assessed to determine if each bicistronic construct contained IRES activity in response to glucose starvation. Surprisingly, there

was an increase in the firefly luciferase and F/R and expression from pRF in response to 30 minutes of glucose starvation and a decrease in the firefly luciferase and F/R expression of pRF in response to 4 hours of glucose starvation (Appendix Figure 22 and Figure 5.4). There was a slight decrease in the firefly luciferase expression from *EGFR* IRES in response to 4 hours of glucose starvation (Appendix Figure 22). However, as there was a reduction in the *Renilla* expression, this resulted in an increase in the F/R expression from *EGFR* IRES activity in response to 4 hours of glucose starvation (Figure 5.4). *β-tubulin* and *HER2* 5' UTR had no effect on the firefly luciferase and the F/R expression in response to glucose starvation (Appendix Figure 22 and Figure 5.4). There was no effect of 4 hours of glucose starvation on the firefly luciferase and F/R expression from constructs containing *HER4* 5' UTR. However, *HER4* 5' UTRs mediated a slight increase in the firefly luciferase expression at the 30 minute timepoint with no effect on the F/R expression in response to glucose starvation (Appendix Figure 22 and Figure 5.4). The data shows that *EGFR* 5' UTR contains an IRES that appears to increase translation in response to 4 hours of glucose starvation while no IRES activity was detected in *HER2* and *HER4* 5' UTR under these conditions. However, as only one independent experiment was conducted statistical testing was not conducted therefore more independent repeats will be needed to confirm the effects shown.

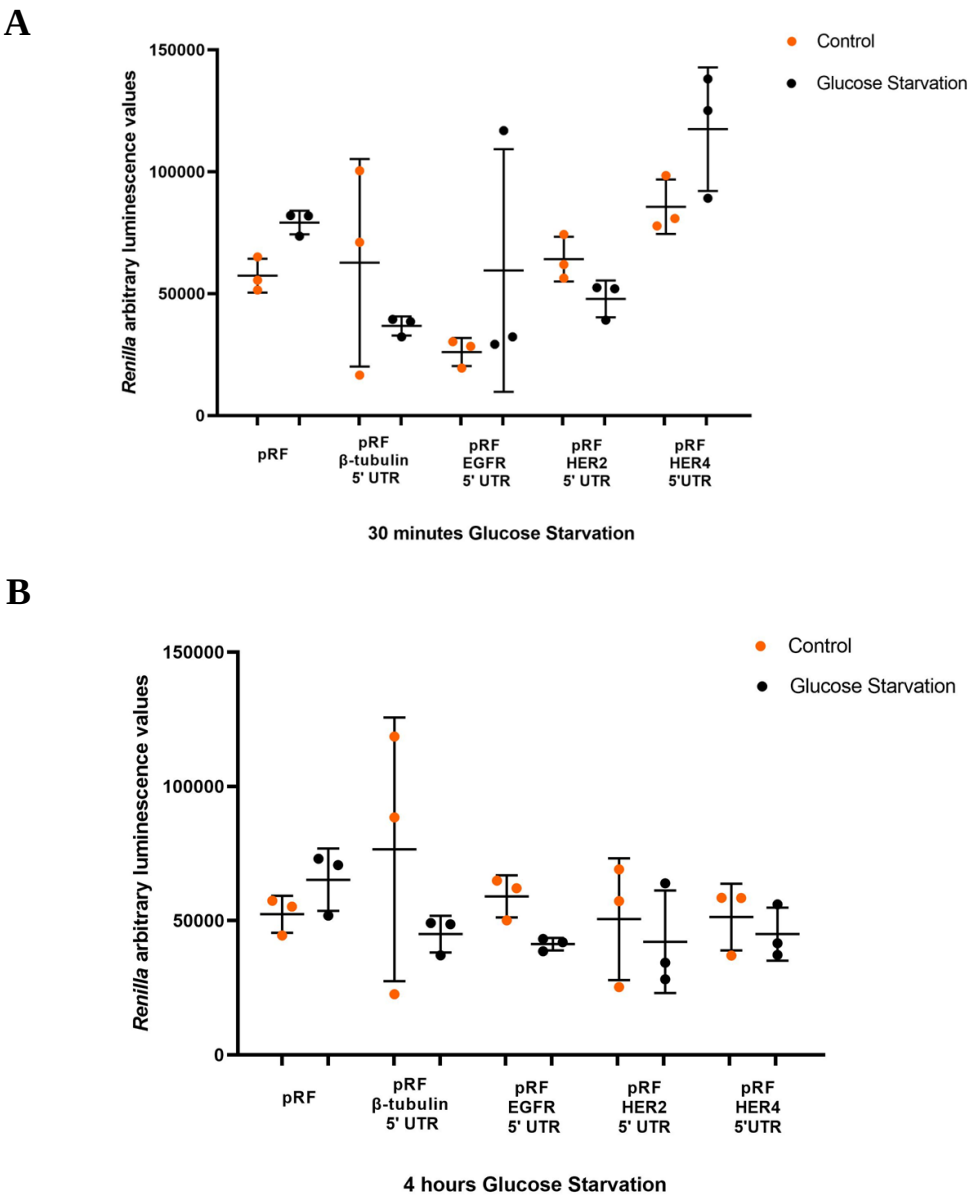

Figure 5.3. Overall, the *Renilla* expression was not reduced in response to glucose starvation. MCF-7 cells were transfected with bicistronic constructs containing both *Renilla* and firefly luciferase open reading frames. 24 hours post-transfection MCF-7 cells were exposed to either DMEM media containing glucose (orange) or DMEM containing no glucose (black). A) 30 minutes glucose starvation. B) 4 hours of glucose starvation. After each timepoint cells were lysed, *Renilla* expression was measured. Data represents the average of one independent experiment carried out in triplicate. All error bars represent the standard deviation.

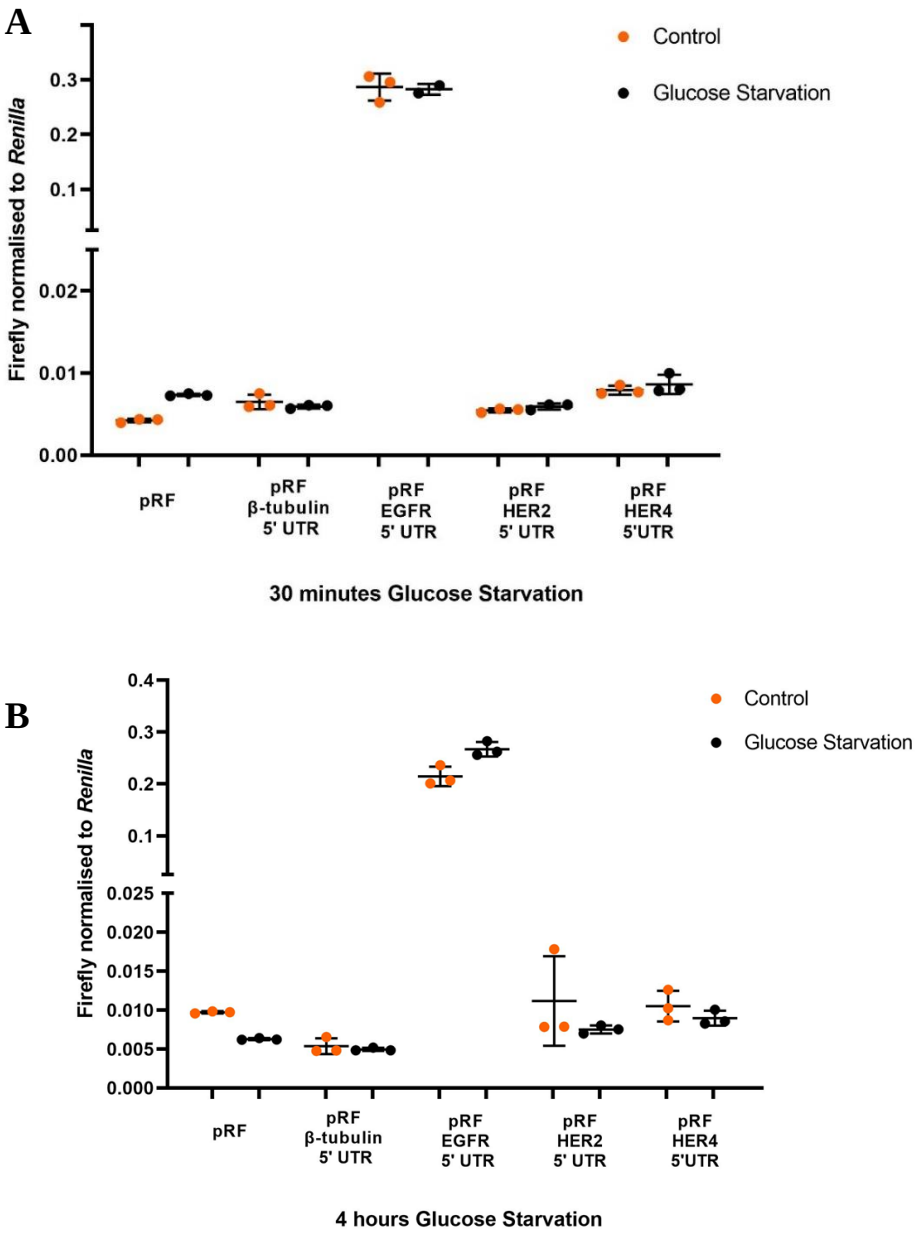

Figure 5.4. No evidence of IRES activity in *HER2* or *HER4* 5' UTRs in response to glucose starvation in contrast to *EGFR* 5' UTR. MCF-7 cells were transfected with bicistronic constructs containing both *Renilla* and firefly luciferase open reading frames. 24 hours post-transfection MCF-7 cells were exposed to either DMEM media containing glucose (orange) or DMEM containing no glucose (black). A) 30 minutes glucose starvation. B) 4 hours of glucose starvation. After each timepoint cells were lysed, and the F/R expression was measured. Data represents the average of one independent experiment carried out in triplicate. All error bars represent the standard deviation.

5.3. Investigating the endogenous HER2 protein and *HER2*/*HER4* mRNA levels in response to glucose starvation

As HER2 has a role in glucose metabolism in cancer cells, next western blots were carried out to investigate if the endogenous HER2 protein was expressed in response to glucose starvation which may support cancer cell growth in response to glucose starvation (Zhao *et al.*, 2009; Wang *et al.*, 2020a). HER2 expression increased in response to 30 minutes of glucose starvation compared to the 30 minute non-starvation control. There was a decrease in HER2 expression in response to 4 hours of glucose starvation compared to the 4 hour non-starvation control. However, HER2 expression in response to 4 hours of glucose starvation was slightly stronger than the expression in response to 30 minutes of glucose starvation (Figure 5.5). This shows that HER2 is expressed in response to glucose starvation, however HER2 expression is stronger in non-stressed conditions at the 4 hour timepoint.

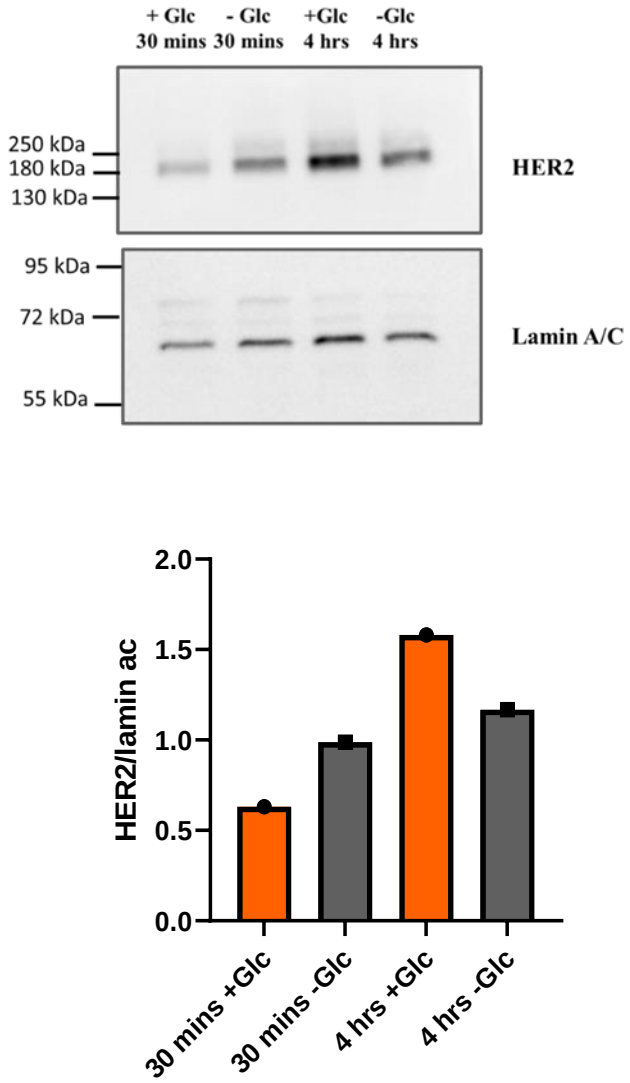

Figure 5.5. HER2 protein expression in response to non-starvation and glucose starvation. Western blots of HER2 (185 kDa) and lamin a/c (loading control) (lamin a; 74 kDa, lamin c; 63 kDa; lamin a/c antibody bands usually observed between 60-80 kDa) were carried out on the lysates from MCF-7 cells starved of glucose for 30 minutes and 4 hours glucose (-Glc). MCF-7 cells incubated in glucose containing media for 30 minutes and 4 hours were used as a control (+Glc). Densitometric analysis shown of HER2 relative to lamin a/c loading control. One independent experiment of each blot was carried out.

To determine if there were any changes on the endogenous mRNA levels of *HER2* in response to glucose starvation, qPCR analysis was carried out. As HER4 also has a role in glucose metabolism, the mRNA levels of *HER4* were measured to determine if there were any transcriptional changes that may control the mRNA expression in response to glucose starvation (Han *et al.*, 2021a). It was found that 30 minutes and 4 hours of glucose starvation has no effect on the mRNA levels of *HER2* ($p=0.100$ and $p=0.700$ respectively) and *HER4* ($p=0.700$ and $p=0.700$ respectively). There was also no change in the mRNA levels of *β-actin* in response to 30 minutes or 4 hours of glucose starvation ($p=0.700$ and $p=0.400$ respectively) (Figure 5.6). This indicates that the expression of *HER2* and *HER4* is not due to changes in the mRNA levels in response to glucose starvation.

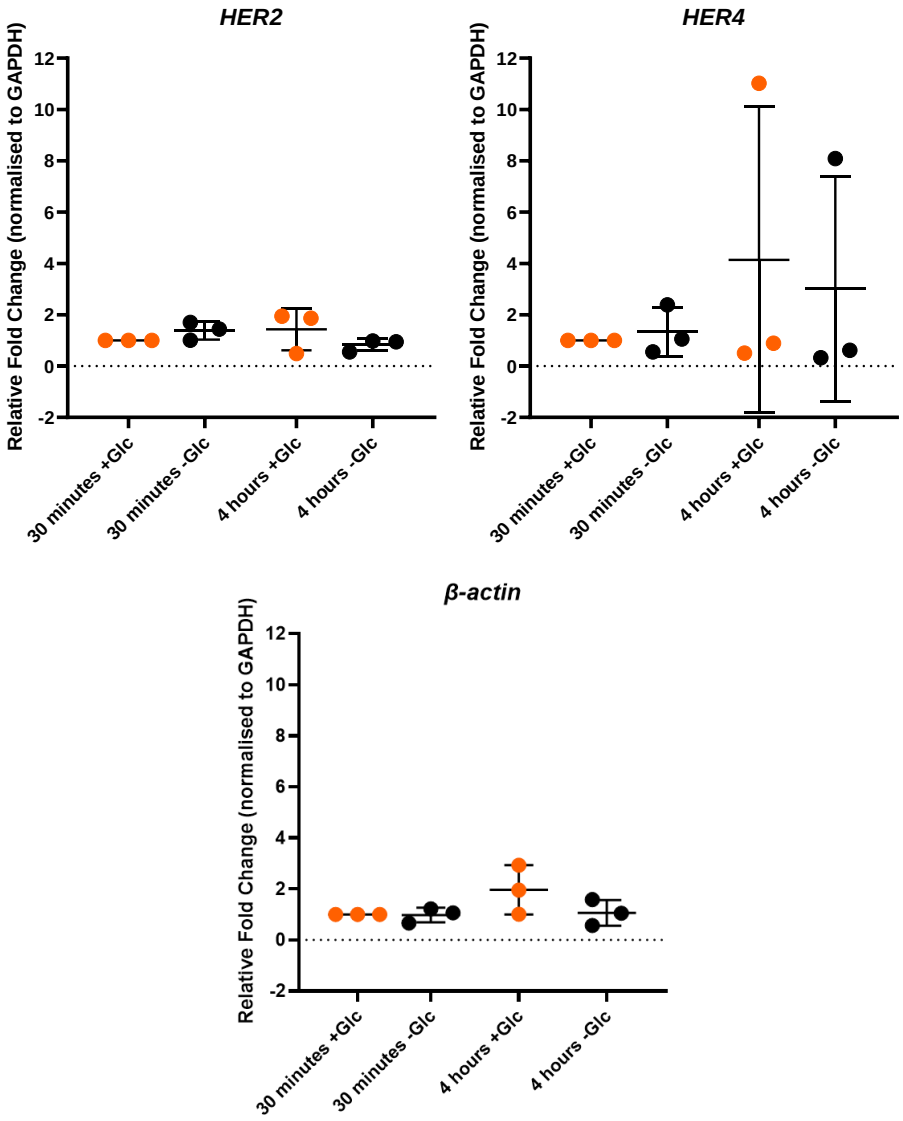

Figure 5.6. The effect of glucose starvation on the mRNA levels of *HER2* and *HER4*. MCF-7 cells were incubated in media containing glucose (+Glc) for 30 minutes or 4 hours as a control (orange) or cells were starved of glucose (-Glc) for 30 minutes or 4 hours (black). After each timepoint total RNA was extracted before being reverse transcribed into cDNA which was used as the qPCR template. Data displayed as fold change normalised to GAPDH house-keeping gene. Data represents the average of three independent experiments carried out in triplicate. $p<0.05$ was determined as statistically significant (*). A Mann-Whitney t-test with Bonferroni-Dunn's correction was used for comparisons of two groups: 30 minutes or 4 hours of glucose starvation to the 30 minute or 4 hour control respectively.

5.4. *HER2* and *HER4* 5' UTRs are unable to increase translation in a monocistronic context in response to glucose starvation

HER2 5' UTR may upregulate translation of *HER2* in response to glucose starvation as previously seen for *ATF4*, to test this monocistronic firefly luciferase constructs containing each 5' UTR were co-transfected with a monocistronic *Renilla* construct in MCF-7 cells.

The *Renilla* expression from the monocistronic p80 construct was measured to determine if cap-dependent translation was reduced in the monocistronic luciferase experiments, in response to 30 minutes and 4 hours of glucose starvation. It was found that the *Renilla* expression was not affected by the glucose starvation conditions (Figure 5.7). This indicates that cap-dependent translation was not reduced in response to glucose starvation.

To determine whether *HER2* or *HER4* 5' UTR could allow an increase in translation in response to glucose starvation conditions in a monocistronic context, the F/R expression was measured. In non-stressed conditions *HER2* and *HER4* 5' UTRs mediated a lower F/R expression than p15 and *EGFR* 5' UTR indicating inefficient translation from *HER2* and *HER4* 5' UTRs. It was found that 30 minutes and 4 hours of glucose starvation had no effect on the firefly luciferase and the F/R expression from p15 ($p=0.219$ and $p=0.777$ respectively) or monocistronic constructs containing *EGFR* 5' UTR ($p=0.853$ and $p=0.194$ respectively), *HER2* 5' UTR ($p=0.687$ and $p=0.210$ respectively) and *HER4* 5' UTR ($p=0.385$ and $p=0.357$ respectively) (Appendix Figure 23) (Figure 5.8). This shows that *HER2* and *HER4* 5' UTRs mediate less efficient translation than

p15 and *EGFR* 5’ UTR in a monocistronic context which is not affected by glucose starvation.

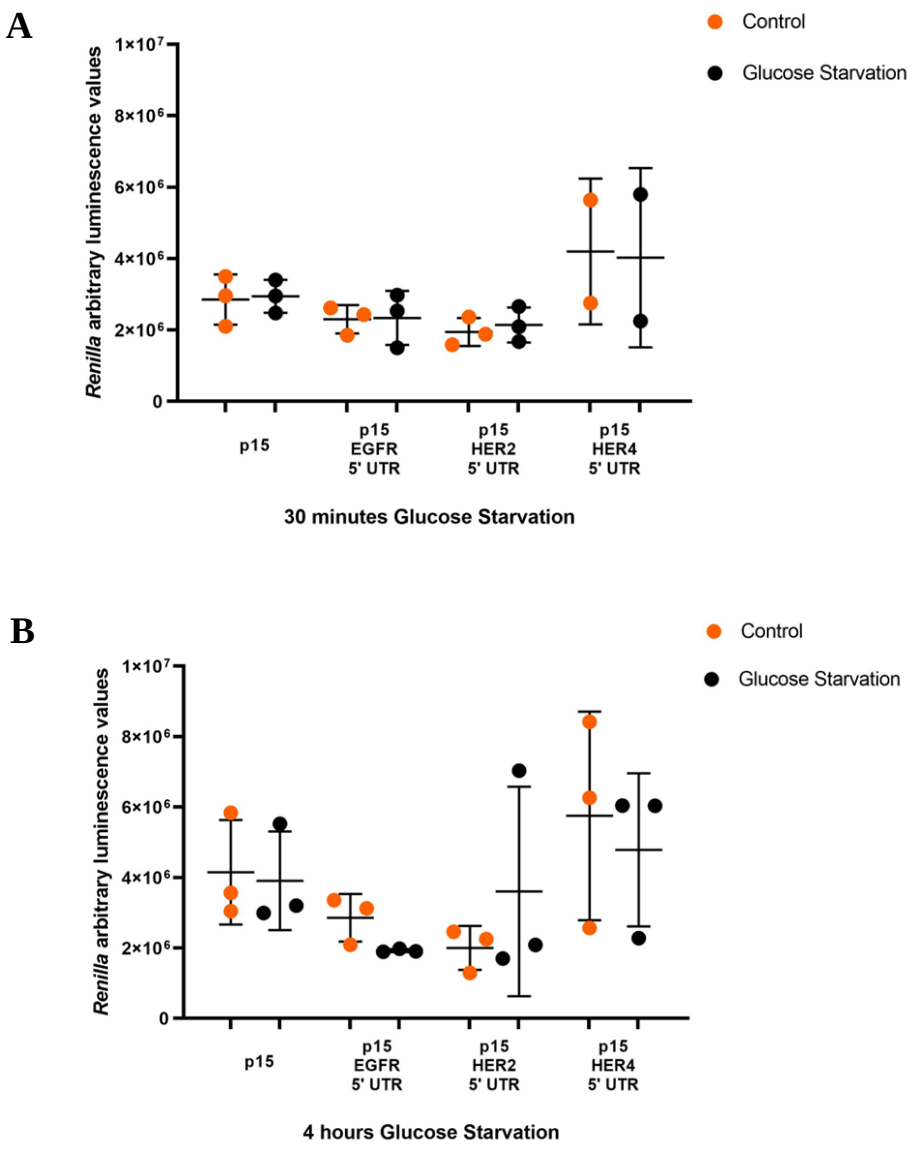

Figure 5.7. The *Renilla* expression co-transfected with each construct was not affected by glucose starvation in a monocistronic context. MCF-7 cells were transfected with firefly luciferase monocistronic constructs containing the 5' UTRs and co-transfected with p80 *Renilla* luciferase construct and 24 hours later were exposed to either DMEM containing glucose control media (orange) or DMEM containing no glucose media (black). After each timepoint cells were lysed, and the *Renilla* expression was measured. A) 30 minutes of glucose starvation. B) 4 hours of glucose starvation. Data represents the average of two-three independent experiment each carried out in triplicate. All error bars represent the standard deviation. $p<0.05$ was determined as statistically significant. A t-test with Bonferroni-Dunn's correction was used for comparisons of each construct in starvation conditions compared to their non-starvation control.

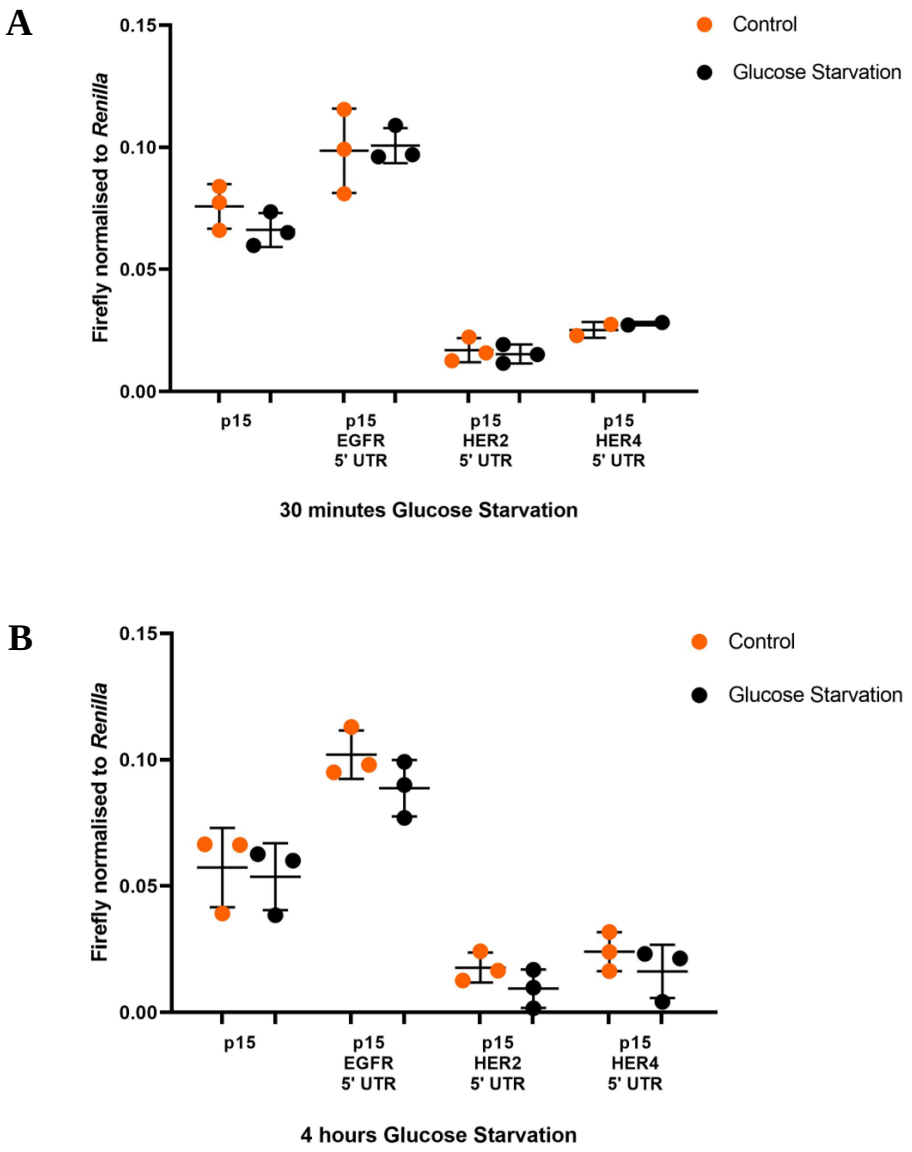

Figure 5.8. *HER2* and *HER4* 5' UTRs mediated inefficient translation in response to glucose starvation. MCF-7 cells were transfected with firefly luciferase monocistronic constructs containing the 5' UTRs and co-transfected with p80 *Renilla* luciferase construct and 24 hours later were exposed to either DMEM containing glucose control media (orange) or DMEM containing no glucose media (black). After each timepoint cells were lysed, and the F/R expression was measured. A) 30 minutes of glucose starvation. B) 4 hours of glucose starvation. Data represents the average of two-three independent experiments each carried out in triplicate. All error bars represent the standard deviation. $p<0.05$ was determined as statistically significant. A t-test with Bonferroni-Dunn's correction was used for comparisons of each construct in starvation conditions compared to their non-starvation control.

Next, to determine if reducing the half-life of firefly luciferase would help detect a difference in translation in response to glucose starvation, the F/R expression from destabilised p15 and destabilised p15-*HER2* 5' UTR constructs was measured. There was found to be no difference in the firefly luciferase from destabilised p15 firefly luciferase constructs and destabilised p15 firefly luciferase constructs containing *HER2* 5' UTR in response to the glucose starvation conditions (Appendix Figure 24). There was also no change in the expression of the *Renilla* reporter co-transfected with both these destabilised plasmids (Appendix Figure 25). This resulted in no change in the F/R expression from destabilised p15 firefly luciferase constructs ($p=0.759$ and $p=0.137$ respectively) and destabilised p15 firefly luciferase constructs containing *HER2* 5' UTR ($p>0.999$ and $p=0.424$ respectively), in response to 30 minutes or 4 hours of glucose starvation (Figure 5.9). This indicates that *HER2* 5' UTR was unable to upregulate translation in response to glucose starvation when the stability of firefly luciferase protein was reduced.

As mentioned, previously the *HER2* 3' UTR has shown to derepress translation in non-stressed MCF-7 cells. However, the data from Chapter 4 found that *HER2* 3' UTR was unable to derepress translation in non-starvation conditions which was not consistent with a previous study (Mehta *et al.*, 2006). As glucose starvation can upregulate translation of mRNAs with uORFs, next it was investigated if *HER2* 3' UTR could derepress the translational inhibition of the *HER2* 5' UTR in these conditions.

First, there was found to be a decrease in the expression of the *Renilla* reporter that was co-transfected with destabilised firefly luciferase constructs containing both *HER2* 5' and 3' UTR in response to 4 hours of glucose starvation

(Appendix Figure 25). This indicates that cap-dependent translation was reduced in cells containing this plasmid at this timepoint. It was found that there was no change in the firefly luciferase from destabilised p15 constructs containing both *HER2* 5' and 3' UTRs in response to 30 minutes or 4 hours of glucose starvation compared to destabilised p15 constructs containing only *HER2* 5' UTR (Appendix Figure 24). This showed no change in the F/R expression in response to 30 minutes and 4 hours of glucose starvation ($p=0.633$ and $p=0.358$ respectively) (Figure 5.9). This indicates that *HER2* 3' UTR was unable to derepress translation in non-starvation and glucose starvation conditions.

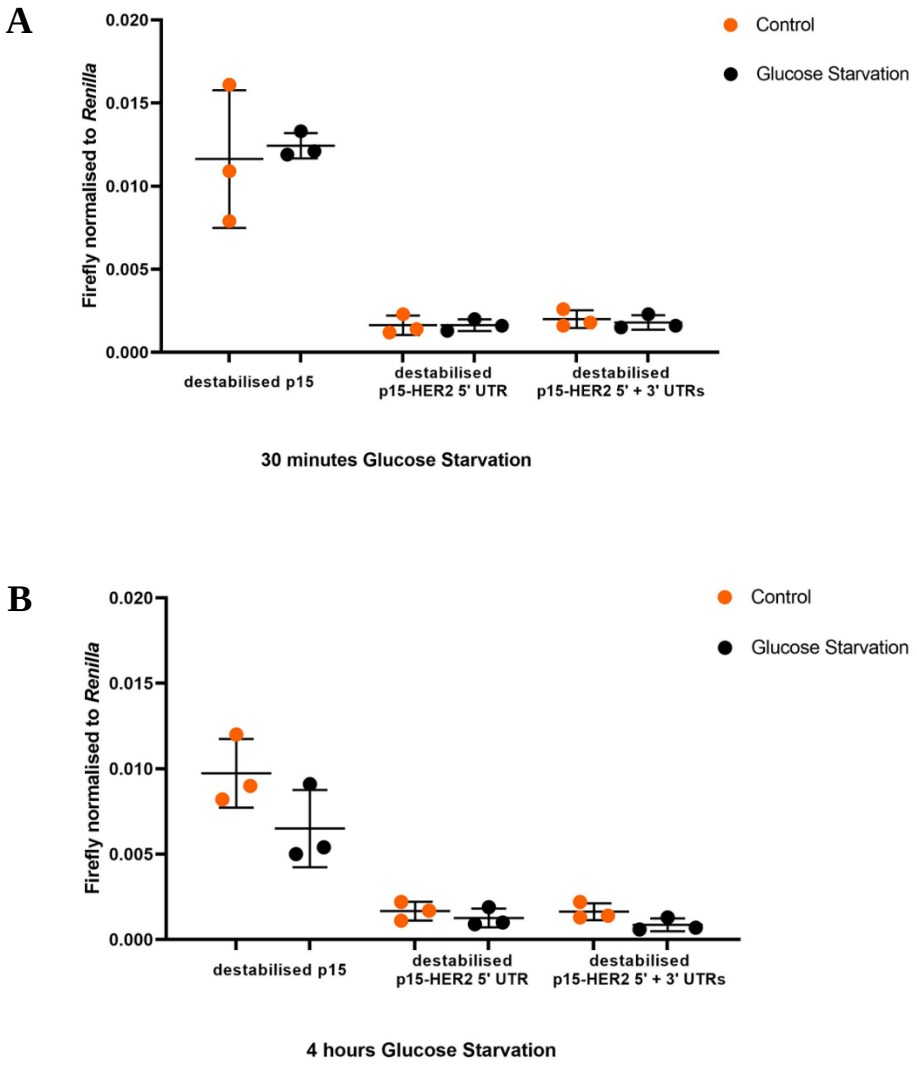

Figure 5.9. *HER2* 3' UTR was unable to derepress translation in non-starvation or glucose starvation conditions. MCF-7 cells transfected for 24 hours with destabilised firefly luciferase monocistronic construct and co-transfected with p80 *Renilla* luciferase construct. Cells were then exposed to DMEM containing glucose (orange) or DMEM containing no glucose (black). A) 30 minutes of glucose starvation B) 4 hours of glucose starvation. After each timepoint cells were lysed, and the F/R expression was measured. Data represents the average of three independent experiments each carried out in triplicate. All error bars represent the standard deviation. $p<0.05$ was determined as statistically significant (*). A t-test with Bonferroni-Dunn's correction was used for comparisons of each construct in starvation conditions compared to their non-starvation control.

5.5 Discussion

The results presented in this chapter demonstrate the translational control of *HER2*, *HER4* and *EGFR* 5' UTRs under conditions of glucose starvation. This work was carried out to give an indication to whether these receptors that drive cancer cell progression can also mediate translation in response to glucose starvation conditions that cancer cells are often subjected too (Conza *et al.*, 2017).

For some of the experiments in Chapters 3-4 the *Renilla* was not reduced in response to stress, so in this chapter an MTT assay was carried out first as an initial indicator to measure if stress was being induced. Short term glucose starvation can increase ROS production in the mitochondria. This can contribute to the disruption of the mitochondrial membrane potential in MCF-7 cells which can lead to apoptosis (Raut *et al.*, 2019). The MTT data showed that there was cell loss at the control conditions in particularly the 30 minute control. During this experiment the control and the starvation conditions underwent PBS washes before the addition of media with or without glucose respectively but this was not conducted for the time-zero condition. Therefore, cell loss may have occurred during this step. In contrast to the glutamine starvation MTT data, 30 minutes and 4 hours of glucose starvation did reduce the viability of MCF-7 cells suggesting that these conditions did induce cell stress. It took long term glutamine starvation to reduce the cell viability. This indicates that MCF-7 cells are more vulnerable to short term glucose starvation compared to short term glutamine starvation. This may be due to the high reliance of cancer cells on glucose to provide rapid energy through glycolysis (Sandulache *et al.*, 2011).

Then in a similar manner to Chapter 4, the effect of glucose starvation on phospho-eIF2α levels was checked which provided a more sensitive read-out of cell stress.Phospho-eIF2α levels increased in response to 30 minute and 4 hours of glucose starvation, with the strongest expression in response to 30 minutes of glucose starvation. Phospho-eIF2α levels were detected in response to non-starvation conditions. This indicates that cells may have also been stressed in non-starvation conditions which may be a reason why no effect was observed in response to glucose starvation in the luciferase assays. Overall, as only one independent of the western blots was carried out more independent repeats will need to be carried out to eliminate confounding factors such as cell health status which could obscure the findings. The addition of a time-zero reading and more glucose starvation time points for the western blots would be useful to measure if eIF2α phosphorylation was consistent over time.

Short term glucose starvation from 30 minutes-6 hours has previously been shown to induce changes in luciferase reporter expression, indicating that the time frames used in this study should be sufficient times to allow changes in reporter activity (Endo *et al.*, 2018; Guzikowski *et al.*, 2022). However, there was generally no change in the raw *Renilla* numbers in response to each condition which indicates that the transfection efficiency between the conditions did not differ. There was overall no effect of glucose starvation on the *Renilla* expression of monocistronic constructs. This contrasts with glutamine starvation where there was a general decrease in the *Renilla* expression, although this was observed at longer timepoints for glutamine starvation. The *Renilla* expression was not efficiently reduced in bicistronic constructs which was also observed for glutamine starvation at the 30 minutes and 4 hour timepoints. For example, for

the bicistronic constructs there was an increase in the *Renilla* expression in response to 30 minutes of glucose starvation from pRF indicating that cap-dependent translation was increased in cells transfected with this plasmid. Additionally, there was a decrease in the *Renilla* expression observed for the bicistronic constructs containing *EGFR* 5' UTR in response to 4 hours of glucose starvation which indicates that cap-dependent translation was reduced in this condition. The inconsistency in the *Renilla* expression in the bicistronic constructs is an issue when drawing conclusions on the expression mediated by each 5' UTR. As mentioned previously the *Renilla* expression should be consistent across plasmids as it is driven by the same promoter therefore this suggests that the *Renilla* stability may differ between constructs or perhaps the promoter activity is inconsistent. It would be useful to carry out qPCR analysis to check the mRNA stability of *Renilla* luciferase from each bicistronic construct.

Another way to check if cap-dependent translation is reduced is to assess the F/R expression of the monocistronic firefly luciferase p15 control construct. As p15 is translated in a cap-dependent manner it is expected that p15 would be reduced in response to glucose starvation. However, there was no reduction in the F/R expression from p15 in response to glucose starvation. The data shows that the *Renilla* expression from bicistronic and monocistronic luciferase constructs was not efficiently reduced in response to glucose starvation indicating that cap-dependent translation is not inhibited in these conditions. Similar to the conclusion from other stress conditions tested in Chapters 3 and 4 it would be useful to check that glucose starvation is inhibiting general protein synthesis by conducting methionine incorporation experiments (Chatterjee *et al.*, 1972).

There was no evidence of IRES activity in *HER2* and *HER4* 5' UTRs in response to glucose starvation, which was similar to the conclusion in response to glutamine starvation. This suggests that the 5' UTRs do not initiate cap-independent translation in these conditions. The results of the bicistronic constructs under conditions of glucose starvation in this chapter together with the bicistronic results from Chapters 3-4 in response to a wide variety of cell stressors support the conclusion that *HER2* and *HER4* 5' UTRs are unlikely to contain an IRES. Unexpectedly, there was an increase in the F/R expression from pRF negative control in response to 30 minutes of glucose starvation. pRF contains does not contain an inserted 5' UTR in the intercistronic region therefore the F/R expression should not be affected by glucose starvation. As the *Renilla* expression was also increased for pRF the change in the F/R expression is likely due to an increase in readthrough signal. In addition, unexpectedly there was a decrease in pRF expression in response to 4 hours of glucose starvation. Despite these changes in firefly luciferase expression from pRF, the expression from pRF was still near background in all conditions therefore unlikely to be biologically relevant. As only one independent experiment was carried out for this experiment more independent replicates are needed to determine if the unexplained changes in firefly luciferase expression from pRF is consistent. It was found that *EGFR* IRES did increase translation in response to 4 hours of glucose starvation. *EGFR* IRES activity also increased in response to 30 minutes and 24 hours of glutamine starvation. However, as pRF seems to be affected by glucose starvation and 30 minutes of glutamine starvation it makes it difficult to draw firm conclusions from the increase seen for *EGFR* IRES in these conditions.

In a monocistronic context, *EGFR* 5' UTR was able to drive efficient translation to levels similar or higher than p15. However, there was no change in the F/R expression mediated by *EGFR* 5' UTR in response to glucose starvation. The monocistronic data in response to glucose starvation differs to the bicistronic data that suggests that *EGFR* IRES may increase firefly luciferase expression in response to 4 hours of glucose starvation. This is because cap-dependent translation takes place in a monocistronic context which reduces the contribution of the *EGFR* IRES.

The data shows that *HER2* and *HER4* 5' UTRs seemed to mediate inefficient translation in monocistronic constructs in non-starved and glucose starved cells compared to p15 and *EGFR* 5' UTR. Similar results were obtained for constructs containing *HER2* 5' UTR or *HER4* 5' UTR in response to glutamine starvation. However, there was a decrease in translation from constructs containing *HER4* 5' UTR in response to glutamine starvation.

As luciferase protein levels accumulate at high levels in monocistronic constructs it can make it more difficult to detect a change in response to stress (Stoneley *et al.*, 2000; Allera-Moreau *et al.*, 2007; Zhao *et al.*, 2022). The focus was on *HER2* as the hypothesis was that *HER2* 5' UTR could mediate an increase in translation in response to glucose starvation via its uORF as previously seen for *ATF4* (Chen *et al.*, 2022). To determine if a change in translation can be detected in response to glucose starvation the firefly luciferase expression from destabilised monocistronic firefly luciferase constructs was tested. However, no change in the F/R expression was detected in response to glucose starvation in destabilised firefly luciferase constructs, indicating that *HER2* 5' UTR may not increase translation in response to glucose starvation.

Further experiments can be carried out to check that the monocistronic firefly luciferase constructs and the destabilised monocistronic firefly luciferase constructs can detect a change in translation. To measure how sensitive the monocistronic constructs are to changes in translation, MCF-7 cells can be transfected with each monocistronic construct and then treated with the translational inhibitor cycloheximide at various times which should demonstrate a rapid decrease in translation over time (Schneider-Poetsch *et al.*, 2010).

Glucose starvation had no effect on the mRNA levels of *HER2* and *HER4* whereas there was an increase in the mRNA levels of these genes in response to glutamine starvation. This suggests that glutamine starvation has an effect on the transcription of these genes which is not observed for glucose starvation.

The western blots did show that HER2 protein expression was detected in response to glucose starvation as well as at the 4 hours non-starvation condition. However, this experiment would need to be repeated and more independent experiments would need to be carried out to confirm the effects shown.

As the *HER2* 3' UTR can derepress the translational inhibition of the *HER2* uORF it was next tested if there was an increase in firefly luciferase translation in destabilised luciferase constructs containing both *HER2* 5' and 3' UTRs. However, it was found that *HER2* 3' UTR did not derepress translation or mediate an increase in translation in response to glucose starvation.

As mentioned, the *HER2* 3' UTR used in the Mehta et al., 2006 was a different isoform to the *HER2* 3' UTR used in this study. It has been observed in SKBR3 breast cancer cells that the 5' end of the 3' UTR is important for derepression activity. This indicates that differences in the derepression activity between

isoforms may also be due to differences in the 5' end of the 3' UTR (Mehta et al., 2006). This demonstrates the importance of the whole nucleotide sequence of the *HER2* 3' UTR being conserved across isoforms on the TDE ability to derepress translation (Mehta et al., 2006).

In conclusion the results from this chapter suggest that *HER2* and *HER4* 5' UTRs do not contain an IRES active in response to glucose starvation. Also, that *HER2* and *HER4* 5' UTR mediate inefficient translation in a monocistronic context which is not affected by glucose starvation. Finally, data from this chapter suggest that HER2 is not regulated at the transcriptional level, or by the *HER2* 5' UTR and *HER2* 3' UTR in response to glucose starvation. However, further experiments would need to be carried out to confidently rule these out. Additional western blot experiments would need to be carried out to accurately determine if HER2 protein levels increase in response to glucose starvation.

Chapter 6 - Discussion

6.1. Summary

The overall aim of this thesis was to investigate whether *HER2* or *HER4* 5' UTRs could mediate translation in response to cell stress conditions associated with cancer and the potential translational mechanisms governing a response to stress. First, it was assessed whether *HER2* or *HER4* 5' UTRs contain IRES activity that could mediate translation in response to stress. Using bicistronic luciferase reporters it was found that *HER2* and *HER4* 5' UTRs do not exhibit IRES activity under the various stress conditions tested in this study. Then it was assessed whether *HER2* or *HER4* 5' UTRs can mediate an increase in translation in response to glutamine or glucose starvation using monocistronic firefly luciferase constructs. The data showed that *HER2* and *HER4* 5' UTRs were unable to increase translation in these conditions. The addition of *HER2* 3' UTR to monocistronic firefly luciferase reporters containing *HER2* 5' UTR did not affect translation under basal conditions or in response to glutamine or glucose starvation.

6.2. Investigating potential IRESs in *HER2* and *HER4* 5' UTRs under various cell stress conditions

The approach to investigate IRES activity in the 5' UTRs of *HER2* and *HER4* was based on previous reports that found that *EGFR* contains an IRES active in response to hypoxic stress which demonstrates that translational regulation may be accounting for EGFR overexpression (Webb *et al.*, 2015). EGFR, HER2 and HER4 are all closely related protein (Monsey *et al.*, 2010). Therefore, it was investigated whether HER2 or HER4 are also regulated at the translational level which may be contributing to their overexpression in breast cancer cells. In

addition, various cell stress conditions were used to screen for potential IRES activity in *HER2* or *HER4* 5' UTRs as IRESs can be active under certain stress inducers but not for others.

First, it was investigated whether *HER2* or *HER4* 5' UTRs contain an IRES active in response to ER stress, a hypoxia mimic, oxidative stress, genotoxic stress, low serum conditions, confluence stress, glucose starvation and glutamine starvation. This is because these stress conditions are biological relevant to cancer, and many of these stress conditions have shown to induce the IRES activity of other cellular mRNAs (Section 1.4.1.3. and Chapter 3). There was no evidence for IRES activity in *HER2* or *HER4* 5' UTRs in response to the various cell stress conditions tested. There was a varied response from *HER2* and *HER4* 5' UTRs in response to UV-B (Figure 3.17) and high cell densities (Appendix Figure 10) as discussed in Chapter 3. However, these effects were still at background levels. This suggests that *HER2* and *HER4* are not upregulated in a cap-independent manner in response to the cell stress conditions tested.

As mentioned, *EGFR* IRES activity has previously been shown to be maintained in response to hypoxia induced by a hypoxic chamber which provided 1% O_2 conditions (Webb *et al.*, 2015). In addition, *EGFR* IRES activity has been tested in response to other cell stress conditions such as low serum conditions, hypoxia mimic $CoCl_2$, genotoxic stress induced by UV radiation and oxidative stress in MCF-7 cells. In these conditions *EGFR* activity was not increased but *EGFR* IRES still maintained the F/R expression (Smalley, 2016; Alamoudi, 2020).

In this study, *EGFR* IRES was used as a positive control as the *EGFR* IRES can maintain activity under stress conditions such as those mentioned above and was found to maintain activity in response to genotoxic stress induced by UV radiation, low serum conditions, hypoxia mimic $CoCl_2$ and confluence stress. There was found to be an increase in the activity of the *EGFR* IRES in response to 30 minutes and 24 hours of glutamine starvation and 4 hours of glucose starvation which was a novel finding (Figure 4.2, Figure 4.4 and Figure 5.4) However, more independent repeats of the bicistronic constructs under glucose starvation and glutamine starvation conditions are needed before concluding that *EGFR* IRES activity is increased in these conditions. The results enhance the understanding of EGFR biology by suggesting that translation of *EGFR* mRNA may increase in response to glutamine starvation or glucose starvation which could aid cancer cell survival in these conditions.

In the future it would be useful to measure if EGFR protein levels increase in response to glucose starvation or glutamine starvation and to measure if there are any changes in *EGFR* mRNA levels in these conditions. This would help determine if the increase in *EGFR* IRES activity in these conditions is meaningful. In addition, conducting siRNA experiments to knock down EGFR expression in response to glutamine or glucose starvation and measuring if there is a significant difference in the viability of breast cancer cells may aid in determining if EGFR expression is important for the survival of cancer cells subjected to these conditions. EGFR overexpression has shown to increase the survival of MCF-7 cells cultured in low glucose conditions (Weihua *et al.*, 2008). EGFR downstream MAPK/ERK and mTOR signalling has shown to be upregulated in response to glutamine starvation and activates the glutamine

transporter SLC1A5 in non-small cell lung cancer (Lee *et al.*, 2020; Liu *et al.*, 2021b).

It would also be useful to test whether *HER2* and *HER4* 5' UTRs exhibit IRES activity under various stress conditions in SKBR-3 and T47D breast cancer cell lines that have a higher expression of these receptors respectively compared to MCF-7 cells (Pontén, *et al.*, 2008). This is because IRES activity can vary between different cells. For example, *EGFR* IRES activity under basal conditions is similar in U87 glioblastoma cells and MCF-7 cells. However, in response to low serum conditions *EGFR* IRES activity is increased in U87 glioblastoma cells, but there is no change in *EGFR* IRES activity in these conditions in MCF-7 cells, potentially due to differences in the availability of ITAFs across cells lines (Smalley, 2016).

A main issue with the bicistronic luciferase assays was that variation in the *Renilla* luciferase expression was commonly observed across the different constructs. The *Renilla* luciferase expression should be consistent between each bicistronic luciferase construct subjected to the same conditions. This is because the *Renilla* luciferase expression is driven by the same SV40 promoter in each bicistronic luciferase construct.

The variation in the *Renilla* luciferase expression may be due to the topology of the bicistronic DNA. Supercoiled DNA has shown to be transfected more efficiently and results in higher expression than non-supercoiled DNA (Tudini *et al.*, 2019; Sudzinová *et al.*, 2021). Therefore, it is important for the topology of the DNA to be the consistent across plasmids. To check this gel electrophoresis can be conducted for each plasmid preparation this can

determine the topology as supercoiled DNA migrates faster on a agarose gel then non-supercoiled DNA (Tudini *et al.*, 2019). Additionally, an alternative normalisation method could be used such as transfecting cells with a bicistronic plasmid containing the *lacZ* gene upstream to firefly luciferase. Firefly luciferase can be normalised to β-galactosidase expression (Martin *et al.*, 1996). However, similar issues with variations could arise so checking the topology of the bicistronic constructs is still needed. Generating stable cell lines where a DNA construct is integrated into the genome would ensure that expression of a construct is consistent within a population of cells. This would eliminate variations due to repeated transfections which is carried out for transiently transfected cells (Hexdall and Zheng, 2001; Lai, Jiang and Li, 2006). Stably transfected cells can also be normalised to total protein (Schagat Trista, *et al.*, 2007). In addition, it would be useful to measure the RNA levels of each luciferase construct to normalise the F/R expression to as variations in transfection efficiency and plasmid quality could be detected at the mRNA level.

As the *Renilla* luciferase expression was often not reduced in response to the stress conditions tested compared to non-stressed cells this suggests that cap-dependent translation was not inhibited. Therefore, this indicates that MCF-7 cells may not be efficiently stressed which makes it is difficult to firmly conclude that *HER2* and *HER4* do not contain IRES activity in response to the various cell stress conditions tested in this study.

To address this issue MTT assays were conducted to investigate if there was a reduction in the cell viability of MCF-7 cells in response to each stress condition to indicate if cell stress was induced. Thapsigargin and UV-B reduced the cell viability potentially by inducing ER stress and DNA damage respectively which

can trigger apoptosis (Wang *et al.*, 1998; Wu *et al.*, 2019). There was an increase in the cell viability in response to 250µM of hydrogen peroxide treatment for 24 hours. This result is in contrast with the literature where 24 hours of exposure to 250µM of hydrogen peroxide decreases the cell viability of MCF-7 cells due to ROS induced cell toxicity. However, at long term exposure to 250µM of hydrogen peroxide, MCF-7 cells can become adapted to hydrogen peroxide induced oxidative stress which is also associated with the upregulation of pro-metastatic genes (Mahalingaiah and Singh, 2014). However, the results in this thesis were insignificant so more repeats are needed to confirm the effects shown. In addition, low serum conditions and hypoxia mimic $CoCl_2$ had no effect on the cell viability of MCF-7 cells. Retrospectively, it would have been best to use a more direct cell stress indicator such as measuring eIF2α phosphorylation in response to each stress condition used in Chapter 3 before testing for IRES activity in *HER2* and *HER4* 5' UTRs.

To firmly conclude that *HER2* and *HER4* 5' UTR do not contain IRES activity in response to cell stress further experiments would need to be carried out. First, various timepoints of each cell stress condition or different concentrations of the chemical treatment used to induce cell stress would need to be conducted. This can be carried out to confirm eIF2α phosphorylation and show that cap-dependent translation is reduced.

This is because IRES activity can vary in response to the exposure time of treatment or starvation as well as at different concentrations of chemical stress inducers. MYC IRES activity increases upon increasing concentrations of ER stress agents thapsigargin and tunicamycin (Shi *et al.*, 2016). Additionally, *SLC7A1* IRES activity increases in a time-dependent manner in response to

glucose starvation up to 9 hrs of starvation then IRES activity declines after this timepoint (Fernandez *et al.*, 2002). In the case of glutamine and glucose starvation further biological repeats of the western blots will need to be carried out, to determine if these starvation conditions show a clear increase in eIF2α phosphorylation in comparison to non-starved cells.

In addition to measuring eIF2α phosphorylation the expression of other key cell stress markers can be measured such as ATF4, phospho-GCN2 and PERK which are upregulated in many stress conditions (Deng *et al.*, 2002; Ye *et al.*, 2010; Iurlaro *et al.*, 2017; Soni *et al.*, 2020). Additionally, stress markers specific for a particular stress conditions can be measured such as HIF-1α for measuring hypoxic stress (Soni *et al.*, 2020).

Additionally, each stress condition can be tested to measure if it is able to reduce total protein synthesis rates. This can be carried out by conducting [^{35} S]-methionine incorporation assays (Chatterjee, Kerwar and Weissbach, 1972). Alternatively, a less toxic and non-radioactive method involving click chemistry can be used. This can involve a methionine analogy, azidohomoalanine (AHA) which contains an azide group that can react to a fluorescently tagged alkyne group. Then the effect of various stress conditions on the incorporation of AHA into newly synthesised proteins can be measured (Hatzenpichler *et al.*, 2014; Wang *et al.*, 2017b; Rothenberg *et al.*, 2018). This would be an important follow up experiment to this project that was investigating IRES-mediated translation in conditions that are expected to inhibit global translation.

In the future, high-throughput screening would be an advantageous method for screening potential IRESs in multiple mRNAs involved in breast cancer under a

range of cancer specific stress conditions. This could involve first incorporating the 5’ UTR of mRNAs into a DNA library. The DNA libraries could contain a range of breast tumour sources with different mutational profiles to reflect the heterogeneity of tumour cells. Such DNA libraries would then be cloned into lentivirus construct between a red fluorescent protein and a GFP protein, the expression of the latter would be indicative of IRES activity. High GFP containing cells can be sorted by fluorescence-activated cell sorting and undergo third generation sequencing which increases the sequencing specificity by allowing sequencing of long reads (Wang et al., 2020b). Although, the high-throughput screening approach described above suggests the use of stress conditions to detect IRESs, there has been little reported in the literature on the use of high-throughput screening methods using stress conditions to detect cellular IRESs (Weingarten-Gabbay *et al.,* 2016).

6.3. Measuring translation in monocistronic firefly luciferase constructs in response to glutamine or glucose starvation

Next, it was investigated whether *HER2* and *HER4* 5' UTR can mediate an increase in translation in response to glutamine starvation or glucose starvation using monocistronic firefly luciferase constructs where translation can occur in a cap-independent or cap-dependent manner. It was found that *HER2* and *HER4* 5' UTRs mediated less efficient translation in non-stressed conditions compared to p15 and *EGFR* 5' UTR. In addition, *HER2* and *HER4* 5' UTRs did not increase translation in response to glutamine starvation or glucose starvation (Figure 4.13 and Figure 5.8). This suggests that the endogenous *HER2* and *HER4* mRNAs may be poorly translated and that *HER2* and *HER4* are not upregulated in response to glutamine starvation or glucose starvation. The *HER2* 5' UTR luciferase data is consistent with reports from the literature that found that *HER2* 5' UTR reduced the translation of β-galactosidase reporter gene in MCF-7 cells, BT474 cells and COS-7 cells compared to the no *HER2* 5' UTR control construct (Child et al., 1999a). It has also been found that *HER2* 5' UTR mediates a lower translation of firefly luciferase in a range of breast cancer cell lines in comparison to controls containing no *HER2* 5' UTR (Mehta et al., 2006).

The *HER2* uORF AUG codon is in an optimal context for translation initiation and has shown to be responsible for the inhibitory effect on translation. This is because mutating the *HER2* uAUG in reporter genes constructs has shown to reduce the inhibitory effects on translation of the downstream cistron in breast cancer cells (Kozak, 1986;Child et al., 1999a; Mehta et al., 2006). In addition to repressing the expression of reporter genes, the *HER2* uORF has shown to repress the protein expression of the endogenous HER2 protein with no effect

on *HER2* RNA levels in COS-7 cells under basal conditions (Child et al., 1999b). Furthermore, it has been shown that translation of the *HER2* mRNA may occur by leaky scanning or by ribosomes reinitiation after translating the *HER2* uORF (Child et al., 1999b). In addition, increasing the intercistronic spacing to at least 50 nucleotides or more has also shown to reduce the translation inhibition caused by the *HER2* uORF in COS-7 cells (Child et al., 1999a).

The control vector, p15 generally produced higher F/R expression levels than *HER2* and *HER4* 5' UTRs in non-starvation and starvation conditions (Figure 4.13 and Figure 5.8). It is expected that p15 would mediate efficient translation as it contains a short 47 nt 5' UTR. Whereas the monocistronic constructs containing *HER2* or *HER4* 5' UTRs contain a 261 nt or 98 nt 5' UTR respectively which is then preceded by a 35 nt intercistronic sequence before the firefly luciferase ORF (Figure 4.11). *HER2* and *HER4* 5' UTRs contain a relatively high GC content of 69.7% and 58.2% respectively, which is often associated with stable secondary structures which can impede ribosome scanning therefore reduce translation rates (Pelletier and Sonenberg, 1985; Chan *et al.*, 2009). 5' UTRs with complex secondary structures or high GC content are often seen in the mRNA of proteins involved in cell growth or dysregulated and implicated in breast cancer progression such as TNF-α, MYC and BRCA1 (Kim *et al.*, 1989; Sobczak and Krzyzosiak, 2002; Wolfe *et al.*, 2014).

However, *EGFR* 5' UTR that is 246 nts and contains a higher GC content of 78% was able to mediate more efficient translation than *HER2* and *HER4* 5' UTRs. Despite this, *HER2* and *HER4* 5' UTRs may contain secondary structure that are more inhibitory to translation than *EGFR* 5'UTR. In addition, *HER2* uORF may be contributing to the inhibitory effects on translation and *EGFR*

IRES may allow translation more efficiently. In the future it would be useful to include a highly structured 5' UTR or a hairpin structure that is inhibitory to translation in addition to testing the firefly luciferase expression from a range of 5' UTRs (Webb, 2012). This can help determine if the structure of *HER2* or *HER4* 5' UTRs is causing less efficient translation compared to a range of cellular 5' UTRs.

The protein expression of the phosphorylated form of eIF2α was detected in response to 48 hours of glutamine starvation but was also expressed in non-starvation conditions at the 48 hour timepoint (Figure 4.7). Additionally, eIF2α phosphorylation was increased in response to glucose starvation but was also detected in non-starvation conditions (Figure 5.2). Glucose starvation induced a strong induction of eIF2α phosphorylation at shorter timepoints such as 30 minutes whereas the increase in eIF2α phosphorylation in response to glutamine starvation was at the 48 hour timepoint. This suggests that shorter exposure to glucose starvation compared to glutamine starvation effects eIF2α phosphorylation and thus global protein synthesis. However, the western blot data suggests that cells were stressed to a certain degree in non-starved cells which would make it difficult to determine if global translation was inhibited in response to glutamine starvation or glucose starvation. Although it is difficult to determine the basal expression of phospho-eIF2α in MCF-7 cells, there should still be a clear increase in expression of the phosphorylated form of eIF2α in starvation conditions. In addition, only one independent experiment was carried out for each eIF2α western blot therefore more repeats would need to be conducted to confirm the effects shown. It is possible that other factors such as

the particular passage of MCF-7 cells may be the reason for the strong eIF2α phosphorylation in non-starved cells.

There was overall no change in the *Renilla* luciferase expression in response to glucose starvation therefore indicating that cap-dependent translation was not decreased. This makes it difficult to determine if cap-dependent translation was reduced. In addition, the starvation conditions used may not reduce cap-dependent translation in MCF-7 cells therefore it is important to conduct methionine incorporation assays as mentioned previously to determine if glutamine starvation or glucose starvation at the timepoints used in this study could efficiently reduce global protein synthesis.

It was then considered if firefly luciferase was the most appropriate assay to detect the effects of glutamine starvation or glucose starvation on translation driven by *HER2* and *HER4* 5' UTRs. As it is possible that no change in translation was observed in response to glutamine starvation or glucose starvation due to a high accumulate of the luciferase protein in cells (Feeney *et al.*, 2016). Therefore, an hCL1 degradation sequence was added downstream of firefly luciferase to reduce the half-life of the protein and increase the response rate (Younis *et al.*, 2010). There was found to be no change in translation in response to glutamine starvation or glucose starvation in destabilised luciferase constructs containing *HER2* 5' UTR. This indicates that *HER2* 5' UTR is unable to mediate an increase in translation in response to glutamine starvation or glucose starvation.

In the future it would be useful to expose cells transfected with monocistronic constructs with and without the hCL1 degradation sequence to the translation

inhibitor, cycloheximide at various timepoints. This would measure how rapid the decrease in firefly luciferase signal from normal and destabilised reporters is following translation inhibition. This would indicate how sensitive the reporters are to a decrease in translation (Schneider-Poetsch *et al.*, 2010).

Previously, it has been shown there are inhibitory effects on translation of firefly luciferase driven by *HER2* 5' UTR in various cell lines including MCF-7 cells. In addition, the *HER2* uORF was directly tested in SKBR-3 cells and demonstrated to be responsible for the inhibitory effects on translation of firefly luciferase. In addition, the *HER2* 3' UTR contains a TDE which is a uridine-rich RNA sequence that is able to derepress the translational inhibition caused by *HER2* 5' UTR in various cell lines, including MCF-7 cells (Mehta, *et al.*, 2006). The TDE is thought to derepress translation due to the interaction of the TDE binding proteins, HuR, hnRNP C1/C2, hnRNP A1 and PABP with the terminating ribosome and eRF3 at the uORF termination codon which interferes with termination efficiency. The TDE binding proteins are thought to be involved in the recycling of the ribosomal subunit and allow translation reinitiation at the *HER2* coding region (Mehta et al., 2006). The derepression activity of the *HER2* 3' UTR has shown to be greater in SKBR-3 cells that contain a higher expression of HER2 compared to MCF-7 cells. This highlights that the translation efficiency mediated by *HER2* 5' and 3' UTRs can vary across different breast cancer cells (Mehta et al., 2006).

As *HER2* 3' UTR has shown to previously derepress the translational inhibition of the *HER2* 5' UTR, next in this project the *HER2* 3' UTR was added downstream of the hCL1 degradation sequence in firefly luciferase constructs containing *HER2* 5' UTR (Mehta, *et al.*, 2006). In contrast to a previous study,

it was found that *HER2* 3' UTR was unable to derepress translation in non-stressed conditions and in response to glutamine starvation or glucose starvation (Figures 4.17 and Figure 5.9). The *HER2* 3' UTR TDE that is responsible for derepression activity differed slightly in nucleotide sequence between this study and the previous study (Mehta, *et al.*, 2006). The *HER2* 3' UTR TDE used in this study differed by a single nucleotide at base 46 (U instead of a C) and had an extra G nucleotide at base 65. Although interestingly, the nucleotide at base 46 in this study was conserved with other mammalian species (Mehta et al., 2006).

However, it is important to mention that in this study one independent experiment showed that the *HER2* 3' UTR was able to derepress translation under basal conditions and in response to glutamine starvation or glucose starvation in comparison to destabilised monocistronic constructs containing only *HER2* 5' UTR. Additionally, there was a decrease in the F/R expression from destabilised *HER2* 5' and 3' UTR monocistronic constructs in response to 4 hours of glucose starvation in comparison to the non-starvation condition (Appendix-Figures 35-36).

The data that showed *HER2* 3' UTR derepression activity (Appendix-Figures 35-36) used a different plasmid preparation to the data reported in this thesis that showed no derepression by *HER2* 3' UTR (Figures 4.17 and Figure 5.9). However, the different plasmid preparations were both were sequenced and confirmed to contain the exact same *HER2* 3' UTR sequence (Appendix Figures 43-44). Therefore, the inconsistence in the results of the experiments with the different destabilised monocistronic *HER2* 5' and 3' UTR plasmid preparations may be due to the conformation of the DNA which can affect the plasmid

expression as discussed previously or differences may be due to the state of the MCF-7 cells between the experiments conducted with the different plasmid preparations. In addition, only one independent experiment was conducted using the plasmid that showed derepression activity whereas three independent experiments were conducted of the data reported in this thesis that used the *HER2* 3' UTR plasmid that was unable to derepress translation. Therefore, more independent experiments would need to be conducted using the plasmid preparation that showed derepression activity to investigate if the effects observed are consistent.

Western blots were carried out to determine the expression of the endogenous HER2 protein in response to glutamine starvation or glucose starvation. HER2 protein had a stronger expression in response to 48 hours of glutamine starvation compared to non-starvation conditions (Figure 4.8). In response to glucose starvation HER2 protein was detected but had a stronger expression at the 4 hours non-starvation timepoint (Figure 5.5). The western blot data suggests that HER2 is expressed in response to glucose starvation but 48 hours of glutamine has a stronger effect. However, it is difficult to determine if HER2 expression is biological significant in response to glucose and glutamine starvation especially as HER2 protein had a higher expression at the 4 hour non-starvation condition for the glucose starvation experiment. Further western blot repeats would need to be carried out due to insufficient number of independent experiments, to confirm HER2 expression under these conditions.

HER2 has a role in the cell response to glutamine and glucose starvation. HER2 can activate PI3K/AKT signalling to stimulate glycolysis to help the survival of cells starved of glutamine (Wang *et al.*, 2020a). In addition, HER2 can regulate

MYC expression. MYC can upregulate glutaminase enzymes that metabolise glutamine and upregulate glutamine transporters providing an energy source for cancer cells starved of other nutrients such as glucose (Chen *et al.*, 2015).

The results from the monocistronic firefly assays suggest that translation of HER2 would not increase in response to glutamine or glucose starvation. This contrasts with the western blot result that showed HER2 protein expression was increased in response to glutamine starvation (Figure 4.8). However, the luciferase assays measured translation specifically whereas western blot data showed the combined result of all gene regulatory steps. In addition, there was no change in *HER2* mRNA levels in response to glucose starvation (Figure 5.6). However, there was an increase in *HER2* mRNA levels in response to glutamine starvation indicating that transcriptional changes may be responsible for an increase in HER2 protein levels in response to glutamine starvation (Figure 4.9).

Analysis of ribosome profiling datasets could be carried to determine the ribosomal occupancy on *HER2* mRNA. Ribosome profiling involves the deep sequencing of ribosome protected mRNA fragments. Translating ribosomes can occupy a ~30 nt portion of an mRNA sequence which protects that portion of mRNA from nuclease degradation (Ingolia *et al.*, 2009). The ribosome protected portions of mRNA corresponds to translating ribosomes and can be used to map the positions of ribosomes on mRNA under specific conditions. This would give an insight into the number of ribosomes synthesising the HER2 protein and the amount of protein being produced (Ingolia *et al.*, 2009). This would reveal if the *HER2* uORF is translated and the effect of this on the translation of *HER2* in response to glutamine or glucose starvation compared to non-starved cells.

Even though the results from the monocistronic luciferase assays suggest that *HER2* uORF was unable to upregulate translation in glutamine or glucose starvation conditions as seen for *ATF4*, in this study the *HER2* uORF was not investigated directly (Gameiro and Struhl, 2018; Zhang *et al.*, 2018; Chen *et al.*, 2022b). To directly test the effects of the *HER2* uORF on translation in response to stress, the uORF AUG codon could be mutated in monocistronic luciferase reporters and then it can be determined whether this changes the response to glutamine or glucose starvation. It is expected that mutating the uORF AUG codon will increase translation as previous studies has shown that mutating the AUG increases translation in basal conditions (Child, *et al.*, 1999; Mehta et al., 2006). This could conclude that translation of the main ORF and its response to glutamine or glucose starvation is affected by the presence of a functional uORF. In addition to mutating the AUG codon of the *HER2* uORF, somatic mutations observed within the *HER2* uORF in cancer cases can be identified and then introduced into the luciferase constructs to represent mutations within the *HER2* uORF that may contribute to oncogenesis.

As work in this study suggests that *HER2* and *HER4* are poorly translated, it is important to highlight that they are commonly overexpression in breast cancer cells. Although gene amplification can contribute to the overexpression of HER2 and HER4, production of malignant splice variations and mutations in HER2 and HER4 such as HER2 CTFs variants and ERBB4-V721I mutations have driven the progression of cancers with aggressive phenotypes (Elster *et al.*, 2018; Maria *et al.*, 2018).

6.4. Conclusion

In this thesis, bicistronic luciferase constructs containing *HER2* or *HER4* 5' UTRs were created and tested to determine if *HER2* or *HER4* 5' UTRs contain an IRES, that could be a therapeutic target for breast cancer cells that often exposed to stress conditions. It was found that *HER2* and *HER4* 5' UTRs do not contain IRES activity in MCF-7 breast cancer cells under the stress conditions tested in this thesis. Future optimisation of the cell stress conditions would need to be carried out to check that they reduce global translation before firmly ruling out the presence of an IRES in the 5' UTRs of *HER2* and *HER4*.

Monocistronic firefly luciferase constructs were also created to determine if *HER2* or *HER4* 5' UTRs could mediate an increase in translation in response to glutamine or glucose starvation. It was found that *HER2* and *HER4* UTRs mediate inefficient translation compared to p15 and *EGFR* 5' UTR in non-starvation conditions and did not increase translation under starvation conditions. Additionally, *HER2* 3' UTR did not derepress the translational inhibition of the *HER2* 5' UTR in response to glutamine or glucose starvation conditions.

In conclusion, this thesis provides an understanding into the efficiency of *HER2* and *HER4* 5' UTRs in mediating translation in response to various cancer related stress conditions. Although, this project did not identify any translational control mechanisms in *HER2* or *HER4* 5' UTRs in response to a range of stress conditions that are biologically relevant to cancer, the approaches used in this project can be used to identify translational mechanisms in other important oncogenes in the future.

References

Abcouwer, S. F., Marjon, P. L., Loper, R. K., and Vander Jagt, D. L. (2002). Response of VEGF expression to amino acid deprivation and inducers of endoplasmic reticulum stress. *Investigative ophthalmology & visual science*, 43(8),2791-2798.

Addess, K. J., Basilion, J. P., Klausner, R. D., Rouault, T. A., and Pardi, A. (1997). Structure and dynamics of the iron responsive element RNA: implications for binding of the RNA by iron regulatory binding proteins. *Journal of molecular biology*, 274(1), 72–83.

Admoun, C., and Mayrovitz, H. (2021). Choosing Mastectomy vs. Lumpectomy-With-Radiation: Experiences of Breast Cancer Survivors. *Cureus*, 13(10), e18433.

Adomavicius, T., Guaita, M., Zhou, Y., Jennings, M. D., Latif, Z., Roseman, A. M., and Pavitt, G. D. (2019). The structural basis of translational control by eIF2 phosphorylation. *Nature communications*, 10(1), 2136.

Aharonov, A., Shakked, A., Umansky, K. B., Savidor, A., Genzelinakh, A., Kain, D., Lendengolts, D., Revach, O. Y., Morikawa, Y., Dong, J., Levin, Y., Geiger, B., Martin, J. F., and Tzahor, E. (2020). ERBB2 drives YAP activation and EMT-like processes during cardiac regeneration. *Nature cell biology*, 22(11), 1346–1356.

Ahn, H. J., Jung, S. J., Kim, T. H., Oh, M. K., and Yoon, H. K. (2015). Differences in Clinical Outcomes between Luminal A and B Type Breast Cancers according to the St. Gallen Consensus 2013. *Journal of breast cancer*, 18(2), 149–159.

Ahuja, D., Karow, D. S., Kilpatrick, J. E., and Imperiale, M. J. (2001). RNA polymerase II-dependent positional effects on mRNA 3' end processing in the adenovirus major late transcription unit. *The Journal of biological chemistry*, 276(45), 41825–41831.

Aigner, A., Juhl, H., Malerczyk, C., Tkybusch, A., Benz, C. C., and Czubayko, F. (2001). Expression of a truncated 100 kDa HER2 splice variant acts as an endogenous inhibitor of tumour cell proliferation. *Oncogene*, 20(17), 2101–2111.

Al-Ajmi, K., Lophatananon, A., Ollier, W., and Muir, K. R. (2018). Risk of breast cancer in the UK biobank female cohort and its relationship to anthropometric and reproductive factors. *PloS one*, 13(7), e0201097.

Alamoudi, A.J. (2020) 'Targeting the Hypoxic Expression of Epidermal Growth Factor Receptor' PhD Thesis, University of Nottingham, Nottingham, UK.

Alfarsi, L. H., El Ansari, R., Craze, M. L., Mohammed, O. J., Masisi, B. K., Ellis, I. O., Rakha, E. A., and Green, A. R. (2021). SLC1A5 co-expression with TALDO1 associates with endocrine therapy failure in estrogen receptor-positive breast cancer. *Breast cancer research and treatment*, 189(2), 317–331.

Allera-Moreau, C., Delluc-Clavières, A., Castano, C., Van den Berghe, L., Golzio, M., Moreau, M., Teissié, J., Arnal, J. F., and Prats, A. C. (2007). Long term expression of bicistronic vector driven by the FGF-1 IRES in mouse muscle. *BMC biotechnology*, 7, 74.

Almanza, A., Carlesso, A., Chintha, C., Creedican, S., Doultsinos, D., Leuzzi, B., Luís, A., McCarthy, N., Montibeller, L., More, S., Papaioannou, A., Püschel, F., Sassano, M. L., Skoko, J., Agostinis, P., de Belleroche, J., Eriksson, L. A., Fulda, S., Gorman, A. M., Healy, S., Kozlov, A., Muñoz-Pinedo, C., Rehm, M., Chevet, E., and Samali, A. (2019). Endoplasmic reticulum stress signalling - from basic mechanisms to clinical applications. *The FEBS journal*, 286(2), 241–278.

Almond, B.D., Zdanovsky, A., Zdanovskaia, M., Ma, D., Stecha, P., Paguio, A., Garvin, D., Wood., K. A Rapid-Fire Solution: Introducing the Rapid Response™ Reporter Vectors. (2004). Promega Corporation (Promega Notes). no. 87.

Alvarado, D., Klein, D. E., and Lemmon, M. A. (2009). ErbB2 resembles an autoinhibited invertebrate epidermal growth factor receptor. *Nature*, 461(7261), 287–291.

Anda, S., Zach, R., and Grallert, B. (2017). Activation of Gcn2 in response to different stresses. *PloS one*, 12(8), e0182143.

Andersen, G. R., Valente, L., Pedersen, L., Kinzy, T. G., and Nyborg, J. (2001). Crystal structures of nucleotide exchange intermediates in the eEF1A-eEF1Balpha complex. *Nature structural biology*, 8(6), 531–534.

Anido, J., Scaltriti, M., Bech Serra, J. J., Santiago Josefat, B., Todo, F. R., Baselga, J., and Arribas, J. (2006). Biosynthesis of tumorigenic HER2 C-terminal fragments by alternative initiation of translation. *The EMBO journal*, 25(13), 3234–3244.

Arcondéguy, T., Lacazette, E., Millevoi, S., Prats, H., and Touriol, C. (2013). VEGF-A mRNA processing, stability and translation: a paradigm for intricate regulation of gene expression at the post-transcriptional level. *Nucleic acids research*, 41(17), 7997–8010.

Argüelles, S., Camandola, S., Cutler, R. G., Ayala, A., and Mattson, M. P. (2014). Elongation factor 2 diphthamide is critical for translation of two IRES-dependent protein targets, XIAP and FGF2, under oxidative stress conditions.

Free radical biology & medicine, 67, 131–138.

Arkhipov, A., Shan, Y., Kim, E. T., Dror, R. O., and Shaw, D. E. (2013). Her2 activation mechanism reflects evolutionary preservation of asymmetric ectodomain dimers in the human EGFR family. *eLife*, 2, e00708.

Arnould, L., Gelly, M., Penault-Llorca, F., Benoit, L., Bonnetain, F., Migeon, C., Cabaret, V., Fermeaux, V., Bertheau, P., Garnier, J., Jeannin, J. F., and Coudert, B. (2006). Trastuzumab-based treatment of HER2-positive breast cancer: an antibody-dependent cellular cytotoxicity mechanism? *British journal of cancer*, 94(2), 259–267.

Ashkenazy-Titelman, A., Atrash, M. K., Boocholez, A., Kinor, N., and Shav-Tal, Y. (2022). RNA export through the nuclear pore complex is directional. *Nature communications*, 13(1), 5881.

Asnani, M., Pestova, T. V., and Hellen, C. U. (2016). Initiation on the divergent Type I cadicivirus IRES: factor requirements and interactions with the translation apparatus. *Nucleic acids research*, 44(7), 3390–3407.

Atanaskova, N., Keshamouni, V. G., Krueger, J. S., Schwartz, J. A., Miller, F., and Reddy, K. B. (2002). MAP kinase/estrogen receptor cross-talk enhances estrogen-mediated signaling and tumor growth but does not confer tamoxifen resistance. *Oncogene*, *21*(25), 4000–4008.

Audigier, S., Guiramand, J., Prado-Lourenco, L., Conte, C., Gonzalez-Herrera, I. G., Cohen-Solal, C., Récasens, M., and Prats, A. C. (2008). Potent activation of FGF-2 IRES-dependent mechanism of translation during brain development. *RNA (New York, N.Y.)*, 14(9), 1852–1864.

Bailur, J. K., Gueckel, B., Derhovanessian, E., and Pawelec, G. (2015). Presence of circulating Her2-reactive CD8 + T-cells is associated with lower frequencies of myeloid-derived suppressor cells and regulatory T cells, and better survival in older breast cancer patients. *Breast cancer research: BCR*, 17(1), 34.

Barthelme, D., Dinkelaker, S., Albers, S. V., Londei, P., Ermler, U., and Tampé, R. (2011). Ribosome recycling depends on a mechanistic link between the FeS cluster domain and a conformational switch of the twin-ATPase ABCE1. *Proceedings of the National Academy of Sciences of the United States of America*, 108(8), 3228–3233.

Baselga, J., Lewis Phillips, G. D., Verma, S., Ro, J., Huober, J., Guardino, A. E., Samant, M. K., Olsen, S., de Haas, S. L., and Pegram, M. D. (2016). Relationship between Tumor Biomarkers and Efficacy in EMILIA, a Phase III Study of Trastuzumab Emtansine in HER2-Positive Metastatic Breast Cancer. *Clinical cancer research: an official journal of the American Association for Cancer Research*, 22(15), 3755–3763.

Baslan, T., Kendall, J., Volyanskyy, K., McNamara, K., Cox, H., D'Italia, S., Ambrosio, F., Riggs, M., Rodgers, L., Leotta, A., Song, J., Mao, Y., Wu, J., Shah, R., Gularte-Mérida, R., Chadalavada, K., Nanjangud, G., Varadan, V., Gordon, A., Curtis, C., Krasnitz, A., Dimitriva, N., Harris, L., Wigler, M., and Hicks., J. (2020). Novel insights into breast cancer copy number genetic heterogeneity revealed by single-cell genome sequencing. eLife, 9, e51480.

Bastide, A., Karaa, Z., Bornes, S., Hieblot, C., Lacazette, E., Prats, H., and Touriol, C. (2008). An upstream open reading frame within an IRES controls expression of a specific VEGF-A isoform. *Nucleic acids research*, 36(7), 2434–2445.

Belsham, G. J., McInerney, G. M., and Ross-Smith, N. (2000). Foot-and-mouth disease virus 3C protease induces cleavage of translation initiation factors eIF4A and eIF4G within infected cells. *Journal of virology*, 74(1), 272–280.

Berkhout, B., Arts, K., and Abbink, T. E. (2011). Ribosomal scanning on the 5'-untranslated region of the human immunodeficiency virus RNA genome. *Nucleic acids research*, 39(12), 5232–5244.

Berndt, SI, Platz, EA, Fallin, MD, Thuita, L. W., Hoffman, S. C., and Helzlsouer, K. J. (2006). Genetic variation in the nucleotide excision repair pathway and colorectal cancer risk. *Cancer Epidemiol Biomarkers Prev,* 15, 2263–2269.

Betney, R., de Silva, E., Mertens, C., Knox, Y., Krishnan, J., and Stansfield, I. (2012). Regulation of release factor expression using a translational negative feedback loop: a systems analysis. *RNA (New York, N.Y.)*, 18(12), 2320–2334.

van den Beucken, T., Magagnin, M. G., Jutten, B., Seigneuric, R., Lambin, P., Koritzinsky, M., and Wouters, B. G. (2011). Translational control is a major contributor to hypoxia induced gene expression. *Radiotherapy and oncology: journal of the European Society for Therapeutic Radiology and Oncology*, 99(3), 379–384.

Bhargava, R., Gerald, W. L., Li, A. R., Pan, Q., Lal, P., Ladanyi, M., and Chen, B. (2005). EGFR gene amplification in breast cancer: correlation with epidermal growth factor receptor mRNA and protein expression and HER-2 status and absence of EGFR-activating mutations. *Modern pathology: an official journal of the United States and Canadian Academy of Pathology, Inc*, 18(8), 1027–1033.

Blau, L., Knirsh, R., Ben-Dror, I., Oren, S., Kuphal, S., Hau, P., Proescholdt, M., Bosserhoff, A. K., and Vardimon, L. (2012). Aberrant expression of c-Jun in glioblastoma by internal ribosome entry site (IRES)-mediated translational activation. *Proceedings of the National Academy of Sciences of the United States*

of America, 109(42), E2875–E2884.

Bloedjes, T. A., de Wilde, G., Maas, C., Eldering, E., Bende, R. J., van Noesel, C. J. M., Pals, S. T., Spaargaren, M., and Guikema, J. E. J. (2020). AKT signaling restrains tumor suppressive functions of FOXO transcription factors and GSK3 kinase in multiple myeloma. *Blood advances*, 4(17), 4151–4164.

Bogorad, A. M., Lin, K. Y., and Marintchev, A. (2017). Novel mechanisms of eIF2B action and regulation by eIF2α phosphorylation. *Nucleic acids research*, *45*(20), 11962–11979.

Bohlen, J., Fenzl, K., Kramer, G., Bukau, B., and Teleman, A. A. (2020). Selective 40S Footprinting Reveals Cap-Tethered Ribosome Scanning in Human Cells. *Molecular cell*, 79(4), 561–574.e5.

Bonnal, S., Schaeffer, C., Créancier, L., Clamens, S., Moine, H., Prats, A. C., and Vagner, S. (2003). A single internal ribosome entry site containing a G quartet RNA structure drives fibroblast growth factor 2 gene expression at four alternative translation initiation codons. *The Journal of biological chemistry*, 278(41), 39330–39336.

Bornes, S., Prado-Lourenco, L., Bastide, A., Zanibellato, C., Iacovoni, J. S., Lacazette, E., Prats, A. C., Touriol, C., and Prats, H. (2007). Translational induction of VEGF internal ribosome entry site elements during the early response to ischemic stress. *Circulation research*, 100(3), 305–308.

Bott, A. J., Peng, I. C., Fan, Y., Faubert, B., Zhao, L., Li, J., Neidler, S., Sun, Y., Jaber, N., Krokowski, D., Lu, W., Pan, J. A., Powers, S., Rabinowitz, J., Hatzoglou, M., Murphy, D. J., Jones, R., Wu, S., Girnun, G., and Zong, W. X. (2015). Oncogenic Myc Induces Expression of Glutamine Synthetase through Promoter Demethylation. *Cell metabolism*, 22(6), 1068–1077.

Bottorff, T. A., Park, H., Geballe, A. P., and Subramaniam, A. R. (2022). Translational buffering by ribosome stalling in upstream open reading frames. *PLoS genetics*, 18(10), e1010460.

Braun, J.E., Huntzinger,E., Fauser, M., and Izaurralde E. (2011). GW182 proteins directly recruit cytoplasmic deadenylase complexes to miRNA targets. *Molecular Cell*. Oct;44(1):120-133.

Braunstein, S., Karpisheva, K., Pola, C., Goldberg, J., Hochman, T., Yee, H., Cangiarella, J., Arju, R., Formenti, S. C., and Schneider, R. J. (2007). A hypoxia-controlled cap-dependent to cap-independent translation switch in breast cancer. *Molecular cell*, 28(3), 501–512.

de Breyne, S., Yu, Y., Unbehaun, A., Pestova, T. V., Hellen, C. U. T., and Doudna, J. A. (2009). Direct Functional Interaction of Initiation Factor elF4G with type 1 internal ribosomal entry sites. *Proceedings of the National Academy*

of Sciences of the United States of America, 106(23), 9197–9202.

Van Tine, B.A. , Mita, M., Barve, M. A., Hamilton, E. P., Brenner, A. J., Valdes, F.,Ahn, D., Hubbard, J., Starr, J., Georgy, A., Pelham, J., Anand, B. S., Strack, T., Sandri, A. M., Wainberg, Z. A.,. (2022). Interim results of a phase 1 study of the novel immunotoxin MT-5111 in patients with HER2+tumors [abstract]. In: Proceedings of the 2021 San Antonio Breast Cancer Symposium; 2021 Dec 7-10; San Antonio, TX. Philadelphia (PA): AACR; *Cancer Res*. 82(4 Suppl):Abstract nr P2-13-45.

Brinton, L. A., Sherman, M. E., Carreon, J. D., and Anderson, W. F. (2008). Recent trends in breast cancer among younger women in the United States. *Journal of the National Cancer Institute*, 100(22), 1643–1648.

Brugiolo, M., Herzel, L., and Neugebauer, K. M. (2013). Counting on co-transcriptional splicing. *F1000prime reports*, 5, 9.

Buttgereit, F., and Brand, M. D. (1995). A hierarchy of ATP-consuming processes in mammalian cells. *The Biochemical journal*, 312 (Pt 1), 163–167.

Canfield, K., Li, J., Wilkins, O. M., Morrison, M. M., Ung, M., Wells, W., Williams, C. R., Liby, K. T., Vullhorst, D., Buonanno, A., Hu, H., Schiff, R., Cook, R. S., & Kurokawa, M. (2015). Receptor tyrosine kinase ERBB4 mediates acquired resistance to ERBB2 inhibitors in breast cancer cells. *Cell cycle (Georgetown, Tex.)*, 14(4), 648–655.

Cano-González, A., Mauro-Lizcano, M., Iglesias-Serret, D., Gil, J., and López-Rivas, A. (2018). Involvement of both caspase-8 and Noxa-activated pathways in endoplasmic reticulum stress-induced apoptosis in triple-negative breast tumor cells. *Cell death & disease*, 9(2), 134.

Carlsson, J., Nordgren, H., Sjöström, J., Wester, K., Villman, K., Bengtsson, N. O., Ostenstad, B., Lundqvist, H., and Blomqvist, C. (2004). HER2 expression in breast cancer primary tumours and corresponding metastases. *Journal of cancer*, 90(12), 2344–2348.

Cava, C., Armaos, A., Lang, B., Tartaglia, G.G., and Castiglioni, I. (2022). Identification of long non-coding RNAs and RNA binding proteins in breast cancer subtypes. *Sci Rep* 12, 693.

Chambers, D. M., Peters, J., and Abbott, C. M. (1998). The lethal mutation of the mouse wasted (wst) is a deletion that abolishes expression of a tissue-specific isoform of translation elongation factor 1alpha, encoded by the Eef1a2 gene. *Proceedings of the National Academy of Sciences of the United States of America*, 95(8), 4463–4468.

Chamond, N., Deforges, J., Ulryck, N., and Sargueil, B. (2014). 40S recruitment in the absence of eIF4G/4A by EMCV IRES refines the model for translation

initiation on the archetype of Type II IRESs. *Nucleic acids research*, 42(16), 10373–10384.

Chan, C.Y., Carmack, C.S., Long, D.D., Maliyekkel, A., Shao, Y., Roninson, B., and Ding, Y. (2009). A structural interpretation of the effect of GC-content on efficiency of RNA interference. *BMC Bioinformatics* 10 (Suppl 1), S33.

Chang, Y. W. E. and Traugh, J.A. (1998). Insulin stimulation of phosphorylation of elongation factor 1 (eEF-1) enhances elongation activity. *European Journal of Biochemistry*, 251: 201-207.

Chappell, S. A., Edelman, G. M., and Mauro, V. P. (2006). Ribosomal tethering and clustering as mechanisms for translation initiation. *Proceedings of the National Academy of Sciences of the United States of America*, 103(48), 18077–18082.

Chard, L. S., Kaku, Y., Jones, B., Nayak, A., and Belsham, G. J. (2006). Functional analyses of RNA structures shared between the internal ribosome entry sites of hepatitis C virus and the picornavirus porcine teschovirus 1 Talfan. *Journal of virology*, 80(3), 1271–1279.

Chatterjee, N. K., Kerwar, S. S., and Weissbach, H. (1972). Initiation of protein synthesis in HeLa cells. *Proceedings of the National Academy of Sciences of the United States of America*, 69(6), 1375–1379.

Chen, R., Zou, Y., Mao, D., Sun, D., Gao, G., Shi, J., Liu, X., Zhu, C., Yang, M., Ye, W., Hao, Q., Li, R., and Yu, L. (2014). The general amino acid control pathway regulates mTOR and autophagy during serum/glutamine starvation. *The Journal of cell biology*, 206(2), 173–182.

Chen, Z., Wang, Y., Warden, C., and Chen, S. (2015). Cross-talk between ER and HER2 regulates c-MYC-mediated glutamine metabolism in aromatase inhibitor resistant breast cancer cells. *The Journal of steroid biochemistry and molecular biology*, 149, 118–127.

Chen, Z., Dempsey, D. R., Thomas, S. N., Hayward, D., Bolduc, D. M., and Cole, P. A. (2016). Molecular Features of Phosphatase and Tensin Homolog (PTEN) Regulation by C-terminal Phosphorylation. *The Journal of biological chemistry*, 291(27), 14160–14169.

Chen, L., Brewer, M. D., Guo, L., Wang, R., Jiang, P., and Yang, X. (2017). Enhanced Degradation of Misfolded Proteins Promotes Tumorigenesis. *Cell reports*, 18(13), 3143–3154.

Chen, C., Zhang, Z., Liu, C., Wang, B., Liu, P., Fang, S., Yang, F., You, Y., and Li, X. (2022). ATF4-dependent fructolysis fuels growth of glioblastoma multiforme. *Nature communications*, 13(1), 6108.

Chi, K. C., Wallis, A. E., Lee, C. H., De Menezes, D. L., Sartor, J., Dragowska, W. H., and Mayer, L. D. (2000). Effects of Bcl-2 modulation with G3139 antisense oligonucleotide on human breast cancer cells are independent of inherent Bcl-2 protein expression. *Breast cancer research and treatment*, 63(3), 199–212.

Chilà, G., Guarini, V., Galizia, D., Geuna, E., and Montemurro, F. (2021). The Clinical Efficacy and Safety of Neratinib in Combination with Capecitabine for the Treatment of Adult Patients with Advanced or Metastatic HER2-Positive Breast Cancer. *Drug design, development, and therapy*, 15, 2711–2720.

Child, S. J., Miller, M. K., and Geballe, A. P. (1999a). Cell type-dependent and -independent control of HER-2/neu translation. *The international journal of biochemistry & cell biology*, 31(1), 201–213.

Child, S. J., Miller, M. K., and Geballe, A. P. (1999b). Translational control by an upstream open reading frame in the HER-2/neu transcript. *The Journal of biological chemistry*, 274(34), 24335–24341.

Choowongkomon, K., Carlin, C. R., and Sönnichsen, F. D. (2005). A structural model for the membrane-bound form of the juxtamembrane domain of the epidermal growth factor receptor. *The Journal of biological chemistry*, 280(25), 24043–24052.

Cobbold, L. C., Spriggs, K. A., Haines, S. J., Dobbyn, H. C., Hayes, C., de Moor, C. H., Lilley, K. S., Bushell, M., and Willis, A. E. (2008). Identification of internal ribosome entry segment (IRES)-trans-acting factors for the Myc family of IRESs. *Molecular and cellular biology*, 28(1), 40–49.

Coldwell, M. J., and Morley, S. J. (2006). Specific isoforms of translation initiation factor 4GI show differences in translational activity. *Molecular and cellular biology*, 26(22), 8448–8460.

Coleman, J and Miskimins, W. K. (2009). Structure and activity of the internal ribosome entry site within the human p27Kip1 5'-untranslated region, *RNA Biology*, 6:1, 84-89,

Conte, C., Ainaoui, N., Delluc-Clavières, A., Khoury, M. P., Azar, R., Pujol, F., Martineau, Y., Pyronnet, S., and Prats, A. C. (2009). Fibroblast growth factor 1 induced during myogenesis by a transcription-translation coupling mechanism. *Nucleic acids research*, 37(16), 5267–5278.

Créancier, L., Mercier, P., Prats, A. C., and Morello, D. (2001). c-myc Internal ribosome entry site activity is developmentally controlled and subjected to a strong translational repression in adult transgenic mice. *Molecular and cellular biology*, 21(5), 1833–1840.

Cullinan, S. B., Zhang, D., Hannink, M., Arvisais, E., Kaufman, R. J., and Diehl,

J. A. (2003). Nrf2 is a direct PERK substrate and effector of PERK-dependent cell survival. *Molecular and cellular biology*, 23(20), 7198–7209.

Czopek, J., Pawlęga, J., Fijorek, K., Püsküllüoğlu, M., Różanowski, P., and Okoń, K. (2013). HER-3 expression in HER-2-amplified breast carcinoma. *Contemporary oncology (Poznan, Poland)*, 17(5), 446–449.

Dai, J., Chen, Y., Tang, C., Wei, X., Gong, Y., Wei, J., Gu, D., and Chen, J. (2020). Pyrotinib in the treatment of human epidermal growth factor receptor 2-positive metastatic breast cancer: A case report. *Medicine*, 99(25), e20809.

Damiano, F., Alemanno, S., Gnoni, G. V., and Siculella, L. (2010). Translational control of the sterol-regulatory transcription factor SREBP-1 mRNA in response to serum starvation or ER stress is mediated by an internal ribosome entry site. *The Biochemical journal*, 429(3), 603–612.

Dangelmaier, C., Manne, B. K., Liverani, E., Jin, J., Bray, P., and Kunapuli, S. P. (2014). PDK1 selectively phosphorylates Thr(308) on Akt and contributes to human platelet functional responses. *Thrombosis and haemostasis*, 111(3), 508–517.

Darb-Esfahani, S., Denkert, C., Stenzinger, A., Salat, C., Sinn, B., Schem, C., Endris, V., Klare, P., Schmitt, W., Blohmer, J. U., Weichert, W., Möbs, M., Tesch, H., Kümmel, S., Sinn, P., Jackisch, C., Dietel, M., Reimer, T., Loi, S., Untch, M., von Minckwitz, G., Nekljudova, V., and Loibl, S. (2016). Role of TP53 mutations in triple negative and HER2-positive breast cancer treated with neoadjuvant anthracycline/taxane-based chemotherapy. *Oncotarget*, 7(42), 67686–67698.

Datta, S. R., Dudek, H., Tao, X., Masters, S., Fu, H., Gotoh, Y., and Greenberg, M. E. (1997). Akt phosphorylation of BAD couples survival signals to the cell-intrinsic death machinery. *Cell*, 91(2), 231–241.

Dave, P., George, B., Sharma, D. K., and Das, S. (2017). Polypyrimidine tract-binding protein (PTB) and PTB-associated splicing factor in CVB3 infection: an ITAF for an ITAF. *Nucleic acids research*, 45(15), 9068–9084.

DeBerardinis, R. J., Mancuso, A., Daikhin, E., Nissim, I., Yudkoff, M., Wehrli, S., and Thompson, C. B. (2007). Beyond aerobic glycolysis: transformed cells can engage in glutamine metabolism that exceeds the requirement for protein and nucleotide synthesis. *Proceedings of the National Academy of Sciences of the United States of America*, 104(49), 19345–19350.

DeBusk, K., Abeysinghe, S., Vickers, A., Nangia, A., Bell, J., Ike, C., Forero-Torres, A., and Blahna, M. T. (2021). Efficacy of tucatinib for HER2-positive metastatic breast cancer after HER2-targeted therapy: a network meta-analysis. *Future oncology (London, England)*, 17(33), 4635–4647.

Deng, J., Harding, H. P., Raught, B., Gingras, A. C., Berlanga, J. J., Scheuner, D., Kaufman, R. J., Ron, D., and Sonenberg, N. (2002). Activation of GCN2 in UV-irradiated cells inhibits translation. *Current biology: CB*, 12(15), 1279–1286.

Dever, T. E., and Green, R. (2012). The elongation, termination, and recycling phases of translation in eukaryotes. *Cold Spring Harbor perspectives in biology*, 4(7), a013706.

Dever, T. E., Dinman, J. D., and Green, R. (2018). Translation Elongation and Recoding in Eukaryotes. *Cold Spring Harbor perspectives in biology*, 10(8), a032649.

Dhalia, R., Marinsek, N., Reis, C. R., Katz, R., Muniz, J. R., Standart, N., Carrington, M., and de Melo Neto, O. P. (2006). The two eIF4A helicases in Trypanosoma brucei are functionally distinct. *Nucleic acids research*, 34(9), 2495–2507.

Di Conza, G., Trusso Cafarello, S., Zheng, X., Zhang, Q., and Mazzone, M. (2017). PHD2 Targeting Overcomes Breast Cancer Cell Death upon Glucose Starvation in a PP2A/B55α-Mediated Manner. *Cell reports*, 18(12), 2836–2844.

Djumagulov, M., Demeshkina, N., Jenner, L., Rozov, A., Yusupov, M., and Yusupova, G. (2021). Accuracy mechanism of eukaryotic ribosome translocation. *Nature*, 600(7889), 543–546.

Doig, J., Griffiths, L. A., Peberdy, D., Dharmasaroja, P., Vera, M., Davies, F. J., Newbery, H. J., Brownstein, D., and Abbott, C. M. (2013). In vivo characterization of the role of tissue-specific translation elongation factor 1A2 in protein synthesis reveals insights into muscle atrophy. *The FEBS journal*, 280(24), 6528–6540.

Dong, J., Qiu, H., Garcia-Barrio, M., Anderson, J., and Hinnebusch, A. G. (2000). Uncharged tRNA activates GCN2 by displacing the protein kinase moiety from a bipartite tRNA-binding domain. *Molecular cell*, *6*(2), 269–279.

Donlin-Asp, P. G., Polisseni, C., Klimek, R., Heckel, A., and Schuman, E. M. (2021). Differential regulation of local mRNA dynamics and translation following long-term potentiation and depression. *Proceedings of the National Academy of Sciences of the United States of America, 118(13), e2017578118.*

Eagle, H., and Levine, E. M. (1967). Growth regulatory effects of cellular interaction. *Nature*, 213(5081), 1102–1106.

Ebert, B. L., and Bunn, H. F. (1998). Regulation of transcription by hypoxia requires a multiprotein complex that includes hypoxia-inducible factor 1, an adjacent transcription factor, and p300/CREB binding protein. *Molecular and cellular biology*, 18(7), 4089–4096.

El-Hashim, A. Z., Khajah, M. A., Renno, W. M., Babyson, R. S., Uddin, M., Benter, I. F., Ezeamuzie, C., and Akhtar, S. (2017). Src-dependent EGFR transactivation regulates lung inflammation via downstream signaling involving ERK1/2, PI3Kδ/Akt and NFκB induction in a murine asthma model. *Scientific reports*, 7(1), 9919.

Elde, N. C., Child, S. J., Geballe, A. P., and Malik, H. S. (2009). Protein kinase R reveals an evolutionary model for defeating viral mimicry. *Nature*, 457(7228), 485–489.

Elenbaas, B., Spirio, L., Koerner, F., Fleming, M. D., Zimonjic, D. B., Donaher, J. L., Popescu, N. C., Hahn, W. C., and Weinberg, R. A. (2001). Human breast cancer cells generated by oncogenic transformation of primary mammary epithelial cells. *Genes & development*, 15(1), 50–65.

Elenius, K., Choi, C. J., Paul, S., Santiestevan, E., Nishi, E., and Klagsbrun, M. (1999). Characterization of a naturally occurring ErbB4 isoform that does not bind or activate phosphatidyl inositol 3-kinase. *Oncogene*, 18(16), 2607–2615.

Elster, N., Toomey, S., Fan, Y., Cremona, M., Morgan, C., Weiner Gorzel, K., Bhreathnach, U., Milewska, M., Murphy, M., Madden, S., Naidoo, J., Fay, J., Kay, E., Carr, A., Kennedy, S., Furney, S., Mezynski, J., Breathhnach, O., Morris, P., Grogan, L., Hill, A., Kennedy, S., Crown, J., Gallagher, W., Hennessy, B., and Eustace, A. (2018). Frequency, impact and a preclinical study of novel *ERBB* gene family mutations in HER2-positive breast cancer. *Therapeutic advances in medical oncology*, 10, 1758835918778297.

Endo, H., Owada, S., Inagaki, Y., Shida, Y., and Tatemichi, M. (2018). Glucose starvation induces LKB1-AMPK-mediated MMP-9 expression in cancer cells. *Scientific reports*, *8*(1), 10122.

Erickson, H. K., Lewis Phillips, G. D., Leipold, D. D., Provenzano, C. A., Mai, E., Johnson, H. A., Gunter, B., Audette, C. A., Gupta, M., Pinkas, J., and Tibbitts, J. (2012). The effect of different linkers on target cell catabolism and pharmacokinetics/pharmacodynamics of trastuzumab maytansinoid conjugates. *Molecular cancer therapeutics*, 11(5), 1133–1142.

Fagard, R., and London, I. M. (1981). Relationship between phosphorylation and activity of heme-regulated eukaryotic initiation factor 2 alpha kinase. *Proceedings of the National Academy of Sciences of the United States of America*, 78(2), 866–870.

Fang, L., Vilas-Boas, J., Chakraborty, S., Potter, Z. E., Register, A. C., Seeliger, M. A., and Maly, D. J. (2020). How ATP-Competitive Inhibitors Allosterically Modulate Tyrosine Kinases That Contain a Src-like Regulatory Architecture. *ACS chemical biology*, 15(7), 2005–2016.

Fedier, A., Schwarz, V. A., Walt, H., Carpini, R. D., Haller, U., and Fink, D. (2001). Resistance to topoisomerase poisons due to loss of DNA mismatch repair. *International journal of cancer*, 93(4), 571–576.

Feeney, K. A., Putker, M., Brancaccio, M., and O'Neill, J. S. (2016). In-depth Characterization of Firefly Luciferase as a Reporter of Circadian Gene Expression in Mammalian Cells. *Journal of biological rhythms*, 31(6), 540–550.

Fernandez, J., Yaman, I., Mishra, R., Merrick, W. C., Snider, M. D., Lamers, W. H., and Hatzoglou, M. (2001). Internal ribosome entry site-mediated translation of a mammalian mRNA is regulated by amino acid availability. *The Journal of biological chemistry*, 276(15), 12285–12291.

Fernandez, J., Bode, B., Koromilas, A., Diehl, J. A., Krukovets, I., Snider, M. D., and Hatzoglou, M. (2002). Translation mediated by the internal ribosome entry site of the cat-1 mRNA is regulated by glucose availability in a PERK kinase-dependent manner. *The Journal of biological chemistry*, 277(14), 11780–11787.

Fernandez, J., Yaman, I., Huang, C., Liu, H., Lopez, A.B., Komar, A.A., Caprara, M.G., Merrick, W.C., Snider, M.D., Kaufman, R.J., Lamers, W.H., and Hatzoglou, M. (2005). Ribosome Stalling Regulates IRES-Mediated Translation in Eukaryotes, a Parallel to Prokaryotic Attenuation, *Molecular Cell*, 17 (3), 405–416. 10.1016

Fernández, I. S., Bai, X. C., Murshudov, G., Scheres, S. H., and Ramakrishnan, V. (2014). Initiation of translation by cricket paralysis virus IRES requires its translocation in the ribosome. *Cell*, 157(4), 823–831.

Ferraro, D. A., Gaborit, N., Maron, R., Cohen-Dvashi, H., Porat, Z., Pareja, F., Lavi, S., Lindzen, M., Ben-Chetrit, N., Sela, M., and Yarden, Y. (2013). Inhibition of triple-negative breast cancer models by combinations of antibodies to EGFR. *Proceedings of the National Academy of Sciences of the United States of America*, *110*(5), 1815–1820.

Fishburn, J., Tomko, E., Galburt, E., and Hahn, S. (2015). Double-stranded DNA translocase activity of transcription factor TFIIH and the mechanism of RNA polymerase II open complex formation. *Proceedings of the National Academy of Sciences of the United States of America*, 112(13), 3961–3966.

Flis, J., Holm, M., Rundlet, E. J., Loerke, J., Hilal, T., Dabrowski, M., Bürger, J., Mielke, T., Blanchard, S. C., Spahn, C. M. T., and Budkevich, T. V. (2018). tRNA Translocation by the Eukaryotic 80S Ribosome and the Impact of GTP Hydrolysis. *Cell reports*, 25(10), 2676–2688.e7.

Ford, L. P., Bagga, P. S., and Wilusz, J. (1997). The poly(A) tail inhibits the assembly of a 3'-to-5' exonuclease in an in vitro RNA stability system.

Molecular and cellular biology, 17(1), 398–406.

Fox, J. T., Shin, W. K., Caudill, M. A., and Stover, P. J. (2009). A UV-responsive internal ribosome entry site enhances serine hydroxymethyltransferase 1 expression for DNA damage repair. *The Journal of biological chemistry*, 284(45), 31097–31108.

Franklin, M. C., Carey, K. D., Vajdos, F. F., Leahy, D. J., de Vos, A. M., and Sliwkowski, M. X. (2004). Insights into ErbB signaling from the structure of the ErbB2-pertuzumab complex. *Cancer cell*, 5(4), 317–328.

Franovic, A., Gunaratnam, L., Smith, K., Robert, I., Patten, D., and Lee, S. (2007). Translational up-regulation of the EGFR by tumor hypoxia provides a nonmutational explanation for its overexpression in human cancer. *Proceedings of the National Academy of Sciences of the United States of America*, 104(32), 13092–13097.

Friis, M. B., Rasmussen, T. B., and Belsham, G. J. (2012). Modulation of translation initiation efficiency in classical swine fever virus. *Journal of virology*, 86(16), 8681–8692.

Fringer, J. M., Acker, M. G., Fekete, C. A., Lorsch, J. R., and Dever, T. E. (2007). Coupled release of eukaryotic translation initiation factors 5B and 1A from 80S ribosomes following subunit joining. *Molecular and cellular biology*, 27(6), 2384–2397.

Fukumura, D., Xu, L., Chen, Y., Gohongi, T., Seed, B., and Jain, R. K. (2001). Hypoxia and acidosis independently up-regulate vascular endothelial growth factor transcription in brain tumors in vivo. *Cancer research*, 61(16), 6020–6024.

Furic, L., Rong, L., Larsson, O., Koumakpayi, I. H., Yoshida, K., Brueschke, A., Petroulakis, E., Robichaud, N., Pollak, M., Gaboury, L. A., Pandolfi, P. P., Saad, F., and Sonenberg, N. (2010). eIF4E phosphorylation promotes tumorigenesis and is associated with prostate cancer progression. *Proceedings of the National Academy of Sciences of the United States of America*, 107(32), 14134–14139.

Furr, B. J., and Jordan, V. C. (1984). The pharmacology and clinical uses of tamoxifen. *Pharmacology & therapeutics*, 25(2), 127–205.

Gaba, A., Wang, Z., Krishnamoorthy, T., Hinnebusch, A.G. and Sachs, M. S. (2001). Physical evidence for distinct mechanisms of translational control by upstream open reading frames. *The EMBO Journal*, 20: 6453-6463.

Gaibar, M., Beltrán, L., Romero-Lorca, A., Fernández-Santander, A., and Novillo, A. (2020). Somatic Mutations in *HER2* and Implications for Current Treatment Paradigms in *HER2*-Positive Breast Cancer. *Journal of oncology*,

2020, 6375956.

Galdadas, I., Carlino, L., Ward, R. A., Hughes, S. J., Haider, S., and Gervasio, F. L. (2021). Structural basis of the effect of activating mutations on the EGF receptor. *eLife*, 10, e65824.

Galicia-Vázquez, G., Chu, J., and Pelletier, J. (2015). eIF4AII is dispensable for miRNA-mediated gene silencing. *RNA (New York, N.Y.)*, 21(10), 1826–1833.

Gameiro, P. A., and Struhl, K. (2018). Nutrient Deprivation Elicits a Transcriptional and Translational Inflammatory Response Coupled to Decreased Protein Synthesis. *Cell reports*, 24(6), 1415–1424.

Gao, P., Tchernyshyov, I., Chang, T. C., Lee, Y. S., Kita, K., Ochi, T., Zeller, K. I., De Marzo, A. M., Van Eyk, J. E., Mendell, J. T., and Dang, C. V. (2009). c-Myc suppression of miR-23a/b enhances mitochondrial glutaminase expression and glutamine metabolism. *Nature*, 458(7239), 762–765.

Garza, K. R., Clarke, S. L., Ho, Y. H., Bruss, M. D., Vasanthakumar, A., Anderson, S. A., and Eisenstein, R. S. (2020). Differential translational control of 5' IRE-containing mRNA in response to dietary iron deficiency and acute iron overload. *Metallomics : integrated biometal science*, 12(12), 2186–2198.

Geltz, N. R., and Augustine, J. A. (1998). The p85 and p110 subunits of phosphatidylinositol 3-kinase-alpha are substrates, in vitro, for a constitutively associated protein tyrosine kinase in platelets. *Blood*, 91(3), 930–939.

Ghee, M., Baker, H., Miller, J. C., and Ziff, E. B. (1998). AP-1, CREB and CBP transcription factors differentially regulate the tyrosine hydroxylase gene. *Brain research. Molecular brain research*, 55(1), 101–114.

Ghosh, R., Narasanna, A., Wang, S. E., Liu, S., Chakrabarty, A., Balko, J. M., González-Angulo, A. M., Mills, G. B., Penuel, E., Winslow, J., Sperinde, J., Dua, R., Pidaparthi, S., Mukherjee, A., Leitzel, K., Kostler, W. J., Lipton, A., Bates, M., and Arteaga, C. L. (2011). Trastuzumab has preferential activity against breast cancers driven by HER2 homodimers. *Cancer research*, 71(5), 1871–1882.

Gingras, A. C., Svitkin, Y., Belsham, G. J., Pause, A., and Sonenberg, N. (1996). Activation of the translational suppressor 4E-BP1 following infection with encephalomyocarditis virus and poliovirus. *Proceedings of the National Academy of Sciences of the United States of America*, 93(11), 5578–5583.

Gingras, A. C., Gygi, S. P., Raught, B., Polakiewicz, R. D., Abraham, R. T., Hoekstra, M. F., Aebersold, R., and Sonenberg, N. (1999). Regulation of 4E-BP1 phosphorylation: a novel two-step mechanism. *Genes & development*, 13(11), 1422–1437.

Giraud, S., Greco, A., Brink, M., Diaz, J. J., and Delafontaine, P. (2001). Translation initiation of the insulin-like growth factor I receptor mRNA is mediated by an internal ribosome entry site. *The Journal of biological chemistry*, 276(8), 5668–5675.

Glaser, W., and Skern, T. (2000). Extremely efficient cleavage of eIF4G by picornaviral proteinases L and 2A in vitro. *FEBS letters*, 480(2-3), 151–155.

Godfrey, J. D., Hejazi, D., Du, X., Wei, C., Rao, E., and Gomez, C. M. (2022). HER2 c-Terminal Fragments Are Expressed via Internal Translation of the HER2 mRNA. *International journal of molecular sciences*, 23(17), 9549.

Goto, N., Bazar, G., Kovacs, Z., Kunisada, M., Morita, H., Kizaki, S., Sugiyama, H., Tsenkova, R., and Nishigori, C. (2015). Detection of UV-induced cyclobutane pyrimidine dimers by near-infrared spectroscopy and aquaphotomics. *Scientific reports*, 5, 11808.

Grau-Bové, X., Ruiz-Trillo, I. and Irimia, M. (2018). Origin of exon skipping-rich transcriptomes in animals driven by evolution of gene architecture. *Genome Biol* 19, 135.

Graves, J. D., Draves, K. E., Craxton, A., Saklatvala, J., Krebs, E. G., and Clark, E. A. (1996). Involvement of stress-activated protein kinase and p38 mitogen-activated protein kinase in mIgM-induced apoptosis of human B lymphocytes. *Proceedings of the National Academy of Sciences of the United States of America*, 93(24), 13814–13818.

Gray, N. K. and Hentze, M. W. (1994). Iron regulatory protein prevents binding of the 43S translation pre-initiation complex to ferritin and eALAS mRNAs, *EMBO Journal*, 13: 3882-3891.

Grishin N. V. (2001). KH domain: one motif, two folds. *Nucleic acids research*, 29(3), 638–643.

Groenewegen, G. and De Gast, G. C. (1999). GM-CSF can cause T cell activation; Results of sequential chemo-immunotherapy, *European Journal of Cancer*, 35(Suppl. 3) 0959-8049.

Gromadski, K. B., Schümmer, T., Strømgaard, A., Knudsen, C. R., Kinzy, T. G., and Rodnina, M. V. (2007). Kinetics of the interactions between yeast elongation factors 1A and 1Balpha, guanine nucleotides, and aminoacyl-tRNA. *The Journal of biological chemistry*, 282(49), 35629–35637.

Grover, R., Ray, P. S., and Das, S. (2008). Polypyrimidine tract binding protein regulates IRES-mediated translation of p53 isoforms. *Cell cycle*, 7(14), 2189–2198.

Gu, S., Jeon, H. M., Nam, S. W., Hong, K. Y., Rahman, M. S., Lee, J. B., Kim, Y., and Jang, S. K. (2022). The flip-flop configuration of the PABP-dimer leads to switching of the translation function. *Nucleic acids research*, 50(1), 306–321.

Guan, B. J., Krokowski, D., Majumder, M., Schmotzer, C. L., Kimball, S. R., Merrick, W. C., Koromilas, A. E., and Hatzoglou, M. (2014). Translational control during endoplasmic reticulum stress beyond phosphorylation of the translation initiation factor eIF2α. *The Journal of biological chemistry*, 289(18), 12593–12611.

Guarneri, V., Barbieri, E., Dieci, M. V., Piacentini, F., and Conte, P. (2010). Anti-HER2 neoadjuvant and adjuvant therapies in HER2 positive breast cancer. *Cancer treatment reviews*, 36 Suppl 3, S62–S66.

Guzikowski, A. R., Harvey, A. T., Zhang, J., Zhu, S., Begovich, K., Cohn, M. H., Wilhelm, J. E., and Zid, B. M. (2022). Differential translation elongation directs protein synthesis in response to acute glucose deprivation in yeast. *RNA biology*, *19*(1), 636–649.

Haghighat, A., Mader, S., Pause, A., and Sonenberg, N. (1995). Repression of cap-dependent translation by 4E-binding protein 1: Competition with p220 for binding to eukaryotic initiation factor-4E', *EMBO Journal*, 14:5701-5709.

Halaby, M. J., Li, Y., Harris, B. R., Jiang, S., Miskimins, W. K., Cleary, M. P., and Yang, D. Q. (2015). Translational Control Protein 80 Stimulates IRES-Mediated Translation of p53 mRNA in Response to DNA Damage. *BioMed research international*, 2015, 708158.

Han, J., Lee, Y., Yeom, K. H., Kim, Y. K., Jin, H., and Kim, V. N. (2004). The Drosha-DGCR8 complex in primary microRNA processing. *Genes & development*, 18(24), 3016–3027.

Han, C. C., and Wan, F. S. (2018). New Insights into the Role of Endoplasmic Reticulum Stress in Breast Cancer Metastasis. *Journal of breast cancer*, 21(4), 354–362.

Han, W., Sfondouris, M. E., Semmes, E. C., Meyer, A. M., and Jones, F. E. (2016). Intrinsic HER4/4ICD transcriptional activation domains are required for STAT5A activated gene expression. *Gene*, 592(1), 221–226.

Han, J., Zhang. Y., Xu, J., Zhnag, T., Wang, H., Wang, Z., Jiang, Y., Zhou, L., Yang, M., Hua, Y., and Cai, Z. (2021a). Her4 promotes cancer metabolic reprogramming via the c-Myc-dependent signaling axis', *Cancer Letters*, 0304-3835.

Han, S., Zhu, L., Zhu, Y., Meng, Y., Li, J., Song, P., Yousafzai, N. A., Feng, L., Chen, M., Wang, Y., Jin, H., and Wang, X. (2021b). Targeting ATF4-dependent pro-survival autophagy to synergize glutaminolysis inhibition. *Theranostics*,

11(17), 8464–8479.

Hanahan, D., and Weinberg, R. A. (2011). Hallmarks of cancer: the next generation. *Cell*, 144(5), 646–674.

Hantelys, F., Godet, A. C., David, F., Tatin, F., Renaud-Gabardos, E., Pujol, F., Diallo, L., Ader, I., Ligat, L., Henras, A.K., Sato, Y., Parini, A., Lacazette, E., Garmy-Susini, B., and Prats A.C.(2019). Vasohibin1, a new IRES trans-acting factor for induction of (lymph)angiogenic factors in early hypoxia. *BioRxiv* 260364

Harami-Papp, H., Pongor, L. S., Munkácsy, G., Horváth, G., Nagy, Á. M., Ambrus, A., Hauser, P., Szabó, A., Tretter, L., and Győrffy, B. (2016). TP53 mutation hits energy metabolism and increases glycolysis in breast cancer. *Oncotarget*, 7(41), 67183–67195.

Harding, H. P., Zhang, Y., Bertolotti, A., Zeng, H., and Ron, D. (2000a). Perk is essential for translational regulation and cell survival during the unfolded protein response. *Molecular cell*, 5(5), 897–904.

Harding, H. P., Novoa, I., Zhang, Y., Zeng, H., Wek, R., Schapira, M., and Ron, D. (2000b). Regulated translation initiation controls stress-induced gene expression in mammalian cells. *Molecular cell*, 6(5), 1099–1108.

Harding, H. P., Zhang, Y., Zeng, H., Novoa, I., Lu, P. D., Calfon, M., Sadri, N., Yun, C., Popko, B., Paules, R., Stojdl, D. F., Bell, J. C., Hettmann, T., Leiden, J. M., and Ron, D. (2003). An integrated stress response regulates amino acid metabolism and resistance to oxidative stress. *Molecular cell*, 11(3), 619–633.

Hart, V., Silipo, M., Satam, S., Gautrey, H., Kirby, J., and Tyson-Capper, A. (2021). HER2-PI9 and HER2-I12: two novel and functionally active splice variants of the oncogene HER2 in breast cancer. *Journal of cancer research and clinical oncology*, 147(10), 2893–2912.

Haskins, J. W., Nguyen, D. X., and Stern, D. F. (2014). Neuregulin 1-activated ERBB4 interacts with YAP to induce Hippo pathway target genes and promote cell migration. *Science signaling*, 7(355), ra116.

Hatzenpichler, R., Scheller, S., Tavormina, P. L., Babin, B. M., Tirrell, D. A., and Orphan, V. J. (2014). In situ visualization of newly synthesized proteins in environmental microbes using amino acid tagging and click chemistry. *Environmental microbiology*, 16(8), 2568–2590.

Hendrickson, D. G., Hogan, D. J., McCullough, H. L., Myers, J. W., Herschlag, D., Ferrell, J. E., and Brown, P. O. (2009). Concordant regulation of translation and mRNA abundance for hundreds of targets of a human microRNA. *PLoS biology*, 7(11), e1000238.

Herbreteau, C. H., Weill, L., Décimo, D., Prévôt, D., Darlix, J. L., Sargueil, B., and Ohlmann, T. (2005). HIV-2 genomic RNA contains a novel type of IRES located downstream of its initiation codon. *Nature structural & molecular biology*, *12*(11), 1001–1007.

Hexdall, L., and Zheng, C. F. (2001). Stable luciferase reporter cell lines for signal transduction pathway readout using GAL4 fusion transactivators. *BioTechniques*, 30(5), 1134–1140.

Hizli, A. A., Chi, Y., Swanger, J., Carter, J. H., Liao, Y., Welcker, M., Ryazanov, A. G., and Clurman, B. E. (2013). Phosphorylation of eukaryotic elongation factor 2 (eEF2) by cyclin A-cyclin-dependent kinase 2 regulates its inhibition by eEF2 kinase. *Molecular and cellular biology*, 33(3), 596–604.

Hoffmann, C., Mao, X., Brown-Clay, J., Moreau, F., Al Absi, A., Wurzer, H., Sousa, B., Schmitt, F., Berchem, G., Janji, B., and Thomas, C. (2018). Hypoxia promotes breast cancer cell invasion through HIF-1α-mediated up-regulation of the invadopodial actin bundling protein CSRP2. *Scientific reports*, 8(1), 10191.

Holgersen, E. M., Gandhi, S., Zhou, Y., Kim, J., Vaz, B., Bogojeski, J., Bugno, M., Shalev, Z., Cheung-Ong, K., Gonçalves, J., O'Hara, M., Kron, K., Verby, M., Sun, M., Kakaradov, B., Delong, A., Merico, D., and Deshwar, A. G. (2021). Transcriptome-Wide Off-Target Effects of Steric-Blocking Oligonucleotides. *Nucleic acid therapeutics*, 31(6), 392–403.

Honegger, A. M., Dull, T. J., Felder, S., Van Obberghen, E., Bellot, F., Szapary, D., Schmidt, A., Ullrich, A., and Schlessinger, J. (1987). Point mutation at the ATP binding site of EGF receptor abolishes protein-tyrosine kinase activity and alters cellular routing. *Cell*, 51(2), 199–209.

Horrell, E. M. W., Wilson, K. and D'Orazio, J. A. (2015). Melanoma — Epidemiology, Risk Factors, and the Role of Adaptive Pigmentation, *Melanoma - Current Clinical Management and Future Therapeutics*, 10.5772/58994.

Howcroft, T. K., Kirshner, S. L., and Singer, D. S. (1997). Measure of transient transfection efficiency using beta-galactosidase protein. *Analytical biochemistry*, 244(1), 22–27.

Hresko, R. C., and Mueckler, M. (2005). mTOR.RICTOR is the Ser473 kinase for Akt/protein kinase B in 3T3-L1 adipocytes. *The Journal of biological chemistry*, 280(49), 40406–40416.

Hsu, P. P., Kang, S. A., Rameseder, J., Zhang, Y., Ottina, K. A., Lim, D., Peterson, T. R., Choi, Y., Gray, N. S., Yaffe, M. B., Marto, J. A., and Sabatini, D. M. (2011). The mTOR-regulated phosphoproteome reveals a mechanism of mTORC1-mediated inhibition of growth factor signaling. *Science (New York, N.Y.)*, 332(6035), 1317–1322.

Hu, Y., Cheng, L., Hochleitner, B. W., and Xu, Q. (1997). Activation of mitogen-activated protein kinases (ERK/JNK) and AP-1 transcription factor in rat carotid arteries after balloon injury. *Arteriosclerosis, thrombosis, and vascular biology*, 17(11), 2808–2816.

Hu, K., Babapoor-Farrokhran, S., Rodrigues, M., Deshpande, M., Puchner, B., Kashiwabuchi, F., Hassan, S. J., Asnaghi, L., Handa, J. T., Merbs, S., Eberhart, C. G., Semenza, G. L., Montaner, S., and Sodhi, A. (2016a). Hypoxia-inducible factor 1 upregulation of both VEGF and ANGPTL4 is required to promote the angiogenic phenotype in uveal melanoma. *Oncotarget*, 7(7), 7816–7828.

Hu, Y. L., Yin, Y., Liu, H. Y., Feng, Y. Y., Bian, Z. H., Zhou, L. Y., Zhang, J. W., Fei, B. J., Wang, Y. G., and Huang, Z. H. (2016b). Glucose deprivation induces chemoresistance in colorectal cancer cells by increasing ATF4 expression. *World journal of gastroenterology*, 22(27), 6235–6245.

Hua, Y., Gorshkov, K., Yang, Y., Wang, W., Zhang, N., and Hughes, D. P. (2012). Slow down to stay alive: HER4 protects against cellular stress and confers chemoresistance in neuroblastoma. *Cancer*, 118(20), 5140–5154.

Huang, J., Tan, PH., Thiyagarajan, J., and Boon-Huat, B. (2003). Prognostic Significance of Glutathione S-Transferase-Pi in Invasive Breast Cancer, *Modern Pathology*, 16, 558–565.

Huang, C., Sheng, S., Li, R., Sun, X., Liu, J., and Huang, G. (2015). Lactate promotes resistance to glucose starvation via upregulation of Bcl-2 mediated by mTOR activation. *Oncology reports*, 33(2), 875–884.

Huang, Y., Ognjenovic, J., Karandur, D., Miller, K., Merk, A., Subramaniam, S., and Kuriyan, J. (2021). A molecular mechanism for the generation of ligand-dependent differential outputs by the epidermal growth factor receptor. *eLife*, 10, e73218.

Huez, I., Créancier, L., Audigier, S., Gensac, M. C., Prats, A. C., and Prats, H. (1998). Two independent internal ribosome entry sites are involved in translation initiation of vascular endothelial growth factor mRNA. *Molecular and cellular biology*, 18(11), 6178–6190.

Huntzinger, E., Kuzuoglu-Öztürk, D., Braun, J. E., Eulalio, A., Wohlbold, L., and Izaurralde, E. (2013). The interactions of GW182 proteins with PABP and deadenylases are required for both translational repression and degradation of miRNA targets. *Nucleic acids research*, 41(2), 978–994.

Iliopoulos, D., Hirsch, H. A., and Struhl, K. (2009). An epigenetic switch involving NF-kappaB, Lin28, Let-7 MicroRNA, and IL6 links inflammation to cell transformation. *Cell*, 139(4), 693–706.

Imataka, H., Gradi, A., and Sonenberg, N. (1998). A newly identified N-terminal

amino acid sequence of human eIF4G binds poly(A)-binding protein and functions in poly(A)-dependent translation. *The EMBO journal*, 17(24), 7480–7489.

Imataka, H., and Sonenberg, N. (1997). Human eukaryotic translation initiation factor 4G (eIF4G) possesses two separate and independent binding sites for eIF4A. *Molecular and cellular biology*, 17(12), 6940–6947.

Inagaki, Y., and Ford Doolittle, W. (2000). Evolution of the eukaryotic translation termination system: origins of release factors. *Molecular biology and evolution*, 17(6), 882–889.

Ingolia, N. T., Ghaemmaghami, S., Newman, J. R., and Weissman, J. S. (2009). Genome-wide analysis in vivo of translation with nucleotide resolution using ribosome profiling. *Science*, 324(5924), 218–223.

Inoki, K., Li, Y., Zhu, T., Wu, J., and Guan, K. L. (2002). TSC2 is phosphorylated and inhibited by Akt and suppresses mTOR signalling. *Nature cell biology*, 4(9), 648–657.

Iurlaro, R., Püschel, F., León-Annicchiarico, C. L., O'Connor, H., Martin, S. J., Palou-Gramón, D., Lucendo, E., and Muñoz-Pinedo, C. (2017). Glucose Deprivation Induces ATF4-Mediated Apoptosis through TRAIL Death Receptors. *Molecular and cellular biology*, 37(10), e00479-16.

Jääskeläinen, A., Roininen, N., Karihtala, P., and Jukkola, A. (2020). High Parity Predicts Poor Outcomes in Patients With Luminal B-Like (HER2 Negative) Early Breast Cancer: A Prospective Finnish Single-Center Study. *Frontiers in oncology*, 10, 1470.

Jadwin, J. A., Curran, T. G., Lafontaine, A. T., White, F. M., and Mayer, B. J. (2018). Src homology 2 domains enhance tyrosine phosphorylation *in vivo* by protecting binding sites in their target proteins from dephosphorylation. *The Journal of biological chemistry*, 293(2), 623–637.

Janapala, Y., Preiss, T., and Shirokikh, N. E. (2019). Control of Translation at the Initiation Phase During Glucose Starvation in Yeast. *International journal of molecular sciences*, 20(16), 4043.

Jang, S. K., Kräusslich, H. G., Nicklin, M. J., Duke, G. M., Palmenberg, A. C., and Wimmer, E. (1988). A segment of the 5' nontranslated region of encephalomyocarditis virus RNA directs internal entry of ribosomes during in vitro translation. *Journal of virology*, 62(8), 2636–2643.

Jarman, E. J., Ward, C., Turnbull, A.K., Martinez-Perez, C., Meehan, J., Xintaropoulou, C., Sims, A.H., and Langdon, S.P. (2019). HER2 regulates HIF-2α and drives an increased hypoxic response in breast cancer, *Breast Cancer Research*, 10.1186/S13058-019-1097-0.

Jeon, M., You, D., Bae, S. Y., Kim, S. W., Nam, S. J., Kim, H. H., Kim, S., and Lee, J. E. (2016). Dimerization of EGFR and HER2 induces breast cancer cell motility through STAT1-dependent ACTA2 induction. *Oncotarget*, 8(31), 50570–50581.

Ji, B., Harris, B. R., Liu, Y., Deng, Y., Gradilone, S. A., Cleary, M. P., Liu, J., and Yang, D. Q. (2017). Targeting IRES-Mediated p53 Synthesis for Cancer Diagnosis and Therapeutics. *International journal of molecular sciences*, 18(1), 93.

Jimenez, C., Hernandez, C., Pimentel, B., and Carrera, A. C. (2002). The p85 regulatory subunit controls sequential activation of phosphoinositide 3-kinase by Tyr kinases and Ras. *The Journal of biological chemistry*, 277(44), 41556–41562.

Jung, S., Wang, M., Anderson, K., Baglietto, L., Bergkvist, L., Bernstein, L., van den Brandt, P. A., Brinton, L., Buring, J. E., Eliassen, A. H., Falk, R., Gapstur, S. M., Giles, G. G., Goodman, G., Hoffman-Bolton, J., Horn-Ross, P. L., Inoue, M., Kolonel, L. N., Krogh, V., Lof, M., Mass, P., Miller, A.B., Neuhouser, M.L., Park, Y., Robien, K., Rohan, T.E., Scarmo, S., Schouten, C.L., Sieri, S., Stevens, V.L., Tsugane, S., Visvanathan, K., Wilkens, L.K., Wolk, A., Weiderpass, E., Willett, W.C., Zeleniuch-Jacquotte, A., Zhang, S.M., Zhang, X., and Zieger, R.G and Smith-Warner, S. A. (2016). Alcohol consumption and breast cancer risk by estrogen receptor status: in a pooled analysis of 20 studies. *International journal of epidemiology*, 45(3), 916–928.

Junttila, T. T., Sundvall, M., Lundin, M., Lundin, J., Tanner, M., Härkönen, P., Joensuu, H., Isola, J., and Elenius, K. (2005). Cleavable ErbB4 isoform in estrogen receptor-regulated growth of breast cancer cells. *Cancer research*, 65(4), 1384–1393.

Kahvejian, A., Svitkin, Y. V., Sukarieh, R., M'Boutchou, M. N., and Sonenberg, N. (2005). Mammalian poly(A)-binding protein is a eukaryotic translation initiation factor, which acts via multiple mechanisms. *Genes & development*, 19(1), 104–113.

Kamenska, A., Simpson, C., Vindry, C., Broomhead, H., Bénard, M., Ernoult-Lange, M., Lee, B. P., Harries, L. W., Weil, D., and Standart, N. (2016). The DDX6-4E-T interaction mediates translational repression and P-body assembly. *Nucleic acids research*, 44(13), 6318–6334.

Kamioka, Y., Yasuda, S., Fujita, Y., Aoki, K., and Matsuda, M. (2010). Multiple decisive phosphorylation sites for the negative feedback regulation of SOS1 via ERK. *The Journal of biological chemistry*, 285(43), 33540–33548.

Kang, S. T., Wang, H. C., Yang, Y. T., Kou, G. H., and Lo, C. F. (2013). The

DNA virus white spot syndrome virus uses an internal ribosome entry site for translation of the highly expressed nonstructural protein ICP35. *Journal of virology*, 87(24), 13263–13278.

Kankia, I. H., Paramasivan, P., Elcombe, M., Langdon, S. P., and Deeni, Y. Y. (2021). Nuclear factor erythroid 2-related factor 2 modulates HER4 receptor in ovarian cancer cells to influence their sensitivity to tyrosine kinase inhibitors. *Exploration of targeted anti-tumor therapy*, 2(2), 187–203.

Karollus, A., Avsec, Ž., and Gagneur, J. (2021). Predicting mean ribosome load for 5' UTR of any length using deep learning. *PLoS computational biology*, 17(5), e1008982.

Kawahara, R., and Simizu, S. (2022). ErbB4-mediated regulation of vasculogenic mimicry capability in breast cancer cells. *Cancer science*, 113(3), 950–959.

Keam, B., Im, S. A., Lee, K. H., Han, S. W., Oh, D. Y., Kim, J. H., Lee, S. H., Han, W., Kim, D. W., Kim, T. Y., Park, I. A., Noh, D. Y., Heo, D. S., and Bang, Y. J. (2011). Ki-67 can be used for further classification of triple negative breast cancer into two subtypes with different response and prognosis. *Breast cancer research: BCR*, 13(2), R22.

Khajah, M. A., Khushaish, S., and Luqmani, Y. A. (2022). Glucose deprivation reduces proliferation and motility, and enhances the anti-proliferative effects of paclitaxel and doxorubicin in breast cell lines in vitro. *PloS one*, 17(8), e0272449.

Khalil, H. S., Langdon, S. P., Goltsov, A., Soininen, T., Harrison, D. J., Bown, J., and Deeni, Y. Y. (2016). A novel mechanism of action of HER2 targeted immunotherapy is explained by inhibition of NRF2 function in ovarian cancer cells. *Oncotarget*, 7(46), 75874–75901.

Khan, D., Katoch, A., Das, A., Sharathchandra, A., Lal, R., Roy, P., Das, S., Chattopadhyay, S., and Das, S. (2015). Reversible induction of translational isoforms of p53 in glucose deprivation. *Cell death and differentiation*, 22(7), 1203–1218.

Kim, S. J., Glick, A., Sporn, M. B., and Roberts, A. B. (1989). Characterization of the promoter region of the human transforming growth factor-beta 1 gene. *The Journal of biological chemistry*, 264(1), 402–408.

Kim, Y. K., Hahm, B., and Jang, S. K. (2000). Polypyrimidine tract-binding protein inhibits translation of bip mRNA. *Journal of molecular biology*, 304(2), 119–133.

Kim, J. W., Zeller, K. I., Wang, Y., Jegga, A. G., Aronow, B. J., O'Donnell, K. A., and Dang, C. V. (2004). Evaluation of myc E-box phylogenetic footprints in

glycolytic genes by chromatin immunoprecipitation assays. *Molecular and cellular biology*, 24(13), 5923–5936.

Kloosterman, W. P., Wienholds, E., Ketting, R. F., and Plasterk, R. H. (2004). Substrate requirements for let-7 function in the developing zebrafish embryo. *Nucleic acids research*, 32(21), 6284–6291.

Komurasaki, T., Toyoda, H., Uchida, D., and Morimoto, S. (1997). Epiregulin binds to epidermal growth factor receptor and ErbB-4 and induces tyrosine phosphorylation of epidermal growth factor receptor, ErbB-2, ErbB-3 and ErbB-4. *Oncogene*, 15(23), 2841–2848.

Komuro, A., Nagai, M., Navin, N. E., and Sudol, M. (2003). WW domain-containing protein YAP associates with ErbB-4 and acts as a co-transcriptional activator for the carboxyl-terminal fragment of ErbB-4 that translocates to the nucleus. *The Journal of biological chemistry*, 278(35), 33334–33341.

Konecny, G. E., Meng, Y. G., Untch, M., Wang, H. J., Bauerfeind, I., Epstein, M., Stieber, P., Vernes, J. M., Gutierrez, J., Hong, K., Beryt, M., Hepp, H., Slamon, D. J., and Pegram, M. D. (2004). Association between HER-2/neu and vascular endothelial growth factor expression predicts clinical outcome in primary breast cancer patients. *Clinical cancer research: an official journal of the American Association for Cancer Research*, 10(5), 1706–1716.

Korotkov, K. V., Novoselov, S. V., Hatfield, D. L., and Gladyshev, V. N. (2002). Mammalian selenoprotein in which selenocysteine (Sec) incorporation is supported by a new form of Sec insertion sequence element. *Molecular and cellular biology*, 22(5), 1402–1411.

Kotagama, K., Babb, C.S., Wolter, J.M., Murphy, R.P., and Mangone, M. (2015). A human 3'UTR clone collection to study post-transcriptional gene regulation', *BMC Genomics*, 16, 1036.

Kovacs, E., Das, R., Wang, Q., Collier, T. S., Cantor, A., Huang, Y., Wong, K., Mirza, A., Barros, T., Grob, P., Jura, N., Bose, R., and Kuriyan, J. (2015). Analysis of the Role of the C-Terminal Tail in the Regulation of the Epidermal Growth Factor Receptor. *Molecular and cellular biology*, 35(17), 3083–3102.

Kozak, M. (1986). Point mutations define a sequence flanking the AUG initiator codon that modulates translation by eukaryotic ribosomes. *Cell*, 44(2), 283–292.

Kozak, M. (2001). New ways of initiating translation in eukaryotes? *Molecular and cellular biology*, 21(6), 1899–1907.

Kozak, M. (2005). A second look at cellular mRNA sequences said to function as internal ribosome entry sites. *Nucleic acids research*, 33(20), 6593–6602.

Krichevsky, A. M., Metzer, E., and Rosen, H. (1999). Translational control of

specific genes during differentiation of HL-60 cells. *The Journal of biological chemistry*, 274(20), 14295–14305.

Krishna, S. S., Majumdar, I., and Grishin, N. V. (2003). Structural classification of zinc fingers: survey and summary. *Nucleic acids research*, 31(2), 532–550.

Laforest, S., Pelletier, M., Denver, N., Poirier, B., Nguyen, S., Walker, B. R., Durocher, F., Homer, N. Z. M., Diorio, C., Andrew, R., and Tchernof, A. (2020). Estrogens and Glucocorticoids in Mammary Adipose Tissue: Relationships with Body Mass Index and Breast Cancer Features. *The Journal of clinical endocrinology and metabolism*, 105(4), e1504–e1516.

Lai, C., Jiang, X., and Li, X. (2006). Development of luciferase reporter-based cell assays. *Assay and drug development technologies*, 4(3), 307–315.

Lang, K. J., Kappel, A., and Goodall, G. J. (2002). Hypoxia-inducible factor-1alpha mRNA contains an internal ribosome entry site that allows efficient translation during normoxia and hypoxia. *Molecular biology of the cell*, 13(5), 1792–1801.

Lanotte, R., Garambois, V., Gaborit, N., Larbouret, C., Musnier, A., Martineau, P., Pèlegrin, A., and Chardès, T. (2020). Biasing human epidermal growth factor receptor 4 (HER4) tyrosine kinase signaling with antibodies: Induction of cell death by antibody-dependent HER4 intracellular domain trafficking. *Cancer science*, 111(7), 2508–2525.

Lattrich, C., Juhasz-Boess, I., Ortmann, O., and Treeck, O. (2008). Detection of an elevated HER2 expression in MCF-7 breast cancer cells overexpressing estrogen receptor beta1. *Oncology reports*, 19(3), 811–817.

Laughner, E., Taghavi, P., Chiles, K., Mahon, P. C., and Semenza, G. L. (2001). HER2 (neu) signaling increases the rate of hypoxia-inducible factor 1alpha (HIF-1alpha) synthesis: novel mechanism for HIF-1-mediated vascular endothelial growth factor expression. *Molecular and cellular biology*, 21(12), 3995–4004.

Le Quesne, J. P., Stoneley, M., Fraser, G. A., and Willis, A. E. (2001). Derivation of a structural model for the c-myc IRES. *Journal of molecular biology*, 310(1), 111–126.

Lee, W., Mitchell, P., and Tjian, R. (1987). Purified transcription factor AP-1 interacts with TPA-inducible enhancer elements. *Cell*, 49(6), 741–752.

Lee, J. C., Laydon, J. T., McDonnell, P. C., Gallagher, T. F., Kumar, S., Green, D., McNulty, D., Blumenthal, M. J., Heys, J. R., Landvatter, S. W., Strickler, J. E., McLaughlin, M. M., Siemens, I. R., Fisher, S. M., Livi, G. P., White, J. R., Adams, J. L., and Young, P. R. (1994). A protein kinase involved in the regulation of inflammatory cytokine biosynthesis. *Nature*, 372(6508), 739–746.

Lee, J. H., Pestova, T. V., Shin, B. S., Cao, C., Choi, S. K., and Dever, T. E. (2002). Initiation factor eIF5B catalyzes second GTP-dependent step in eukaryotic translation initiation. *Proceedings of the National Academy of Sciences of the United States of America*, 99(26), 16689–16694.

Lee, Y., Kim, M., Han, J., Yeom, K. H., Lee, S., Baek, S. H., and Kim, V. N. (2004). MicroRNA genes are transcribed by RNA polymerase II. *The EMBO journal*, 23(20), 4051–4060.

Lee, N. Y., Hazlett, T. L., and Koland, J. G. (2006). Structure and dynamics of the epidermal growth factor receptor C-terminal phosphorylation domain. *Protein science : a publication of the Protein Society*, 15(5), 1142–1152.

Lee, S. W., and Commisso, C. (2020). Metabolic regulation of EGFR effector and feedback signaling in pancreatic cancer cells requires K-Ras. *Biochemical and biophysical research communications*, 533(3), 424–428.

Lemmon, M. A., Ladbury, J. E., Mandiyan, V., Zhou, M., and Schlessinger, J. (1994). Independent binding of peptide ligands to the SH2 and SH3 domains of Grb2. *The Journal of biological chemistry*, 269(50), 31653–31658.

Leonetti, M. D., Sekine, S., Kamiyama, D., Weissman, J. S., and Huang, B. (2016). A scalable strategy for high-throughput GFP tagging of endogenous human proteins. *Proceedings of the National Academy of Sciences of the United States of America*, 113(25), E3501–E3508.

Leprivier, G., Remke, M., Rotblat, B., Dubuc, A., Mateo, A. R., Kool, M., Agnihotri, S., El-Naggar, A., Yu, B., Somasekharan, S. P., Faubert, B., Bridon, G., Tognon, C. E., Mathers, J., Thomas, R., Li, A., Barokas, A., Kwok, B., Bowden, M., Smith, S., Wu, X., Korshunov, A., Hielscher, T., Northcott, P. A., Galpin, J. D., Ahern, C. A., Wang, Y., McCabe, M. G., Collins, V. P., Jones, R. G, Pollak, M., Delattre, O., Gleave, M. E., Jan, E., Pfister, S. M., Proud, C. G., Derry, W. B., Taylor, M. D., and Sorensen, P. H. (2013). The eEF2 kinase confers resistance to nutrient deprivation by blocking translation elongation. *Cell*, 153(5), 1064–1079.

Lewis Phillips, G. D., Li G., Dugger, D. L., Crocker, L. M., Parsons, K. L., Mai, E., Blättler, W. A., Lambert, J. M., Chari, R.V., Lutz, R. J., Wong, W. L., Jacobson, F. S., Koeppen, H., Schwall, R. H., Kenkare-Mitra, S. R., Spencer, S. D., and Sliwkowski, M. X. (2008). Targeting HER2-positive breast cancer with trastuzumab-DM1, an antibody-cytotoxic drug conjugate. *Cancer Res*. 68(22):9280-90.

Lewis, S. M., Cerquozzi, S., Graber, T. E., Ungureanu, N. H., Andrews, M., and Holcik, M. (2008). The eIF4G homolog DAP5/p97 supports the translation of select mRNAs during endoplasmic reticulum stress. *Nucleic acids research*,

36(1), 168–178.

Li, Y., Li, Y., Zhang, J., Zheng, C., Zhu, H., Yu, H., and Fan, L. (2016). Circulating Insulin-Like Growth Factor-1 Level and Ovarian Cancer Risk. *Cellular physiology and biochemistry: international journal of experimental cellular physiology, biochemistry, and pharmacology*, 38(2), 589–597.

Li, J., Xiao, Q., Bao, Y., Wang, W., Goh, J., Wang, P., and Yu, Q. (2019). HER2-L755S mutation induces hyperactive MAPK and PI3K-mTOR signaling, leading to resistance to HER2 tyrosine kinase inhibitor treatment. *Cell cycle* 18(13), 1513–1522.

Liang, X. H., Sun, H., Nichols, J. G., and Crooke, S. T. (2017). RNase H1-Dependent Antisense Oligonucleotides Are Robustly Active in Directing RNA Cleavage in Both the Cytoplasm and the Nucleus. *Molecular therapy: the journal of the American Society of Gene Therapy*, 25(9), 2075–2092.

Liebermeister, W., Noor, E., Flamholz, A., Davidi, D., Bernhardt, J., and Milo, R. (2014). Visual account of protein investment in cellular functions. *Proceedings of the National Academy of Sciences of the United States of America*, 111(23), 8488–8493.

Lin, J. Y., Brewer, G., and Li, M. L. (2015). HuR and Ago2 Bind the Internal Ribosome Entry Site of Enterovirus 71 and Promote Virus Translation and Replication. *PloS one*, 10(10), e0140291.

Lind, C. and Åqvist, J. (2016). Principles of start codon recognition in eukaryotic translation initiation, *Nucleic Acids Research*, 44(17).

Liu, Y., Tamimi, R. M., Collins, L. C., Schnitt, S. J., Gilmore, H. L., Connolly, J. L., and Colditz, G. A. (2011). The association between vascular endothelial growth factor expression in invasive breast cancer and survival varies with intrinsic subtypes and use of adjuvant systemic therapy: results from the Nurses' Health Study. *Breast cancer research and treatment*, 129(1), 175–184.

Liu, P., Cleveland, T. E., 4th, Bouyain, S., Byrne, P. O., Longo, P. A., and Leahy, D. J. (2012). A single ligand is sufficient to activate EGFR dimers. *Proceedings of the National Academy of Sciences of the United States of America*, 109(27), 10861–10866.

Liu, C. Y., Hung, M. H., Wang, D. S., Chu, P. Y., Su, J. C., Teng, T. H., Huang, C. T., Chao, T. T., Wang, C. Y., Shiau, C. W., Tseng, L. M., and Chen, K. F. (2014). Tamoxifen induces apoptosis through cancerous inhibitor of protein phosphatase 2A-dependent phospho-Akt inactivation in estrogen receptor-negative human breast cancer cells. *Breast cancer research: BCR*, 16(5), 431.

Liu, W., Li, C., Shan, J., Wang, Y., and Chen, G. (2021a). Insights into the aggregation mechanism of RNA recognition motif domains in TDP-43: a

theoretical exploration. *Royal Society open science*, 8(8), 210160.

Liu, Y., Ge, X., Pang, J., Zhang, Y., Zhang, H., Wu, H., Fan, F., and Liu, H. (2021b). Restricting Glutamine Uptake Enhances NSCLC Sensitivity to Third-Generation EGFR-TKI Almonertinib. *Frontiers in pharmacology*, 12, 671328.

Lohse, I., Reilly, P., and Zaugg, K. (2011). The CPT1C 5'UTR contains a repressing upstream open reading frame that is regulated by cellular energy availability and AMPK. *PloS one*, 6(9), e21486.

Lowman, X. H., Hanse, E. A., Yang, Y., Ishak Gabra, M. B., Tran, T. Q., Li, H., and Kong, M. (2019). p53 Promotes Cancer Cell Adaptation to Glutamine Deprivation by Upregulating Slc7a3 to Increase Arginine Uptake. *Cell reports*, 26(11), 3051–3060.e4.

Lu, L., Han, A. P., and Chen, J. J. (2001). Translation initiation control by heme-regulated eukaryotic initiation factor 2alpha kinase in erythroid cells under cytoplasmic stresses. *Molecular and cellular biology*, 21(23), 7971–7980.

Ma, J., Haldar, S., Khan, M. A., Sharma, S. D., Merrick, W. C., Theil, E. C., and Goss, D. J. (2012). Fe2+ binds iron responsive element-RNA, selectively changing protein-binding affinities and regulating mRNA repression and activation. *Proceedings of the National Academy of Sciences of the United States of America*, 109(22), 8417–8422.

Macejak, D. G., and Sarnow, P. (1991). Internal initiation of translation mediated by the 5' leader of a cellular mRNA. *Nature*, 353(6339), 90–94.

Madson, J. G., Lynch, D. T., Svoboda, J., Ophardt, R., Yanagida, J., Putta, S. K., Bowles, A., Trempus, C. S., Tennant, R. W., & Hansen, L. A. (2009). Erbb2 suppresses DNA damage-induced checkpoint activation and UV-induced mouse skin tumorigenesis. *The American journal of pathology*, 174(6), 2357–2366.

Mahalingaiah, P. K., and Singh, K. P. (2014). Chronic oxidative stress increases growth and tumorigenic potential of MCF-7 breast cancer cells. *PloS one*, 9(1), e87371.

Mailloux, R. J., Singh, R., Brewer, G., Auger, C., Lemire, J., and Appanna, V. D. (2009). Alpha-ketoglutarate dehydrogenase and glutamate dehydrogenase work in tandem to modulate the antioxidant alpha-ketoglutarate during oxidative stress in Pseudomonas fluorescens. *Journal of bacteriology*, 191(12), 3804–3810.

Malygin, A. A., Kossinova, O. A., Shatsky, I. N., and Karpova, G. G. (2013). HCV IRES interacts with the 18S rRNA to activate the 40S ribosome for subsequent steps of translation initiation. *Nucleic acids research*, 41(18), 8706–8714.

Marcotrigiano, J., Gingras, A. C., Sonenberg, N., and Burley, S. K. (1997). Cocrystal structure of the messenger RNA 5' cap-binding protein (eIF4E) bound to 7-methyl-GDP. *Cell*, 89(6), 951–961.

Maria, A. M., El-Shebiney, M., El-Saka, A. M., and Zamzam, Y. (2018). Expression of truncated HER2 and its prognostic value in HER2-positive breast cancer patients. *Journal of the Egyptian National Cancer Institute*, 30(2), 49–55.

Martin-Fernandez, M. L., Clarke, D. T., Roberts, S. K., Zanetti-Domingues, L. C., and Gervasio, F. L. (2019). Structure and Dynamics of the EGF Receptor as Revealed by Experiments and Simulations and Its Relevance to Non-Small Cell Lung Cancer. *Cells*, 8(4), 316.

Martín-Nieto, J., and Villalobo, A. (1998). The human epidermal growth factor receptor contains a juxtamembrane calmodulin-binding site. *Biochemistry*, 37 (1),227-236.

Martín-Pérez, R., Palacios, C., Yerbes, R., Cano-González, A., Iglesias-Serret, D., Gil, J., Reginato, M. J., and López-Rivas, A. (2014). Activated ERBB2/HER2 licenses sensitivity to apoptosis upon endoplasmic reticulum stress through a PERK-dependent pathway. *Cancer research*, 74(6), 1766–1777.

Martin, C. S., Wight, P. A., Dobretsova, A., and Bronstein, I. (1996). Dual luminescence-based reporter gene assay for luciferase and beta-galactosidase. *BioTechniques*, 21(3), 520–524.

Martin, E. T., Blatt, P., Nguyen, E., Lahr, R., Selvam, S., Yoon, H. A. M., Pocchiari, T., Emtenani, S., Siekhaus, D. E., Berman, A., Fuchs, G., and Rangan, P. (2022). A translation control module coordinates germline stem cell differentiation with ribosome biogenesis during Drosophila oogenesis. *Developmental cell*, 57(7), 883–900.e10.

Martínez, A., Sesé, M., Losa, J. H., Robichaud, N., Sonenberg, N., Aasen, T., and Ramón Y Cajal, S. (2015). Phosphorylation of eIF4E Confers Resistance to Cellular Stress and DNA-Damaging Agents through an Interaction with 4E-T: A Rationale for Novel Therapeutic Approaches. *PloS one*, 10(4), e0123352.

Martinez-Outschoorn, U. E., Goldberg, A., Lin, Z., Ko, Y. H., Flomenberg, N., Wang, C., Pavlides, S., Pestell, R. G., Howell, A., Sotgia, F., and Lisanti, M. P. (2011). Anti-estrogen resistance in breast cancer is induced by the tumor microenvironment and can be overcome by inhibiting mitochondrial function in epithelial cancer cells. *Cancer biology & therapy*, 12(10), 924–938.

Mazloomian, A., Araki, S., Ohori, M., El-Naggar, A. M., Yap, D., Bashashati, A., Nakao, S., Sorensen, P. H., Nakanishi, A., Shah, S., and Aparicio, S. (2019). Pharmacological systems analysis defines EIF4A3 functions in cell-cycle and

RNA stress granule formation. *Communications biology*, 2, 165.

Mazor, K.M., Dong, L., Mao, Y, Swanda, R.V., Qian, S.B., and Stipanuk, M. H. (2018). Effects of single amino acid deficiency on mRNA translation are markedly different for methionine versus leucine, *Scientific Reports.* 8, 8076.

McCaughan, K. K., Brown, C. M., Dalphin, M. E., Berry, M. J., and Tate, W. P. (1995). Translational termination efficiency in mammals is influenced by the base following the stop codon. *Proceedings of the National Academy of Sciences of the United States of America*, 92(12), 5431–5435.

McFarland, M. R., Keller, C. D., Childers, B. M., Adeniyi, S. A., Corrigall, H., Raguin, A., Romano, M. C., and Stansfield, I. (2020). The molecular aetiology of tRNA synthetase depletion: induction of a GCN4 amino acid starvation response despite homeostatic maintenance of charged tRNA levels. *Nucleic acids research*, 48(6), 3071–3088.

McGillivray, P., Ault, R., Pawashe, M., Kitchen, R., Balasubramanian, S., and Gerstein, M. (2018). A comprehensive catalog of predicted functional upstream open reading frames in humans. *Nucleic acids research*, 46(7), 3326–3338.

Mehta, A., Trotta, C. R., and Peltz, S. W. (2006). Derepression of the Her-2 uORF is mediated by a novel post-transcriptional control mechanism in cancer cells. *Genes & development*, 20(8), 939–953.

Milholland, B., Auton, A., Suh, Y., and Vijg, J. (2015). Age-related somatic mutations in the cancer genome. *Oncotarget*, 6(28), 24627–24635.

Miller, P. F., and Hinnebusch, A. G. (1989). Sequences that surround the stop codons of upstream open reading frames in GCN4 mRNA determine their distinct functions in translational control. *Genes & development*, 3(8), 1217–1225.

Miller, D. L., Dibbens, J. A., Damert, A., Risau, W., Vadas, M. A., and Goodall, G. J. (1998). The vascular endothelial growth factor mRNA contains an internal ribosome entry site. *FEBS letters*, 434(3), 417–420.

Mitchell, S. A., Spriggs, K. A., Coldwell, M. J., Jackson, R. J., and Willis, A. E. (2003). The Apaf-1 internal ribosome entry segment attains the correct structural conformation for function via interactions with PTB and unr. *Molecular cell*, 11(3), 757–771.

Mittendorf, E. A., Lu, B., Melisko, M., Price Hiller, J., Bondarenko, I., Brunt, A. M., Sergii, G., Petrakova, K., and Peoples, G. E. (2019). Efficacy and Safety Analysis of Nelipepimut-S Vaccine to Prevent Breast Cancer Recurrence: A Randomized, Multicenter, Phase III Clinical Trial. *Clinical cancer research: an official journal of the American Association for Cancer Research*, 25(14), 4248–4254.

Modi, S., Saura, C., Yamashita, T., Park, Y. H., Kim, S. B., Tamura, K., Andre, F., Iwata, H., Ito, Y., Tsurutani, J., Sohn, J., Denduluri, N., Perrin, C., Aogi, K., Tokunaga, E., Im, S. A., Lee, K. S., Hurvitz, S. A., Cortes, J., Lee, C., Chen, S., Zhang, L., Shahidi, J., Yver, A., and Krop, I. (2020). Trastuzumab Deruxtecan in Previously Treated HER2-Positive Breast Cancer. *The New England journal of medicine*, 382(7), 610–621.

Monje, P., Hernández-Losa, J., Lyons, R. J., Castellone, M. D., and Gutkind, J. S. (2005). Regulation of the transcriptional activity of c-Fos by ERK. A novel role for the prolyl isomerase PIN1. *The Journal of biological chemistry*, 280(42), 35081–35084.

Monsey, J., Shen, W., Schlesinger, P., and Bose, R. (2010). Her4 and Her2/neu tyrosine kinase domains dimerize and activate in a reconstituted in vitro system. *The Journal of biological chemistry*, 285(10), 7035–7044.

Moro, S. G., Hermans, C., Ruiz-Orera, J., and Albà, M. M. (2021). Impact of uORFs in mediating regulation of translation in stress conditions. *BMC molecular and cell biology*, 22(1), 29.

Morrison, M. M., Hutchinson, K., Williams, M. M., Stanford, J. C., Balko, J. M., Young, C., Kuba, M. G., Sánchez, V., Williams, A. J., Hicks, D. J., Arteaga, C. L., Prat, A., Perou, C. M., Earp, H. S., Massarweh, S., and Cook, R. S. (2013). ErbB3 downregulation enhances luminal breast tumor response to antiestrogens. *The Journal of clinical investigation*, 123(10), 4329–4343.

Moteki, S., and Price, D. (2002). Functional coupling of capping and transcription of mRNA. *Molecular cell*, *10*(3), 599–609.

Muraoka-Cook, R. S., Sandahl, M. A., Strunk, K. E., Miraglia, L. C., Husted, C., Hunter, D. M., Elenius, K., Chodosh, L. A., and Earp, H. S., 3rd. (2009). ErbB4 splice variants Cyt1 and Cyt2 differ by 16 amino acids and exert opposing effects on the mammary epithelium in vivo. *Molecular and cellular biology*, 29(18), 4935–4948.

Murray, J., Savva, C. G., Shin, B. S., Dever, T. E., Ramakrishnan, V., and Fernández, I. S. (2016). Structural characterization of ribosome recruitment and translocation by type IV IRES. *eLife*, 5, e13567.

Mohd Nafi, S. N., Generali, D., Kramer-Marek, G., Gijsen, M., Strina, C., Cappelletti, M., Andreis, D., Haider, S., Li, J. L., Bridges, E., Capala, J., Ioannis, R., Harris, A. L., and Kong, A. (2014). Nuclear HER4 mediates acquired resistance to trastuzumab and is associated with poor outcome in HER2 positive breast cancer. *Oncotarget*, 5(15), 5934–5949.

Nagelreiter, F., Coats, M. T., Klanert, G., Gludovacz, E., Borth, N., Grillari, J., and Schosserer, M. (2018). OPP Labeling Enables Total Protein Synthesis

Quantification in CHO Production Cell Lines at the Single-Cell Level. *Biotechnology journal*, 13(4), e1700492.

Nair, R., Roden, D. L., Teo, W. S., McFarland, A., Junankar, S., Ye, S., Nguyen, A., Yang, J., Nikolic, I., Hui, M., Morey, A., Shah, J., Pfefferle, A. D., Usary, J., Selinger, C., Baker, L. A., Armstrong, N., Cowley, M. J., Naylor, M. J., Ormandy, C. J., Lakhani, S. R., Herschkowitz, J. I., Perou, C. M., Kaplan, W., O'Toole, S. A., and Swarbrick, A. (2014). c-Myc and Her2 cooperate to drive a stem-like phenotype with poor prognosis in breast cancer. *Oncogene*, 33(30), 3992–4002.

Nanayakkara, A. K., Follit, C. A., Chen, G., Williams, N. S., Vogel, P. D., and Wise, J. G. (2018). Targeted inhibitors of P-glycoprotein increase chemotherapeutic-induced mortality of multidrug resistant tumor cells. *Scientific reports*, 8(1), 967.

Nanbru, C., Lafon, I., Audigier, S., Vagner, S., Huez, G., and Prats, A.C. (1997). 'Alternative translation of the proto-oncogene c-myc by an internal ribosome entry site.', *The Journal of biological chemistry*, 272(51)

Naresh, A., Long, W., Vidal, G. A., Wimley, W. C., Marrero, L., Sartor, C. I., Tovey, S., Cooke, T. G., Bartlett, J. M., and Jones, F. E. (2006). The ERBB4/HER4 intracellular domain 4ICD is a BH3-only protein promoting apoptosis of breast cancer cells. *Cancer research*, 66(12), 6412–6420.

Nassar, L. R., Barber, G. P., Benet-Pagès, A., Casper, J., Clawson, H., Diekhans, M., Fischer, C., Gonzalez, J. N., Hinrichs, A. S., Lee, B. T., Lee, C. M., Muthuraman, P., Nguy, B., Pereira, T., Nejad, P., Perez, G., Raney, B. J., Schmelter, D., Speir, M. L., Wick, B. D., Zweig, A. S., Haussler D, Kuhn, R. M., Haeussler, M., and Kent, W. J. (2023). The UCSC Genome Browser database: 2023 update. *Nucleic acids research*, 51(D1), D1188–D1195.

Navaraj, A., Mori, T., and El-Deiry, W. S. (2005). Cooperation between BRCA1 and p53 in repair of cyclobutane pyrimidine dimers. *Cancer biology & therapy*, 4(12), 1409–1414.

Nelde, A., Flötotto, L., Jürgens, L., Szymik, L., Hubert, E., Bauer, J., Schliemann, C., Kessler, T., Lenz, G., Rammensee, H. G., Walz, J. S., and Wethmar, K. (2022). Upstream open reading frames regulate translation of cancer-associated transcripts and encode HLA-presented immunogenic tumor antigens. *Cellular and molecular life sciences: CMLS*, 79(3), 171.

Nowacka, M., Boccaletto, P., Jankowska, E., Jarzynka, T., Bujnicki, J. M., and Dunin-Horkawicz, S. (2019). RRMdb-an evolutionary-oriented database of RNA recognition motif sequences. *Database: the journal of biological databases and curation*, 10.1093.

Nyikó, T., Auber, A., Szabadkai, L., Benkovics, A., Auth, M., Mérai, Z., Kerényi, Z., Dinnyés, A., Nagy, F., and Silhavy, D. (2017). Expression of the eRF1 translation termination factor is controlled by an autoregulatory circuit involving readthrough and nonsense-mediated decay in plants. *Nucleic acids research*, 45(7), 4174–4188.

Ogden, A., Bhattarai, S., Sahoo, B., Mongan, N. P., Alsaleem, M., Green, A. R., Aleskandarany, M., Ellis, I. O., Pattni, S., Li, X. B., Moreno, C. S., Krishnamurti, U., Janssen, E. A., Jonsdottir, K., Rakha, E., Rida, P., and Aneja, R. (2020). Combined HER3-EGFR score in triple-negative breast cancer provides prognostic and predictive significance superior to individual biomarkers. *Scientific reports*, 10(1), 3009.

Ogiso, H., Ishitani, R., Nureki, O., Fukai, S., Yamanaka, M., Kim, J. H., Saito, K., Sakamoto, A., Inoue, M., Shirouzu, M., and Yokoyama, S. (2002). Crystal structure of the complex of human epidermal growth factor and receptor extracellular domains. *Cell*, 110(6), 775–787.

Okamura, K., Ishizuka, A., Siomi, H., and Siomi, M. C. (2004). Distinct roles for Argonaute proteins in small RNA-directed RNA cleavage pathways. *Genes & development*, 18(14), 1655–1666.

Oltean, S., and Banerjee, R. (2005). A B12-responsive internal ribosome entry site (IRES) element in human methionine synthase. *The Journal of biological chemistry*, 280(38), 32662–32668.

Ørom, U. A., Nielsen, F. C., and Lund, A. H. (2008). MicroRNA-10a binds the 5'UTR of ribosomal protein mRNAs and enhances their translation. *Molecular cell*, 30(4), 460–471.

Ovchinnikov, L. P., Motuz, L. P., Natapov, P. G., Averbuch, L. J., Wettenhall, R. E., Szyszka, R., Kramer, G., and Hardesty, B. (1990). Three phosphorylation sites in elongation factor 2. *FEBS letters*, 275(1-2), 209–212.

Paatero, I., Jokilammi, A., Heikkinen, P. T., Iljin, K., Kallioniemi, O. P., Jones, F. E., Jaakkola, P. M., and Elenius, K. (2012). Interaction with ErbB4 promotes hypoxia-inducible factor-1α signaling. *The Journal of biological chemistry*, 287(13), 9659–9671.

Paatero, I., Seagroves, T. N., Vaparanta, K., Han, W., Jones, F. E., Johnson, R. S., and Elenius, K. (2014). Hypoxia-inducible factor-1α induces ErbB4 signaling in the differentiating mammary gland. *The Journal of biological chemistry*, 289(32), 22459–22469.

Paek, K. Y., Hong, K. Y., Ryu, I., Park, S. M., Keum, S. J., Kwon, O. S., and Jang, S. K. (2015). Translation initiation mediated by RNA looping. *Proceedings of the National Academy of Sciences of the United States of*

America, 112(4), 1041–1046.

Palacino, J., Bai, C., Yi, Y., Skaletskaya, A., Takrouri, K., Wong,W., Kim, M-S., Choi, D-K., Kim, D-Y., Yang, Y.,Kook, J., Lee, P., Jeong, H., Jee, S-M., Park, J.,Chang, K-H., Fishkin, N.,Park, P. U ,. (2022). ORM-5029: A first-in-class targeted protein degradation therapy using antibody neodegrader conjugate (AnDC) for HER2-expressing breast cancer [abstract]. In: Proceedings of the American Association for Cancer Research Annual Meeting 2022; Apr 8-13. Philadelphia (PA): AACR; *Cancer Res*. ;82(12_Suppl):Abstract nr 3933.

Park, K., Kwak, K., Kim, J., Lim, S., and Han, S. (2005). c-myc amplification is associated with HER2 amplification and closely linked with cell proliferation in tissue microarray of nonselected breast cancers. *Human pathology*, 36(6), 634–639.

Park, S.-J., Lee, B-J., Park, M.-H., Choi, J., Park, Y., Park, M.-J., Lim, J.-H., Lee, J., Hwang, S., Lee, J., and Shin, Y.G. (2021). Quantification for Antibody-Conjugated Drug in Trastuzumab Emtansine and Application to In Vitro Linker Stability and In Vivo Pharmacokinetic Study in Rat Using an Immuno-Affinity Capture Liquid Chromatography-Mass Spectrometric Method, *Applied Sciences*, 11(20):9437.

Parra-Palau, J. L., Pedersen, K., Peg, V., Scaltriti, M., Angelini, P. D., Escorihuela, M., Mancilla, S., Sánchez Pla, A., Ramón Y Cajal, S., Baselga, J., and Arribas, J. (2010). A major role of p95/611-CTF, a carboxy-terminal fragment of HER2, in the down-modulation of the estrogen receptor in HER2-positive breast cancers. *Cancer research*, 70(21), 8537–8546.

Passmore, L. A., Schmeing, T. M., Maag, D., Applefield, D. J., Acker, M. G., Algire, M. A., Lorsch, J. R., and Ramakrishnan, V. (2007). The eukaryotic translation initiation factors eIF1 and eIF1A induce an open conformation of the 40S ribosome. *Molecular cell*, 26(1), 41–50.

Patel, J., McLeod, L.E., Vries, R.G.J., Flynn, A., Wang, X. and Proud, C.G. (2002). Cellular stresses profoundly inhibit protein synthesis and modulate the states of phosphorylation of multiple translation factors', *European Journal of Biochemistry*, 269: 3076-3085.

Pause, A., Belsham, G. J., Gingras, A. C., Donzé, O., Lin, T. A., Lawrence, J. C., Jr, and Sonenberg, N. (1994). Insulin-dependent stimulation of protein synthesis by phosphorylation of a regulator of 5'-cap function. *Nature*, 371(6500), 762–767.

Pedersen, K., Angelini, P. D., Laos, S., Bach-Faig, A., Cunningham, M. P., Ferrer-Ramón, C., Luque-García, A., García-Castillo, J., Parra-Palau, J. L., Scaltriti, M., Ramón y Cajal, S., Baselga, J., and Arribas, J. (2009). A naturally

occurring HER2 carboxy-terminal fragment promotes mammary tumor growth and metastasis. *Molecular and cellular biology*, 29(12), 3319–3331.

Pelletier, J., and Sonenberg, N. (1985). Insertion mutagenesis to increase secondary structure within the 5' noncoding region of a eukaryotic mRNA reduces translational efficiency. *Cell*, 40(3), 515–526.

Pelletier, J., and Sonenberg, N. (1988). Internal initiation of translation of eukaryotic mRNA directed by a sequence derived from poliovirus RNA. *Nature*, 334(6180), 320–325.

Peng, R., Hawkins, I., Link, A. J., and Patton, J. G. (2006). The splicing factor PSF is part of a large complex that assembles in the absence of pre-mRNA and contains all five snRNPs. *RNA biology*, 3(2), 69–76.

Perou C. M. (2011). Molecular stratification of triple-negative breast cancers. *The oncologist*, 16 Suppl 1, 61–70.

Pyronnet, S., Imataka, H., Gingras, A. C., Fukunaga, R., Hunter, T., and Sonenberg, N. (1999). Human eukaryotic translation initiation factor 4G (eIF4G) recruits mnk1 to phosphorylate eIF4E. *The EMBO journal*, 18(1), 270–279.

Philippe, C., Dubrac, A., Quelen, C., Desquesnes, A., Van Den Berghe, L., Ségura, C., Filleron, T., Pyronnet, S., Prats, H., Brousset, P., and Touriol, C. .(2016). PERK mediates the IRES-dependent translational activation of mRNAs encoding angiogenic growth factors after ischemic stress. *Science signaling*, 9(426), ra44.

Philpott, C. C., Klausner, R. D., and Rouault, T. A. (1994). The bifunctional iron-responsive element binding protein/cytosolic aconitase: the role of active-site residues in ligand binding and regulation. *Proceedings of the National Academy of Sciences of the United States of America*, 91(15), 7321–7325.

Picard, F., Loubière, P., Girbal, L., and Cocaign-Bousquet, M. (2013). The significance of translation regulation in the stress response, *BMC Genomics*, 14, 588.

Pisarev, A. V., Hellen, C. U., and Pestova, T. V. (2007). Recycling of eukaryotic posttermination ribosomal complexes. *Cell*, 131(2), 286–299.

Pisarev, A. V., Skabkin, M. A., Pisareva, V. P., Skabkina, O. V., Rakotondrafara, A. M., Hentze, M. W., Hellen, C. U., and Pestova, T. V. (2010). The role of ABCE1 in eukaryotic posttermination ribosomal recycling. *Molecular cell*, 37(2), 196–210.

Pontén, F., Jirström, K., and Uhlen, M. (2008). The Human Protein Atlas--a tool for pathology. *The Journal of pathology*, 216(4), 387–393.

Poudel, P., Nyamundanda, G., Patil, Y., Cheang, M.C.U., and Sadanandam, A. (2019). Heterocellular gene signatures reveal luminal-A breast cancer heterogeneity and differential therapeutic responses, *npj Breast Cancer*, 5 21.

Poulin, F., Gingras, A. C., Olsen, H., Chevalier, S., and Sonenberg, N. (1998). 4E-BP3, a new member of the eukaryotic initiation factor 4E-binding protein family. *The Journal of biological chemistry*, 273(22), 14002–14007.

Powell, E., and Xu, W. (2008). Intermolecular interactions identify ligand-selective activity of estrogen receptor alpha/beta dimers. *Proceedings of the National Academy of Sciences of the United States of America*, 105(48), 19012–19017.

Preis, A., Heuer, A., Barrio-Garcia, C., Hauser, A., Eyler, D. E., Berninghausen, O., Green, R., Becker, T., and Beckmann, R. (2014). Cryoelectron microscopic structures of eukaryotic translation termination complexes containing eRF1-eRF3 or eRF1-ABCE1. *Cell reports*, 8(1), 59–65.

Preiss, T., and W Hentze, M. (2003). Starting the protein synthesis machine: eukaryotic translation initiation. *BioEssays : news and reviews in molecular, cellular and developmental biology*, 25(12), 1201–1211.

Promega Corporation. (Revised Nov, 2020). pGL4 Luciferase Reporter Vectors Technical Manual #TM259. Madison, WI, USA. Revised. p10-11. (Accessed: Nov 2022). [Online]. Available at: https://www.promega.co.uk/-/media/files/resources/protocols/technical-manuals/0/pgl4-luciferase-reporter-vectors-protocol.pdf?rev=d1a2cdb9503847cf90a1a732b2212c57&sc_lang=en

Qie, S., Chu, C., Li, W., Wang, C., and Sang, N. (2014). ErbB2 activation upregulates glutaminase 1 expression which promotes breast cancer cell proliferation. *Journal of cellular biochemistry*, 115(3), 498–509.

Rabindran, S. K., Discafani, C. M., Rosfjord, E. C., Baxter, M., Floyd, M. B., Golas, J., Hallett, W. A., Johnson, B. D., Nilakantan, R., Overbeek, E., Reich, M. F., Shen, R., Shi, X., Tsou, H. R., Wang, Y. F., and Wissner, A. (2004). Antitumor activity of HKI-272, an orally active, irreversible inhibitor of the HER-2 tyrosine kinase. *Cancer research*, 64(11), 3958–3965.

Raut, G. K., Chakrabarti, M., Pamarthy, D., and Bhadra, M. P. (2019). Glucose starvation-induced oxidative stress causes mitochondrial dysfunction and apoptosis via Prohibitin 1 upregulation in human breast cancer cells. *Free radical biology & medicine*, 145, 428–441.

Ray, P. S., Grover, R., and Das, S. (2006). Two internal ribosome entry sites mediate the translation of p53 isoforms. *EMBO reports*, 7(4), 404–410.

Redpath, N. T., Foulstone, E. J. and Proud, C. G. (1996). Regulation of translation elongation factor-2 by insulin via a rapamycin-sensitive signalling

pathway, *EMBO Journal*, 15(9), 2291-2297.

Reim, F., Dombrowski, Y., Ritter, C., Buttmann, M., Häusler, S., Ossadnik, M., Krockenberger, M., Beier, D., Beier, C. P., Dietl, J., Becker, J. C., Hönig, A., and Wischhusen, J. (2009). Immunoselection of breast and ovarian cancer cells with trastuzumab and natural killer cells: selective escape of CD44high/CD24low/HER2low breast cancer stem cells. *Cancer research*, 69(20), 8058–8066.

Resch, A. M., Ogurtsov, A. Y., Rogozin, I. B., Shabalina, S. A., and Koonin, E. V. (2009). Evolution of alternative and constitutive regions of mammalian 5'UTRs. *BMC genomics*, 10, 162.

Riley, A., Jordan, L. E., and Holcik, M. (2010). Distinct 5' UTRs regulate XIAP expression under normal growth conditions and during cellular stress. *Nucleic acids research*, 38(14), 4665–4674.

Rio, C., Buxbaum, J. D., Peschon, J. J., and Corfas, G. (2000). Tumor necrosis factor-alpha-converting enzyme is required for cleavage of erbB4/HER4. *The Journal of biological chemistry*, 275(14), 10379–10387.

Risom, T., Wang, X., Liang, J., Zhang, X., Pelz, C., Campbell, L. G., Eng, J., Chin, K., Farrington, C., Narla, G., Langer, E. M., Sun, X. X., Su, Y., Daniel, C. J., Dai, M. S., Löhr, C. V., and Sears, R. C. (2020). Deregulating MYC in a model of HER2+ breast cancer mimics human intertumoral heterogeneity. *The Journal of clinical investigation*, 130(1), 231–246.

Robichaux, J.P., Elamin, Y.Y., Tan ,Z., Carter ,B.W., Zhang ,S., Liu, S., Li, S., Chen, T., Poteete, A., Estrada-Bernal, A., Le, A.T., Truini, A., Nilsson, M.B., Sun, H., Roarty, E., Goldberg, S.B., Brahmer J.R., Altan ,M., Lu, C., Papadimitrakopoulou , V., Politi, K., Doebele, R.C., Wong, K.K., and Heymach J.V. (2018). Mechanisms and clinical activity of an EGFR and HER2 exon 20-selective kinase inhibitor in non-small cell lung cancer. *Nature medicine*, 24(5), 638–646.

Rothenberg, D. A., Taliaferro, J. M., Huber, S. M., Begley, T. J., Dedon, P. C., and White, F. M. (2018). A Proteomics Approach to Profiling the Temporal Translational Response to Stress and Growth. *iScience*, 9, 367–381.

Rozen, F., Edery, I., Meerovitch, K., Dever, T. E., Merrick, W. C., and Sonenberg, N. (1990). Bidirectional RNA helicase activity of eucaryotic translation initiation factors 4A and 4F. *Molecular and cellular biology*, 10(3), 1134–1144.

Ruan, H., Li, X., Xu, X., Leibowitz, B. J., Tong, J., Chen, L., Ao, L., Xing, W., Luo, J., Yu, Y., Schoen, R. E., Sonenberg, N., Lu, X., Zhang, L., and Yu, J. (2020). eIF4E S209 phosphorylation licenses myc- and stress-driven

oncogenesis. *eLife*, 9, e60151.

Sáez, R., Molina, M. A., Ramsey, E. E., Rojo, F., Keenan, E. J., Albanell, J., Lluch, A., García-Conde, J., Baselga, J., and Clinton, G. M. (2006). p95HER-2 predicts worse outcome in patients with HER-2-positive breast cancer. *Clinical cancer research : an official journal of the American Association for Cancer Research*, 12(2), 424–431.

Salas-Marco, J. and Bedwell, D. M. (2004). GTP Hydrolysis by eRF3 Facilitates Stop Codon Decoding during Eukaryotic Translation Termination, *Molecular and Cellular Biology*, 24(17), 7769–7778.

Salaün, P., Pyronnet, S., Morales, J., Mulner-Lorillon, O., Bellé, R., Sonenberg, N., and Cormier, P. (2003). eIF4E/4E-BP dissociation and 4E-BP degradation in the first mitotic division of the sea urchin embryo. *Developmental biology*, 255(2), 428–439.

Sancak, Y., Peterson, T. R., Shaul, Y. D., Lindquist, R. A., Thoreen, C. C., Bar-Peled, L., and Sabatini, D. M. (2008). The Rag GTPases bind raptor and mediate amino acid signaling to mTORC1. *Science (New York, N.Y.)*, 320(5882), 1496–1501.

Sanchez, A. M., Flamini, M. I., Baldacci, C., Goglia, L., Genazzani, A. R., and Simoncini, T. (2010). Estrogen receptor-alpha promotes breast cancer cell motility and invasion via focal adhesion kinase and N-WASP. *Molecular endocrinology (Baltimore, Md.)*, 24(11), 2114–2125.

Sanchez, M., Lin, Y., Yang, C. C., McQuary, P., Rosa Campos, A., Aza Blanc, P., and Wolf, D. A. (2019). Cross Talk between eIF2α and eEF2 Phosphorylation Pathways Optimizes Translational Arrest in Response to Oxidative Stress. *iScience*, 20, 466–480.

Sanders, J. M., Wampole, M. E., Thakur, M. L., and Wickstrom, E. (2013). Molecular determinants of epidermal growth factor binding: a molecular dynamics study. *PloS one*, 8(1), e54136.

Sandulache, V. C., Ow, T. J., Pickering, C. R., Frederick, M. J., Zhou, G., Fokt, I., Davis-Malesevich, M., Priebe, W., and Myers, J. N. (2011). Glucose, not glutamine, is the dominant energy source required for proliferation and survival of head and neck squamous carcinoma cells. *Cancer*, *117*(13), 2926–2938.

Savolainen-Peltonen, H., Vihma, V., Leidenius, M., Wang, F., Turpeinen, U., Hämäläinen, E., Tikkanen, M.J., and Mikkola, T.S. (2014). Breast adipose tissue estrogen metabolism in postmenopausal women with or without breast cancer, *Journal of Clinical Endocrinology and Metabolism*, 1945-7197.

Scaltriti, M., Rojo, F., Ocaña, A., Anido, J., Guzman, M., Cortes, J., Di Cosimo, S., Matias-Guiu, X., Ramon y Cajal, S., Arribas, J., and Baselga, J. (2007).

Expression of p95HER2, a truncated form of the HER2 receptor, and response to anti-HER2 therapies in breast cancer. *Journal of the National Cancer Institute* 99(8), 628–638.

Scaltriti, M., Chandarlapaty, S., Prudkin, L., Aura, C., Jimenez, J., Angelini, P. D., Sánchez, G., Guzman, M., Parra, J. L., Ellis, C., Gagnon, R., Koehler, M., Gomez, H., Geyer, C., Cameron, D., Arribas, J., Rosen, N., and Baselga, J. (2010). Clinical benefit of lapatinib-based therapy in patients with human epidermal growth factor receptor 2-positive breast tumors coexpressing the truncated p95HER2 receptor. *Clinical cancer research: an official journal of the American Association for Cancer Research*, 16(9), 2688–2695.

Schagat, T., Paguio, A., and Kopish, K. (2007). What is Normalization? What Methods are used for Normalization? *Promega Corporation*: *Cell Notes*, Issue 17 2007.

Scheper, G. C., van Kollenburg, B., Hu, J., Luo, Y., Goss, D. J., and Proud, C. G. (2002). Phosphorylation of eukaryotic initiation factor 4E markedly reduces its affinity for capped mRNA. *The Journal of biological chemistry*, 277(5), 3303–3309.

Schneider-Poetsch, T., Ju, J., Eyler, D. E., Dang, Y., Bhat, S., Merrick, W. C., Green, R., Shen, B., and Liu, J. O. (2010). Inhibition of eukaryotic translation elongation by cycloheximide and lactimidomycin. *Nature chemical biology*, 6(3), 209–217.

Schwartzenberg-Bar-Yoseph, F., Armoni, M., and Karnieli, E. (2004). The tumor suppressor p53 down-regulates glucose transporters GLUT1 and GLUT4 gene expression. *Cancer research*, 64(7), 2627–2633.

Segev, N., and Gerst, J. E. (2018). Specialized ribosomes and specific ribosomal protein paralogs control translation of mitochondrial proteins. *The Journal of cell biology*, 217(1), 117–126.

Seli, E. U. (2009). Translational Regulation of Gene Expression During Oocyte and Early Embryo Development. *Biology of Reproduction*, 1529-7268.

Sencan, S., Tanriover, M., Ulasli, M., Karakas, D., and Ozpolat, B. (2021). UV radiation resistance-associated gene (UVRAG) promotes cell proliferation, migration, invasion by regulating cyclin-dependent kinases (CDK) and integrin-β/Src signaling in breast cancer cells. *Molecular and cellular biochemistry*, 476(5), 2075–2084.

Shen, D. W., Goldenberg, S., Pastan, I., and Gottesman, M. M. (2000). Decreased accumulation of [14C] carboplatin in human cisplatin-resistant cells results from reduced energy-dependent uptake. *Journal of cellular physiology*, 183(1), 108–116.

Shi, Y., Sharma, A., Wu, H., Lichtenstein, A., and Gera, J. (2005). Cyclin D1 and c-myc internal ribosome entry site (IRES)-dependent translation is regulated by AKT activity and enhanced by rapamycin through a p38 MAPK- and ERK-dependent pathway. *The Journal of biological chemistry*, 280(12), 10964–10973.

Shi, F., Telesco, S. E., Liu, Y., Radhakrishnan, R., and Lemmon, M. A. (2010). ErbB3/HER3 intracellular domain is competent to bind ATP and catalyze autophosphorylation. *Proceedings of the National Academy of Sciences of the United States of America*, 107(17), 7692–7697.

Shi, Y., Yang, Y., Hoang, B., Bardeleben, C., Holmes, B., Gera, J., and Lichtenstein, A. (2016). Therapeutic potential of targeting IRES-dependent c-myc translation in multiple myeloma cells during ER stress. *Oncogene*, 35(8), 1015–1024.

Shveygert, M., Kaiser, C., Bradrick, S. S., and Gromeier, M. (2010). Regulation of eukaryotic initiation factor 4E (eIF4E) phosphorylation by mitogen-activated protein kinase occurs through modulation of Mnk1-eIF4G interaction. *Molecular and cellular biology*, 30(21), 5160–5167.

Sierke, S. L., Cheng, K., Kim, H. H., and Koland, J. G. (1997). Biochemical characterization of the protein tyrosine kinase homology domain of the ErbB3 (HER3) receptor protein. *The Biochemical journal*, 757–763.

Silipo, M., Gautrey, H., Satam, S., Lennard, T., and Tyson-Capper, A. (2017). How is Herstatin, a tumor suppressor splice variant of the oncogene HER2, regulated? *RNA biology*, 14(5), 536–543.

Singh, N., Joshi, R., and Komurov, K. (2015). HER2-mTOR signaling-driven breast cancer cells require ER-associated degradation to survive. *Science signaling*, 8(378), ra52.

Singhi, A. D., Cimino-Mathews, A., Jenkins, R. B., Lan, F., Fink, S. R., Nassar, H., Vang, R., Fetting, J. H., Hicks, J., Sukumar, S., De Marzo, A. M., and Argani, P. (2012). MYC gene amplification is often acquired in lethal distant breast cancer metastases of unamplified primary tumors. *Modern pathology: an official journal of the United States and Canadian Academy of Pathology, Inc*, 25(3), 378–387.

Siu, F., Bain, P. J., LeBlanc-Chaffin, R., Chen, H., and Kilberg, M. S. (2002). ATF4 is a mediator of the nutrient-sensing response pathway that activates the human asparagine synthetase gene. *The Journal of biological chemistry*, 277(27), 24120–24127.

Smalley, D.S. (2016). 'Translational Control of Epidermal Growth Factor Receptor in Neurodegenerative Diseases'. PhD Thesis, University of

Nottingham, Nottingham, UK.

Sobczak, K., and Krzyzosiak, W. J. (2002). Structural determinants of BRCA1 translational regulation. *The Journal of biological chemistry*, 277(19), 17349–17358.

Sokabe, M., and Fraser, C. S. (2014). Human eukaryotic initiation factor 2 (eIF2)-GTP-Met-tRNAi ternary complex and eIF3 stabilize the 43 S preinitiation complex. *The Journal of biological chemistry*, 289(46), 31827–31836.

Soni, H., Bode, J., Nguyen, C. D. L., Puccio, L., Neßling, M., Piro, R. M., Bub, J., Phillips, E., Ahrends, R., Eipper, B. A., Tews, B., and Goidts, V. (2020). PERK-mediated expression of peptidylglycine α-amidating monooxygenase supports angiogenesis in glioblastoma. *Oncogenesis*, 9(2), 18.

South, J. C. M., Blackburn E., Brown, I.R., and Gullick, W. J. (2013). The neuregulin system of ligands and their receptors in rat islets of Langerhans, *Endocrinology*, 154(7).

Spevak, C. C., Park, E. H., Geballe, A. P., Pelletier, J., and Sachs, M. S. (2006). her-2 upstream open reading frame effects on the use of downstream initiation codons. *Biochemical and biophysical research communications*, 350(4), 834–841.

Spriggs, K. A., Cobbold, L. C., Ridley, S. H., Coldwell, M., Bottley, A., Bushell, M., Willis, A. E., and Siddle, K. (2009). The human insulin receptor mRNA contains a functional internal ribosome entry segment. *Nucleic acids research*, 37(17), 5881–5893.

Stansfield, I., Eurwilaichitr, L., Akhmaloka, and Tuite, M. F. (1996). Depletion in the levels of the release factor eRF1 causes a reduction in the efficiency of translation termination in yeast. *Molecular microbiology*, 20(6), 1135–1143.

Stein, I., Itin, A., Einat, P., Skaliter, R., Grossman, Z., and Keshet, E. (1998). Translation of vascular endothelial growth factor mRNA by internal ribosome entry: implications for translation under hypoxia. *Molecular and cellular biology*, 18(6), 3112–3119.

Stoneley, M., Paulin, F. E., Le Quesne, J. P., Chappell, S. A., and Willis, A. E. (1998). C-Myc 5' untranslated region contains an internal ribosome entry segment. *Oncogene*, 16(3), 423–428.

Stoneley, M., Subkhankulova, T., Le Quesne, J. P., Coldwell, M. J., Jopling, C. L., Belsham, G. J., and Willis, A. E. (2000). Analysis of the c-myc IRES; a potential role for cell-type specific trans-acting factors and the nuclear compartment. *Nucleic acids research*, 28(3), 687–694.

Stoneley, M., and Willis, A. E. (2004). Cellular internal ribosome entry segments: structures, trans-acting factors and regulation of gene expression. *Oncogene*, 23(18), 3200–3207.

Strand, E., Hollås, H., Sakya, S. A., Romanyuk, S., Saraste, M. E. V., Grindheim, A. K., Patil, S. S., and Vedeler, A. (2021). Annexin A2 binds the internal ribosomal entry site of c-*myc* mRNA and regulates its translation. *RNA biology*, 18(sup1), 337–354.

Strunk, K. E., Husted, C., Miraglia, L.C., Sandahl, M., Rearick, W.A., Hunter, D.M., Earp, S., and Muraoka-Cook, R.S. (2007). HER4 D-box sequences regulate mitotic progression and degradation of the nuclear HER4 cleavage product, s80HER4, *Cancer research*, 67 (14): 6582–6590.

Subkhankulova, T., Mitchell, S. A., and Willis, A. E. (2001). Internal ribosome entry segment-mediated initiation of c-Myc protein synthesis following genotoxic stress. *The Biochemical journal*, 359(Pt 1), 183–192.

Sudzinová, P., Kambová, M., Ramaniuk, O., Benda, M., Šanderová, H., and Krásný, L. (2021). Effects of DNA Topology on Transcription from rRNA Promoters in *Bacillus subtilis*. *Microorganisms*, 9(1), 87.

Sundaram, A., and Grant, C. M. (2014). A single inhibitory upstream open reading frame (uORF) is sufficient to regulate Candida albicans GCN4 translation in response to amino acid starvation conditions. *RNA*,20(4), 559–567.

Swain, S. M., Shastry, M., and Hamilton, E. (2023). Targeting HER2-positive breast cancer: advances and future directions. *Nature reviews. Drug discovery*, *22*(2), 101–126.

Sweeney, T. R., Abaeva, I. S., Pestova, T. V., and Hellen, C. U. (2014). The mechanism of translation initiation on Type 1 picornavirus IRESs. *The EMBO journal*, 33(1), 76–92.

Takagi, M., Absalon, M. J., McLure, K. G., and Kastan, M. B. (2005). Regulation of p53 translation and induction after DNA damage by ribosomal protein L26 and nucleolin. *Cell*, 123(1), 49–63.

Tallet-Lopez, B., Aldaz-Carroll, L., Chabas, S., Dausse, E., Staedel, C., and Toulmé, J. J. (2003). Antisense oligonucleotides targeted to the domain IIId of the hepatitis C virus IRES compete with 40S ribosomal subunit binding and prevent in vitro translation. *Nucleic acids research*, 31(2), 734–742.

Talwar, T., Vidhyasagar, V., Qing, J., Guo, M., Kariem, A., Lu, Y., Singh, R. S., Lukong, K. E., and Wu, Y. (2017). The DEAD-box protein DDX43 (HAGE) is a dual RNA-DNA helicase and has a K-homology domain required for full nucleic acid unwinding activity. *The Journal of biological chemistry*, 292(25), 10429–10443.

Tan, W., Dean, M., and Law, A. J.(2010). Molecular cloning and characterization of the human ErbB4 gene: identification of novel splice isoforms in the developing and adult brain. *PloS one*, 5(9), e12924.

Taniuchi, S., Miyake, M., Tsugawa, K., Oyadomari, M., and Oyadomari, S. (2016). Integrated stress response of vertebrates is regulated by four eIF2α kinases. *Scientific reports*, 6, 32886.

Tariki, M., Dhanyamraju, P. K., Fendrich, V., Borggrefe, T., Feldmann, G., and Lauth, M. (2014). The Yes-associated protein controls the cell density regulation of Hedgehog signaling. *Oncogenesis*, 3(8), e112.

Taylor, D., Unbehaun, A., Li, W., Das, S., Lei, J., Liao, H. Y., Grassucci, R. A., Pestova, T. V., and Frank, J. (2012). Cryo-EM structure of the mammalian eukaryotic release factor eRF1-eRF3-associated termination complex. *Proceedings of the National Academy of Sciences of the United States of America*, 109(45), 18413–18418.

Törnroos, R., Tina, E., and Göthlin Eremo, A. (2022). SLC7A5 is linked to increased expression of genes related to proliferation and hypoxia in estrogen-receptor-positive breast cancer. *Oncology reports*, 47(1), 17.

Torrence, M. E., MacArthur, M. R., Hosios, A. M., Valvezan, A. J., Asara, J. M., Mitchell, J. R., and Manning, B. D. (2021). The mTORC1-mediated activation of ATF4 promotes protein and glutathione synthesis downstream of growth signals. *eLife*, 10, e63326.

Trobro, S., and Aqvist, J. (2007). A model for how ribosomal release factors induce peptidyl-tRNA cleavage in termination of protein synthesis. *Molecular cell*, 27(5), 758–766.

Tsai, P. Y., Lee, M. S., Jadhav, U., Naqvi, I., Madha, S., Adler, A., Mistry, M., Naumenko, S., Lewis, C. A., Hitchcock, D. S., Roberts, F. R., DelNero, P., Hank, T., Honselmann, K. C., Morales Oyarvide, V., Mino-Kenudson, M., Clish, C. B., Shivdasani, R. A., and Kalaany, N. Y. (2021). Adaptation of pancreatic cancer cells to nutrient deprivation is reversible and requires glutamine synthetase stabilization by mTORC1. *Proceedings of the National Academy of Sciences of the United States of America*, 118(10), e2003014118.

Tudini, E., Burke, L. J., Whiley, P. J., Sevcik, J., Spurdle, A. B., and Brown, M. A. (2019). Caution: Plasmid DNA topology affects luciferase assay reproducibility and outcomes. *BioTechniques*, 67(3), 94–96.

Ueda, T., Watanabe-Fukunaga, R., Fukuyama, H., Nagata, S., and Fukunaga, R. (2004). Mnk2 and Mnk1 are essential for constitutive and inducible phosphorylation of eukaryotic initiation factor 4E but not for cell growth or development. *Molecular and cellular biology*, 24(15), 6539–6549.

Ungureanu, N. H., Cloutier, M., Lewis, S. M., de Silva, N., Blais, J. D., Bell, J. C., and Holcik, M. (2006). Internal ribosome entry site-mediated translation of Apaf-1, but not XIAP, is regulated during UV-induced cell death. *The Journal of biological chemistry*, 281(22), 15155–15163.

Van Eden, M. E., Byrd, M. P., Sherrill, K. W., and Lloyd, R. E. (2004). Demonstrating internal ribosome entry sites in eukaryotic mRNAs using stringent RNA test procedures. *RNA*, 10(4), 720–730.

Van Geldermalsen, M., Wang, Q., Nagarajah, R., Marshall, A. D., Thoeng, A., Gao, D., Ritchie, W., Feng, Y., Bailey, C. G., Deng, N., Harvey, K., Beith, J. M., Selinger, C. I., O'Toole, S. A., Rasko, J. E., and Holst, J. (2016). ASCT2/SLC1A5 controls glutamine uptake and tumour growth in triple-negative basal-like breast cancer. *Oncogene*, 35(24), 3201–3208.

Vattem, K. M., and Wek, R. C. (2004). Reinitiation involving upstream ORFs regulates ATF4 mRNA translation in mammalian cells. *Proceedings of the National Academy of Sciences of the United States of America*, 101(31), 11269–11274.

Victorino, V. J., Campos, F. C., Herrera, A. C., Colado Simão, A. N., Cecchini, A. L., Panis, C., and Cecchini, R. (2014). Overexpression of HER-2/neu protein attenuates the oxidative systemic profile in women diagnosed with breast cancer. *Tumour biology: the journal of the International Society for Oncodevelopmental Biology and Medicine*, 35(4), 3025–3034.

Volpi, C. C., Pietrantonio, F., Gloghini, A., Fucà, G., Giordano, S., Corso, S., Pruneri, G., Antista, M., Cremolini, C., Fasano, E., Saggio, S., Faraci, S., Di Bartolomeo, M., de Braud, F., Di Nicola, M., Tagliabue, E., Pupa, S. M., and Castagnoli, L. (2019). The landscape of d16HER2 splice variant expression across HER2-positive cancers. *Scientific reports*, 9(1), 3545.

Vuković, L., Koh, H. R., Myong, S., and Schulten, K. (2014). Substrate recognition and specificity of double-stranded RNA binding proteins. *Biochemistry*, 53(21), 3457–3466.

Wander, S. A., Cohen, O., Gong, X., Johnson, G. N., Buendia-Buendia, J. E., Lloyd, M. R., Kim, D., Luo, F., Mao, P., Helvie, K., Kowalski, K. J., Nayar, U., Waks, A. G., Parsons, S. H., Martinez, R., Litchfield, L. M., Ye, X. S., Yu, C., Jansen, V. M., Stille, J. R., Smith, P.S., Oakley, G.J., Chu, Q.S., Batist, G., Hughes, M.E., Kremer, J.D., Garraway, L.A., Winer, E.P., Tolaney, S.M., Lin, N.U., Buchanan, S.G., and Wagle, N. (2020). The Genomic Landscape of Intrinsic and Acquired Resistance to Cyclin-Dependent Kinase 4/6 Inhibitors in Patients with Hormone Receptor-Positive Metastatic Breast Cancer. *Cancer discovery*, 10(8), 1174–1193.

Wang, Y., Rosenstein, B., Goldwyn, S., Zhang, X., Lebwohl, M., and Wei, H. (1998). Differential regulation of P53 and Bcl-2 expression by ultraviolet A and B. *The Journal of investigative dermatology*, 111(3), 380–384.

Wang, W., Caldwell, M.C., Lin, S., Furneaux, H and Gorospe, M. (2000). 'HuR regulates cyclin A and cyclin B1 mRNA stability during cell proliferation', *The EMBO Journal*, 19: 2340-2350.

Wang, E. T., Sandberg, R., Luo, S., Khrebtukova, I., Zhang, L., Mayr, C., Kingsmore, S. F., Schroth, G. P., and Burge, C. B. (2008). Alternative isoform regulation in human tissue transcriptomes. *Nature*, 456(7221), 470–476.

Wang, J. B., Erickson, J. W., Fuji, R., Ramachandran, S., Gao, P., Dinavahi, R., Wilson, K. F., Ambrosio, A. L., Dias, S. M., Dang, C. V., and Cerione, R. A. (2010). Targeting mitochondrial glutaminase activity inhibits oncogenic transformation. *Cancer cell*, 18(3), 207–219.

Wang, H. M., Yang, H. L., Thiyagarajan, V., Huang, T. H., Huang, P. J., Chen, S. C., Liu, J. Y., Hsu, L. S., Chang, H. W., and Hseu, Y. C. (2017a). Coenzyme Q_0 Enhances Ultraviolet B-Induced Apoptosis in Human Estrogen Receptor-Positive Breast (MCF-7) Cancer Cells. *Integrative cancer therapies*, 16(3), 385–396.

Wang, J., Zhang, J., Lee, Y. M., Ng, S., Shi, Y., Hua, Z. C., Lin, Q., and Shen, H. M. (2017b). Nonradioactive quantification of autophagic protein degradation with L-azidohomoalanine labeling. *Nature protocols*, 12(2), 279–288.

Wang, H., Sun, W., Sun, M., Fu, Z., Zhou, C., Wang, C., Zuo, D., Zhou, Z., Wang, G., Zhang, T., Xu, J., Chen, J., Wang, Z., Yin, F., Duan, Z., Hornicek, F. J., Cai, Z., and Hua, Y. (2018a). HER4 promotes cell survival and chemoresistance in osteosarcoma via interaction with NDRG1. *Biochimica et biophysica acta. Molecular basis of disease*, 1864(5 Pt A), 1839–1849.

Wang, Z., Zhang, J., Zhang, Y., Deng, Q., and Liang, H. (2018b). Expression and mutations of BRCA in breast cancer and ovarian cancer: Evidence from bioinformatics analyses. *International journal of molecular medicine*, 42(6), 3542–3550.

Wang, J., Ji, H., Niu, X., Yin, L., Wang, Y., Gu, Y., Li, D., Zhang, H., Lu, M., Zhang, F., and Zhang, Q. (2020a). Sodium-Dependent Glucose Transporter 1 (SGLT1) Stabled by HER2 Promotes Breast Cancer Cell Proliferation by Activation of the PI3K/Akt/mTOR Signaling Pathway in HER2+ Breast Cancer. *Disease markers*, 2020, 6103542.

Wang, L. Y., Cui, J. J., Guo, C. X., and Yin, J. Y. (2020b). A New Way to Discover IRESs in Pathology or Stress Conditions? Harnessing Latest High-Throughput Technologies. *BioEssays: news and reviews in molecular, cellular*

and developmental biology, 42(3), e1900180.

Wang, X., Wang, L., Yu, Q., Liu, Z., Li, C., Wang, F., and Yu, Z. (2021). The Effectiveness of Lapatinib in HER2-Positive Metastatic Breast Cancer Patients Pretreated With Multiline Anti-HER2 Treatment: A Retrospective Study in China. *Technology in cancer research & treatment*, 20, 15330338211037812.

Warburg, O. (1925). The Metabolism of Carcinoma Cells. *The Journal of Cancer Research*, 9 (1): 148–163.

Webb, T.E., (2012). 'UNDERSTANDING THE ROLE OF EIF4A IN GENE REGULATION IN HEALTH AND DISEASE'. PhD Thesis, University of Nottingham, Nottingham, UK.

Webb, T. E., Hughes, A., Smalley, D. S., and Spriggs, K. A. (2015). An internal ribosome entry site in the 5' untranslated region of epidermal growth factor receptor allows hypoxic expression. *Oncogenesis*, 4(1), e134.

Wege, A. K., Chittka, D., Buchholz, S., Klinkhammer-Schalke, M., Diermeier-Daucher, S., Zeman, F., Ortmann, O., and Brockhoff, G. (2018). HER4 expression in estrogen receptor-positive breast cancer is associated with decreased sensitivity to tamoxifen treatment and reduced overall survival of postmenopausal women. *Breast cancer research: BCR*, 20(1), 139.

Weihua, Z., Tsan, R., Huang, W. C., Wu, Q., Chiu, C. H., Fidler, I. J., and Hung, M. C. (2008). Survival of cancer cells is maintained by EGFR independent of its kinase activity. *Cancer cell*, 13(5), 385–393.

Weil-Malherbe, H. and Gordon, J. (1971). AMINO ACID METABOLISM AND AMMONIA FORMATION IN BRAIN SLICES', *Journal of Neurochemistry*, 18: 1659-1672.

Weingarten-Gabbay, S., Elias-Kirma, S., Nir, R., Gritsenko, A. A., Stern-Ginossar, N., Yakhini, Z., Weinberger, A., and Segal, E. (2016). Comparative genetics. Systematic discovery of cap-independent translation sequences in human and viral genomes. *Science (New York, N.Y.)*, 351(6270), aad4939.

Weisman, P., Ospina-Romero, M., Yu, Q., Wisinski, K., and Xu, J. (2022). HER2-positive/ER-low breast carcinoma shows a response to neoadjuvant chemotherapy similar to that of HER2-positive/ER-negative breast carcinoma. *Pathology, research and practice*, 238, 154087.

Wen, W., Chen, W. S., Xiao, N., Bender, R., Ghazalpour, A., Tan, Z., Swensen, J., Millis, S. Z., Basu, G., Gatalica, Z., and Press, M. F. (2015). Mutations in the Kinase Domain of the HER2/ERBB2 Gene Identified in a Wide Variety of Human Cancers. *The Journal of molecular diagnostics: JMD*, 17(5), 487–495.

Wiegmans, A. P., Ward, A., Ivanova, E., Duijf, P. H. G., Adams, M. N., Najib,

I. M., Van Oosterhout, R., Sadowski, M. C., Kelly, G., Morrical, S. W., O'Byrne, K., Lee, J. S., and Richard, D. J. (2021). Genome instability and pressure on non-homologous end joining drives chemotherapy resistance via a DNA repair crisis switch in triple negative breast cancer. *NAR cancer*, 3(2), zcab022.

Wilczynska, A., Gillen, S. L., Schmidt, T., Meijer, H. A., Jukes-Jones, R., Langlais, C., Kopra, K., Lu, W. T., Godfrey, J. D., Hawley, B. R., Hodge, K., Zanivan, S., Cain, K., Le Quesne, J., and Bushell, M. (2019). eIF4A2 drives repression of translation at initiation by Ccr4-Not through purine-rich motifs in the 5'UTR. *Genome biology*, 20(1), 262.

Wild , C. P, Weiderpass, E, Stewart, B. W. (2020). World Cancer Report: Cancer Research for Cancer Prevention. Lyon, France: International Agency for Research on Cancer. Available from: http://publications.iarc.fr/586. Licence: CC BY-NC-ND 3.0 IGO

Wilusz, J. (2013). Putting an 'End' to HIV mRNAs: capping and polyadenylation as potential therapeutic targets. *AIDS Res Ther,* 10, 31.

Wolf-Yadlin, A., Kumar, N., Zhang, Y., Hautaniemi, S., Zaman, M., Kim, H. D., Grantcharova, V., Lauffenburger, D. A., and White, F. M. (2006). Effects of HER2 overexpression on cell signaling networks governing proliferation and migration. *Molecular systems biology*, 2, 54.

Wolfe, A. L., Singh, K., Zhong, Y., Drewe, P., Rajasekhar, V. K., Sanghvi, V. R., Mavrakis, K. J., Jiang, M., Roderick, J. E., Van der Meulen, J., Schatz, J. H., Rodrigo, C. M., Zhao, C., Rondou, P., de Stanchina, E., Teruya-Feldstein, J., Kelliher, M. A., Speleman, F., Porco, J. A., Jr, Pelletier, J., Rätsch, G., and Wendel, H. G. (2014). RNA G-quadruplexes cause eIF4A-dependent oncogene translation in cancer. *Nature*, 513(7516), 65–70.

Wolff, M. S., and Weston, A. (1997). Breast cancer risk and environmental exposures. *Environmental health perspectives, 105 Suppl 4*(Suppl 4), 891–896.

Won, S., Eidenschenk, C., Arnold, C. N., Siggs, O. M., Sun, L., Brandl, K., Mullen, T. M., Nemerow, G. R., Moresco, E. M., and Beutler, B. (2012). Increased susceptibility to DNA virus infection in mice with a GCN2 mutation. *Journal of virology*, 86(3), 1802–1808.

Woo, P. C., Lau, S. K., Choi, G. K., Huang, Y., Teng, J. L., Tsoi, H. W., Tse, H., Yeung, M. L., Chan, K. H., Jin, D. Y., and Yuen, K. Y. (2012). Natural occurrence and characterization of two internal ribosome entry site elements in a novel virus, canine picodicistrovirus, in the picornavirus-like superfamily. *Journal of virology*, 86(5), 2797–2808.

Wood, E. R., Truesdale, A. T., McDonald, O. B., Yuan, D., Hassell, A., Dickerson, S. H., Ellis, B., Pennisi, C., Horne, E., Lackey, K., Alligood, K. J.,

Rusnak, D. W., Gilmer, T. M., and Shewchuk, L. (2004). A unique structure for epidermal growth factor receptor bound to GW572016 (Lapatinib): relationships among protein conformation, inhibitor off-rate, and receptor activity in tumor cells. *Cancer research*, 64(18), 6652–6659.

Wu, L., Huang, X., Kuang, Y., Xing, Z., Deng, X., and Luo, Z. (2019). Thapsigargin induces apoptosis in adrenocortical carcinoma by activating endoplasmic reticulum stress and the JNK signaling pathway: an in vitro and in vivo study. *Drug design, development and therapy*, *13*, 2787–2798.

Xia, X., and Holcik, M. (2009). Strong eukaryotic IRESs have weak secondary structure. *PloS one*, 4(1), e4136.

Xiao, W., Sun, Y., Xu, J., Zhang, N., and Dong, L. (2022). uORF-Mediated Translational Regulation of ATF4 Serves as an Evolutionarily Conserved Mechanism Contributing to Non-Small-Cell Lung Cancer (NSCLC) and Stress Response. *Journal of molecular evolution*, 90(5), 375–388.

Xu, X., De Angelis, C., Burke, K. A., Nardone, A., Hu, H., Qin, L., Veeraraghavan, J., Sethunath, V., Heiser, L. M., Wang, N., Ng, C. K. Y., Chen, E. S., Renwick, A., Wang, T., Nanda, S., Shea, M., Mitchell, T., Rajendran, M., Waters, I., Zabransky, D. J., Scott, K.L., Gutierrez, C., Nagi, C., Geyer, F.C., Chamness, G.C., Park, B.H., Shaw, C.A., Hilsenbeck, S.G., Rimawi, M.F., Gray, J.W., Weigelt, B., Reis-Filho J.S., Osborne, C.K., and Schiff, R. (2017). HER2 Reactivation through Acquisition of the HER2 L755S Mutation as a Mechanism of Acquired Resistance to HER2-targeted Therapy in HER2^{+} Breast Cancer. *Clinical cancer research: an official journal of the American Association for Cancer Research*, 23(17), 5123–5134.

Yaman, I. Fernandez, J, Liu, H, Caprara, M, Komar, A. A, Koromilas, A. E, Zhou, L, Snider, M. D, Scheuner, D, Kaufman, R. J, and Hatzoglou, M. (2003) .'The zipper model of translational control: A small upstream ORF is the switch that controls structural remodeling of an mRNA leader', *Cell*, 113(4), pp. 519–531.

Yamashita, H., Ishida, N., Hatanaka, Y., Hagio, K., Oshino, T., Takeshita, T., Kanno-Okada, H., Shimizu, A. I., Hatanaka, K. C., and Matsuno, Y. (2020). Gene Amplification in ER-positive HER2 Immunohistochemistry 0 or 1+ Breast Cancer With Early Recurrence. *Anticancer research*, 40(2), 645–652.

Yan, Y., Song, Q., Yao, L., Zhao, L., and Cai, H. (2022). YAP Overexpression in Breast Cancer Cells Promotes Angiogenesis through Activating YAP Signaling in Vascular Endothelial Cells. *Analytical cellular pathology*, 5942379.

Yang, R., Wek, S. A., and Wek, R. C. (2000). Glucose limitation induces GCN4

translation by activation of Gcn2 protein kinase. *Molecular and cellular biology*, 20(8), 2706–2717.

Yang, D. Q., Halaby, M. J., and Zhang, Y. (2006). The identification of an internal ribosomal entry site in the 5'-untranslated region of p53 mRNA provides a novel mechanism for the regulation of its translation following DNA damage. *Oncogene*, 25(33), 4613–4619.

Yang, R., Li, X., Wu, Y., Zhang, G., Liu, X., Li, Y., Bao, Y., Yang, W., and Cui, H. (2020). EGFR activates GDH1 transcription to promote glutamine metabolism through MEK/ERK/ELK1 pathway in glioblastoma. *Oncogene*, 39(14), 2975-2986.

Yang, G., Yang, Y., Liu, R., Li, W., Xu, H., Hao, X., Li, J., Xing, P., Zhang, S., Ai, X., Xu, F., and Wang, Y. (2022). First-line immunotherapy or angiogenesis inhibitor plus chemotherapy for *HER2*-altered NSCLC: a retrospective real-world POLISH study. *Therapeutic advances in medical oncology*, *14*, 17588359221082339.

Yarden, Y., and Schlessinger, J. (1987). Self-phosphorylation of epidermal growth factor receptor: evidence for a model of intermolecular allosteric activation. *Biochemistry*, 26(5), 1434–1442.

Ye, J., Kumanova, M., Hart, L. S., Sloane, K., Zhang, H., De Panis, D. N., Bobrovnikova-Marjon, E., Diehl, J. A., Ron, D., and Koumenis, C. (2010). The GCN2-ATF4 pathway is critical for tumour cell survival and proliferation in response to nutrient deprivation. *The EMBO journal*, 29(12), 2082–2096.

Yi, R., Qin, Y., Macara, I. G., and Cullen, B. R. (2003). Exportin-5 mediates the nuclear export of pre-microRNAs and short hairpin RNAs. *Genes & development*, 17(24), 3011–3016.

Yin, O., Xiong, Y., Endo, S., Yoshihara, K., Garimella, T., AbuTarif, M., Wada, R., and LaCreta, F. (2021). Population Pharmacokinetics of Trastuzumab Deruxtecan in Patients With HER2-Positive Breast Cancer and Other Solid Tumors. *Clinical pharmacology and therapeutics*, 109(5), 1314–1325.

Yoshiji, H., Harris, S. R., and Thorgeirsson, U. P. (1997). Vascular endothelial growth factor is essential for initial but not continued in vivo growth of human breast carcinoma cells. *Cancer research*, 57(18), 3924–3928.

Young, A. T. L., Moore, R. B., Murray, A. G., Mullen, J. C., and Lakey, J. R. T. (2004). Assessment of Different Transfection Parameters in Efficiency Optimization. *Cell transplantation*, 13(2), 179–185.

Young, D. J., Makeeva, D. S., Zhang, F., Anisimova, A. S., Stolboushkina, E. A., Ghobakhlou, F., Shatsky, I. N., Dmitriev, S. E., Hinnebusch, A. G., and Guydosh, N. R. (2018). Tma64/eIF2D, Tma20/MCT-1, and Tma22/DENR

Recycle Post-termination 40S Subunits In Vivo. *Molecular cell*, 71(5), 761–774.e5.

Younis, I., Berg, M., Kaida, D., Dittmar, K., Wang, C., and Dreyfuss, G. (2010). Rapid-response splicing reporter screens identify differential regulators of constitutive and alternative splicing. *Molecular and cellular biology*, 30(7), 1718–1728.

Yu, Y., Abaeva, I. S., Marintchev, A., Pestova, T. V., and Hellen, C. U. (2011). Common conformational changes induced in type 2 picornavirus IRESs by cognate trans-acting factors. *Nucleic acids research*, 39(11), 4851–4865.

Yuan, C. X., Lasut, A. L., Wynn, R., Neff, N. T., Hollis, G. F., Ramaker, M. L., Rupar, M. J., Liu, P., and Meade, R. (2003). Purification of Her-2 extracellular domain and identification of its cleavage site. *Protein expression and purification*, 29(2), 217–222.

Yuan, Y., Hilliard, G., Ferguson, T., and Millhorn, D. E. (2003). Cobalt inhibits the interaction between hypoxia-inducible factor-alpha and von Hippel-Lindau protein by direct binding to hypoxia-inducible factor-alpha. *The Journal of biological chemistry*, 278(18), 15911–15916.

Zaborowska, I., Kellner, K., Henry, M., Meleady, P., and Walsh, D. (2012). Recruitment of host translation initiation factor eIF4G by the Vaccinia Virus ssDNA-binding protein I3. *Virology*, 425(1), 11–22.

Zeng, P., Sun, S., Li, R., Xiao, Z. X., and Chen, H. (2019). HER2 Upregulates ATF4 to Promote Cell Migration via Activation of ZEB1 and Downregulation of E-Cadherin. *International journal of molecular sciences*, 20(9), 2223.

Zeng, Y., Yi, R., and Cullen, B. R. (2005). Recognition and cleavage of primary microRNA precursors by the nuclear processing enzyme Drosha. *The EMBO journal*, 24(1), 138–148.

Zenin, V., Ivanova, J., Pugovkina, N., Shatrova, A., Aksenov, N., Tyuryaeva, I., Kirpichnikova, K., Kuneev, I., Zhuravlev, A., Osyaeva, E., Lyublinskaya, E., Gazizova, I., Guriev, N., and Lyublinskaya, O. (2022). Resistance to H_2O_2-induced oxidative stress in human cells of different phenotypes. *Redox biology*, 50, 102245.

Zhang, P. McGrath, B. C., Reinert, J., Olsen, D. S., Lei, L., Gill, S., Wek, S. A., Vattem, K. M., Wek, R. C., Kimball, S. R., Jefferson, L. S., and Cavener, D. R. (2002). 'The GCN2 eIF2α Kinase Is Required for Adaptation to Amino Acid Deprivation in Mice', *Molecular and Cellular Biology*, 22(19), p. 6681.

Zhang, C., Liu, J., Liang, Y., Wu, R., Zhao, Y., Hong, X., Lin, M., Yu, H., Liu, L., Levine, A. J., Hu, W., and Feng, Z. (2013). Tumour-associated mutant p53 drives the Warburg effect. *Nature communications*, 4, 2935.

Zhang, N., Yang, X., Yuan, F., Zhang, L., Wang, Y., Wang, L., Mao, Z., Luo, J., Zhang, H., Zhu, W. G., and Zhao, Y. (2018). Increased Amino Acid Uptake Supports Autophagy-Deficient Cell Survival upon Glutamine Deprivation. *Cell reports*, 23(10), 3006–3020.

Zhang, H. S., Zhang, Z. G., Du, G. Y., Sun, H. L., Liu, H. Y., Zhou, Z., Gou, X. M., Wu, X. H., Yu, X. Y., and Huang, Y. H. (2019a). Nrf2 promotes breast cancer cell migration via up-regulation of G6PD/HIF-1α/Notch1 axis. *Journal of cellular and molecular medicine*, 23(5), 3451–3463.

Zhang, M., Jang, H., and Nussinov, R. (2019b). The mechanism of PI3Kα activation at the atomic level. *Chemical science*, 10(12), 3671–3680.

Zhang, Y., Wu, S., Zhuang, X., Weng, G., Fan, J., Yang, X., Xu, Y., Pan, L., Hou, T., Zhou, Z., and Chen, S. (2019c). Identification of an Activating Mutation in the Extracellular Domain of HER2 Conferring Resistance to Pertuzumab. *OncoTargets and therapy*, 12, 11597–11608.

Zhao, B., Ye, X., Yu, J., Li, L., Li, W., Li, S., Yu, J., Lin, J. D., Wang, C. Y., Chinnaiyan, A. M., Lai, Z. C., and Guan, K. L. (2008). TEAD mediates YAP-dependent gene induction and growth control. *Genes & development*, 22(14), 1962–1971.

Zhao, Y. H., Zhou, M., Liu, H., Ding, Y., Khong, H. T., Yu, D., Fodstad, O., and Tan, M. (2009). Upregulation of lactate dehydrogenase A by ErbB2 through heat shock factor 1 promotes breast cancer cell glycolysis and growth. *Oncogene*, 28(42), 3689–3701.

Zhao, E. M., Mao, A. S., de Puig, H., Zhang, K., Tippens, N. D., Tan, X., Ran, F. A., Han, I., Nguyen, P. Q., Chory, E. J., Hua, T. Y., Ramesh, P., Thompson, D. B., Oh, C. Y., Zigon, E. S., English, M. A., and Collins, J. J. (2022). RNA-responsive elements for eukaryotic translational control. *Nature biotechnology*, 40(4), 539-545.

Zheng, D., Wang, R., Ding, Q., Wang, T., Xie, B., Wei, L., Zhong, Z., and Tian, B. (2018). Cellular stress alters 3'UTR landscape through alternative polyadenylation and isoform-specific degradation *Nature communications*, 9(1),2268.

Zhou, B. P., and Hung, M. C. (2003). Dysregulation of cellular signaling by HER2/neu in breast cancer. *Seminars in oncology*, 30(5 Suppl 16), 38–48.

Zhou, D., Palam, L. R., Jiang, L., Narasimhan, J., Staschke, K. A., and Wek, R. C. (2008). Phosphorylation of eIF2 directs ATF5 translational control in response to diverse stress conditions. *The Journal of biological chemistry*, 283(11), 706-7073.

Zhu, Y., Sullivan, L. L., Nair, S. S., Williams, C. C., Pandey, A. K., Marrero,

L., Vadlamudi, R. K., and Jones, F. E. (2006). Coregulation of estrogen receptor by ERBB4/HER4 establishes a growth-promoting autocrine signal in breast tumor cells. *Cancer research*, 66(16), 7991–7998.

Ziemba, B. P., Pilling, C., Calleja, V., Larijani, B., and Falke, J. J. (2013). The PH domain of phosphoinositide-dependent kinase-1 exhibits a novel, phospho-regulated monomer-dimer equilibrium with important implications for kinase domain activation: single-molecule and ensemble studies. *Biochemistry*, 52(28), 4820–4829.

Appendices

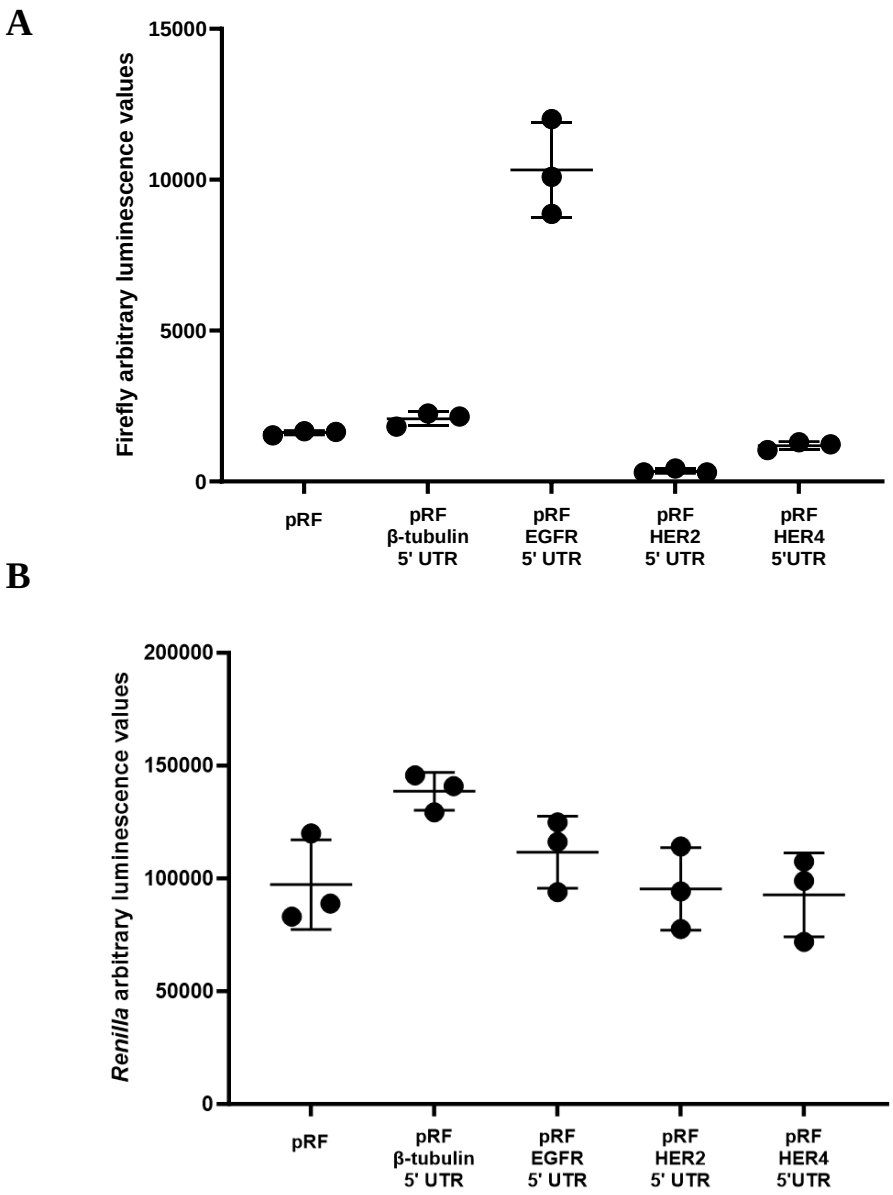

Appendix Figure 1. Raw bicistronic luciferase reporter data in non-stressed conditions. MCF-7 cells were transfected with bicistronic constructs containing both *Renilla* and firefly luciferase open reading frames. 24 hours post-transfection cells were lysed and the A) raw firefly luciferase and B) *Renilla* luciferase expression was measured. Data represents one independent experiment taken in triplicate. All error bars represent the standard deviation.

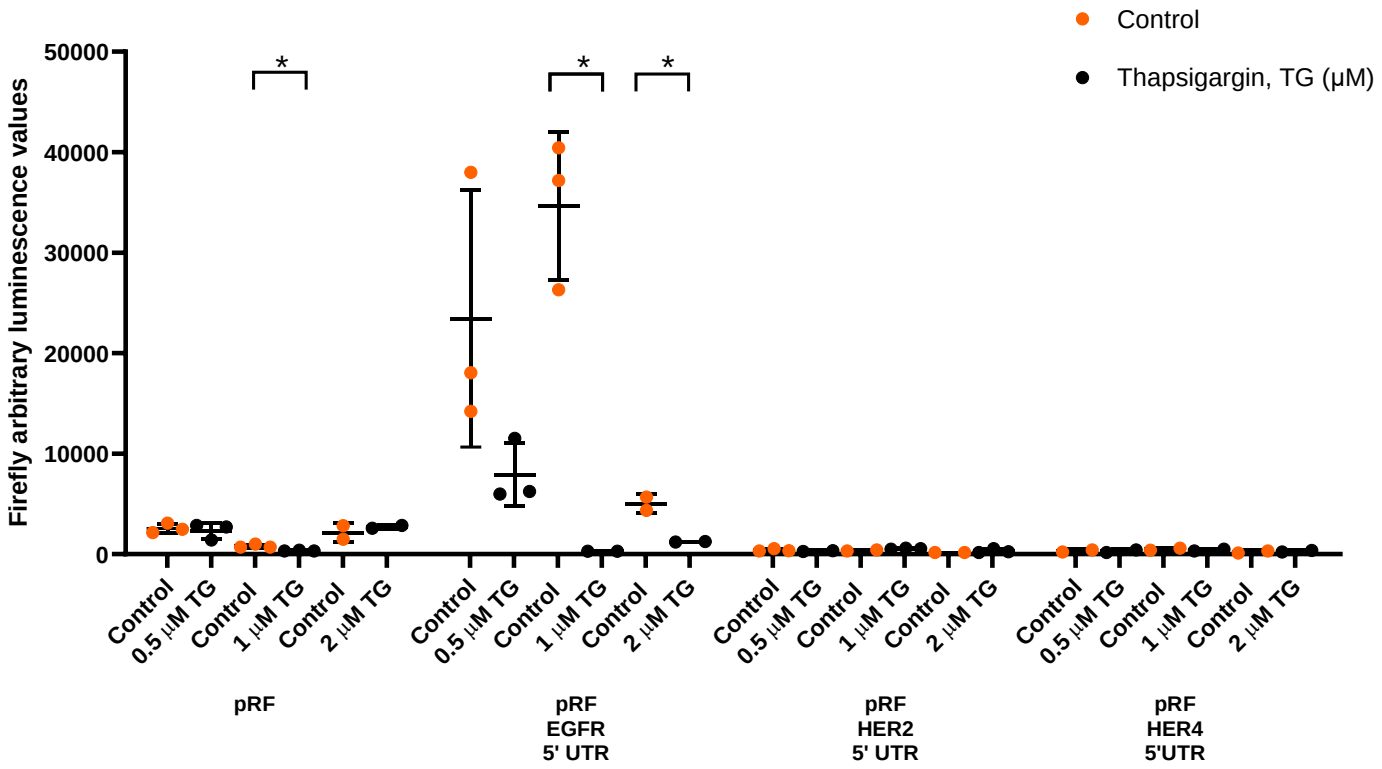

Appendix Figure 2. Raw bicistronic firefly luciferase data in response to thapsigargin. MCF-7 cells were transfected with bicistronic constructs containing both *Renilla* luciferase and firefly luciferase open reading frames. 24 hours post-transfection MCF-7 cells were exposed to either 0.5 μM, 1 μM or 2 μM of thapsigargin (black) or respective DMSO controls (orange). 24 hours later cells were lysed and the firefly activity was measured. Data represents the average of two-three independent experiments each carried out in triplicate. All error bars represent the standard deviation. $p<0.05$ was determined statistically significant using a t-test with Bonferroni-Dunn's correction.

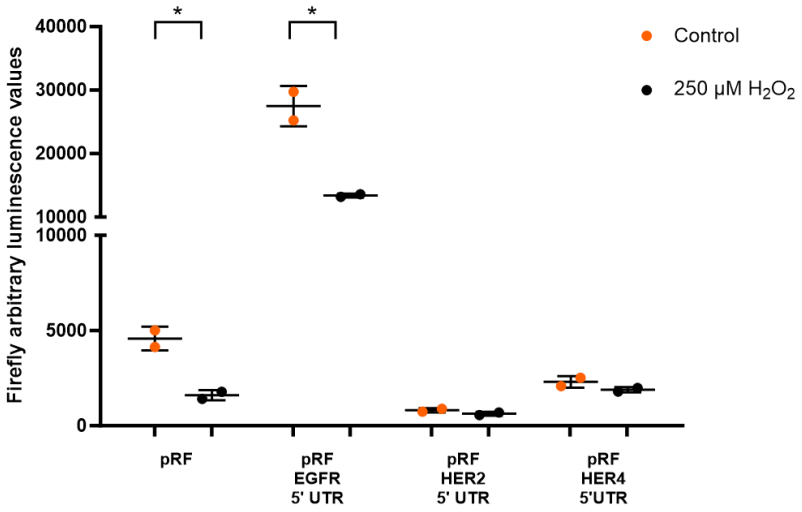

Appendix Figure 3. Raw bicistronic firefly luciferase data in response to 250 µM of hydrogen peroxide. MCF-7 cells were transfected with bicistronic constructs. 24 hours post-transfection MCF-7 cells were exposed to 250 µM of hydrogen peroxide (H_2O_2) (black) or were untreated (orange) for 24 hours. 24 hours later cells were lysed and the firefly luciferase activity was measured. Data represents the average of two independent experiments each carried out in triplicate. All error bars represent the standard deviation. $p<0.05$ was determined statistically significant using a t-test with Bonferroni-Dunn's correction.

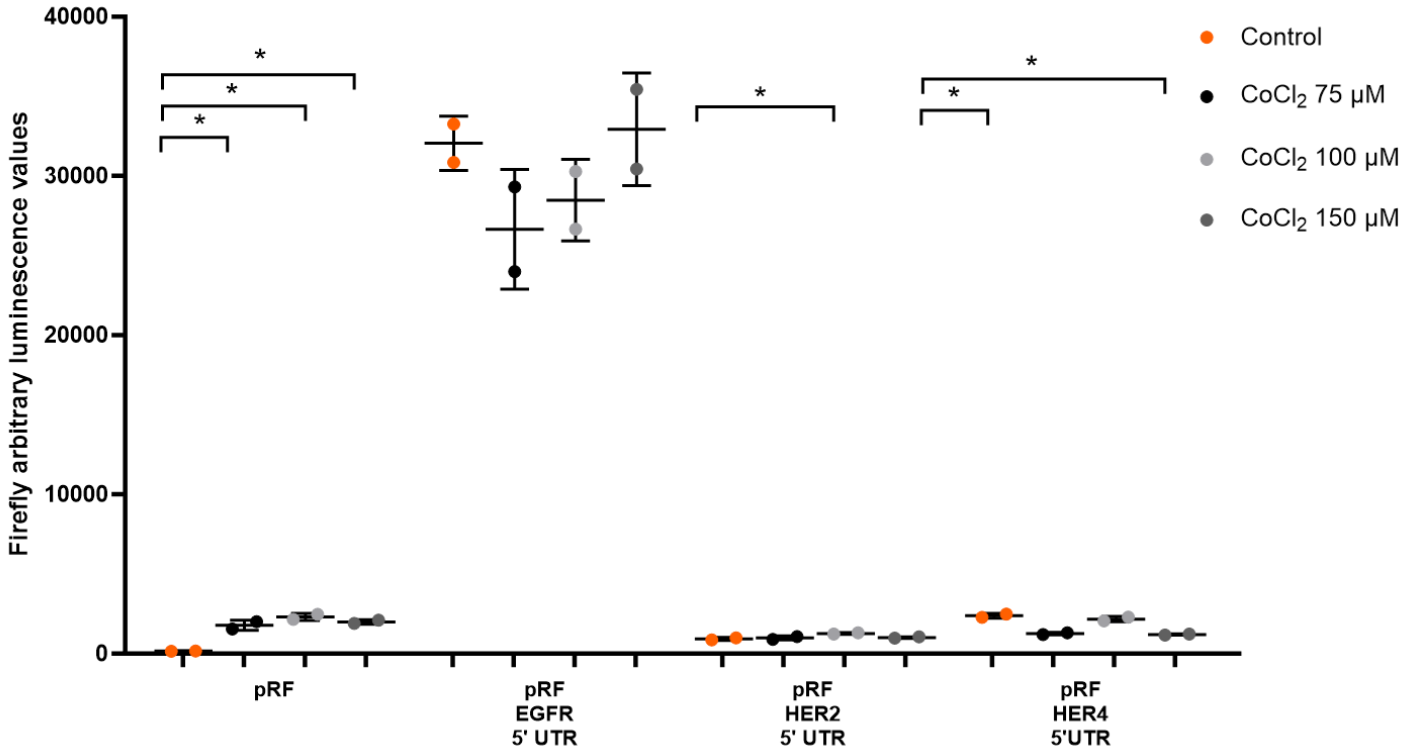

Appendix Figure 4. Raw bicistronic firefly luciferase data in response to $CoCl_2$. MCF-7 cells were transfected with bicistronic constructs containing both *Renilla* and firefly luciferase open reading frames. 24 hours post-transfection MCF-7 cells were exposed to 75 µM, 100 µM or 150 µM of $CoCl_2$ (black, light grey or dark grey respectively) or were untreated (orange) for 24 hours. Then cells were lysed and the firefly luciferase expression was measured. Data represents the average of two independent experiments each carried out in triplicate. All error bars represent the standard deviation. $p<0.05$ was determined statistically significant using a t-test with Bonferroni-Dunn's correction.

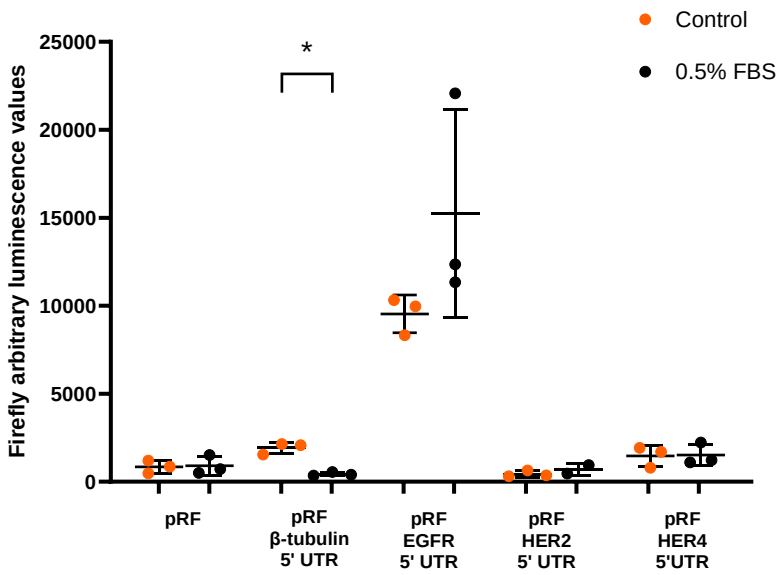

Appendix Figure 5. Raw bicistronic firefly luciferase data in response to low serum conditions. MCF-7 cells were transfected with bicistronic constructs. 24 hours later MCF-7 cells were exposed to media containing 0.5% FBS to provide low serum conditions (black) or media containing 10% FBS as a control (orange) for 24 hours. Then cells were lysed and the firefly luciferase expression was measured. Data represents the average of three biological repeats each carried out in triplicate. All error bars represent the standard deviation. $p<0.05$ was determined statistically significant using a t-test with Bonferroni-Dunn's correction.

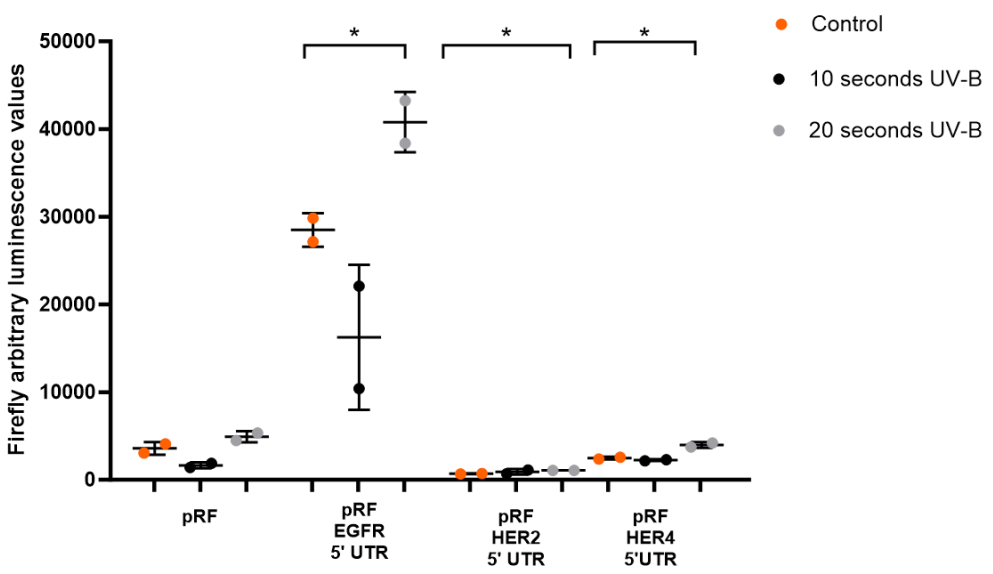

Appendix Figure 6. Raw bicistronic firefly luciferase data in response to UV radiation. MCF-7 cells were transfected with bicistronic constructs. 24 hours post-transfection MCF-7 cells were exposed to UV-B radiation (302 nm) for 10 seconds (black) or 20 seconds (grey) to induce genotoxic stress or were untreated (orange) for 24 hours. After each timepoint cells were lysed, and the firefly activity was measured. Data represents the average of two independent experiments each carried out in triplicate. All error bars represent the standard deviation. $p<0.05$ was determined as statistically significant using a t-test with Bonferroni-Dunn's correction.

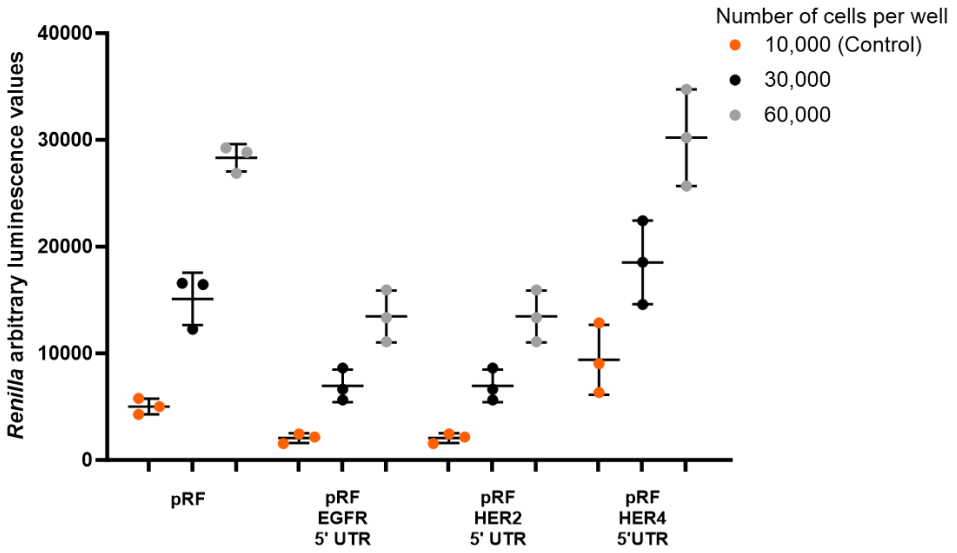

Appendix Figure 7. Raw bicistronic *Renilla* luciferase reporter data in response to high cell densities. (second independent experiment). MCF-7 cells were seeded at high cell densities; 30,000 (black) and 60,000 (grey) or at the original cell density of 10,000 cells per well (orange). 24 hours later MCF-7 cells were transfected with bicistronic constructs. 24 hours post-transfection cells were lysed, and the *Renilla* luciferase expression was measured. Data of one independent experiment carried out in triplicate but representative of two independent experiments.

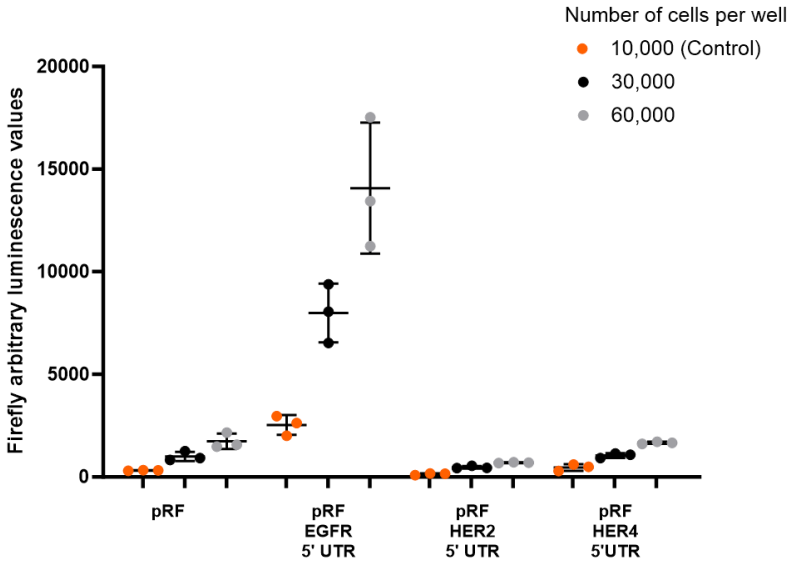

Appendix Figure 8. Raw bicistronic firefly luciferase reporter data in response to high cell densities. (first independent experiment-data corresponding to Figures 3.19-3.20). MCF-7 cells were seeded at high cell densities; 30,000 (black) and 60,000 (grey) or at the original cell density of 10,000 cells per well (orange). 24 hours later MCF-7 cells were transfected with bicistronic constructs. 24 hours post-transfection cells were lysed, and the firefly activity was measured. Data of one independent experiment carried out in triplicate but representative of two independent experiments.

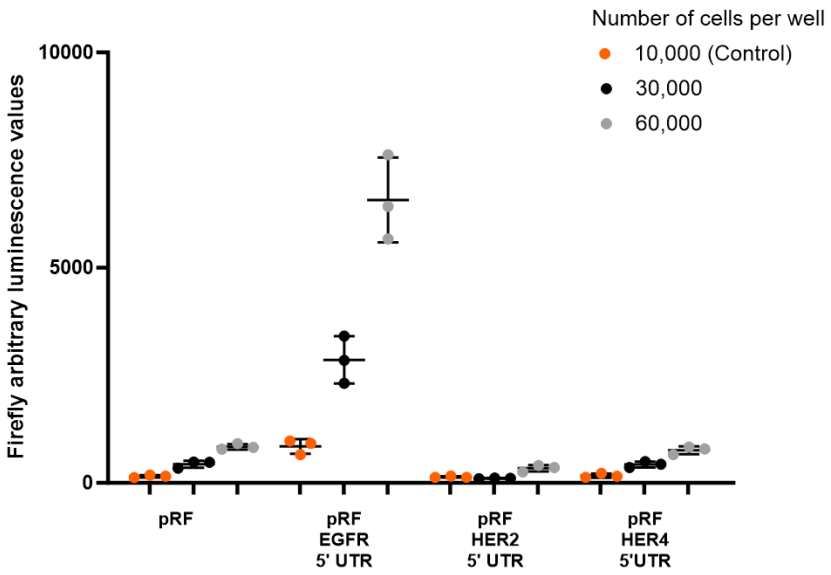

Appendix Figure 9. Raw bicistronic firefly luciferase reporter data in response to high cell densities from a second independent experiment. MCF-7 cells were seeded at high cell densities; 30,000 (black) and 60,000 (grey) or at the original cell density of 10,000 cells per well (orange). 24 hours later MCF-7 cells were transfected with bicistronic constructs. 24 hours post-transfection cells were lysed, and the firefly activity was measured. Data of one independent experiment carried out in triplicate but representative of two independent experiments.

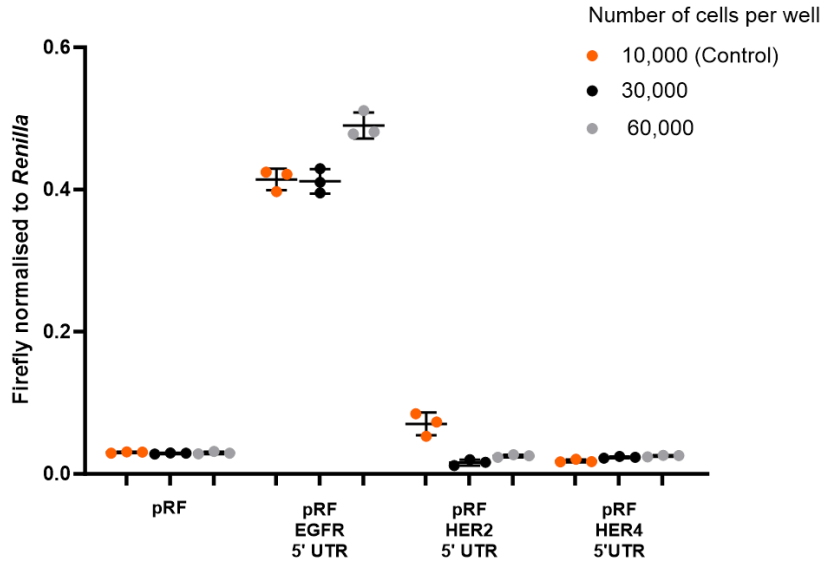

Appendix Figure 10. F/R data in response to high cell densities from a second independent experiment. MCF-7 cells were seeded at high cell densities; 30,000 (black) and 60,000 (grey) or at the original cell density of 10,000 cells per well (orange). 24 hours later MCF-7 cells were transfected with bicistronic constructs. 24 hours post-transfection cells were lysed, and the F/R activity was measured. Data represents one independent experiment carried out in triplicate.

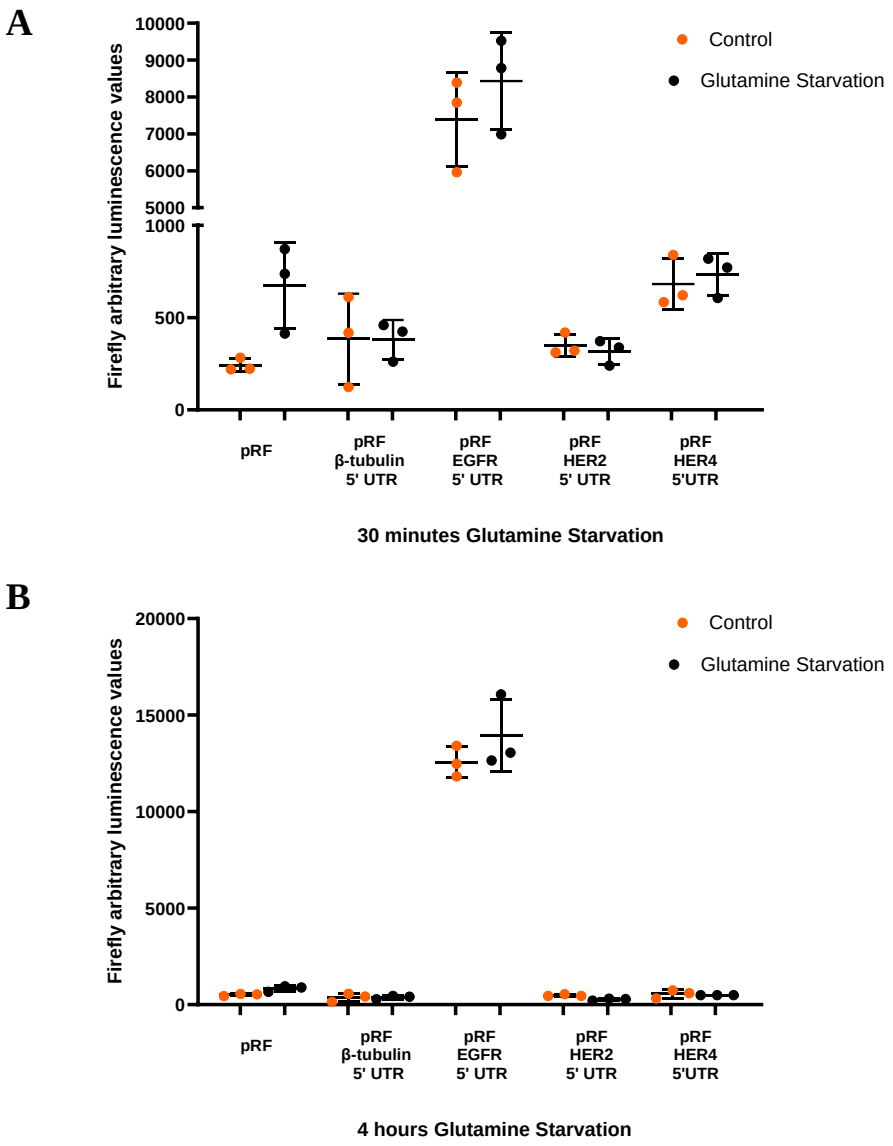

Appendix Figure 11. Raw bicistronic firefly luciferase reporter data in response to short-term glutamine starvation. MCF-7 cells were transfected with each bicistronic construct. 24 hours post-transfection cells were starved of glutamine for 30 minutes or 4 hours (black) or non-starved (orange). After each timepoint cells were then lysed, and the firefly expression was measured. A) 30 minutes of glutamine starvation. B) 4 hours of glutamine starvation. Data represents one independent experiment carried out in triplicate. All error bars represent the standard deviation.

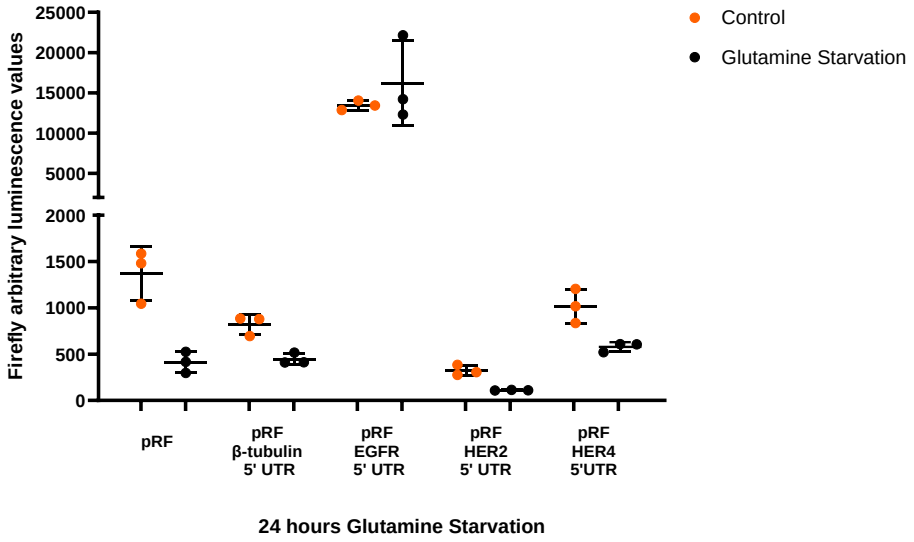

Appendix Figure 12. Raw bicistronic firefly luciferase reporter data in response to 24 hours of glutamine starvation. MCF-7 cells were transfected with each bicistronic construct. 24 hours post-transfection cells were starved of glutamine for 24 hours (black) or non-starved (orange). Cells were then lysed, and the firefly expression was measured. Data represents one independent experiment carried out in triplicate. All error bars represent the standard deviation.

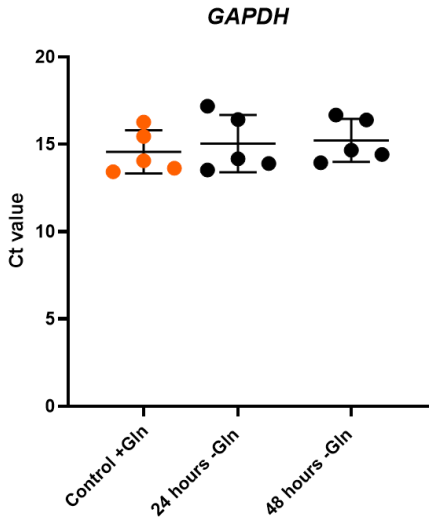

Appendix Figure 13. Glutamine starvation experiment: Raw Ct values for GAPDH. MCF-7 cells were incubated in media containing glutamine (+Gln) for 24 hours as a control (orange) or cells were starved of glutamine (-Gln) for 24 hours or 48 hours (black). After each timepoint total RNA was extracted before being reverse transcribed into cDNA which was used as the qPCR template. Data represents the average of five independent experiments each carried out in triplicate. All error bars represent the standard deviation. $p<0.05$ was determined as statistically significant (*). A Mann-Whitney t-test with Bonferroni-Dunn's correction was used for comparisons of two groups: 24 hours and 48 hours of glutamine starvation conditions compared separately to the 24 hour non-starvation control. No statistical significance was determined for GAPDH in response to glutamine starvation.

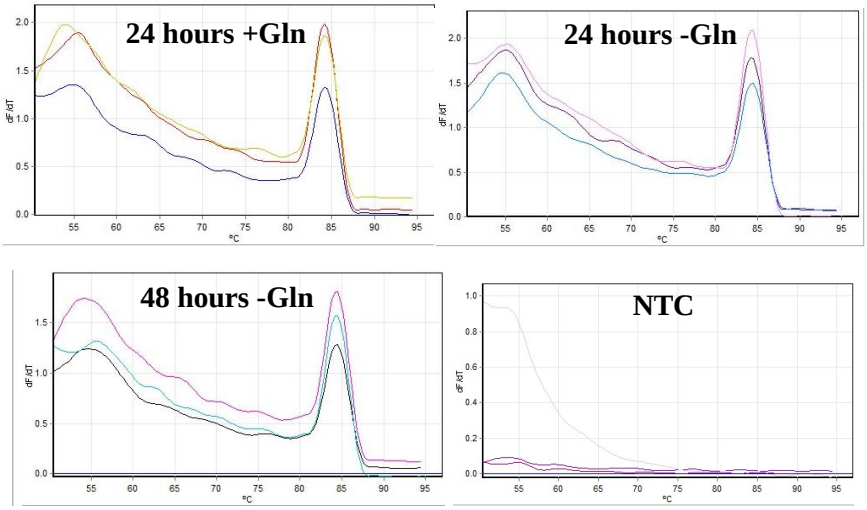

Appendix-Figure 14. Melt curves for qPCR primers targeting GAPDH house-keeping gene in response to glutamine starvation or control. Representative melt curve from a single experiment. +Gln= non-starvation (with glutamine), -Gln= glutamine starvation, NTC= non-template control.

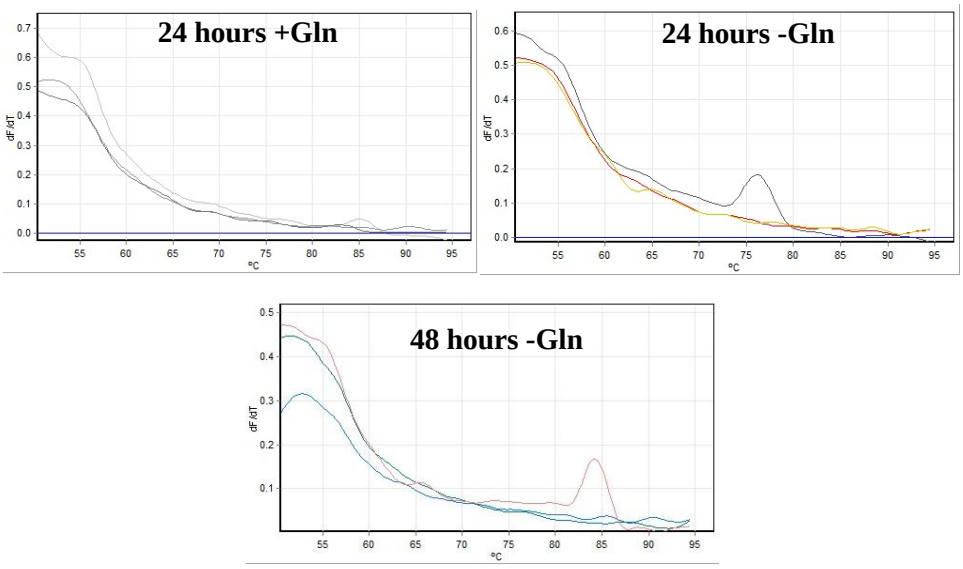

Appendix-Figure 15. -RT control melt curves for qPCR primers targeting GAPDH house-keeping gene in response to glutamine starvation or control. Representative melt curve from a single experiment. +Gln= non-starvation (with glutamine), -Gln= glutamine starvation.

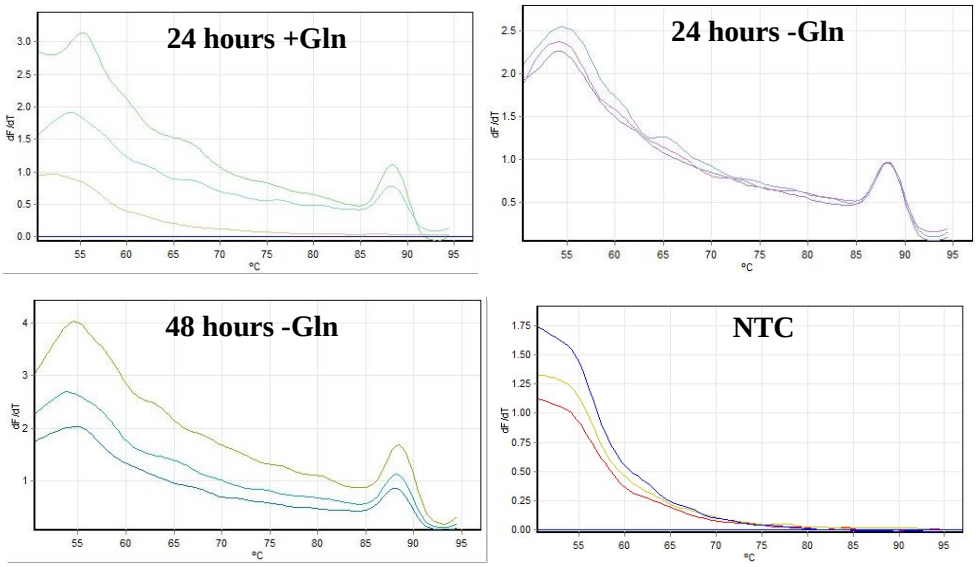

Appendix-Figure 16. Melt curves for qPCR primers targeting *β-actin* reference gene in response to glutamine starvation or control. Representative melt curve from a single experiment. +Gln= non-starvation (with glutamine), -Gln= glutamine starvation , NTC= non-template control.

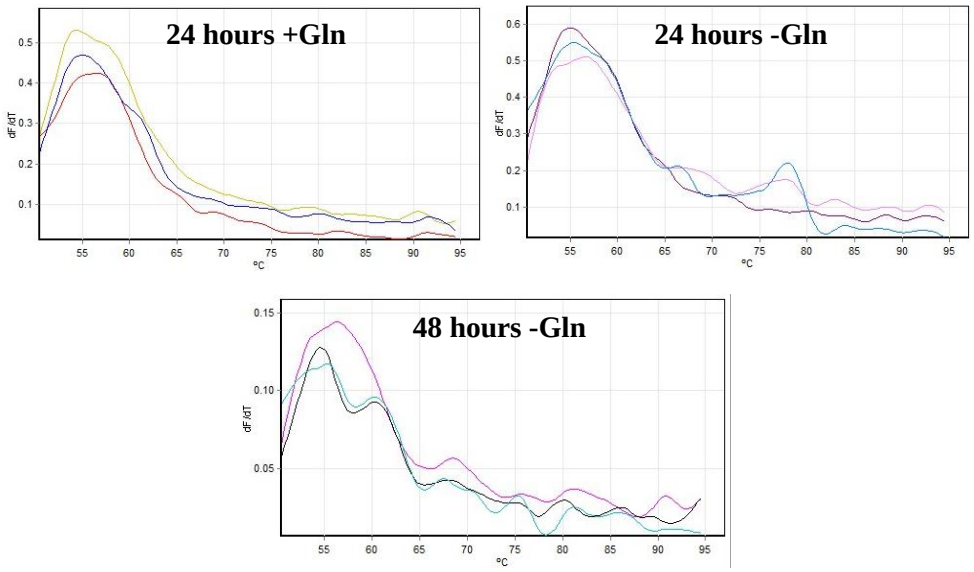

Appendix-Figure 17. -RT control melt curves for qPCR primers targeting *β-actin* reference gene in response to glutamine starvation or control. Representative melt curve from a single experiment. +Gln= non-starvation (with glutamine), -Gln= glutamine starvation.

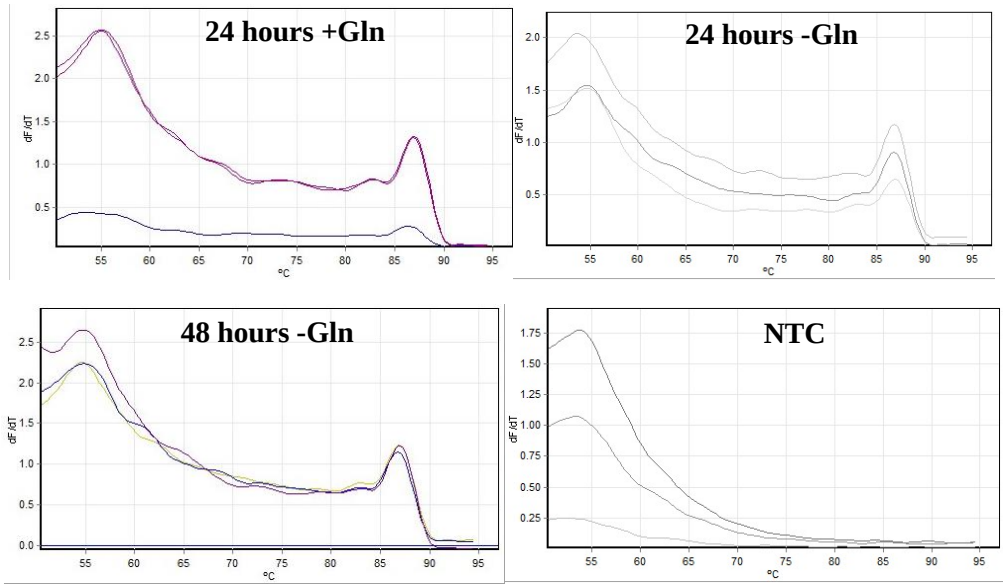

Appendix-Figure 18. Melt curves for qPCR primers targeting *HER2* mRNA in response to glutamine starvation or control. Representative melt curve from a single experiment. +Gln= non-starvation (with glutamine), -Gln= glutamine starvation, NTC= non-template control.

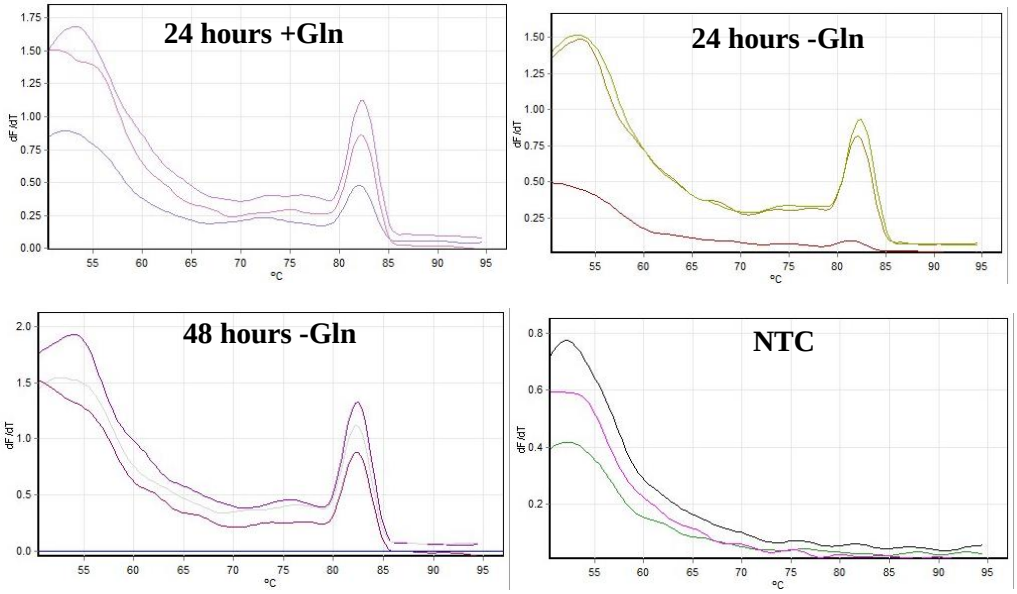

Appendix-Figure 19. Melt curves for qPCR primers targeting *HER4* mRNA in response to glutamine starvation or control. Representative melt curve from a single experiment. +Gln= non-starvation (with glutamine), -Gln= glutamine starvation, NTC= non-template control.

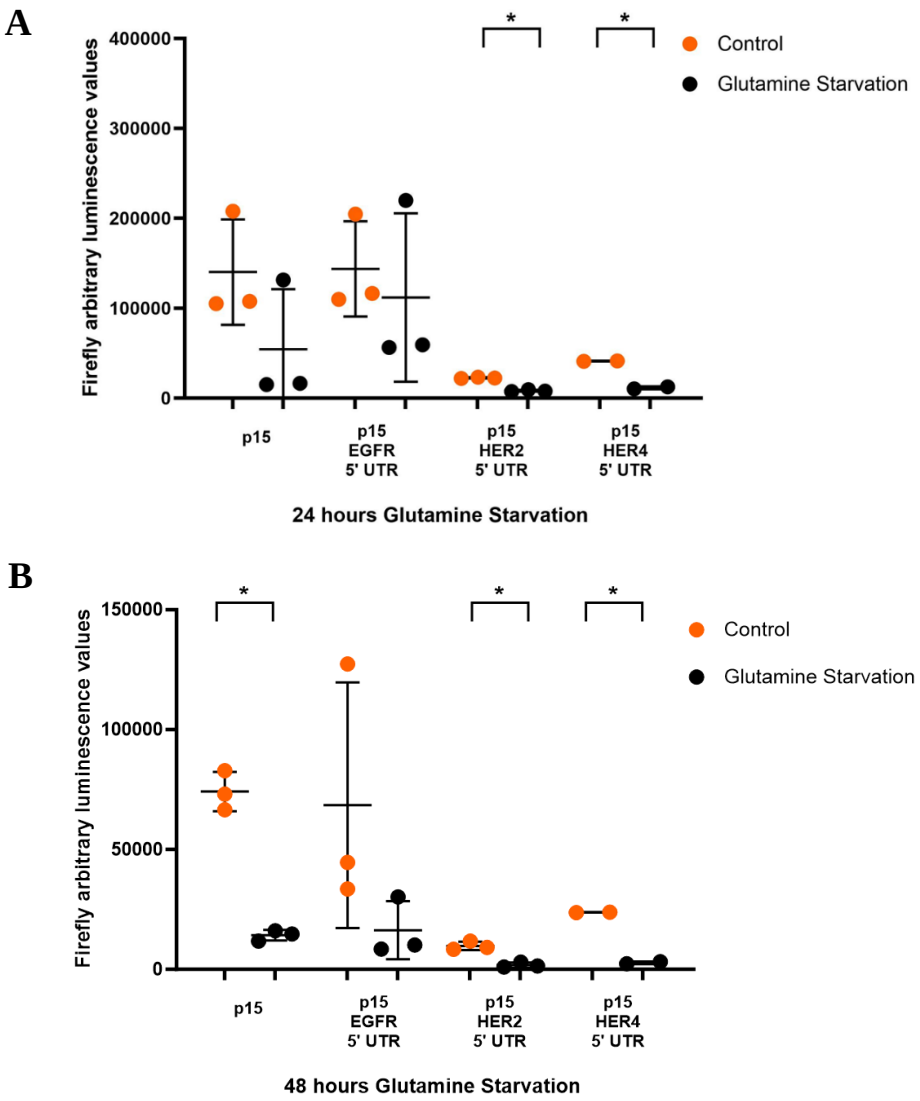

Appendix Figure 20. Raw monocistronic firefly luciferase reporter data in response in response to 24 and 48 hours of glutamine starvation. MCF-7 cells were transfected with firefly monocistronic constructs containing the 5' UTRs and co-transfected with p80 *Renilla* luciferase construct. 24 hours later were exposed to either DMEM containing glutamine control media (orange) or DMEM containing no glutamine media (black). After each timepoint cells were lysed, and the firefly expression was measured. A) 24 hours of glutamine starvation. B) 48 hours of glutamine starvation. Data represents the average of two-three independent experiments each carried out in triplicate. All error bars represent the standard deviation. $p<0.05$ was determined as statistically significant (*). A t-test with Bonferroni-Dunn's correction was used for comparisons of each construct in starvation conditions compared to their non-starvation control.

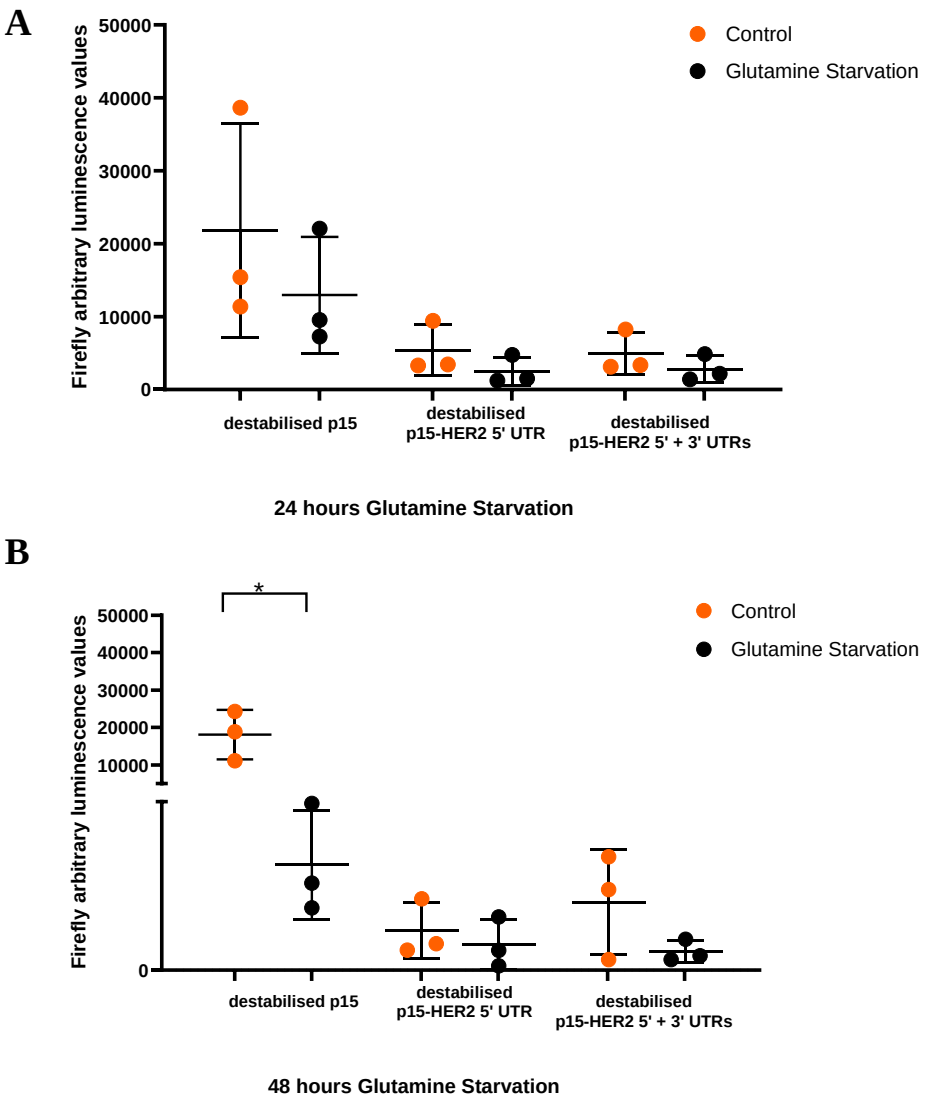

Appendix Figure 21. Raw destabilised monocistronic firefly luciferase reporter data in response to 24 and 48 hours of glutamine starvation. MCF-7 cells were transfected for 24 hours with destabilised firefly monocistronic constructs; destabilised p15, destabilised p15-*HER2* 5' UTR and destabilised *HER2* 5' + 3' UTR and co-transfected with p80 *Renilla* luciferase construct. After each timepoint cells were lysed after being exposed to DMEM containing glutamine (orange) or DMEM containing no glutamine (black). A) 24 hours of glutamine starvation. B) 48 hours of glutamine starvation. Then the firefly activity was measured. Data represents the average of three independent experiments each carried out in triplicate. All error bars represent the standard deviation. $p<0.05$ was determined as statistically significant using a t-test with Bonferroni-Dunn's correction.

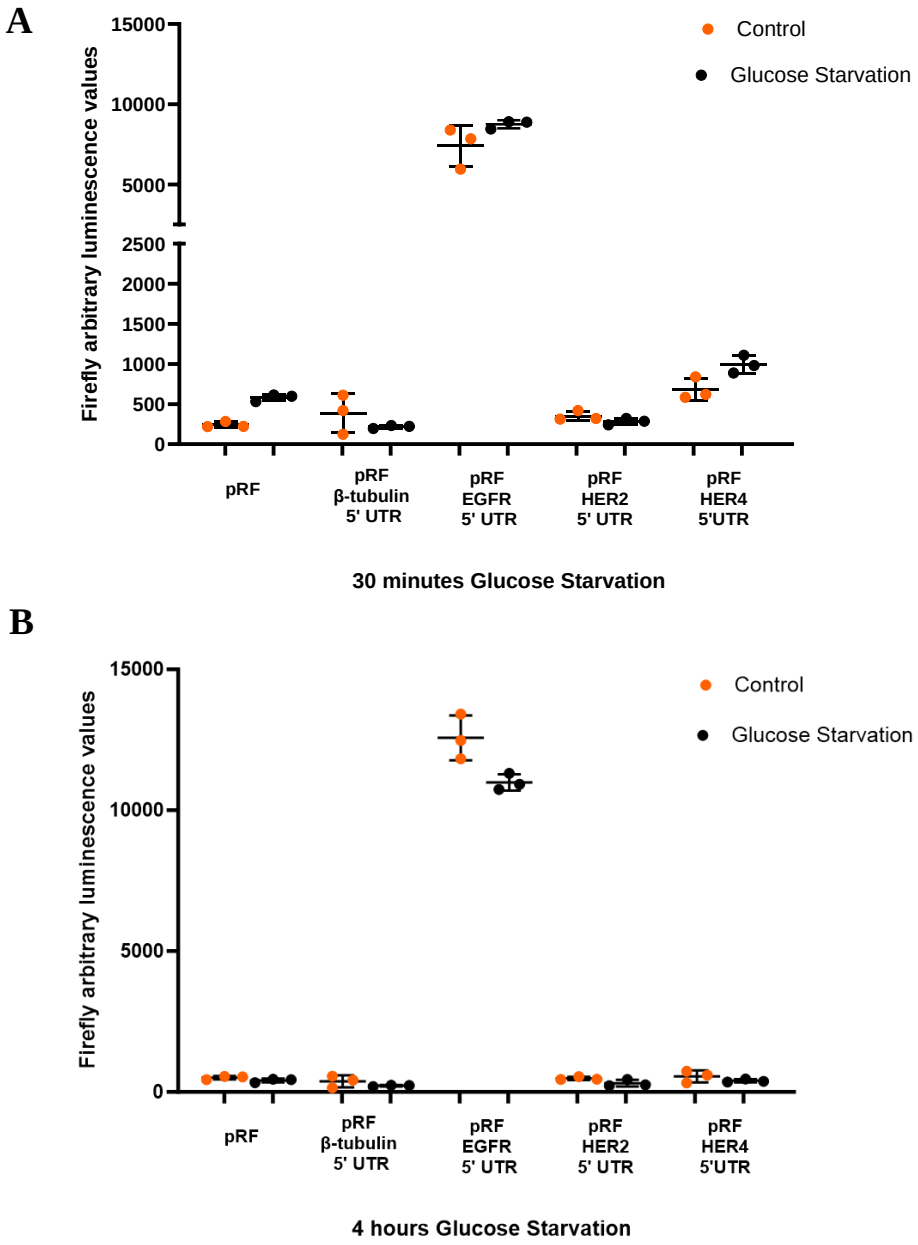

Appendix Figure 22. Raw bicistronic firefly luciferase reporter data in response to glucose starvation. MCF-7 cells were transfected with bicistronic constructs containing both *Renilla* and firefly luciferase open reading frames. 24 hours post-transfection MCF-7 cells were exposed to either DMEM media containing glucose (orange) or DMEM containing no glucose (black). A) 30 minutes of glucose starvation. B) 4 hours of glucose starvation. After each timepoint cells were lysed, and the firefly expression was measured. Data represents one independent experiment carried out in triplicate. All error bars represent the standard deviation.

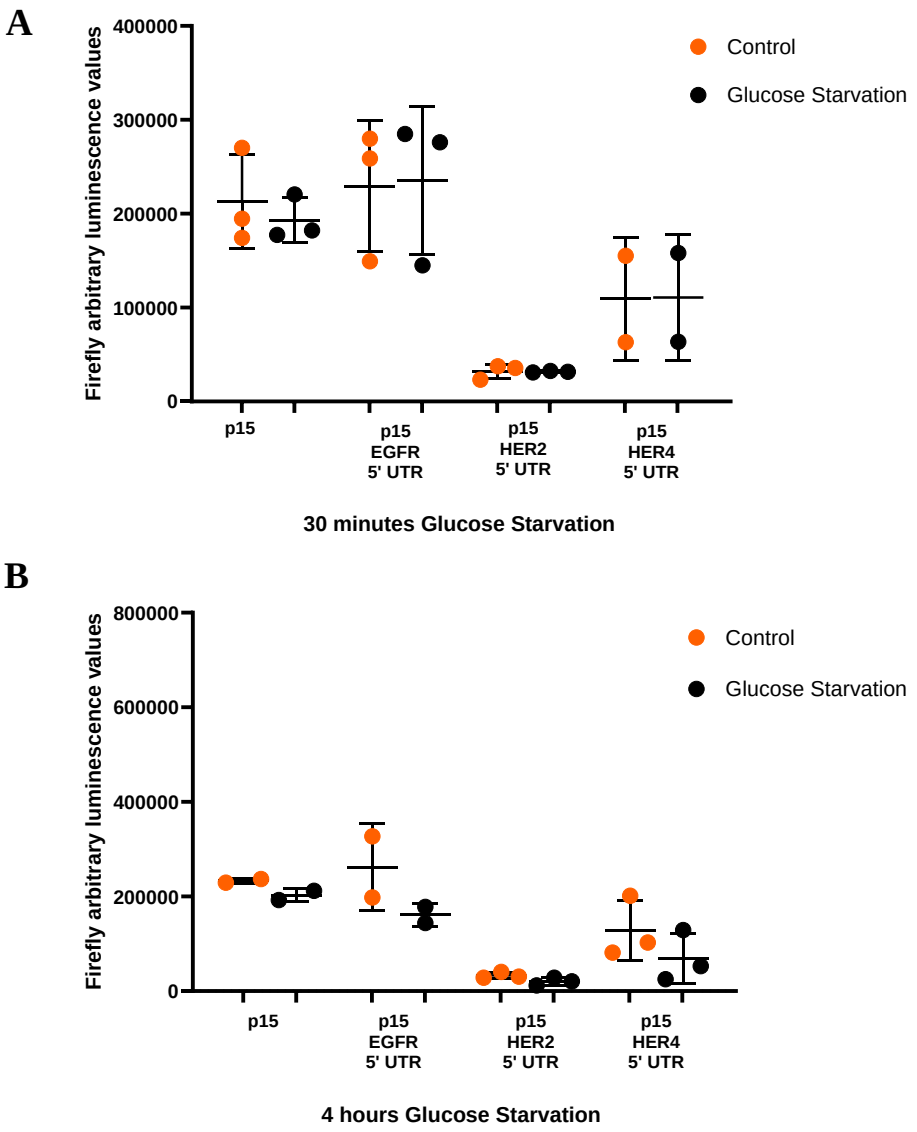

Appendix Figure 23. Raw monocistronic firefly luciferase reporter data in response to glucose starvation. MCF-7 cells were transfected with firefly monocistronic constructs containing the 5' UTRs and co-transfected with p80 *Renilla* luciferase construct and 24 hours later were exposed to either DMEM containing glucose control media (orange) or DMEM containing no glucose media (black). After each timepoint cells were lysed, and the firefly expression was measured. A) 30 minutes of glucose starvation. B) 4 hours of glucose starvation. Data represents the average of two-three independent experiments each carried out in triplicate. All error bars represent the standard deviation. $p<0.05$ was determined as statistically significant. A t-test with Bonferroni-Dunn's correction was used for comparisons of each construct in starvation conditions compared to their non-starvation control.

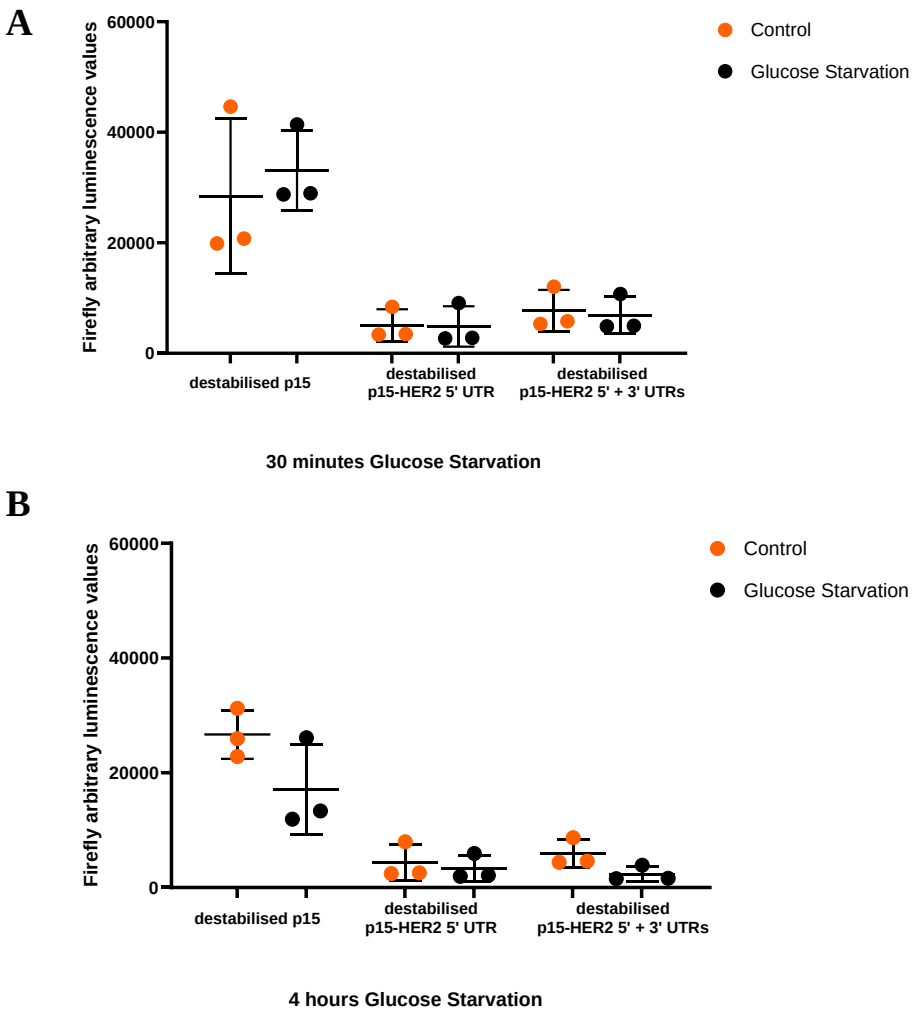

Appendix Figure 24. Raw destabilised monocistronic firefly luciferase reporter data in glucose starvation conditions. MCF-7 cells transfected for 24 hours with destabilised firefly monocistronic construct and co-transfected with p80 *Renilla* luciferase construct. Cells were then exposed to DMEM containing glucose (orange) or DMEM containing no glucose (black). A) 30 minutes of glucose starvation, B) 4 hours of glucose starvation. After each timepoint cells were lysed, and the firefly expression was measured. Data represents the average of three independent experiments each carried out in triplicate. All error bars represent the standard deviation. $p<0.05$ was determined as statistically significant (*). A t-test with Bonferroni-Dunn's correction was used for comparisons of each construct in starvation conditions compared to their non-starvation control.

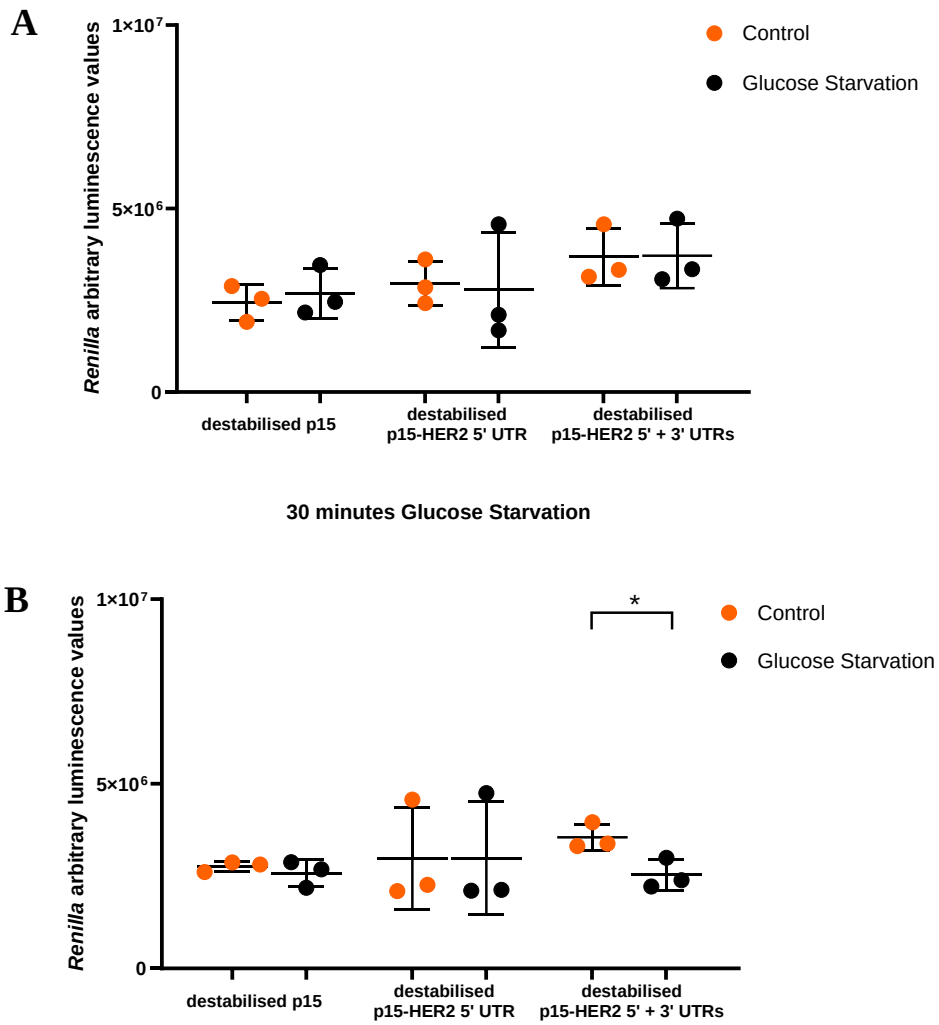

Appendix Figure 25. Raw monocistronic *Renilla* luciferase data co-transfected with destabilised firefly reporters in glucose starvation conditions. MCF-7 cells transfected for 24 hours with destabilised firefly monocistronic construct and co-transfected with p80 *Renilla* luciferase construct. Cells were then exposed to DMEM containing glucose (orange) or DMEM containing no glucose (black). A) 30 minutes of glucose starvation, B) 4 hours of glucose starvation. After each timepoint cells were lysed, and the *Renilla* expression was measured. Data represents the average of three independent experiments each carried out in triplicate. All error bars represent the standard deviation. $p<0.05$ was determined as statistically significant (*). A t-test with Bonferroni-Dunn's correction was used for comparisons of each construct in starvation conditions compared to their non-starvation control.

Appendix -Table 1. Fold increase of the average arbitrary firefly units of MCF-7 cells transfected with destabilised p15 constructs compared to untransfected MCF-7 cells in non-starvation conditions.

	destabilised p15	**destabilised p15-*HER2* 5' UTR**	**destabilised p15-*HER2* 3+5' UTR**
24 hours control	2846.3	702.5	636.7
48 hours control	1356.1	87.5	163.6

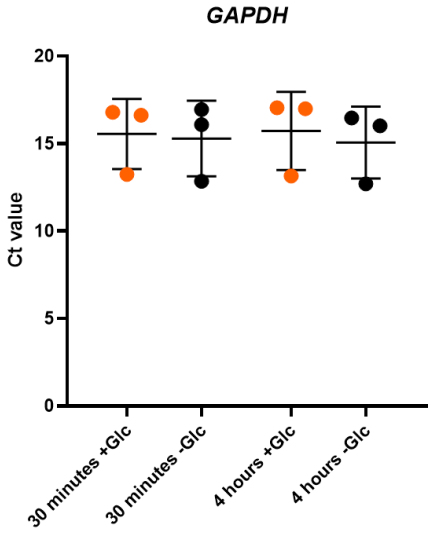

Appendix Figure 26. Glucose starvation experiment: Raw Ct values for GAPDH. MCF-7 cells were incubated in media containing glucose (+Glc) for 30 minutes or 4 hours as a control (orange) or cells were starved of glucose (-Glc) for 30 minutes or 4 hours (black). After each timepoint total RNA was extracted before being reverse transcribed into cDNA which was used as the qPCR template. Data represents the average of three independent experiments carried out in triplicate. $p<0.05$ was determined as statistically significant (*). A Mann-Whitney t-test with Bonferroni-Dunn's correction was used for comparisons of two groups: 30 minutes or 4 hours of glucose starvation to the 30 minute or 4 hour control respectively. No statistical significance was determined for GAPDH in response to glucose starvation.

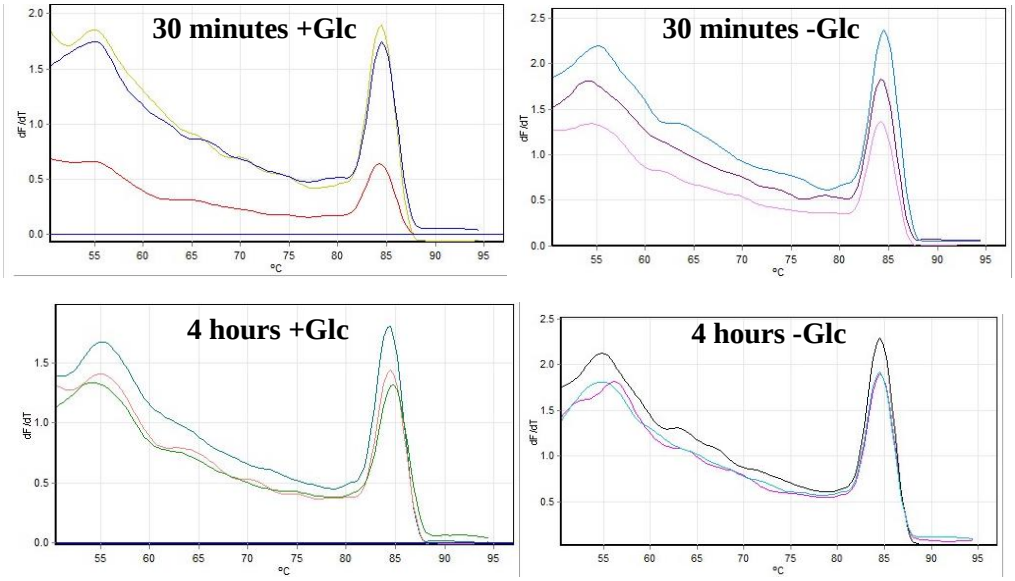

Appendix-Figure 27. Melt curves for qPCR primers targeting GAPDH house-keeping gene in response to glucose starvation or control. Representative melt curve from a single experiment. +Glc= non-starvation (with glucose), -Glc= glucose starvation.

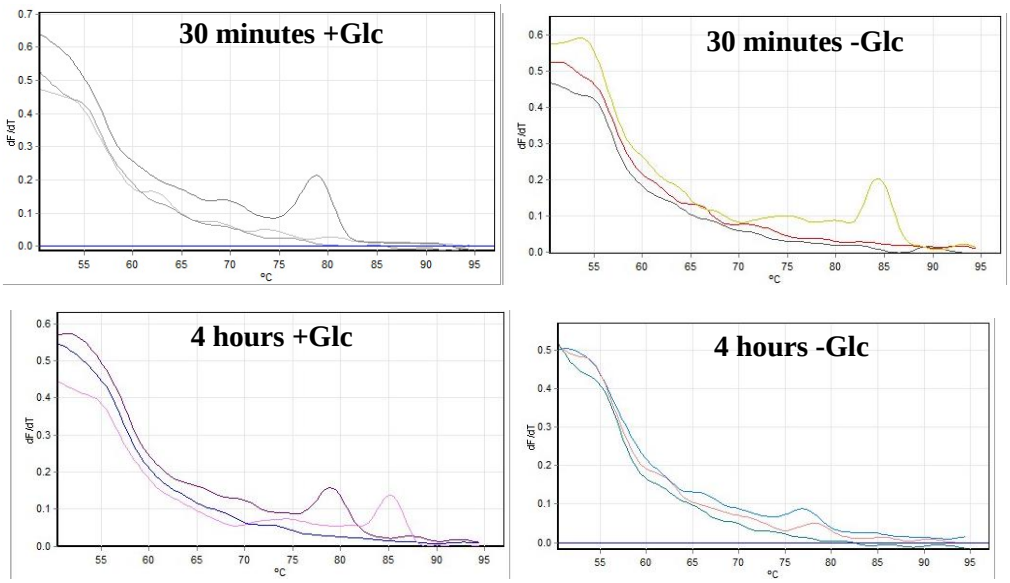

Appendix-Figure 28. -RT control melt curves for qPCR primers targeting GAPDH house-keeping gene in response to glucose starvation or control. Representative melt curve from a single experiment. +Glc= non-starvation (with glucose), -Glc= glucose starvation.

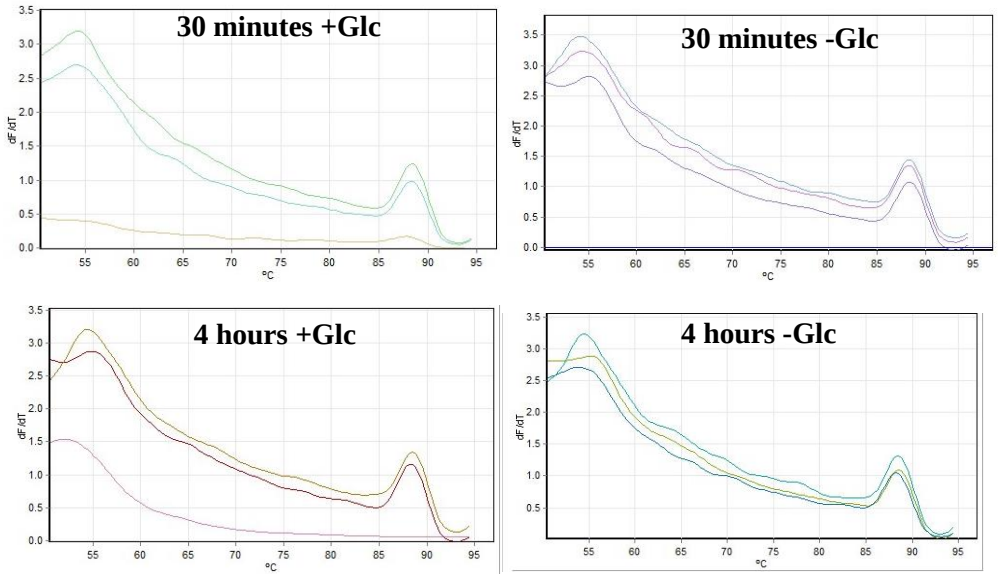

Appendix-Figure 29. Melt curves for qPCR primers targeting *β-actin* reference gene in response to glucose starvation or control. Representative melt curve from a single experiment. +Glc= non-starvation (with glucose),-Glc= glucose starvation. NTC= non-template control.

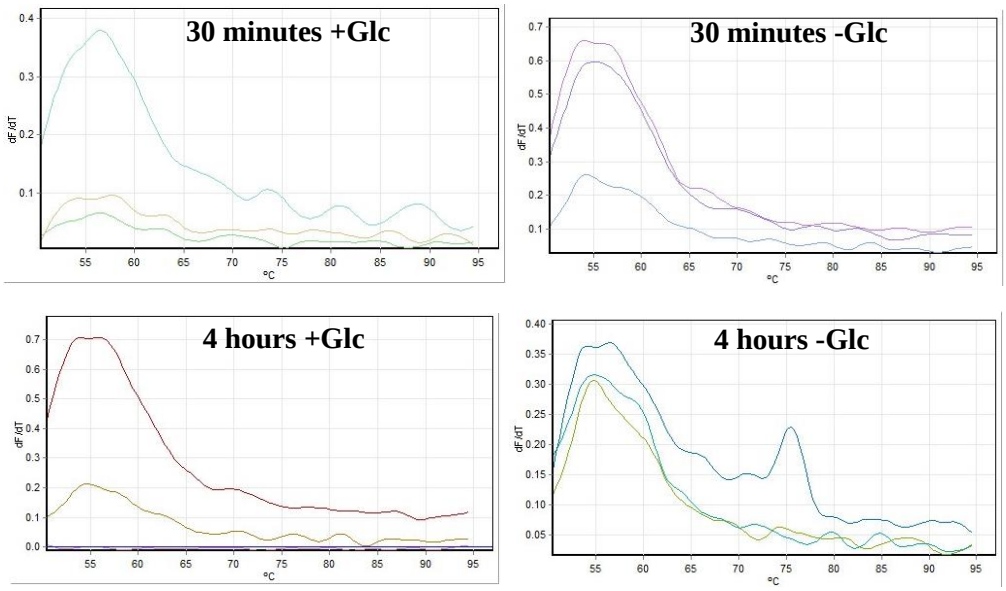

Appendix-Figure 30. -RT control melt curves for qPCR primers targeting *β-actin* reference gene in response to glucose starvation or control. +Glc= non-starvation (with glucose), -Glc= glucose starvation. Representative melt curve from a single experiment.

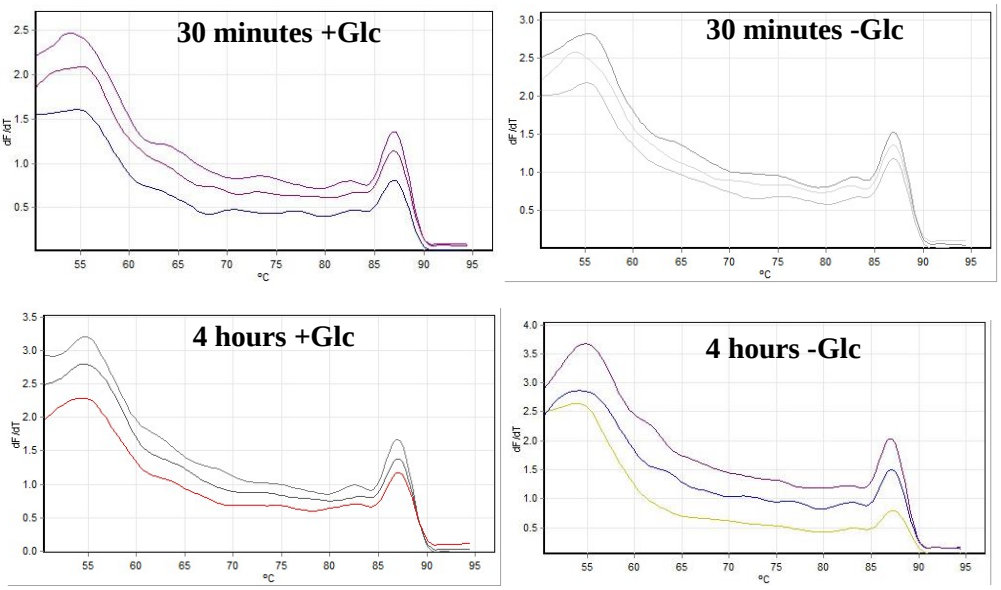

Appendix-Figure 31. Melt curves for qPCR primers targeting *HER2* mRNA in response to glucose starvation or control. Representative melt curve from a single experiment. +Glc= non-starvation (with glucose), -Glc= glucose starvation. NTC= non-template control.

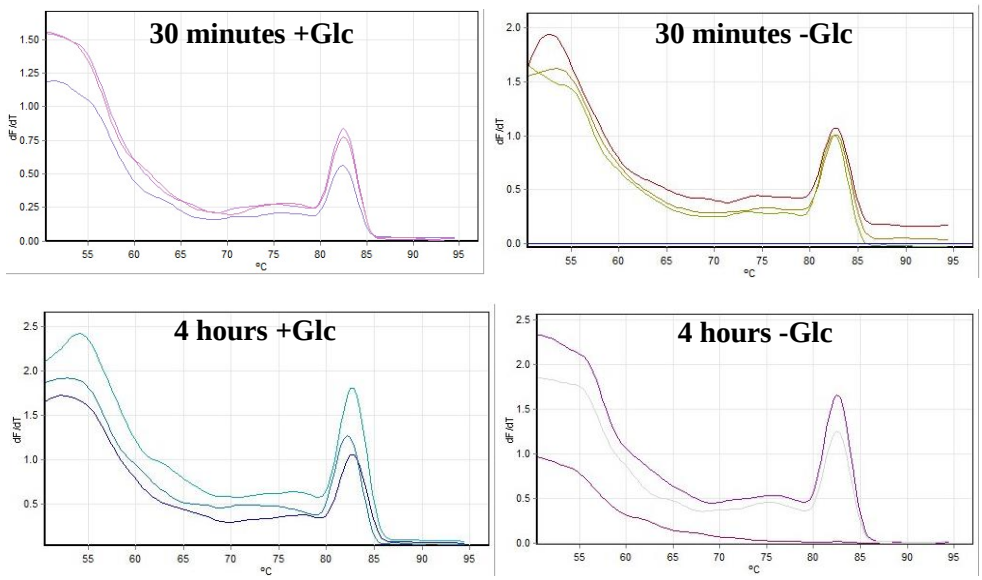

Appendix-Figure 32. Melt curves for qPCR primers targeting *HER4* mRNA in response to glucose starvation or control. Representative melt curve from a single experiment. +Glc= non-starvation (with glucose), -Glc= glucose starvation. NTC= non-template control.

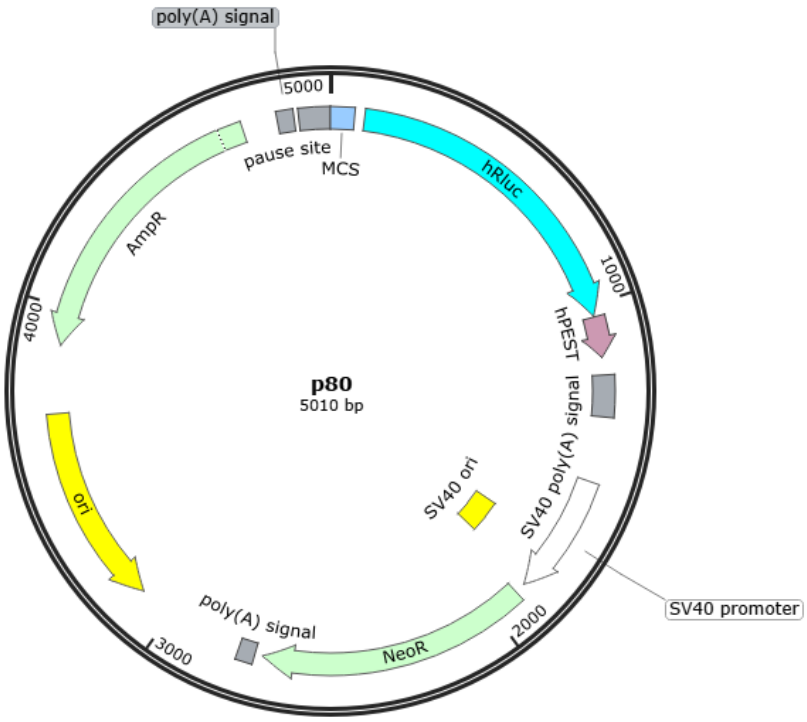

Appendix-Figure 33. Monocistronic *Renilla* construct-p80 vector map. p80 originally from pGL4.180 with a cytomegalovirus (CMV) promoter upstream to *Renilla* luciferase. p80 was used as a transfection control to normalise the firefly expression from p15 and destabilised p15 constructs.

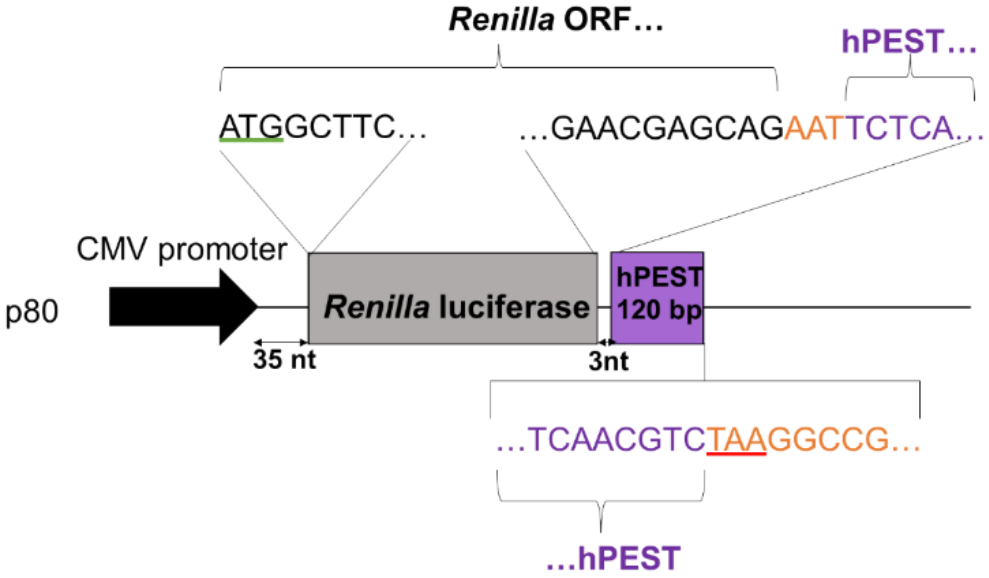

Appendix-Figure 34. Schematic of monocistronic *Renilla* constructs used in the project. p80 contained *Renilla* luciferase downstream to the CMV promotor and was used as a co-transfection control. Start codons are underlined green and stop codons are underlined red.

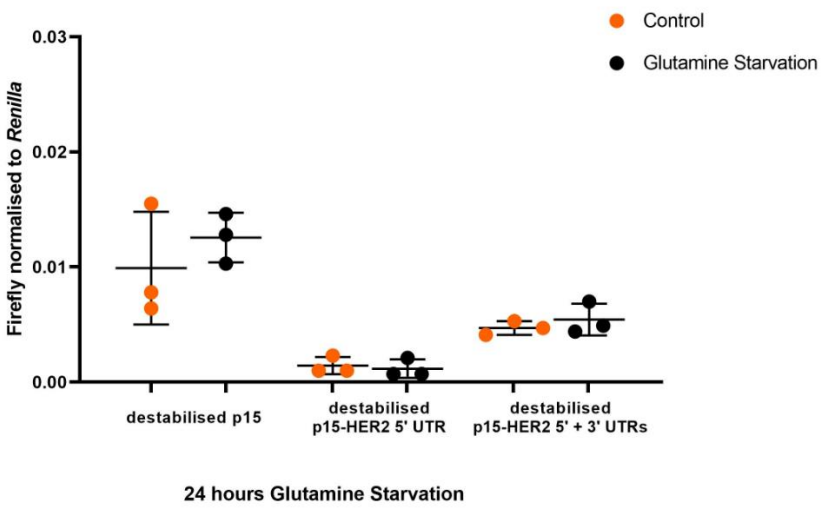

Appendix-Figure 35. *HER2* 3' UTR does derepress *HER2* 5' UTR under non-starvation conditions and in response to glutamine starvation. MCF-7 cells were transfected for 24 hours with destabilised firefly monocistronic constructs; destabilised p15, destabilised p15-*HER2* 5' UTR and destabilised *HER2* 5' + 3' UTR and co-transfected with p80 *Renilla* luciferase construct. Cells were lysed after being exposed to DMEM containing glutamine (orange) or DMEM containing no glutamine (black) for 24 hours. Then the F/R activity was measured. Data represents one independent experiment carried out in triplicate. All error bars represent the standard deviation.

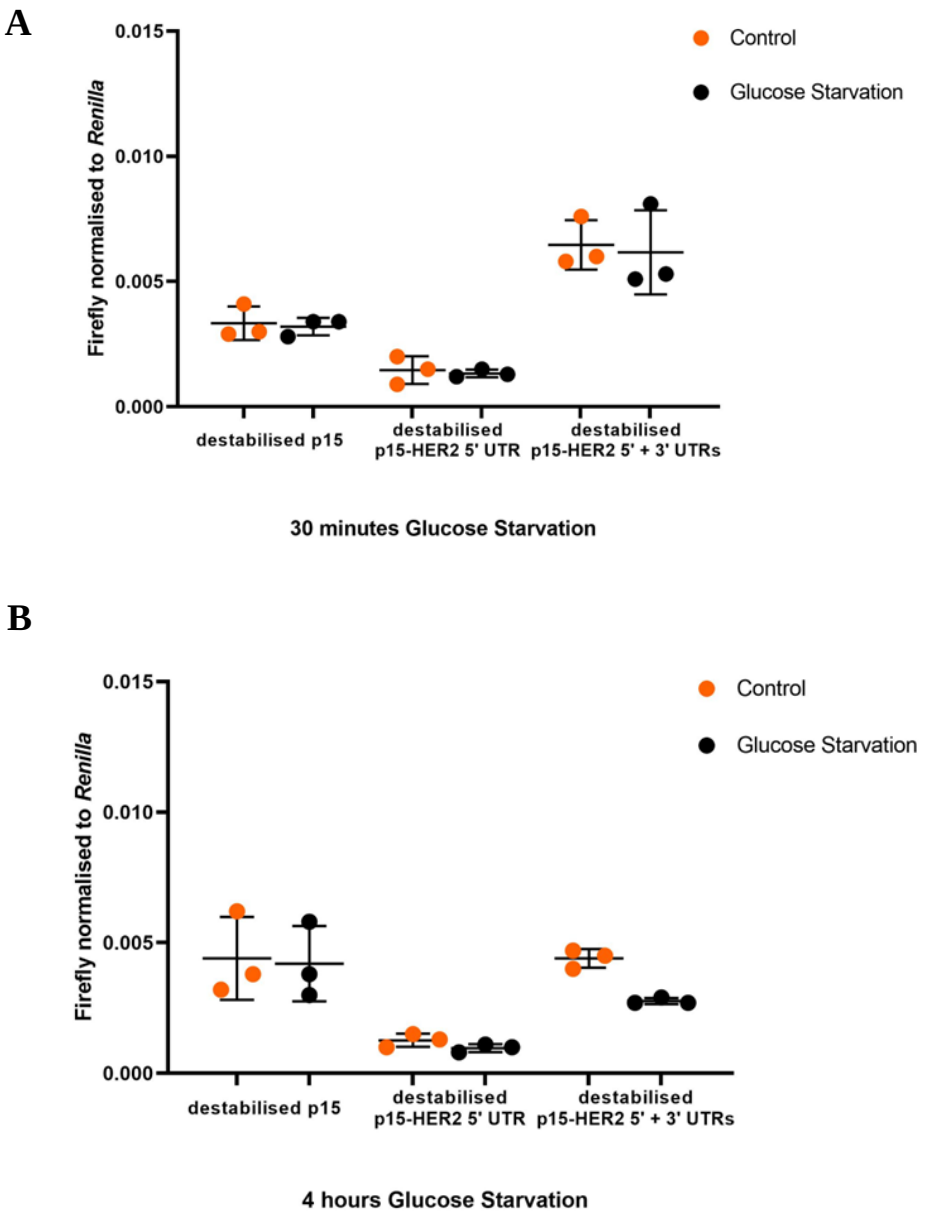

Appendix-Figure 36. *HER2* 3' UTR derepresses translation and mediates a decrease in translation in response to 4 hours of glucose starvation. MCF-7 cells transfected for 24 hours with destabilised firefly monocistronic construct and co-transfected with p80 *Renilla* luciferase construct. Cells were then exposed to DMEM containing glucose (orange) or DMEM containing no glucose (black). A) 30 minutes of glucose starvation. B) 4 hours of glucose starvation. After each timepoint cells were lysed, and the F/R expression was measured. Data represents one independent experiment carried out in triplicate. All error bars represent the standard deviation.

Appendix Table 2. Sequencing primers

Sequencing Primer Name	Sequences (5'-3')
RNase (F)	GCAAGAAGATGCACCTGATG
T7 promoter (F)	TAATACGACTCACTATAGGG
CL1-PEST (F)	ACGGTAAAACCATGACCGAG
HER2 3' UTR (F)	TTCCCTCCCGAGGTGGAG

Appendix-Figure 37. Sequencing data of cloning *HER2* 5' UTR into pRF bicistronic plasmid. Part of pRF sequence= green. *HER2* 5' UTR sequence=blue. Part of firefly luciferase sequence= red. Sequenced with RNase F primer.

NNNNNNNNNNCGTTCGTTGAGCGAGTTCTCAAAATGAACAATAATTCTAGAGCTTATCGA
TACCGTCGACCTCGAATCACTAGTCAGCTGGAATTCGCTTGCTCCCAATCACAGGAGAAG
GAGGAGGTGGAGGAGGAGGGCTGCTTGAGGAAGTATAAGAATGAAGTTGTGAAGCTGAGA
TTCCCCTCCATTGGGACCGGAGAAACCAGGGGAGCCCCCCGGGCAGCCGCGCGCCCCTTC
CCACGGGGCCCTTTACTGCGCCGCGCGCCCGGCCCCCACCCCTCGCAGCACCCCGCGCCC
CGCGCCCTCCCAGCCGGGTCCAGCCGGAGCCATGGGGCCGGAGCCGCAGTGAGCACCATG
TCATGGAAGACGCCAAAAACATAAAGAAAGGCCCGGCGCCATTCTATCCGCTGGAAGATG
GAACCGCTGGAGAGCAACTGCATAAGGCTATGAAGAGATACGCCCTGGTTCCTGGAACAA
TTGCTTTTACAGATGCACATATCGAGGTGGACATCACTTACGCTGAGTACTTCGAAATGT
CCGTTCGGTTGGCAGAAGCTATGAAACGATATGGGCTGAATACAAATCACAGAATCGTCG
TATGCAGTGAAAACTCTCTTCAATTCTTTATGCCGGTGTTGGGCGCGTTATTTATCGGAG
TTGCAGTTGCGCCCGCGAACGACATTTATAATGAACGTGAATTGCTCAACAGTATGGGCA
TTTCGCAGCCTACCGTGGTGTTCGTTTCCAAAAAGGGGTTGCAAAAAATTTTGAACGTGC
AAAAAAAGCTCCCAATCATCCAAAAAATTATTATCATGGATTCTAAAACGGATTACCAGG
GATTTCAGTCGATGTACACGTTCGTCACATCTCATCTACCTCCCGGTTTTAATGAATACG
ATTTTGTGCCAGAGTCCTTCGATAGGGACAAGACAATTGCACTGATCATGAACTCCTCTG
GATCTACTGGTCTGCCTAAAGGTGTCGCTCTGCCTCATAGAACTGCCTGCGTGAGATTCT
CGCATGCCAGAGATCCTATTTTTGGCAATCAAATCATTCCGGATACTGCGATTTTAAGTG
TTGTTCCATTCCATCACGGTTTTGGAATGTTTACTACACTCGGATATTTGATATGTGGAT
TTCGAGTCGTCTTAATGTATAGATTTGAAGAAGAGCTGTTTCTGAGGAGCCTTCAGGATT
ACAAGATTCAAAGTGCGCTGCTGGTGCCAACCCTATTCTCCTTCTTCGCCAAAAGCACTC
TGATTGACAAATACGATTTATCTAATTTACACGAAATTGCTTCTGGTGGCGCTCCCCTCT
CTAAGGAAGTCGGGGAANCGGTTGCCAAGAGGTTCCANCTGCCAGGTATCNGGCAAGGAN
NTGGGNCTNCCTGAGACTANNNNCANNNNTTNNGANTNNCCCCCAAGGGGNANNNAAAAA
C

Appendix-Figure 38. Sequencing data of cloning *HER4* 5' UTR into pRF bicistronic plasmid. Part of pRF sequence= green. *HER4* 5' UTR sequence= blue. Part of firefly luciferase sequence= red. Sequenced with T7 promoter (F) primer.

NNNNNNNNNCNNTCNTTGAGCGAGTTCTCAAAATGAACAATAATTCTAGAGCTTATCGAT
ACCGTCGACCTCGAATCACTAGTCAGCTGGAATTCCACGCGCGCCCGGCTGGGGGATCTC
CTCCGCGTGCCCGAAAGGGGGATATGCCATTTGGACATGTAATTGTCAGCACGGGATCTG
AGACTTCCAAAAAATGCCATGGAAGACGCCAAAAACATAAAGAAAGGCCCGGCGCCATTC
TATCCGCTGGAAGATGGAACCGCTGGAGAGCAACTGCATAAGGCTATGAAGAGATACGCC
CTGGTTCCTGGAACAATTGCTTTTACAGATGCACATATCGAGGTGGACATCACTTACGCT
GAGTACTTCGAAATGTCCGTTCGGTTGGCAGAAGCTATGAAACGATATGGGCTGAATACA

AATCACAGAATCGTCGTATGCAGTGAAAACTCTCTTCAATTCTTTATGCCGGTGTTGGGC
GCGTTATTTATCGGAGTTGCAGTTGCGCCCGCGAACGACATTTATAATGAACGTGAATTG
CTCAACAGTATGGGCATTTCGCAGCCTACCGTGGTGTTCGTTTCCAAAAAGGGGTTGCAA
AAAATTTTGAACGTGCAAAAAAAGCTCCCAATCATCCAAAAAATTATTATCATGGATTCT
AAAACGGATTACCAGGGATTTCAGTCGATGTACACGTTCGTCACATCTCATCTACCTCCC
GGTTTTAATGAATACGATTTTGTGCCAGAGTCCTTCGATAGGGACAAGACAATTGCACTG
ATCATGAACTCCTCTGGATCTACTGGTCTGCCTAAAGGTGTCGCTCTGCCTCATAGAACT
GCCTGCGTGAGATTCTCGCATGCCAGAGATCCTATTTTTGGCAATCAAATCATTCCGGAT
ACTGCGATTTTAAGTGTTGTTCCATTCCATCACGGTTTTGGAATGTTTACTACACTCGGA
TATTTGATATGTGGATTTCGAGTCGTCTTAATGTATAGATTTGAAGAAGAGCTGTTTCTG
AGGAGCCTTCAGGATTACAAGATTCAAAGTGCGCTGCTGGTGCCAACCCTATTCTCCTTC
TTCGCCAAAAGCACTCTGATTGACAAATACGATTTATCTAATTTANNCGAAATTGCTTCT
GGNGGCGCTCCCCTCTCTAAGGAAGTCGGGGAANNCGGTTGCCAAGAGGTTCCATCTGCC
AGGTATCAGGCAAGGAAATGGNCTNANTGAGACTACNTCAGCTATTNNGATTANNCCCCA
AGGGGGAAGAATAAAC

Appendix-Figure 39. Sequencing data of cloning *HER2* 5' UTR into p15 monocistronic plasmid. *HER2* 5' UTR sequence= blue. Part of p15 sequence= green. Part of firefly luciferase sequence= red. Sequenced with T7 promoter (F) primer.

NNNNNNNNNNGTNANTTAGCTTGCTTGCTCCCAATCACAGGAGAAGGAGGAGGTGGAGGA
GGAGGGCTGCTTGAGGAAGTATAAGAATGAAGTTGTGAAGCTGAGATTCCCCTCCATTGG
GACCGGAGAAACCAGGGGAGCCCCCCGGGCAGCCGCGCGCCCCTTCCCACGGGGCCCTTT
ACTGCGCCGCGCGCCCGGCCCCCACCCCTCGCAGCACCCCGCGCCCCGCGCCCTCCCAGC
CGGGTCCAGCCGGAGCCATGGGGCCGGAGCCGCAGTGAGCACCAAGCTTGGCAATCCGGT
ACTGTTGGTAAAGCCACCATGGAAGATGCCAAAAACATTAAGAAGGGCCCAGCGCCATTC
TACCCACTCGAAGACGGGACCGCCGGCGAGCAGCTGCACAAAGCCATGAAGCGCTACGCC
CTGGTGCCCGGCACCATCGCCTTTACCGACGCACATATCGAGGTGGACATTACCTACGCC
GAGTACTTCGAGATGAGCGTTCGGCTGGCAGAAGCTATGAAGCGCTATGGGCTGAATACA
AACCATCGGATCGTGGTGTGCAGCGAGAATAGCTTGCAGTTCTTCATGCCCGTGTTGGGT
GCCCTGTTCATCGGTGTGGCTGTGGCCCCAGCTAACGACATCTACAACGAGCGCGAGCTG
CTGAACAGCATGGGCATCAGCCAGCCCACCGTCGTATTCGTGAGCAAGAGAGGGCTGCAA
AAGATCCTCAACGTGCAAAAGAAGCTACCGATCATACAAAAGATCATCATCATGGATAGC
AAGACCGACTACCAGGGCTTCCAAAGCATGTACACCTTCGTGACTTCCCATTTGCCACCC
GGCTTCAACGAGTACGACTTCGTGCCCGAGAGCTTCGACCGGGACAAAACCATCGCCCTG
ATCATGAACAGTAGTGGCAGTACCGGATTGCCCAAGGGCGTAGCCCTACCGCACCGCACC
GCTTGTGTCCGATTCAGTCNTGCCCGCGACCTCATCTTCGGCAACCAGATCATCGCCGAC
ACCGCTATCCTCAGGGGGTGCCATTTCACCACGGCTTCGGCATGTTCACCACGCTGGGCT
ACTTGATCTGCGGCTTTCG

Appendix-Figure 40. Sequencing data of cloning *HER4* 5' UTR into p15 monocistronic plasmid. *HER4* 5' UTR sequence= blue. Part of p15 sequence= green. Part of firefly luciferase sequence= red. Sequenced with T7 promoter (F) primer.

NNNNNNNNNNNNNNANTTNAGCTTNNCGCGCGCCCGGCTGGGGGATCTCCTCCGCGTGCC
CGAAAGGGGGATATGCCATTTGGACATGTAATTGTCAGCACGGGATCTGAGACTTCCAAA
AAAAGCTTCACGCGCGCCCGGCTGGGGGATCTCCTCCGCGTGCCCGAAAGGGGGATATGC
CATTTGGACATGTAATTGTCAGCACGGGATCTGAGACTTCCAAAAAAAGCTTGGCAATCC
GGTACTGTTGGTAAAGCCACCATGGAAGATGCCAAAAACATTAAGAAGGGCCCAGCGCCA
TTCTACCCACTCGAAGACGGGACCGCCGGCGAGCAGCTGCACAAAGCCATGAAGCGCTAC
GCCCTGGTGCCCGGCACCATCGCCTTTACCGACGCACATATCGAGGTGGACATTACCTAC
GCCGAGTACTTCGAGATGAGCGTTCGGCTGGCAGAAGCTATGAAGCGCTATGGGCTGAAT
ACAAACCATCGGATCGTGGTGTGCAGCGAGAATAGCTTGCAGTTCTTCATGCCCGTGTTG
GGTGCCCTGTTCATCGGTGTGGCTGTGGCCCCAGCTAACGACATCTACAACGAGCGCGAG

CTGCTGAACAGCATGGGCATCAGCCAGCCCACCGTCGTATTCGTGAGCAAGAAAGGGCTG
CAAAAGATCCTCAACGTGCAAAAGAAGCTACCGATCATACAAAAGATCATCATCATGGAT
AGCAAGACCGACTACCAGGGCTTCCAAAGCATGTACACCTTCGTGACTTCCCATTTGCCA
CCCGGCTTCAACGAGTACGACTTCGTGCCCGAGAGCTTCGACCGGGACAAAACCATCGCC
CTGATCATGAACAGTAGTGGCAGTACCGGATTGCCCAAGGGCGTAGCCCTACCGCACCGC
ACCGCTTGTGTCCGATTCAGTCATGCCCGCGACCCCATCTTCGGCAACCAGATCATCCCC
GACACCGCTATCCTCAGCGTGGTGCCATTTCACCACGGCTTCGGCATGTTCACCACGCTG
GGCTACTTGATCTGCGGCTTTCGGGTCGTGCTCATGTACCGCTTCGAGGAGGAGCTATTC
TTGCGCAGCTTGCAAGACTATAAGATTCAATCTGCCCTGCTGGTGCCCACACTATTTAGC
TTCTTCGCTAAGAGCACTCTCATCGACAAGTACGACCTAAGCAACTTGCACGANATCGCC
AGCGGCGGGGCGCCGCTCANCAAGGAGGT

Appendix-Figure 41. Sequencing data of cloning hCLl-hPEST into p15. Part of firefly luciferase sequence= red. hCLl-hPEST sequence= purple. Vector sequence between hCL1 and hPEST= orange. Part of p15 sequence= green. Sequenced with CL1-PEST (F) primer.

NNNNNNNNNNNNNGNNNNNNNNGGTTNNACCGCCAGAAGCTGCGCGGTGGTGTTGTGTTC
GTGGACGAGGTGCCTAAAGGACTGACCGGCAAGTTGGACGCCCGCAAGATCCGCGAGATT
CTCATTAAGGCCAAGAAGGGCGGCAAGATCGCCGTGAATTCTGCTTGCAAGAACTGGTTC
AGTAGCTTAAGCCACTTTGTGATCCACCTTAACAGCCACGGCTTCCCTCCCGAGGTGGAG
GAGCAGGCCGCCGGCACCCTGCCCATGAGCTGCGCCCAGGAGAGCGGCATGGATAGACAC
CCTGCTGCTTGCGCCAGCGCCAGGATCAACGTCCACGTGCAGTCTAGATGGCCGGCCGCT
TCGAGCAGACATGATAAGATACATTGATGAGTTTGGACAAACCACAACTAGAATGCAGTG
AAAAAAATGCTTTATTTGTGAAATTTGTGATGCTATTGCTTTATTTGTAACCATTATAAG
CTGCAATAAACAAGTTAACAACAACAATTGCATTCATTTTATGTTTCAGGTTCAGGGGGA
GGTGTGGGAGGTTTTTTAAAGCAAGTAAAACCTCTACAAATGTGGTAAAATCGATAAGGA
TCCGTTTGCGTATTGGGCGCTCTTCCGCTGATCTGCGCAGCACCATGGCCTGAAATAACC
TCTGAAAGAGGAACTTGGTTAGCTACCTTCTGAGGCGGAAAGAACCAGCTGTGGAATGTG
TGTCAGTTAGGGTGTGGAAAGTCCCCAGGCTCCCCAGCAGGCAGAAGTATGCAAAGCATG
CATCTCAATTAGTCAGCAACCAGGTGTGGAAAGTCCCCAGGCTCCCCAGCAGGCAGAAGT
ATGCAAAGCATGCATCTCAATTAGTCAGCAACCATAGTCCCGCCCCTAACTCCGCCCATC
CCGCCCCTAACTCCGNCCAGTTCCGCCCATTCTCCGCCCCATGGCTGACTANTTTTTTTT
ATTTATGCNNAGGCCGAGGCCGCCTCTGCCTCTGAGCTATTCAGAAGTAGTGACGAGGCT
TTTTTGGAGGCCTAAGCTTTTGCAAAAAGCTCGATTCTTCTGANNCTAANNNCCCCANAA
AAAACCCCAACTCCCNGNNNNCNNCGTTAAAAANTTNNNAATCCAAANGTNNNACGGGGN
NNNGNC

Appendix-Figure 42. Sequencing data of cloning hCLl-hPEST into p15-*HER2* 5' UTR. Part of firefly luciferase sequence= red. hCLl-hPEST sequence= purple. Vector sequence between hCL1 and hPEST = orange. Part of p15 sequence= green. Sequenced with CL1-PEST (F) primer.

NNNNNNNNNNNNNNNNNNNNNNNNNNNNTTACNNCCGCCAAGAAGCTGCGCGGTGGTGTTG
TGTTCGTGGACGAGGTGCCNNNNGGACTGACCGGCAAGTTGGACGCCCGCAAGATCCGCG
AGATTCTCATTAAGGCCAAGAAGGGCGGCAAGATCGCCGTGAATTCTGCTTGCAAGAACT
GGTTCAGTAGCTTAAGCCACTTTGTGATCCACCTTAACAGCCACGGCTTCCCTCCCGAGG
TGGAGGAGCAGGCCGCCGGCACCCTGCCCATGAGCTGCGCCCAGGAGAGCGGCATGGATA
GACACCCTGCTGCTTGCGCCAGCGCCAGGATCAACGTCCACGTGCAGTCTAGATGGCCGG
CCGCTTCGAGCAGACATGATAAGATACATTGATGAGTTTGGACAAACCACAACTAGAATG
CAGTGAAAAAAATGCTTTATTTGTGAAATTTGTGATGCTATTGCTTTATTTGTAACCATT
ATAAGCTGCAATAAACAAGTTAACAACAACAATTGCATTCATTTTATGTTTCAGGTTCAG
GGGGAGGTGTGGGAGGTTTTTTAAAGCAAGTAAAACCTCTACAAATGTGGTAAAATCGAT
AAGGATCCGTTTGCGTATTGGGCGCTCTTCCGCTGATCTGCGCAGCACCATGGCCTGAAA
TAACCTCTGAAAGAGGAACTTGGTTAGCTACCTTCTGAGGCGGAAAGAACCAGCTGTGGA

ATGTGTGTCAGTTAGGGTGTGGAAAGTCNCCAGGCTCCCCAGCACGCACAACTATGCAAA
GCATGCATCTCNATTANTCNNCCACCANGTGTGGANGTCTCAGNNCCCCCGCCACGAANN
NTATGCAACCNGCACNGCAANAANCNNCNNCATAGGCCNGCCCNNACTCCNCCAACCCGC
CCCNANACNACCANNNCCACCAGTNNNCACCCCATGGNCGAACA

Appendix-Figure 43. Sequencing data of cloning *HER2* 3' UTR into destabilised p15-*HER2* 5'UTR. Part of hPEST sequence= purple. *HER2* 3' UTR (plasmid preparation used in Chapter 4 and 5) = blue. Part of p15 sequence= green. Sequenced with *HER2* 3' UTR (F) primer.

NNNNNNNNNNCNTGNNCTGCGCCCAGGAGAGCGGCATGGATAGACACCCTGCTGCTTGCG
CCAGCGCCAGGATCAACGTCCACGTGACCAGAAGGCCAAGTCCGCAGAAGCCCTGATGTG
TCCTCAGGGAGCAGGGAAGGCCTGACTTCTGCTGGCATCAAGAGGTGGGAGGGCCCTCCG
ACCACTTCCAGGGGAACCTGCCATGCCAGGAACCTGTCCTAAGGAACCTTCCTTCCTGCT
TGAGTTCCCAGATGGCTGGAAGGGGTCCAGCCTCGTTGGAAGAGGAACAGCACTGGGGAG
TCTTTGTGGATTCTGAGGCCCTGCCCAATGAGACTCTAGGGTCCAGTGGATGCCACAGCC
CAGCTTGGCCCTTTCCTTCCAGATCCTGGGTACTGAAAGCCTTAGGGAAGCTGGCCTGAG
AGGGGAAGCGGCCCTAAGGGAGTGTCTAAGAACAAAAGCGACCCATTCAGAGACTGTCCC
TGAAACCTAGTACTGCCCCCCATGAGGAAGGAACAGCAATGGTGTCAGTATCCAGGCTTT
GTACAGAGTGCTTTTCTGTTTAGTTTTTACTTTTTTTGTTTTGTTTTTTTAAAGATGAAA
TAAAGACCCAGGGGGAGAATGGGTGTTGTATGGGGAGGCAAGTGTGGGGGGTCCTTCTCC
ACACCCACTTTGTCCATTTGCAAATATATTTTGGAAAACAGCTGGCCGGCCGCTTCGAGC
AGACATGATAAGATACATTGATGAGTTTGGACAAACCACAACTAGAATGCAGTGAAAGAA
ATGCTTTATTTGTGAAATTTGTGATGCTATTGCTTTATTTGTAACCATTATAAGCTGCAA
TAAACAAGTTAACAACAACAATTGCATTCATTTTATGTTTCAGGTTCAGGGGGATGTGTG
GGAGGTTTTTAAAACAAGNNCACCACCACCCTGCGCTAANNCGATAAGNTNCNATAAGAA
TAGNNCGCCNNNNNGN

Appendix-Figure 44. Sequencing data of cloning *HER2* 3' UTR into destabilised p15-*HER2* 5'UTR. Part of hPEST sequence= purple. *HER2* 3' UTR (plasmid preparation used in the Appendix Figures 35-36) =blue. Part of p15 sequence= green. Sequenced with *HER2* 3' UTR (F) primer.

NNNNNNNNNNCNTGANCTGCGCCCAGGAGAGCGGCATGGATAGACACCCTGCTGCTTGCG
CCAGCGCCAGGATCAACGTCCACGTGACCAGAAGGCCAAGTCCGCAGAAGCCCTGATGTG
TCCTCAGGGAGCAGGGAAGGCCTGACTTCTGCTGGCATCAAGAGGTGGGAGGGCCCTCCG
ACCACTTCCAGGGGAACCTGCCATGCCAGGAACCTGTCCTAAGGAACCTTCCTTCCTGCT
TGAGTTCCCAGATGGCTGGAAGGGGTCCAGCCTCGTTGGAAGAGGAACAGCACTGGGGAG
TCTTTGTGGATTCTGAGGCCCTGCCCAATGAGACTCTAGGGTCCAGTGGATGCCACAGCC
CAGCTTGGCCCTTTCCTTCCAGATCCTGGGTACTGAAAGCCTTAGGGAAGCTGGCCTGAG
AGGGGAAGCGGCCCTAAGGGAGTGTCTAAGAACAAAAGCGACCCATTCAGAGACTGTCCC
TGAAACCTAGTACTGCCCCCCATGAGGAAGGAACAGCAATGGTGTCAGTATCCAGGCTTT
GTACAGAGTGCTTTTCTGTTTAGTTTTTACTTTTTTTGTTTTGTTTTTTTAAAGATGAAA
TAAAGACCCAGGGGGAGAATGGGTGTTGTATGGGGAGGCAAGTGTGGGGGGTCCTTCTCC
ACACCCACTTTGTCCATTTGCAAATATATTTTGGAAAACAGCTGGCCGGCCGCTTCGAGC
AGACATGATAAGATACATTGATGAGTTTGGACAAACCACAACTAGAATGCAGTGAAAAAA
ATGCTTTATTTGTGAAATTTGTGATGCTATTGCTTTATTTGTAACCATTATAAGCTGCAA
TAAACAAGTTAACAACAACAATTGCATTCATTTTATGTTTCAGGTTCAGGGGGAGGTGTG
GGAGGTTTTTTAAAGCAAGTAAAACCTCTACAAATGTGGTAAAATCGATAAGGATCCGTT
TGCGTATTGGGCGCTCTTCCGCTGATCTGCGCAGCACCATGGCCTGAAATAACCTCTGAA
AGAGGAACTTGGTTAGCTACCTTCTGAGGCGGAAAGAACCAGCTGTGGAATGTGTGTCAG
TTAGGNTGTGGAAAGTCCNNAGGCTCCCNAGCAGGCAGAAAGTATGCAAAGCATGCATCT
CAATTAGTCAGCAACCAGGGTGNGGAAAGTCCCCAGGCTCCCCANNCAGGCAAGAAGTNT
GCAAAGNATGCATCTCCATTAAGTCANCAACNNTAGTTCCCGCCCCTAAANNCNNCCNAT
CCCGCCCCTAACTNCGCCCANNTCCNNCCAATCTCCCGACCNNNGGTTGNCNNANTTGTT
TTNANTTTATNNNAAGGCCCNAGGCCNCCANNNNNCCNNNAGAACTAT

PIP Reflective Statement

Note to examiners:

This statement is included as an appendix to the thesis in order that the thesis accurately captures the PhD training experienced by the candidate as a BBSRC Doctoral Training Partnership student.

The Professional Internship for PhD Students is a compulsory 3-month placement which must be undertaken by DTP students. It is usually centred on a specific project and must not be related to the PhD project. This reflective statement is designed to capture the skills development which has taken place during the student's placement and the impact on their career plans it has had.

PIP Reflective Statement:

I completed a 3-month internship (28th February 2022-27th May 2022) at APIS Assays Technologies which is a biotechnology company in Manchester that focuses on researching and producing diagnostic assays. During my internship, I worked across two different disciplines, pneumonia and complicated urinary tract infections, which allowed me to adapt my scientific knowledge to different disease areas and quickly adjust to projects with different goals. My role when working on the pneumonia project involved determining the limit of detection of a series of pneumonia pathogen targets using a QIAstat (Qiagen) qPCR machine and to benchmark results against a competitor brand. This allowed me to carry out work that I had no prior experience in. In addition, I gained experience working with machinery used in industry and working with biological samples. I was able to work within a team but was quickly given

responsibilities to work independently which developed my confidence. When working on the complicated urinary tract infections project, I gained experience in a different aspect of assay development which involved developing multiplex tests for the detection of different targets in a single PCR experiment and conducting sensitivity tests of targets using the QS5 qPCR machine and the QIAstat. I also gained experience crafting QIAstat cartridges containing different primer/probes for the use in the QIAstat machine. This also gave me experience working in a manufacturing laboratory.

I enjoyed working as part of a team during my internship such as liaising work with other team members. I was involved in writing and reviewing experimental protocols for the team. I also developed confidence with my verbal communication by reporting my progress to my colleagues at daily team 'stand up' meetings and I was made to feel like a valuable team member.

Overall, my internship has developed my interest in a career outside academia and has given me experience in working at a biotechnology company which will be advantageous for exploring a career in industry. My internship has given me an opportunity to understand how diagnostic assays are developed for the detection of different diseases and experience of working as a team to improve and progress projects.